

PERFORMANCE, EMISSION AND COMBUSTION STUDIES OF A RENEWABLE DIESEL IN A COMPRESSION IGNITION ENGINE

**A thesis submitted to the Delhi Technological University, Delhi in fulfilment of
the requirements for the award of the degree of**

DOCTOR OF PHILOSOPHY

in

Mechanical Engineering

by

RASHI KOUL

(2K17/PhD/ME/17)

Under the supervision of

Dr. NAVEEN KUMAR

(Professor, Guide)

&

Dr. R. C. SINGH

(Professor, Co-Guide)



(Mechanical Engineering Department)

Delhi Technological University

Shahbad, Daulatpur Bawana Road

Delhi – 110042, INDIA

February, 2023

© DELHI TECHNOLOGICAL UNIVERSITY-2023

ALL RIGHTS RESERVED

DECLARATION

I hereby declare that the PhD thesis entitled “**PERFORMANCE, EMISSION AND COMBUSTION STUDIES OF A RENEWABLE DIESEL IN A COMPRESSION IGNITION ENGINE**” is an original work carried out by me under the supervision of Dr. NaveenKumar, Professor, and Dr. R. C. Singh, Professor, Mechanical Engineering Department, Delhi Technological University, Delhi. This thesis has been prepared in conformity with the rules and regulations of the Delhi Technological University, Delhi. The research work reported, and results presented in the thesis have not been submitted either in part or full to any other university or institute for the award of any other degree or diploma.

(Rashi Koul)

2K17/PhD/ME/17

Research Scholar

Mechanical Engineering Department

Delhi Technological University

Delhi-110042

Date:

Place: Delhi

CERTIFICATE

This is to certify that the work embodied in the thesis entitled “**PERFORMANCE, EMISSION AND COMBUSTION STUDIES OF A RENEWABLE DIESEL IN A COMPRESSION IGNITION ENGINE**” by **Rashi Koul**, (Roll No.-2K17/PhD/ME/17) in partial fulfillment of requirements for the award of Degree of **DOCTOR OF PHILOSOPHY** in Mechanical Engineering, is an authentic record of student’s own work carried by her under our supervision.

This is also certified that this work has not been submitted to any other University or Institute for the award of any other diploma or degree.

(Dr. Naveen Kumar)

Professor

Mechanical Engineering

Department Delhi Technological

University

Delhi-110042

(Dr. R. C. Singh)

Professor Mechanical

Engineering Department Delhi

Technological University

Delhi-110042

Dedicated to
My Father
Prof. P. K. Koul

ACKNOWLEDGEMENTS

The present research work was carried out under the esteemed supervision of my learned guide Prof. Naveen Kumar and co-guide Prof. R. C. Singh. It is my honour and privilege to express a deep sense of gratitude to both of them for their helping attitude, critical and valuable comments and constant inspiration. I am grateful for Prof. Naveen Kumar's mentorship, his active participation, constant encouragement and 'never give up' perspective, especially during difficult times, have always led me to become a good researcher. I am grateful for his understanding and his blessings. I also express my gratitude to Smt. Sumeeta Garg, for her blessings and affection for me.

I would also like to extend my gratitude to Prof. S.K.Garg, DRC Chairman, and Head, Prof. Rajiv Chaudhary, and Late Prof. Vikas Rastogi Mechanical Engineering Department, Delhi Technological University, Delhi for their guidance and support.

I am grateful and blessed to have supportive colleagues of Centre for Advanced Studies and Research in Automotive Engineering (CASRAE), DTU, Delhi; in particular, ex-researchers, Dr. H.S. Pali, Assistant Professor, NIT Srinagar, Dr. Sidharth Bansal, Assistant Professor, MAIT, Delhi, Dr. Parvesh Kumar, Assistant Professor, VCE, Warangal, Dr. Ankit Sonthalia, Assistant Professor, SRMIST, Ghaziabad UP, Dr. Mukul Tomar, Post-Doc Fellow, University of Illinois, Chicago, Dr. Roshan Raman, Assistant Professor, NCU, Gurgaon and existing scholars Mr. Hansham Dewal, Mr. Pawan Jha, Ms. Khushbu Yadav, Mr. Vipul, Mr. Chandrashekar, Mr. Dushyant Mishra for their valuable guidance, persistent help and support.

I am grateful to Mr. Kamal Nain for the cooperation in the laboratory along with Mr. Surender Singh and Mrs. Neetu Mishra, support staff of CASRAE, DTU, Delhi, Mr. Deepak Ridhlan, support staff, ME Dept. DTU.

I am grateful to management of Amity University Haryana, particularly Prof. P. B. Sharma,

Vice-chancellor, AUH, and my esteemed colleagues Dr. Rajesh Arora, Dr. Sandeep Phogat, Mr. Avinash Dholiwal, Ms. Sakshi Gupta, Mr. Manish Bharti, Mr. Rajat Butola, and Mr. Narender Kumar for providing all possible support and helping me in my official duties, which has enabled me to focus on the present work.

There are some friends and colleagues who have helped me along the way for the successful completion of this research work. I take this opportunity to thank Dr. Mukul Tomar, Dr. Ankit Sonthalia, Mr Hansham, Dr. Harveer Singh Pali, and Dr. Parvesh Kumar for their valuable contribution, timely help, great suggestions and ready to help attitude will always be cherished by me throughout my life. I would also like to thank Mr. Sandeep, Mr. Sheel Bhadra, Mr. Deepak, Mr Ankur, Mr Abhishek Goyal, Mr. BharatYadav, and Dr. S. K. Singh.

I am also grateful to my small community of friends Mr. Sagar Kadecha, Mr. Jaydeep Parmar, Mr. Anush, Mr. Nishikant, Mr. Amit, Mr. Ashwin ji, Mr. Sushant Tripathi, Ms. Surya, Ms. Shriveni, Ms. Anamika, Ms. Anjali ji, Ms. Sheetal and Dr. Shabeena for always encouraging and believing in my dream

I shall ever cherish the affection and blessings showered on me by my parents, Prof. P.K.Koul and Mrs. Indra Mattoo. Whatever I have achieved in my professional life it is all because of them. I cannot express in words the efforts and encouragement given by them to nurture me. I place my sincere respect and a deep sense of gratitude to my mother-in-law Mrs. Santosh Kaul and father-in-law Mr. Jawahar Kaul, for always being there as a strong support system and a source of an encouragement. Without their continuous support this journey would have been difficult. I am also indebted to my grandparents, my aunt, and my relatives who always encouraged and blessed me. I am grateful for my younger sister Mrs. Vibha Koul Razdan and my sister-in-law Mrs. Anvika Kaul Bopana who always blessed and wished me good.

Finally, I am unable to express my sincere gratitude in words for the affection, encouragement

and moral support given by my husband Mr. Amit Kaul and limitless love by my wise and sensible daughter Ms. Vriti Kaul during the research work. I am ever beholden to my husband Mr. Amit Kaul, and daughter Vriti Kaul for not giving due attention and time during the present work. Last but not the least I thank the Almighty for giving me the strength and patience to complete this work in all respects, leading to the path of success.

Rashi Koul

Delhi

ABSTRACT

India is a developing country and major parts of its transportation, agriculture, and energy sectors are all diesel-dependent. The exhaust gases emitted by the combustion of diesel fuel have led to an increase in air pollution and global warming. These exhaust emissions have affected the lives of animals and humans in numerous ways. Extensive research has been done on alternative fuels, biodiesel being a common one. However, due to biodiesel's limitations, it cannot replace diesel in existing CI engines. All over the world, researchers, academicians, and industrialists are exploring alternative fuels, which can be sustainable in such a way that they can replace diesel as fuel. Renewable diesel is such a fuel, which is produced from non-edible vegetable oil undergoing hydroprocessing at high pressure and temperature in presence of a catalyst. The molecular structure of renewable diesel is similar to diesel. Renewable diesel can use the same pipeline infrastructure as is used for diesel fuel. It is also called a 'drop-in fuel'.

The objective of the present research work is to produce renewable diesel by hydroprocessing. The catalyst used during the hydroprocessing process was chosen as manganese, cerium promoted ruthenium-based catalyst supported on Al_2O_3 . Various blends of diesel and renewable diesel and ternary blends of renewable diesel, diesel, and ethanol were prepared in different proportions and their performance, emission, and combustion characteristics were compared to the baseline data of conventional fuel, diesel. Percentage of ethanol was limited to 15% due to its insolubility in diesel fuel. Physicochemical properties like kinematic viscosity, density, cold flow properties, cetane index, etc. were evaluated and found suitable for use as per ASTM D standards.

Response surface methodology (RSM) optimization technique was implemented to study various response variables like brake thermal efficiency (BTE), carbon monoxide (CO), unburnt hydrocarbon (HC), nitrogen oxide (NO) emissions, and smoke opacity by using input factors like

brakemean effective pressure (BMEP) and percentage of renewable diesel and ethanol by volume in diesel.

For getting the most accurate solutions, a face-centered model of Central Composite Design (CCD) was chosen. This helps researchers predict results very precisely with fewer experiments to be conducted. The results obtained from RSM were validated with experimental data. RSM optimizer tool showed that 30% of Renewable diesel and 7% of ethanol at BMEP of 2.6 bar can give optimized output. The predicted values for BTE, CO, HC, NO, and smoke were found to be 29.21%, 5.5g/kWh, 4.32g/kWh, 4.47g/kWh, and 19.46% respectively.

Renewable diesel was mixed with diesel from 10% to 50% by volume and was named D90R10, D80R20, D70R30, D60R40, and D50R50. The results for renewable diesel (R100) and diesel (D100) blends indicate that with an increase in the percentage of renewable diesel, brake thermal efficiency decreases. There is a decrease of 16.7%, 3.51%, 6.35%, 8.66%, 10.91% and 12.65% of BTE for R100, D90R10, D80R20, D70R30, D60R40 and D50R50 respectively. In addition, the heat release rate (HRR) for diesel fuel is more than for renewable diesel and its blends. This is because of the earlier ignition of renewable diesel. Exhaust emissions like CO, HC, and smoke opacity are found to decrease up to 30% blend, after which it increases. At full load, there is a decrease of 5.79%, 10.31%, and 14.47% in HC emissions for R10D90, R20D80, and R30D70 blends. For CO exhaust emissions, 5.09%, 9.55%, and 13.38% decrease until renewable diesel is up to 30% of the blend. Beyond 30% renewable diesel in a blend, the percentage of CO exhaust emissions starts increasing. NO emissions were lower for all blends than diesel. The lowest NO emission for neat renewable diesel is 3.1014 g/kWh which is 23.2% lesser than that emitted by diesel fuel. At full load, smoke opacity was lowest for R30D70 which is 54.1% than that of diesel which was 62.4%.

It was observed that R20D80 gave better BTE and D70R30 gave lesser emissions. Keeping

these two blends into consideration and to improve the shortcomings of both, ethanol was added. 5%, 10% and 15% of ethanol were blended with 20% and 30% of renewable diesel. The experiments concluded that HRR increased with an addition of ethanol due to a low cetane index which increased ignition delay. Values of HRR for ternary blends were found to be more than diesel. BTE increased with an increase in the percentage of ethanol till E10. Beyond E10, BTE decreased. R30E15 has the least BTE of 23.8% on full load which is 24.8% lesser than diesel fuel. With an increase in the percentage of ethanol, HRR increased. At full load, the maximum HRR for R20E15 was 61.74J/°CA whereas, for D80R20 it was 50.16J/°CA. With an increase in addition of ethanol pressure also increased. Ethanol percentage up to 10% by volume in a blend is acceptable as otherwise, it can lead to a further decrease in the BTE. This is due to the lower calorific value of both renewable diesel and ethanol. Low calorific value also leads to more consumption of fuel with an increase of renewable diesel and ethanol percentage in a ternary blend. With an increase in the percentage of ethanol, CO and HC emission increases however, CO emissions are lesser than diesel. Moreover, with an increase in ethanol percentage smoke opacity and NO decreases. Ternary blend R30E10 has the lowest NO and smoke emissions. NO and smoke opacity were reduced by 24.25% and 20.35% respectively.

LIST OF CONTENTS

		Page No.
	Declaration	i
	Certificate	ii
	Dedication	iii
	Acknowledgements	iv
	Abstract	vii
	List of Contents	x
	List of Figures	xv
	List of Plates	xx
	List of Tables	xxi
	Nomenclature	xxii
CHAPTER 1	INTRODUCTION	1 - 13
1.1	Motivation	1
1.2	Energy Scenario in India	1
1.3	Diesel engine	4
1.4	Environmental Degradation	5
	1.4.1 Alternative fuels and its effect on exhaust emissions	6
	1.4.2 Jatropha oil as a potential alternative fuel	8
1.5	Hydrogenation of Triglycerides based Biomass	10
1.6	Role of hydrogen and methanol in producing biofuel	12
1.7	Organization of Thesis	12
CHAPTER 2	LITERATURE REVIEW	14 - 47
2.1	Introduction	14
2.2	Hydroprocessing Unit	15
2.3	Various Techniques used for the production of Renewable Diesel	15
	2.3.1 Hydroprocessing	16
	2.3.2 Thermal Conversion	16
	2.3.3 Biomass to Liquid	17

2.4	Various reaction mechanism for the production of Renewable Diesel through hydroprocessing technique	19
2.5	Several operating Parameters and its consequence on Production of Renewable Diesel	23
	2.5.1 Catalyst and its effect on production of Renewable Diesel	25
	2.5.2 Temperature and its effect on production of Renewable Diesel	32
	2.5.3 Effect of Hydrogen Pressure on production of Renewable Diesel	35
2.6	Characteristics of Renewable Diesel used in CI Engines	37
	2.6.1 Physio-chemical Properties of a Renewable Diesel	37
	2.6.2 Performance Characteristics of a Renewable Diesel	39
	2.6.3 Emission Characteristics of a Renewable Diesel	42
2.7	Summary	44
2.8	Research Gaps	46
2.9	Objectives	46
CHAPTER 3 SYSTEM DEVELOPMENT AND METHODOLOGY		
3.1	Introduction	48 - 79
3.2	Selection of vegetable oil and catalyst	48
3.3	Preparation of catalyst	49
3.4	Production of Renewable Diesel using Hydroprocessing	49
3.5	Production of Biodiesel	50
	3.5.1 Esterification of Jatropha oil	51
	3.5.2 Transesterification of Esterified Jatropha oil	52
3.6	Ethanol	53
3.7	Preparation Fuel sample Test Blends	53
3.8	Test Methods for determination of Physicochemical Properties	55
	3.8.1 Kinematic Viscosity	55
	3.8.2 Density Meter	56
	3.8.3 Calorific Value	57
	3.8.4 Flash Point	58
	3.8.5 Cetane Index	58
	3.8.6 Distillation	59

	3.8.7	Cold Flow Properties	59
	3.8.7.1	Cloud Point and Pour Point	60
	3.8.7.2	Cold Filter Plugging Point	60
	3.8.8	Lubricity	61
	3.8.9	Gas Chromatograph and Mass Spectrometer (GC-MS)	62
	3.8.10	Fourier Transform Infra-Red Spectroscopy (FTIR)	63
3.9		Selection of Compression Ignition Engine	64
3.10		Selection of Engine Test Parameters	67
3.11		Observation and Calculation Methods	68
	3.11.1	Brake Power (BP) and Brake Mean Effective Pressure (BMEP)	68
	3.11.2	Measurement of Engine Speed	69
	3.11.3	Measurement of Air Flow Rate	70
	3.11.4	Measurement of Fuel Consumption Rate	71
	3.11.5	Measurement of Temperature	71
	3.11.6	Measurement of In-cylinder pressure	72
	3.11.7	Measurement of Exhaust Emissions	72
	3.11.8	Calculation of Heat release Rate (HRR)	73
3.12		Engine Trial Methodology	74
3.13		Experimental Accuracies and Uncertainties	74
3.14		Optimization of output parameters using Response Surface Methodology	76
CHATER 4 RESULTS AND DISCUSSIONS			80 - 148
4.1		Introduction	80
4.2		Catalyst Characterization	80
4.3		Product Analysis	81
	4.3.1	GC-MS of Biodiesel derived from Jatropha oil	82
	4.3.2	GC-MS of Renewable Diesel derived from Jatropha oil	82
	4.3.3	FTIR analysis of Biodiesel derived from Jatropha oil	83
	4.3.4	FTIR analysis of Renewable Diesel derived from Jatropha oil	84
4.4		Phyiso-chemical Properties of fuel and its blends	85
	4.4.1	Density	86

	4.4.2	Kinematic Viscosity	88
	4.4.3	Calorific Value	90
	4.4.4	Distillation	91
	4.4.5	Cetane Index	92
	4.4.6	Cold Flow Properties	94
	4.4.7	Flash Point	96
	4.4.8	Lubricity	97
4.5		Storage Stability and its effect on fuel properties	98
4.6		Engine Combustion Characteristics for Diesel, Renewable Diesel and their Blends	101
	4.6.1	Heat Release Rate (HRR)	101
	4.6.2	In-cylinder Pressure (P- θ curve)	102
	4.6.3	Variation in In-cylinder pressure at various loads	103
	4.6.4	Ignition Delay (ID)	104
	4.6.5	Combustion Duration (CD)	105
	4.6.6	Burning Rate at different crank angles	106
4.7		Engine Performance Characteristics of Diesel, Renewable Diesel and their blends	107
	4.7.1	Brake Thermal Efficiency (BTE)	107
	4.7.2	Brake Specific energy Consumption (BSEC)	108
	4.7.3	Exhaust Gas Temperature (EGT)	109
4.8		Engine Exhaust Emission Characteristics of Diesel, Renewable Diesel and their Blends	109
	4.8.1	Hydrocarbon Emissions (HC)	110
	4.8.2	Carbon-monoxide Emissions (CO)	111
	4.8.3	Nitrogen-oxide Emission (NO)	112
	4.8.4	Smoke Opacity	113
4.9		Combustion Characteristics of Diesel, Renewable Diesel and Ethanol blends (Ternary blends)	114
	4.9.1	Heat Release Rate for Ternary Blends	114
	4.9.2	In-cylinder Pressure (P- θ Curve) for Ternary Blends	116
	4.9.3	Variation in In-cylinder pressure of Ternary Blends at various loads	118
	4.9.4	Variation in Ignition Delay for Ternary Blends	119
	4.9.5	Variation in Combustion Duration for Ternary Blends	121

4.10	Engine Performance for Ternary Blends	123
	4.10.1 Brake Thermal Efficiency	123
	4.10.2 Brake Specific Energy Consumption of Ternary Blends	125
	4.10.3 Exhaust Gas Temperature for Ternary Blends	126
4.11	Engine Exhaust Emissions for Ternary Blends	128
	4.11.1 Hydro-carbon Emissions for Ternary Blends	128
	4.11.2 Carbon-monoxide Emissions of Ternary Blends	130
	4.11.3 Nitrogen-oxide Emission for Ternary Blends	131
	4.11.4 Smoke Opacity of Ternary Blends	133
4.12	Response Surface Methodology	135
4.13	Surface and Contour Plots for Input Factors and Response Variables	137
	4.13.1 Optimization Plot and Validation Test	146
CHAPTER 5		
	Conclusions and Future Scope	149 - 151
	5.1 Conclusions	149
	5.2 Scope for Future Work	151
REFERENCES		
		152 - 167

Appendices		
Appendix 1	Test Engine Technical Specifications	168
Appendix 2	AVL Smoke-meter Technical specifications	169
Appendix 3	AVL Di-Gas Analyser Technical Specifications	170
Appendix 4	Optimization Data equations	171

List of Publications		172
Biographical Sketch		173
Curriculum Vitae		174 - 178

LIST OF FIGURES

S.No.	Title	Page No.
Figure 1.1	Production and consumption of oil by various region in million barrels daily	2
Figure 1.2	Trend of consumption of aviation, petrol and diesel fuel in India	3
Figure 1.3	Carbon-dioxide emission (%) world-wide from fuel combustion	6
Figure 1.4	Jatropha fruit, seed, shell and its various by-products	9
Figure 2.1	Catalytic hydroprocessing for organic transformation and progress to fuel	19
Figure 2.2	Different alleyways of triglycerides over hydroprocessing catalyst	20
Figure 3.1	Research Methodology Flowchart	48
Figure 3.2	Schematic diagram of HPSR	51
Figure 3.3	Chemical reaction during transesterification process	53
Figure 3.4	Engine experimental set-up	66
Figure 3.5	Step-by-step mechanism for applying RSM model	76
Figure 3.6	Geometric structure of CCFC	78
Figure 4.1	XRD profile of a catalyst	81
Figure 4.2	SEM images of a catalyst at 20 μ m, 10 μ m and 5 μ m	81
Figure 4.3	Gas- chromatograph of a biodiesel derived from Jatropha oil	82
Figure 4.4	Gas- chromatograph of a Renewable diesel derived from Jatropha oil	83
Figure 4.5	FTIR analysis of Biodiesel derived from Jatropha oil	84
Figure 4.6	FTIR analysis of Renewable diesel derived from Jatropha oil	85
Figure 4.7	Density variation for test fuel samples	87
Figure 4.8	Density variation for ternary test fuel samples	88
Figure 4.9	Kinematic viscosity variation for test fuel samples	89
Figure 4.10	Kinematic viscosity variation for ternary test fuel samples	89
Figure 4.11	Calorific value variation for test fuel samples	90
Figure 4.12	Calorific value variation for ternary test fuel samples	91
Figure 4.13	Distillation at 10%, 50%, 90% and 98% recovery for diesel, Renewablediesel, biodiesel and blends of Renewable diesel and diesel.	92
Figure 4.14	Cetane index variation for various diesel, Renewable diesel and binary test fuel samples	93

Figure 4.15	Cetane index variation for diesel, ethanol, Renewable diesel and ternary blends	93
Figure 4.16	Cloud Point variation for various diesel, Renewable diesel and binary test fuel samples	95
Figure 4.17	Cloud point variation for diesel, Renewable diesel and ternary blends of ethanol, diesel and Renewable diesel	95
Figure 4.18	Cold filter plugging point variation for diesel, Renewable diesel and binary test fuel samples	95
Figure 4.19	Cold filter plugging point variation for diesel, Renewable diesel, ethanol and their ternary blends	96
Figure 4.20	Flash point variation for diesel, Renewable diesel and binary test fuel samples	97
Figure 4.21	Flash point variation for diesel, Renewable diesel, ethanol and their ternary blends	97
Figure 4.22	Lubricity variation for diesel, Renewable diesel and binary test fuel samples	98
Figure 4.23	Lubricity variation for diesel, Renewable diesel and ternary blends of ethanol, diesel and Renewable diesel	98
Figure 4.24	Variation in Kinematic Viscosity of diesel, Renewable diesel and their blends for twelve months	100
Figure 4.25	Variation in Density of diesel, Renewable diesel and their blends for twelve months	100
Figure 4.26	Variation in calorific value of diesel, Renewable diesel and their blends for twelve months	101
Figure 4.27	Heat release rate variation of diesel, Renewable diesel and their blends at full load	102
Figure 4.28	Variation in in-cylinder pressure of diesel, Renewable diesel and their blends at different crank angles at full load	103
Figure 4.29	Variation in peak pressure of diesel, Renewable diesel and their blends at varying loads	104
Figure 4.30	Variation in ignition delay of diesel, Renewable diesel and their blends at varying loads	104
Figure 4.31	Variation in combustion duration of diesel, Renewable diesel and their blends at varying loads	105
Figure 4.32	Variation in crank angle at MFB at 10, 50 and 90% for diesel, Renewable diesel and their blends at varying loads	106
Figure 4.33	Brake thermal efficiency of various fuel samples at varying load	108
Figure 4.34	Brake specific energy consumption of various fuel samples at varying	108

	load	
Figure 4.35	Exhaust Gas Temperature of various fuel samples at varying load	109
Figure 4.36	Hydrocarbon emissions by different fuel samples at varying load conditions	111
Figure 4.37	Carbon-monoxide emissions by different fuel samples at varying load conditions	112
Figure 4.38	Nitrogen-oxide emissions by different fuel samples at varying load conditions	113
Figure 4.39	Smoke Opacity of different fuel samples at varying load conditions	114
Figure 4.40	Heat Release Rate at peak load with 5% blending of an ethanol	115
Figure 4.41	Heat Release Rate at peak load with 10% blending of an ethanol	116
Figure 4.42	Heat Release Rate at peak load with 15% blending of an ethanol	116
Figure 4.43	Variation in in-cylinder peak pressure at peak load with 5% blending of an ethanol	117
Figure 4.44	Variation in in-cylinder peak pressure at peak load with 10% blending of an ethanol	117
Figure 4.45	Variation in in-cylinder peak pressure at peak load with 15% blending of an ethanol	117
Figure 4.46	Variation in in-cylinder peak pressure at various load with 5% blending of an ethanol	119
Figure 4.47	Variation in in-cylinder peak pressure at various load with 10% blending of an ethanol	119
Figure 4.48	Variation in in-cylinder peak pressure at various load with 15% blending of an ethanol	119
Figure 4.49	Variation in ignition delay at various load with 5% blending of an ethanol	120
Figure 4.50	Variation in ignition delay at various load with 10% blending of an ethanol	120
Figure 4.51	Variation in ignition delay at various load with 15% blending of an ethanol	121
Figure 4.52	Variation in combustion duration at various load with 5% blending of an ethanol	122
Figure 4.53	Variation in combustion duration at various load with 10% blending of an ethanol	122
Figure 4.54	Variation in combustion duration at various load with 15% blending of an ethanol	122
Figure 4.55	Variation in Brake Thermal efficiency at different loads with 5% blending	124

	of an ethanol	
Figure 4.56	Variation in Brake Thermal efficiency at different loads with 5% blending of an ethanol	124
Figure 4.57	Variation in Brake Thermal efficiency at different loads with 15% blending of an ethanol	124
Figure 4.58	Variation in Brake specific energy consumption at different loads with 5% blending of an ethanol	125
Figure 4.59	Variation in Brake specific energy consumption at different loads with 10% blending of an ethanol	126
Figure 4.60	Variation in Brake specific energy consumption at different loads with 15% blending of an ethanol	126
Figure 4.61	Variation in exhaust gas temperature at different loads with 5% blending of an ethanol	127
Figure 4.62	Variation in exhaust gas temperature at different loads with 10% blending of an ethanol	127
Figure 4.63	Variation in exhaust gas temperature at different loads with 15% blending of an ethanol	127
Figure 4.64	Variation in hydro-carbon emission at different loads with 5% blending of an ethanol	129
Figure 4.65	Variation in hydro-carbon emission at different loads with 10% blending of an ethanol	129
Figure 4.66	Variation in hydro-carbon emission at different loads with 15% blending of an ethanol	129
Figure 4.67	Variation in carbon-monoxide emission at different loads with 5% blending of an ethanol	130
Figure 4.68	Variation in carbon-monoxide emission at different loads with 10% blending of an ethanol	131
Figure 4.69	Variation in carbon-monoxide emission at different loads with 15% blending of an ethanol	131
Figure 4.70	Variation in Nitrogen-oxide emission at different loads with 5% blending of an ethanol	132
Figure 4.71	Variation in Nitrogen-oxide emission at different loads with 10% blending of an ethanol	132
Figure 4.72	Variation in Nitrogen-oxide emission at different loads with 15% blending of an ethanol	133

Figure 4.73	Variation in Smoke opacity at different loads with 5% blending of an ethanol	134
Figure 4.74	Variation in Smoke opacity at different loads with 10% blending of an ethanol	134
Figure 4.75	Variation in Smoke opacity at different loads with 15% blending of an ethanol	134
Figure 4.76	3D-Surface and contour plots of BTE vs. various input variables	139
Figure 4.77	3D-Surface and contour plots of CO emissions vs. various input variables	141
Figure 4.78	3D-Surface and contour plots of HC emissions vs. various input variables	143
Figure 4.79	3D-Surface and contour plots of NO emissions vs. various input variables	144 - 145
Figure 4.80	3D-Surface and contour plots of Smoke Opacity vs. various input variables	146
Figure 4.81	Optimization plot for smoke, CO, NO, HC and BTE	148

LIST OF PLATES

S.No.	Title	Page No.
Plate 3.1	Experimental set-up for Renewable diesel production high pressure stirred reactor (HPSR)	51
Plate 3.2.	Steps in biodiesel production from Jatropha oil	53
Plate 3.3	Fuel sample blends of Diesel and Renewable diesel	54
Plate 3.4	Ternary fuel samples blends of Diesel, Renewable diesel and ethanol	55
Plate 3.5	Phase separation in fuel sample blends with 20% as ethanol	55
Plate 3.6	Viscometer	56
Plate 3.7	Density meter	57
Plate 3.8	Bomb Calorimeter	57
Plate 3.9	Flash point apparatus	58
Plate 3.10	Distillation equipment	59
Plate 3.11	Cloud Point and Pour Point equipment	60
Plate 3.12	Cold Filter Plugging Point Apparatus	61
Plate 3.13	High Frequency Reciprocating Rig	62
Plate 3.14	Gas Chromatograph and Mass Spectrometer	63
Plate 3.15	FTIR set-up	64
Plate 3.16	Test Engine	65
Plate 3.17	Eddy current dynamometer	66
Plate 3.18	Strain gauge and RPM sensor	66
Plate 3.19	Rotameters	66
Plate 3.20	NI USB 6210 Data acquisition system	66
Plate 3.21	AVL DISMOKE smoke meter and AVL DITEST gas analyser	67
Plate 3.22	Air flow sensor	70
Plate 3.23	Fuel flow sensor	71
Plate 3.24	K-type thermocouple	72
Plate 3.25	Kubeler piezoelectric transducer	72

LIST OF TABLES

S.No	Title	Page No.
Table 1.1	India's oil production and oil consumption	3
Table 1.2	Physiochemical properties of various feedstock used for an alternative fuel	8
Table 1.3	Physio-chemical properties of Diesel and Jatropha oil	10
Table 2.1	Production of Renewable diesel from different feedstock at varying parameters	23
Table 3.1	Composition of various fuel samples blends of Diesel and Renewable diesel	54
Table 3.2	Composition of ternary fuel sample blends of diesel Renewable diesel and ethanol	54
Table 3.3	Accuracy of measuring instruments	75
Table 3.4	Various input factors and their levels	77
Table 3.5	Design array of experimental trials	79
Table 4.1	Comparison in Properties of Diesel, Biodiesel, Renewable Diesel, and blends	85
Table 4.2	Properties of Various fuel samples	86
Table. 4.3	ANOVA for BTE	136
Table 4.4	ANOVA for CO and HC Emissions	136
Table 4.5	ANOVA for NO Emissions and Smoke Opacity	137
Table 4.6	Model Evaluation	137
Table 4.7	Optimization values	147
Table 4.8	Validation Test	148

NOMENCLATURE

ANNOVA	Analysis of Variance
ASTM	American Society for Testing and Materials
AVL-437	AVL-437 Smoke Meter
BDC	Bottom Dead Centre
BSEC	Brake Specific Energy Consumption
BSFC	Brake Specific Fuel Consumption
BTE	Brake Thermal Efficiency
BS-VI	Bharat Stage Emission Standards
B100	Biodiesel 100%
cSt	Centistokes
°C	Degree Celsius
°CA	Degree Crank Angle
CA50	Crank Angle with 50% of heat released
CA90	Crank Angle with 90% of heat released
CCD	Central Composite Design
CCFD	Central Composite Face Centred
CFPP	Cold Filter Plug Point
CI	Compression Ignition
CO	Carbon Monoxide
CO ₂	Carbon Dioxide
CoMo	Cobalt Molybdenum catalyst
CP	Cloud Point
CV	Calorific Value
DPF	Diesel Particulate Filter
D90R10	Diesel 90% Renewable Diesel 10%
D80R20	Diesel 80% Renewable Diesel 20%
D70R30	Diesel 70% Renewable Diesel 30%
D60R40	Diesel 60% Renewable Diesel 40%

D50R50	Diesel 50% Renewable Diesel 50%
EGR	Exhaust Gas Recirculation
EGT	Exhaust Gas Temperature
Eq	Equation
EN	European Union Standards
E100	Ethanol 100%
FAME	Fatty Acid Methyl Ester
FFA	Free Fatty Acids
FTIR	Fourier Transform Infrared
GC-MS	Gas Chromatography Mass Spectrometry
g/kWhr	Gram per KiloWatt hour
HC	Hydrocarbon
HDC	Hydrocracking
HDCX	Hydrodecarboxylation
HDCN	Hydrodecarbonylation
HDN	Hydrodenitrogenation
HDO	Hydrodeoxygenation
HDS	Hydrodesulfurization
hr	Hour
HVO	Hydroprocessed Vegetable Oil
HFRR	High Frequency Reciprocating Rig
HRR	Heat Release Rate
HPSR	High Pressure Stirred Reactor
JO	Jatropha Oil
J/kg	Joules/Kilogram
Kg	Kilogram
kW	Kilowatt
LHSV	Liquid Hourly Space Velocity
ltr	Litre
MJ/kg	Mega Joules / Kilogram

MMT	Million Metric Tonnes
Mm	Millimetre
NiMo	Nickel Molybdenum catalyst
NO _x	Oxides of Nitrogen
NO	Nitrogen-oxide
PID	Proportional-Integral-Derivative
PAH	Polynuclear Aromatic Hydrocarbons
Pd	Palladium
Pd/C	Palladium/Carbon catalyst
PM	Particulate Matter
Pt	Platinum
PP	Pour Point
P- θ	Pressure-Crank Angle
ppm	Parts per million
PTSA	p-toulene sulphonic acid
Rh	Rhodium
rpm	Revolutions per minute
RSM	Response Surface Methodology
Ru	Ruthenium
R100	Renewable Diesel 100%
R20E5	Renewable Diesel 20% Ethanol 5%, 75% Diesel
R20E10	Renewable Diesel 20% Ethanol 10%, 70% Diesel
R20E15	Renewable Diesel 20% Ethanol 15%, 65% Diesel
R30E5	Renewable Diesel 30% Ethanol 5%, 65% Diesel
R30E10	Renewable Diesel 30% Ethanol 10%, 60% Diesel
R30E15	Renewable Diesel 30% Ethanol 15%, 55% Diesel
SFA	Saturated Fatty Acids
SMD	Sauter Mean Diameter
SO ₂	Sulphur-di-oxide
TDC	Top Dead Centre

UFA	Unsaturated Fatty Acids
ULSD	Ultra Low Speed Diesel
v/v	Volume by Volume
wt	Weight
w/w	Weight by Weight
WCO	Waste Cooking Oil
WHSV	Weight Hourly Space Velocity

INTRODUCTION

1.1 Motivation

India is a developing country where economy is diesel dependent. A never-ending increasing demand, increasing price, scarcity of Diesel and massive harmful exhaust emissions, has led researchers, academicians and industrialists to find explicitly a sustainable alternative fuel, which can replace diesel fuel. Exhaust emissions caused due to combustion of diesel fuel has invited hazardous health concerns, increase in earth's temperature by few degrees and global warming. Amongst alternative fuels, biodiesel is a much-researched alternative fuel but it has its limitations and can be used as neat only after engine modifications are done on existing CI engines. Renewable diesel is such a fuel, which is produced from third and fourth generation feedstock by hydroprocessing. Also, fuel modifications are cheaper in comparison to an engine modification. It is a promising substitute to biodiesel and has a tendency to replace diesel fuel. In the present work, Renewable diesel and its blends are explored to help in overcoming the scarcity of diesel fuel in coming years and reduction in emissions and mitigating climate changes which is a need of the hour.

1.2 Energy Scenario in India

Our country is a Diesel driven economy. China and the United States are the top two energy consumers in the world, respectively, with India third on the list [1]. Agricultural sector, power sector and transportation are majorly dependent on diesel fuel. About two million CI engines are used only within agriculture sector. It has created a dependency on other countries for importing diesel fuel to India. It is a known fact that fossil fuel is depleting and prices are sky-rocketing which is creating a perturbation. With such a huge

demand, India has to find some sustainable alternative fuel for itself so that it can become economically resilient and recuperate with environmental conditions.

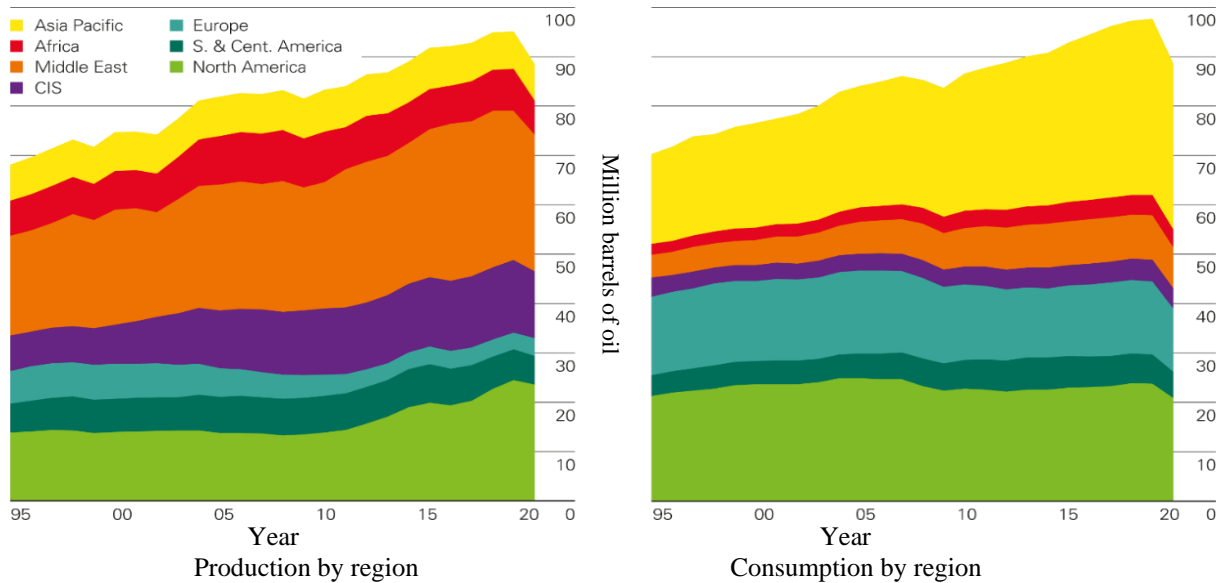


Figure 1.1. Production and consumption of oil by various region in million barrels daily [2]

Figure 1.1 presents production and consumption of oil in various regions all over the world from the year 1995 till 2020 [2]. It is evident from Figure 1.1 that consumption of Asia Pacific, Europe and North America is more than their production rate. India spent almost 88 billion USD in importing 217.08 MT of crude oil in the fiscal year 2018 [3]. India has 138 crore population and only 0.8% of world’s known oil reserves [3]. India’s primary energy demand is expected to grow at CAGR of 4.2% during 2017-2040 [3–5]. Consumption of India has increased from 213.22 MMT in 2018 - 2019 to 214.13 MMT in 2019 – 2020 [2]. India produced 32.17 MMT which is 5.9% less than 2018-19. Table 1.1 represents the statistics of oil production and oil consumption in India since 2010 till date.

Table 1.1 India's oil production and oil consumption [2]

Year	India's Oil Production (MMT)	India's Oil Consumption (MMT)	Self-reliance (%)
2010	41.3	154.0	26.8
2012	42.5	172.0	24.7
2014	41.6	179.1	23.2
2016	40.2	214.3	18.8
2018	39.5	229.0	17.2
2020	35.1	213.1	16.5
2021	32.17	214.13	15.0

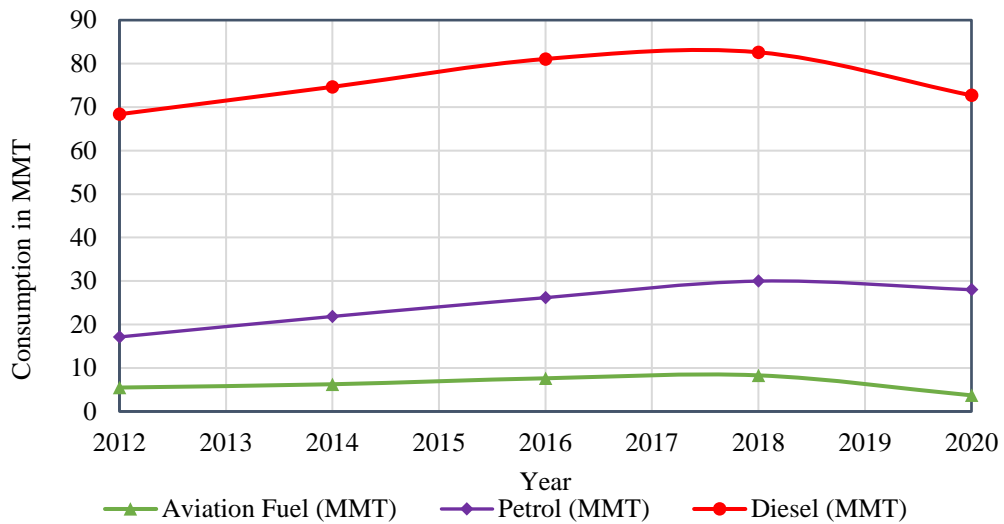


Figure 1.2. Trend of consumption of aviation, petrol and diesel fuel in India [2,6]

Figure 1.2 shows the increasing trend in the consumption of aviation, petrol and diesel fuel with each passing year [2]. However, a decline is observed in 2020, which, is due to the current pandemic situation (Covid-19), wherein the whole country was under lockdown. It also resulted in slight decrease in the percentage of air pollutants. However, this event is temporary. Once the earth is free from pandemic, the dependency on imported crude oil will further increase. Therefore, it is imperative to create sustainable and

alternative fuels that can replace fossil fuels and improve self-reliance in the energy sector [7].

1.3 Diesel Engine

Diesel engine is the most promising and prominent engine used in India. It is used in every sector, be it agriculture, power industry, automobiles, railways or shipping industry. Diesel engine develops good power, consumes specific fuel and is sturdy. Due to these salient features, it continues to dominate across sectors of India.

Due to the fact that diesel engines feed air into the cylinder, which is compressed to a high temperatures and pressures, they are also known as compression ignition engines. Then, diesel fuel is injected swiftly through nozzles in the fuel injector tip, where it atomizes into tiny droplets and combines with the compressed air already in the combustion chamber. After a brief delay caused by a few crank angles, combustion begins [8]. Diesel fuel is a fossil fuel made up of hydrocarbon compounds having higher molecular weights. During the spray of fuel from fuel injector significant pyrolysis takes place and leads to carbon-monoxide (CO) and unburnt hydrocarbon (HC) emissions. Sometimes locally lean mixtures lead to no ignition, no flame propagation, resulting in incomplete combustion. Diesel fuel's incomplete combustion is the main cause of particulate pollution. The emission rates are typically from 0.2g/km to 0.6g/km and 0.5 to 1.5g/brake kW/h in light duty and heavy duty vehicles respectively [8]. In diesel engines, NO₂ is usually found in between 10 to 30% of the total exhaust emissions[8]. All these emissions are hazardous for any life on the planet. These emissions can lead to various life threatening diseases. Apart from doing modifications on an engine or using devices to reduce emissions, which is a costly affair, the world is trying to explore an alternative drop-in fuel produced from renewable resources, which will be able to replace or at least lower the burden on fossil fuel, and is environmentally friendly.

1.4 Environmental Degradation

As mentioned earlier, tackling exhaust emissions from diesel engines is need of an hour. Enhancement in vehicle emission control system can reduce CO and NO emissions by 95% and 85% respectively if they are designed in that manner [9]. However, such designs lead to intricacies and surge in cost. That is why each country has put certain mandatory standards on emission regulations, which every automobile industry follows world-wide. Indian government is also coming up with stringent emission laws. BS-VI norms is applied from 1st April 2020 is one of the rigorous action taken up by the government.

Diesel engine is the most used engine on road, in industries, in power generation plants etc. Due to high efficiency of diesel engine than petrol engine, consumption of diesel is greater than petrol. However, it produces lot of exhaust emissions, which are very perilous for the environment and humanity. India stands at third position world-wide in PM_{2.5} concentration that is 51.9 $\mu\text{g}/\text{m}^3$ annually [10]. Increase in levels of exhaust emissions such as CO, CO₂, particulate matter (PM), oxides of nitrogen (NO_x), smoke, and soot have led to global warming, melting of polar ice caps, untimely season change, droughts, floods, increase in sea-levels, countless health problems and poor air quality index [11–13]. Energy security and reducing the carbon footprint is the need of an hour which has made researchers, environmentalist etc. to quest for an alternate fuel which is both viable and environment friendly [14].

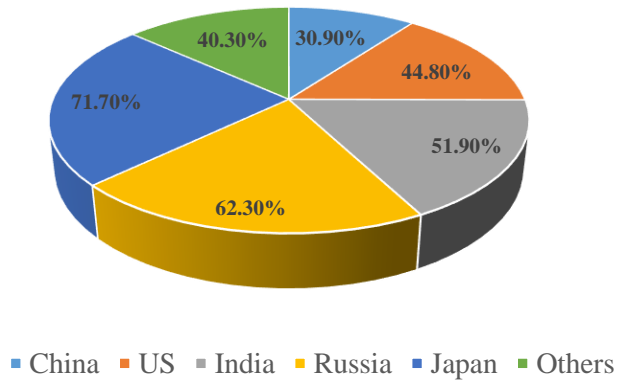


Figure 1.3. Carbon-dioxide emission (%) world-wide from fuel combustion

1.4.1 Alternative Fuels and its Effect on Exhaust Emissions

Alternative fuels derived from renewable sources like plant oil, animal fats, alga, lingo cellulosic biomass and waste cooking oil have played a major role in research and exploration of a viable solution to conventional fuel, Diesel. Since 1900, vegetable oil derived from various plants, has undergone a lot of research and different chemical processes.

Now a days third and fourth generation feedstock is used which usually consists of non-edible plant oil so that there is no struggle with the food crops. These feedstocks are minimalistic. They require less maintenance and can usually grow in all weather conditions. Some of these feedstock's can be cultivated on barren lands with minimum requirement of water. Non-edible content in biomass are as follows:

- Lignin: It is an intricate aromatic arrangement of molecules which is high in energy and does not allow any biochemical reactions to take place. It is usually in a range of 15 to 20%.
- Hemi-cellulose: Xylose is the second most abundant sugar in the biosphere [15]. It is usually in a range of 23%–32% but it has a marginal biochemical feed.

-
- Cellulose: In the biosphere, cellulose is the most prevalent type of carbon. It is a rich biochemical substrate and primarily a polymer of glucose. It is in the range of 38 to 50%.

Diesel and vegetable oil can be analyzed in terms of physiochemical characteristics like density and calorific value [16]. The flash and fire point of plant oil is high thus can be stored and handled safely. However, viscosity of vegetable oil (30 mm/s^2) is exorbitant and does not even lie within ASTM D range. The kinematic viscosity of diesel fuel is 3 mm/s^2 . High viscosity causes poor atomization, improper mingling of fuel and air that causes filter clogging, and heavy smoke. Volatility of vegetable oil is also low ensuing in poor thermal cracking and carbon deposition in a combustion chamber. They have low cetane number than Diesel. Vegetable oil also has a tendency to dilute lubricating oil and leads to formation of sludge. Therefore, it becomes necessary for a vegetable oil to undergo some chemical processes, which can reduce the viscosity and used as a transportation fuel. Several feedstock utilized for production of an alternative fuel are presented in Table 1.2 below. The fuel should be economically viable so that the dependence on oil imports can be reduced largely.

Vegetable oil is biodegradable, ecological, non-hazardous and energy efficient. Emissions produced from diesel fuel is hazardous but vegetable oil produces fewer emissions on combustion in diesel engine. Sulfur dioxide emissions are eliminated when vegetable oil is used in diesel engines because the oil is sulfur-free, resulting in less acid rain. It emits lesser CO_2 , CO and hydrocarbons, thus is environmentally friendly.

Table 1.2 Physiochemical properties of various feedstock used for an alternative fuel

Feedstock (oil)	Kinematic Viscosity at 40°C mm ² /sec	Cetane no.	Heating value (MJ/kg) approx.	Cloud Point (°C)	Pour Point (°C)	Flash Point (°C)	Density (kg /l)	References
Corn	35	38	40.5	- 1.1	-40	277	0.909	[17–20]
Cottonseed	34	42	40.6	1.7	- 15	234	0.915	[18,21]
Jatropha oil	38	51.1	38	9.0	3	235	0.920	[17,20,22,23]
Linseed oil	27	35	39	1.7	- 15	241	0.924	[18,24–26]
Palm oil	40	42	-	31.0	-	267	0.918	[27–30]
Peanut oil	40	42	40	12.8	- 6.7	271	0.903	[18,31–33]
Rapeseed oil	37	38	40.3	- 3.9	- 31.7	246	0.912	[34–36]
Sesame oil	36	40	39	- 3.9	- 9.4	260	0.913	[22,34]
Soybean oil	32	38	40	- 3.9	- 12.2	254	0.914	[37–39]
Sunflower oil	34	37	40	7.2	- 15	274	0.916	[18,40–42]

1.4.2 Jatropha Oil as a Potential Alternative Fuel

Governments from different parts of the world have campaigned to fulfil the diesel demand by concentrating on different renewable resources, owing to environmental concerns and a desire to lessen dependence on fossil fuels. Jatropha is thought to be one of the most suitable biofuel alternatives. There are 175 species of Jatropha in the Euphorbiaceae family [43]. It first originated in tropical America and since then has spread to Asia and Africa's tropics and subtropics [43]. More than 1,000,000 acres of Jatropha have been propagated over the world. About 85% of Jatropha is present in many Asian countries, such as India, Myanmar, and China. India is the world's largest producer of Jatropha. After reaching maturity stage, the Jatropha plant will tend to bear fruit for another 50 years [2]. From Jatropha fruit to making of Jatropha oil cakes as shown in Figure 1.4, everything is utilized.



Figure 1.4 Jatropha fruit, seed, shell and its various by-products [44].

The physiognomies of Jatropha seed oil are similar to that of diesel fuel [45,46]. Jatropha oil comprises of 35% - 45% of oil in its seeds, 50% - 60% of oil in its kernel [47-49]. It has 70 - 72% of unsaturated fatty acids (UFA) and 28 - 30 % of saturated fatty acids (SFA) [49]. SFA mainly includes 21% and 7.23% of Palmitic acid and stearic acid respectively, whereas, UFA comprises of 40% and 32% of oleic acid and linolenic acid respectively [49,50]. Jatropha seed contains toxic proteins namely, curcin and phorbol which makes it non-edible. It can be cultivated on barren lands with sufficient sunlight and low to medium rain showers. Jatropha oil cakes is used as a manure as it contains potassium, nitrogen and phosphorous which are good for plant growth containing all essential nutrients [23]. The leaves, twigs also help in increasing the microbial activity making it environment friendly. Planting more Jatropha trees can help in averting soil erosion, utilizing barren lands, small gestation period, pest resistance, low maintenance, cheaper, curbing emissions, controlling global warming makes it a suitable feedstock for an alternative fuel [23]. Some of the physiochemical characteristics of Jatropha oil and Diesel are shown in Table 1.3 below.

Table 1.3. Physio-chemical properties of Diesel and Jatropha oil

Properties	Diesel	Jatropha oil
Density at 15°C (g/cm ³)	0.840	0.920
Viscosity at 40°C (cSt)	2.41	52
Flash point (°C)	52 to 96	240 °C
Fire point (°C)	94	271 to 277
Cloud point (°C)	-5	8 to 10
Pour point (°C)		3 to 5
Cetane number	45 to 55	38
Calorific value (MJ/kg)	42	38.2
Auto ignition temperature (°C)	260	
Sulphur (% wt.)	0.149	0
Oxygen (% wt.)	0	11.06
Iodine number		94

1.5 Hydrogenation of Triglycerides based Biomass

Biomass is a renewable organic material that initiates from the plants and animals.

Triglycerides based biomass are usually edible, inedible plant oil, animal fats, microalgae etc.

Triglyceride is the prime component of oil. The biofuel is classified into Ist, IInd, IIIrd and IVth-generation fuels based on the obtainability of raw organic compounds. The first generation biofuels are made by extracting oil from food crops and further transforming them to biofuel [20,51,52]. However, there is a limit because it causes a scarcity of crops for human use and raises food prices. The second-generation include wastes from the plant which are not consumed by human-beings like straw, stem, twigs, leaves, dry leaves, shells etc. for e.g. Jatropha, Miscanthus as feedstock [53–56]. Second generation biofuels are not in race with foodstuff vegetation. Third generation biofuels are extracted from waste cooking oil, animal fats, algae etc. [51,53,57]. Algae has achieved a breakthrough as it can be converted into

petrol and Diesel but it has sustainability issues. Fourth-generation involves many new techniques which are still worked upon to curb the environmental pollution. These techniques include carbon-dioxide capturing and inserted into the underground reservoirs. This way it makes environment carbon negative.

Second and third generation biofuels are produced by undergoing transesterification process in existence of methyl alcohol and base catalyst which gives Fatty Acid Methyl Esters (FAME) called as biodiesel [20,53,58–60]. Biodiesel are a good source of plummeting various exhaust emissions from compression ignition engines like carbon monoxide (CO), oxides of nitrogen (NO_x) particulate matter (PM). However, biodiesel also has few disadvantages like high viscosity, poor cold flow properties, poor oxidation steadiness, corrosion of seals etc. Neat biodiesel cannot be run on CI engines. CI engines have to undergo the modification which is not possible in current scenario.

Although transesterification process is much-researched, in contrary hydroprocessing is attaining a lot of consideration amongst industrialists, researchers and academicians [20]. In hydroprocessing, plant oil or animal fat undergoes hydrogenation at a raised temperature and raised pressure along with an existence of a catalyst producing Renewable diesel, which is similar in its molecular structure to Diesel [20,61,62]. Due to its molecular structure the pipeline infrastructure laid down for Diesel can be used for Renewable diesel without undergoing any moderation [20,49]. Hydroprocessing is also termed as hydrogenation, hydro-deoxygenation (HDO), hydrodesulphurization (HDS), hydro-denitrogenation (HDN) to remove heteroatoms like sulphur, nitrogen, oxygen etc. These chemical reactions are used to convert triglycerides to straight carbon chain, alkanes. Other terms used for Renewable diesel are hydroprocessed vegetable oil [63–65], green Diesel [66–68], hydrogenated oil [69,70], paraffinic Renewable diesel [71,72] etc. Renewable diesel has high cetane number, better cold flow properties and almost negligible oxygen in its molecular structure [20,65,73,74]. Exhaust

emissions produced by combustion of Renewable diesel like CO, PM, NO_x and smoke are lesser than Diesel and biodiesel both [68,73,74]. Also, due to high cetane index of Renewable diesel, ignition delay (ID) is short [20,65].

1.6 Importance of Hydrogen and Methanol in Producing Biofuel

Methanol or ethanol is used to make biodiesel, whereas hydrogen is utilized to make Renewable diesel. Methanol may be made from a variety of renewable resources [75]. As a result, almost 95% of fatty acids with C-16 to C-18 atoms are derived from renewable sources [57]. The ratio of molecular weights of methanol to feedstock is kept at 6:1 [57]. It is mandatory to be vigilant on intake of H₂ in process of making of Renewable diesel [68]. Highly saturated vegetable oil require less quantity of hydrogen and unsaturated feedstocks are usually chosen for enhancing low temperature operation ability [57]. Hydrogen along with removing heteroatoms, also helps in converting unsaturated to saturated compounds. Due to Renewable diesel's similar molecular structure to that of Diesel, same pipeline infrastructure can be used, thus lowering the cost on engine modification [20].

1.7 Organization of Thesis

The thesis is divided into six chapters and its outline are enumerated below.

Chapter 1 deliberates about the energy scenario in India and its dependence on the fossil fuel is increasing with each passing year. It also brings about the urge to find an alternative fuel which can replace diesel fuel and reduce the carbon footprints to a great extent. It is shown that how second-generation fuel, especially vegetable oil has physiochemical properties at par with diesel and its advantages are discussed. Chemical mechanism of transesterification and hydroprocessing is discussed in brief. It shows how hydroprocessing converts vegetable oil into sustainable and suitable transportation fuel. The properties of hydro-processed fuel is at par with diesel and enhanced than biodiesel.

Chapter 2 elucidates an exhaustive literature review is done. Renewable diesel and its essential properties are discussed and compared with Diesel. The Renewable diesel production techniques are enumerated and the effect of its reaction temperature, reaction time and hydrogen pressure on the conversion efficacy of Renewable diesel is also discussed. Importance in choosing catalyst is also discussed. The various performance and emission physiognomies of Renewable diesel are enumerated. Research gaps, and objectives are also conferred.

Chapter 3 includes the procedure of the production of renewable diesel. Blend formation of different proportions is listed by mixing renewable diesel and diesel and ternary blends by blending renewable diesel, diesel and ethanol. The measuring instruments, specifications, accuracy, uncertainty, and working procedure are discussed. Also, engine set-up development and the test procedure is described.

Chapter 4 discusses the importance of catalysts in producing renewable diesel. It further includes the production and characterization of the noble metal catalyst, which is chosen for the present work to produce renewable diesel from Indian feedstock. It also includes the various results, comparison of physiochemical properties of blends. It also covers GC and FTIR respectively for renewable diesel and biodiesel. The engine test conducted on renewable diesel and its blends with diesel and ethanol are presented with the help of graphs. The best blend of renewable diesel and diesel were chosen, and ethanol was added to them in three proportions to study its effect on the engine performance. These findings are then thoroughly examined and compared to that of diesel. RSM technique is also used for renewable diesel, ethanol and diesel blends to optimize the various performance and emission characteristics.

Chapter 5 includes conclusion pointing out main findings from the research work and future scope.

Literature Review**2.1 Introduction**

Dr. Rudolph Diesel created an engine that bears his name, "Diesel engine," as it is the best option available globally for its exceptional fuel efficiency, high output, and reliability [32]. Since 1900, vegetable oil has been the best substitute for fossil fuel [49,76]. The French government and Dr. Rudolph Diesel, believed vegetable oil could be a fuel source to run initial diesel engines for agricultural applications, participated in the early research on an engine using neat vegetable oil as a fuel. [75,77–80]. Following Rudolph's demise, the diesel engine was created to be in accord with the characteristics of diesel fuel in order to operate properly [78]. Consequently, as time went on, the deterioration of the environment and the irresponsible use of petrol-diesel prompted the search for an alternate fuel. Due to the high viscosity, it is not possible to utilize vegetable oil in CI engines directly, so, vegetable oil undergoes various chemical processes to get converted into the transportation fuel. Some of those chemical processes are transesterification, pyrolysis, emulsification and hydroprocessing [49]. Hydroprocessing process is one of the processes which converts vegetable oil, animal fats etc. into n-paraffins and iso-paraffins fuel called as Renewable diesel. Renewable diesel has higher cetane number, higher heating value, better cold flow properties and better steadiness than other biofuels [20,81].

This chapter emphasizes usage and significance of diesel engine in India and discusses about the ongoing research in the field of alternative fuels, especially Renewable diesel produced from hydroprocessing. It also discusses the production technique for the Renewable diesel using different feedstock. A comparative analysis was done between much-researched biodiesel and newly introduced Renewable diesel. This chapter also enumerated the

performance, emissions and combustion for Diesel, Renewable diesel and biodiesel. The outcome of the exhaustive literature reviewed is also highlighted in the chapter. Finally, the research gap, problem statement and objectives of the research are outlined.

2.2 Hydroprocessing Unit

It is very imperative to acknowledge that hydrogen pressure, reaction temperature and selection of catalyst plays a pivotal part in making of a Renewable diesel. Usually a hydroprocessing element comprises of three sub elements as follows:

- a) Feed preparation
- b) Catalyst-feed reaction
- c) Separation of product

The process begins by first purging the hydrogen into first subunit so as to remove the presence of an oxygen if any. After that the selected feedstock is allowed to mix with hydrogen at a high pressure and high temperature and from there it makes a pathway to the fixed bed reactor where the mix is reacted through selected catalyst and product is formed. The product (mixture of both liquid and gas) formed is put into the last sub-element (separator) which separates gases from liquids [20]. Various gases that are separated are CO₂, CO, H₂S and unreacted excess H₂. Liquid is further sent for fractional distillation to obtain products like diesel, kerosene and naphtha [74].

2.3 Various Techniques Used for the Production of Renewable Diesel

Hydrodeoxygenation, esterification, hydrothermal liquefaction and catalytic hydroprocessing are some of the chemical reactions that a vegetable oil or animal fats undergo to produce a biofuel [82]. Figure 2.1 shows the catalytic hydroprocessing for both wet and solid biomass. As discussed in earlier chapter, Renewable diesel is gaining much attention. It can be produced by undergoing thermal conversion, biomass to liquid (BTL), hydroprocessing are some of the chemical processes used for production of Renewable diesel [20,74].

2.3.1 Hydroprocessing

In hydroprocessing triglycerides are reacted with catalyst in presence of hydrogen at an elevated temperature and an elevated pressure to yield Renewable diesel. The Renewable diesel produced is either a normal paraffin or branched paraffin with the molecular arrangement like diesel [20]. Feedstock that is used for either transesterification or esterification process, same feedstock is utilized for production of Renewable diesel. Hydroprocessing can follow three different trails which are: decarboxylation, decarbonylation or hydrodeoxygenation. All these three different pathways are explained in detail in section 2.4, below.

2.3.2. Thermal Conversion

Thermal conversion converts organic compounds such as waste oils from industries, sewage, sludges and domestic vegetable wastes into clean, environment friendly transportation fuel [83]. The reaction happens at raised temperature and pressure. It includes combustion, gasification or pyrolysis processes [84,85].

- a) Combustion: Combustion is a process in which feedstock or any biomass is burnt in presence of ample amount of oxygen and liberates heat. It gives out byproducts like carbon-dioxide and water which have more stronger bond energy and hence gives out more energy [86].
- b) Gasification: In this process, biomass is burnt in presence of insufficient amount of oxygen to liberate heat and the product is called producer gas. Producer gas carries combination of different gases like N_2 (46 to 51%), CO (17 to 23%), CO_2 (9 to 11%), H_2 (7 to 13%), methane (1.6 to 4.6%) [87,88]. Gasification of biomass uses less oxygen and takes place at lesser temperature with a catalyst [89]. In an absence of a catalyst, higher temperature is required, however the product formed is free from tar and methane gas. At a lower temperature reaction catalyst like dolomite, olivine,

nickel, Fe/Alumina etc. can be used to avert development of tar and methane. Moreover, the formation of coke deposits, reduces the catalyst activity [21,90,91].

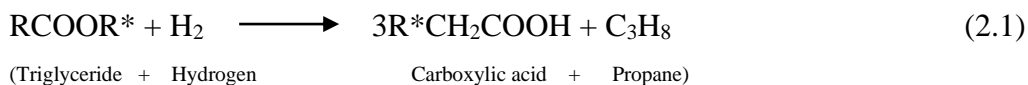
- c) Pyrolysis: In this process, biomass is burnt in absence of oxygen and produces pyrolysis oil and by-product as char [92]. When pyrolysis process is carried out at 500C and fast with vapour residence time as only 2 sec, it can yield pyrolysis oil in between 75 to 80%, syn gas 13 to 18% and char 12 to 17%. Pyrolysis oil is used to form additives in transportation fuel as well. It has more CV than feedstock. Moreover, pyrolysis oil has comparable molecular ratio to that of fossil fuels which is $H_2 : C = 1:2$ [89]. However its stability is a point of concern as it contains water and oxygen in its structure which can lead to corrosiveness and instability [93–95].

2.3.3 Biomass To Liquid (BTL)

BTL is known as two-step process where solid biomass under chemical treatment gets formed into liquid. In the first step, Fischer-tropsch process converts biomass to syngas ($CO+H_2$). Then in second step, this syn gas is polymerized to form hydrocarbon compounds which are similar to diesel in molecular structure called as Renewable diesel [68,85,96–98]. The biggest advantage of BTL technique is that it a plant's oil, cellulose, starch as well as sugar can be used in converting it to transportation fuel [68]. Liquid biomass undergoes follows different ways under catalytic treatment as cracking, saturation, heteroatom removal or isomerization processes.

- a) Cracking: Heavy weight hydro-carbon molecules under the impact of high pressure in presence of catalysts are fragmented down into lighter weight hydrocarbon molecules called as cracking [27,99–101]. Cracking is being performed on crude oil to get petrol and diesel on a commercial scale. Equation 2.1 below shows how a triglycerides under cracking when reacted with hydrogen produces carboxylic acid

and propane. In addition to this, the carboxylic acid can undergo pyrolysis as well as deoxygenation to produce Renewable diesel [68,102].



- b) Saturation: In saturation, unsaturated compounds and cyclic compounds are converted to saturated compounds and aromatic compounds respectively by breaking double bonds to single bonds in presence of excess quantity of H₂ [68]. Changing a double bond to a single one aids in decreasing oxidation and averting corrosion in engines. They also don't react easily due to their stable and less active nature. Under saturation, carboxylic acid produced via cracking can be converted to saturated compounds by removing oxygen in its molecular structure.
- c) Heteroatom removal: As the name suggests, elimination of heteroatom is done in this process to prevent the undesirable effect caused by the presence of heteroatoms like S, N₂, and O₂. These elements when undergo reaction can produce hydrogen sulphide, ammonia, water and can interfere in the oxidation stability and reduce calorific value of the fuel as well [68]. With formation of such compounds, it will affect the operation ability of an engine and reduce its efficiency. Equations 2.2, 2.3 and 2.4 represent various reaction mechanism used to remove heteroatoms.
- d) Isomerization: Isomerization is also called as branched paraffin. When unsaturated H-C compounds are converted to saturated H-C compounds, it improves its calorific value, oxidation stability, viscosity, density and cetane number in comparison to its original form (triglycerides). However these n-paraffin have decreased cold flow properties which is one of the important property which helps in running of an engine in extreme low temperature regions. With isomerization, although cetane number decreases but cold flow properties improves [20,41,68,73,103,104].

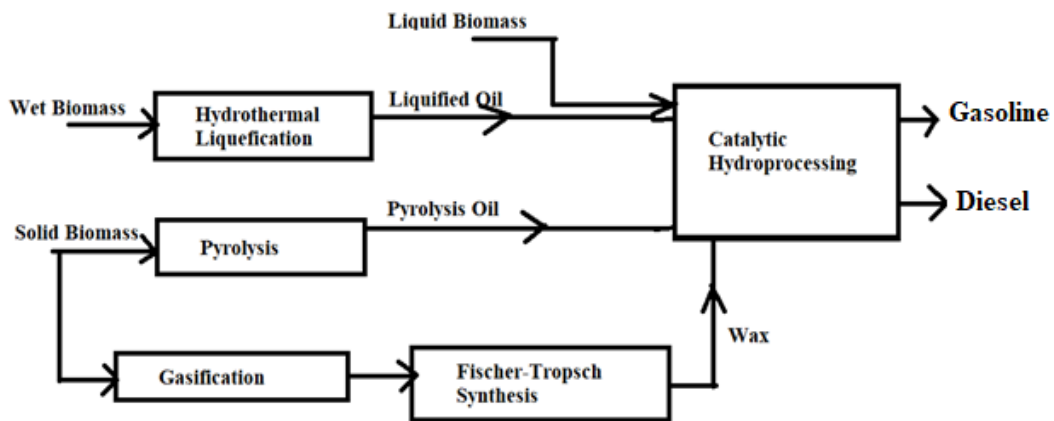


Figure 2.1. Catalytic hydroprocessing for organic transformation and progress to fuel [20,105].

2.4 Various Reaction Mechanism for the Production of Renewable Diesel through Hydroprocessing Technique

Feedstock are basically triglycerides are reacted at a high temperature, and pressure in existence of a catalytic agent to form Renewable diesel [106]. Molecular arrangement of R100 is similar to diesel as shown in Figure 2.2. As stated earlier, hydroprocessing is used in industries to remove heteroatom. Likewise from the Figure 2.2 it is clearly shown that with an addition of hydrogen, oxygen atom is removed making Renewable diesel more stable than other biofuels. Hydroprocessing can take place following three distinct pathways as follows:

- a) Decarboxylation (DCX): It forms saturated odd number of hydrocarbon compound with CO_2 as a by-product.
- b) Decarbonylation (DCN): It also forms a saturated odd number of hydrocarbon compound with carbon-monoxide and water as by-product on further addition of hydrogen ,and
- c) Hydrodeoxygenation (HDO): Saturated even number of hydrocarbon compound is formed with water as by-product.

Figure 2.2 below shows the reaction mechanism for different pathways followed in hydroprocessing.

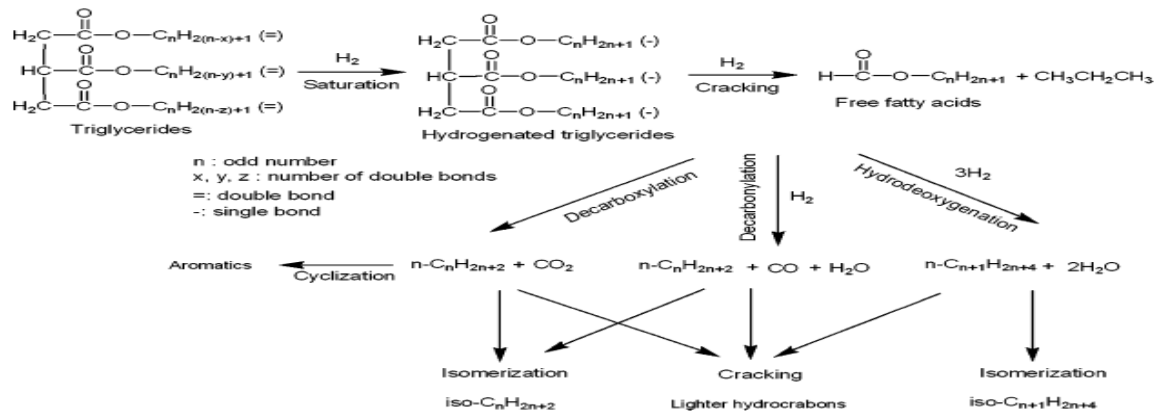
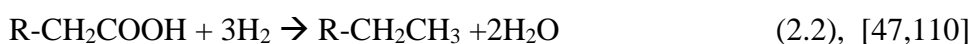


Figure 2.2. Different alleyways of triglycerides over hydroprocessing catalyst [20,64]

From the above mentioned three processes and the Figure 2.2 it is shown that oxygen is removed by following DCX, DCN or HDO reaction mechanism. Figure 2.2 clearly illustrates first triglyceride (any vegetable oil) is reacted in presence of hydrogen (6MPa-20 MPa) and temperature (250°C-450°C) to convert unsaturated compound to saturated compound by breaking double bond [35,64,107,108]. Then more hydrogen is added to carry out the cracking process. Cracking is usually carried out to reduce the hydrocarbon chain length and its boiling point falls in the range similar to that of diesel fuel. After cracking hydrogenated triglycerides is converted to free fatty acids (FFA) giving C_3H_6 as a byproduct. DCX, DCN or HDO can then be used to convert FFA into n-paraffins. These different pathways are illustrated in the form of chemical equations (eq 2.2 to eq 2.4) as below. Further isomerization, cyclization and cracking can form iso-alkanes, aromatics and lighter HC respectively [64]. N-paraffins obtained have high cetane number and good cold flow properties like cloud-point (CP), cold-filter plugging point (CFPP). When n-paraffins undergo isomerization, isomers are formed which have better CP and CFPP than n-paraffins but reduced cetane number [109].





By-products like CO₂, CO and H₂O which are produced during hydroprocessing can partake in methanation reaction and H₂O-gas-shift reaction. Methanation reaction consumes more hydrogen to form methane (CH₄) and water, thus being an expensive reaction mechanism. When the production of methane is almost negligible then the molar ratio of CO₂/CO displays an assessment for DCX and DCN reaction [64]. The reactions are shown below in equations 2.5 to 2.7.

Carbon-dioxide methanation



Carbon-monoxide methanation



Water-Gas shift reaction



Many researchers used various feedstocks following different pathway reactions. A. Srifa et al [70] hydroprocessed Palm oil under a nonstop stream in a fixed-bed reactor with working parameters as temperature (270°C to 420°C), hydrogen pressure (15bar-80bar), LHSV (0.25/hr to 5/hr), H₂ : oil (250 to 2000 N/cm³), concluded that HDO, DCN, DCX have their own optimized and limited conditions. When temperature was kept high and pressure low DCN and DCX were more prominent than HDO. Kikhtyanin et.al [41] worked on Sunflower oil and observed that with rise in temperature C₋₁₇ / C₋₁₈ ratio increased which concluded that DCN/DCX had a higher rate of reaction than the HDO reaction pathway. Guzman et al. [113] and Krar et al. [114] observed that when hydrogen pressure is low, HDO conversion from FFA to n-paraffins is not fully attained due to low molar ratio of C₋₁₇ / C₋₁₈, and C₋₁₅/C₋₁₆ in a Palm oil [115]. Also, Krar et al. [42] in their another research concluded from their

experiments that DCX and DCN are promoted and facilitated by a rise in the hydrogen:oil ratio. Oil conversion reduced as the WHSV increased, while the product yield rose was shown by Nimkarde et al. [55] in their study on Karanja oil. Bezergianni et al. showed in their experiments that the outcome of temperature and LHSV on the production quality of the used cooking oil and enumerated that moderate reaction temperatures and LHSVs lead to conventional fuel (diesel) like alternative fuel production and elevated temperatures and lesser LHSVs are supplementary for gasoline-like alternative fuel production [105]. Whereas, Yang et al. [116] argued that LHSV has no major role in the production of Renewable diesel following any of the reaction mechanism (DCX, DCN, HDO). Simacek et al. [117] showed in their work that when Rapeseed oil's reaction temperature was less than 310°C gives transitional products like FFA and little percentage of triglycerides.

Crude soyabean oil was hydrocracked over ZSM5 zeolite following three different reaction pathways. It was shown that HDO lead to the production of C-18 H-C chain from stearic acid (18:0) and C-15 H-C chain from C-16 fatty acids with water as major by-product. Due to deactivation of hydrocracking over NaZSM5, HDO was also affected with increase in fatty acids. [118]. Veriansyah et al. [64] did experimentation on hydroprocessing of soyabean oil. From their observation, it was found that catalyst like nickel-molybdenum (Ni-Mo), Cobalt-Molybdenum (Co-Mo) and Platinum (Pt) favored HDO reaction and Ruthenium (Ru, Nickel (Ni) and Palladium (Pd) favored DCX reaction. The highest yield of C-17/C-18 ratio was found for Ru/Al₂O₃ which was 39.6. NiMo was potent for HDO and SiO₂-Al₂O₃ provided the suitable acidity for isomerization or cracking of Jatropha oil [119]. Ni with base as Al₂O₃ yields only DCX H-C chain products [120–123] and Mo with base as Al₂O₃ yielded only HDO H-C chain products [77]. Whereas, Kiatkittipong et. al showed that with bimetallic catalyst NiMo and base as γ - Al₂O₃ showed DCX/DCN higher C-15 to C-16 ratio in the range of 4.8 to 5.8 due to deficiency of hydrogen in the feed [69].

2.5 Several Operating Parameters and its Consequence on Production of Renewable Diesel

Many researchers have shown that temperature, pressure and catalyst are pivotal for the making of Renewable diesel. Each parameter have their importance and are dependent on each other. Renewable diesel are the hydrocarbon chain having C-15 to C-18 carbon atoms in their structure with cetane number ranging in between 65 to 90. Many feedstock like Palm oil, Jatropha oil, Karanja seed oil, Rubber seed oil, Sunflower oil, waste cooking oil, Rapeseed oil, Soyabean oil have been used to convert them into Renewable diesel at temperature stretching from 250°C to 450°C and pressure from 1.5MPa to 20MPa under various catalyst like NiMo/ γ Al₂O₃, Pd/ γ -Al₂O₃CoMoS/ γ -Al₂O₃, Mo/Al₂O₃, Ni/Al₂O₃, NiMo/B₂O₃-aluminium oxide, sulfidedNiMo/ γ Al₂O₃, Pd/C, Mesoporous α -alumina etc [64,65,124]. The Table 2.1 below shows the various experiments conducted at different operating parameters by different researchers.

Table 2.1 Production of Renewable diesel from different feedstock at varying parameters

Feedstock	Operating parameters Temperature, Temp (°C), Pressure, Pr (MPa), LHSV or WHSV (h ⁻¹)	Catalyst utilized	Reference
Karanja Oil	Temp =300 to 380, Pr=1.5 to 3.5, WHSV=1.1 to 5; H ₂ /oil ratio= 400 to 600 v/v	Commercially sulfide CoMo and NiMo catalyst supported on Al ₂ O ₃	[55,65]
Jatropha oil	Temp= 320 to 420; Pr= 8; WHSV= 1 to 2	NiMoS catalyst supported on thermostable mesoporous silica doped titania	[125]
Jatropha oil	Temp= 200 to 350, Pr= 4, LHSV= 7.6	Ni-Mo/SiO ₂ -Al ₂ O ₃ ;	[119]
Jatropha oil	Temp= 300 to 400, Pr= 6 to 8, LHSV= 1-10, H ₂ :oil ratio= 1000 to 2000 lit/hr	Mesoporous α -alumina TMN/ α -Al ₂ O ₃	[126]
Sunflower oil	Temp: 280 to 380, Pr: 2 to 8, LHSV = 0.75 to 3, H ₂ /oil :400 to 600 Nm ³ /m ³	NiMo/Al ₂ O ₃ /F	[54]
Sunflower oil	Temp= 360 to 420, rP= 18, LFF (Sunflower oil) and H ₂ flow = 49g/h and 0.049 N m ³ /h respectively	commercial hydrocracking supported metal sulfides	[35]

Sunflower oil	Temp= 280 to 380, Pr= 3 to 8, WHSV= 1 to 4, H ₂ /oil = 250 to 400 N m ³ /m ³	Pt/HZSM-22 supported on Al ₂ O ₃ and Pt/SAPO-11	[114]
Sunflower oil	Temp= 310 to 360, Pr= 2, WHSV= 0.9 to 1.6, H ₂ /oil = 1000 N m ³ /m ³	Pd/SAPO-31	[41]
Palm oil	Temp= 350 to 450, Pr= 2 to 6, Reaction time= 0.25 to 5 hr	Commercialized 5% by wt Pd/C & synthesized NiMo/ γ -Al ₂ O ₃ ,	[69]
Palm oil	Temp= 350, Pr= 40 to 90, WHSV= 2, H ₂ /oil= 20 mol/mol	NiMo/ γ - aluminum oxide	[113]
Palm oil	Temp= 300 to 400, Pr= 3 to 6, H ₂ /oil molar ratio of 20:1	NiMo/ γ - Al ₂ O ₃	[67]
Rapeseed Oil	Temp= 310, Pr= 3.5, WHSV= 2, H ₂ /feed = 100 mol/mol	multiple grades of sulfide CoMo/ γ -Al ₂ O ₃	[127]
Rapeseed Oil	Temp= 310 to 360, Pr= 7 to 15, WHSV= 1.0, H ₂ /oil= 920 N m ³ /m ³	NiMo/Al ₂ O ₃	[128]
Rapeseed Oil	Temp= 260 to 280, Pr= 3.5, WHSV= 0.25 to 4.0	NiMo/Al ₂ O ₃ , Mo/Al ₂ O ₃ , Ni/Al ₂ O ₃	[120]
Rapeseed Oil	Temp= 260 to 340, Pr= 7, LHSV= 1h ⁻¹ , H ₂ /oil= 22 g h ⁻¹	NiO and MoO ₃ concentration in varying proportions	[129]
Rapeseed Oil	Temp= 260, Pr= 3.5, WHSV= 1 to 4, H ₂ /feed= 50 mol/mol	Sulfided NiMo/ γ -Al ₂ O ₃	[65,121]
Rapeseed Oil	Temp= 320 to 380, Pr= 4, WHSV= 1h ⁻¹ , H ₂ /oil= 240m ³ /m ³	Co-Mo / Al ₂ O ₃ +SiO ₂	[65,130]
Soybean Oil	Temp= 350 to 400, Pr= 1 to 20, batch process	NiMo/ γ - Al ₂ O ₃	[131]
Soybean Oil	Temp= 360, Pr= 14, batch	NiMo/ γ - Al ₂ O ₃	[132]
Soybean Oil	Temp= 400, Pr= 9.2, batch	NiMo/ γ - Al ₂ O ₃ , Pd/ γ -Al ₂ O ₃ CoMoS/ γ - Al ₂ O ₃ , Ni/SiO ₂ - Al ₂ O ₃ / γ - Al ₂ O ₃ , Ru/ Al ₂ O ₃	[64]
Waste Cooking oil	Temp= 350 to 390, Pr= 13.8, WHSV= 1.5, H ₂ /oil= 6000 scfb	commercial hydrocracking catalyst	[65,105]
Waste Cooking oil	Temp= 370, Pr= 8.27 to 9.65, H ₂ /Oil ratio= 543 to 890 nm ³ /m ³ , LHSV: 0.5 to 1.5 h ⁻¹	commercial hydrocracking catalyst	[102]
Waste Cooking oil	Temp= 300 to 350, Pr= 7, batch	NiMo /B ₂ O ₃ supported on Al ₂ O ₃	[133]
Waste Cooking oil	Temp= 330 to 398, Pr= 8.3, WHSV= 1.0, H ₂ /oil= 4000 scfb	commercial hydrotreating catalyst	[53,65]

2.5.1 Catalyst and its Effect on Production of Renewable Diesel

Catalyst involvement in producing a Renewable diesel is of a lot of significance. Selecting an appropriate catalyst in terms of its dynamic nature, supporter selection, stability, permeability and to handle the unsaturated vegetable oil for high yield of a transportation fuel is very important [134]. The catalyst selection's reduction rate and yield is also dependent upon the type of feedstock chosen for conversion to alternative fuel [111]. Other effective characteristics like temperature, pressure, LHSV, WHSV and H₂:molar ratio also effect the catalyst selection criteria [135]. Increased temperature can reduce catalyst activity which can be improved by inserting more hydrogen, but with increase in hydrogen concentration, chances of water formation gets increased. So similar things have to be taken into consideration while selecting catalyst for the experiments [68].

Catalyst is broadly classified into two terms:

- a) Noble metals
- b) Transition metals

Noble metal catalyst are very active and have thermal stability. Noble metals also help in oxidation of CO, HC and Nitrogen. However these catalysts are expensive and short-lived. Few of the frequently utilized noble metal catalysts are ruthenium (Ru), Palladium (Pd), Platinum (Pt) and Rhodium (Rh) etc [41,69,114]. Transition metal catalyst are not as much active as noble metals and have low thermal stability. Some of the commonly used transition metal catalyst are Cobalt (Co), Nickle (Ni), Molybdenum (Mo), and Tungsten (W) [63,77,113,121,136,137]. Transition metal catalyst can further be sub divided into two categories that is homogeneous and heterogeneous. Homogeneous are already listed above and heterogeneous are like NiMo, NiCo, CoMo etc. Out of these two sub-categories, heterogeneous catalyst are more active than homogeneous and can deoxygenate at a faster rate [120]. Since the reaction is taken in existence of a catalyst is an exothermic reaction so

the reaction temperature rises and coke formation takes place. Coke formation decreases catalyst activity and hence more hydrogen is to be supplied to keep the reaction in a working condition. However, addition of more and more hydrogen leads to the formation of water vapours which has an undesirable effect on activity and stability [68]. Various authors have pointed out many reasons for catalyst's deactivation like:

- a) Deposits of coke on catalyst surface due to exothermic reactions.
- b) Chemisorption of heteroatoms like Nitrogen and Sulphur.
- c) Sintering or a thermal action that causes clustering and a decrease in the surface:volume ratio of the catalyst. Usually, this causes the catalyst's structure to change, losing active sites.
- d) Decrease in strength of catalyst due to impregnation

So it becomes important to check the nature, temperature, consumption of hydrogen as well during hydroprocessing process to keep the activity of a catalyst high. As, replacing catalyst on each reaction can be a costly affair. It is the tendency of catalyst to undergo reversible or irreversible deactivation during hydro-de-oxygenation process [77]. As per Furimsky E [138] molybdenum carbides and molybdenum nitrides have capacity to adsorb, activate and transfer active hydrogen to the reactant molecule. Active hydrogen existing on catalyst surface decides the reaction rate for hydroprocessing mechanism. Reactant molecule's adsorption rate should be slower than hydrogen adsorption and active rate reaction [77]. Carbides and nitrides deactivate catalyst because of coke development which is not the case in sulfides [77]. However, sulfide catalyst are an unease to the environment. Coke formation is usually seen to be lower amid temperature range of 350°C to 375°C. Noble metals have a tendency to carry out reaction at lower temperature which will enhance the catalytic activity and increasing the conversion rate. Kikhtyanin et al. [41] performed experiment on Sunflower oil using Pd/SAPO-31 catalyst, temp. 310°C to 360°C, pr. of 2MPa with WHSV

as 0.9 – to 6 h⁻¹ to improve its low-temperature properties. Products formed were in the range of C₁₇ and C₁₈ with normal and branched paraffins. High initial reactivity for the hydro-conversion of Sunflower oil and good isomerization capabilities were shown by the Pd/SAPO-31 catalyst, although deactivation was seen after a few hours of procedure taking place. At a temperature of 360°C with high WHSV resulted a dip in iso-alkane/n-alkane ratio due to fast deactivation. This deactivation was due to the thermal action of the metal particles. The concentration of Pd was same before and after reaction, but the dispersion reduced to 11% from 50%. It was also concluded in their study that during de-carboxylation of dodecanoic acid over Pd/C catalyst and time-on-stream the fatty acids blocked the SAPO-31 acidic sites which prevented conversion of isomers from normal alkanes. Yanyong et al. [119] deoxygenated both fatty acids and triglycerides waste cooking oil over two different catalysts, sulfided Ni-Mo/Al13-Mont and Ru/Al13-montmorillonite. Sulfided Ni-Mo/Al13-montmorillonite showed slow deactivation in first 10hrs, after which it increased due to NiMoS collapse. Whereas, Ru/Al13-Mont showed no deactivation as it was on-stream for 72 hours and after specified time, there was no Sulphur found in WCO and gave a yield of 83.6%. Whereas, sulfided Ni-Mo/Al13-Mont yield decreased from 83.5% to 76.8% after 72 hrs due to deactivation of a catalyst.

Transition metal catalyst like sulfides of Ni, Co and Mo actively help in hydrodesulfurization, hydrodeoxygenation and hydrodenitrogenation. Reaction temperature in case of sulfides (hydrogen-sulfide and carbon di sulfide) range from 280°C to 350°C. Hydrogen consumed and coke deposition is less in case of H₂S. Senol et al. [139] in their work have shown that the conversion rate of methyl heptanoate increased with the increased concentration of H₂S from 67-76% on NiMo catalyst and 34-55% on CoMo catalyst. Similarly for ethyl heptanoate conversion was from 63 to 83% and 37 to 65% on NiMo and CoMo catalyst respectively. Whereas, CS₂ had not much effect on the conversion due to production

of coke. Kiatkittipong et al. [69] and Keng et al. [124] did experiment on three different types of oil, crude Palm oil (CPO), degummed Palm oil (DPO) and Palm fatty acid distillate (PFAD) to convert them to hydroprocessed fuel. CPO under the operating conditions of 400°C and 4MPa in presence of Pd/C catalyst gave maximum yield of 51%. They also observed that Pd/C was more active in nature than Pd/C than sulfided NiMo/ γ -Al₂O₃ for FFA. Removing of degummed from Palm oil can lead to more yield of 81% and at mild conditions of temperature 375°C and half an hour for reaction time. High acid content of waste cooking oil was hydrotreated on ruthenium catalyst supported on al-polyoxocation-pillared montmorillonite by Yanyong et al. and Young et al. [119,140–142]. Operating parameters selected were temperature 350°C, pressure 20 bar with LHSV as 15.2 h⁻¹, and hydrogen to oil ratio as 400 ml/ml. With catalyst Ru-SiO₂ improved pour point to 20°C and with addition of Al13-mont, it was further improved to -15°C and produced n-paraffins and iso-paraffins in the range of C15 to C18. Ru/H-Y was incapable of producing diesel like structure, however it produced gasoline like similar structure (C5 to C10).

Sotelo et al. [143] hydrotreated Rapeseed oil using noble metal with zeolite as support and transition metals with alumina as support, Pt/H-Y, Pt/H-ZSM and NiMo/ γ -Al₂O₃ [144]. It was concluded from their results that liquid hydrocarbon of highest yield was obtained using NiMo/ γ -Al₂O₃ catalyst with poor cold flow temperature due to its moderate acidic nature. Whereas, zeolite catalysts produced more of branched paraffins in the boiling temperature range of C₅ to C₂₂ [144]. Authors have also concluded that since transition metal catalyst have higher capacity to remove oxygen and have low cost, so they are mostly suited for converting triglycerides to hydro-processed fuel using hydroprocessing.

Commercial hydrocracking catalyst have been used by many researchers on Sunflower oil, Palm oil and waste cooking oil [35,102,145]. Daria et al. [130] evaluated the percentage of Rapeseed oil getting converted to n-alkanes using three different processes like hydro-

decarbonylation, hydro-decarboxylation, and hydro-deoxygenation with a commercial CoMo/Al₂O₃-SiO₂ hydrotreating catalyst. With rise in temperature, 320°C to 380°C, proportion of C₁₇ and C₁₈ increased from 16% to 28% by weight. Also, with increase in temperature, hydro-deoxygenation overpowered other two reaction mechanism. CoMo/supporter catalyst helped in dipping the quantity of monoaromatic and polycyclic aromatic hydrocarbons in the Rapeseed oil. Bezergianni et al. [102] performed similar experiment on WCO with three different commercial catalyst based on hydrocracking intensity. Catalyst A was hydrocracking catalyst, B was mild and third one was severe hydrocracking catalyst. Highest yield was seen for catalyst A. Catalyst B removed maximum heteroatoms and saturated 99% of unsaturated bonds. Catalyst C had low efficiency with more gases produced. Toba et al. [133] showed that Ni based catalyst are better than Co based catalyst for hydro-deoxygenation and converted 100% of WCO into hydrocarbon chain. The non-sulfided NiPTA/Al₂O₃ catalyst was developed by Liu et al. [146] for hydrotreatment of Jatropha oil. This catalyst was initially prepared by Ni/ Al₂O₃ and then it was further co-precipitated with impregnation of Ni/ Al₂O₃ with PTA solution. 98.5% of Jatropha oil was converted to green diesel at 360°C, 30bar and 0.8h⁻¹. It was inferred that non-sulfided catalyst are exceedingly active along with environment friendly. The carinata oil was hydrotreated by Zhao et al. [147] with Zn/Mo/ Al₂O₃ and only Al₂O₃. Hydroprocessed fuel that was produced with Zn and Mo on support with Al₂O₃ had lesser acidity than Al₂O₃ alone. Al₂O₃ with metal helps in hydro-deoxygenation mechanism and increases H-C content. For maximum yield Zn/Mo molar ratio was 2:1, beyond which the H-C content started to decrease as it led to deactivation of a catalyst. In presence of single transition metal catalyst like Ni or Mo, H-C conversion went from 30 to 80% from 260°C to 270°C. However when bi-metallic transition metal catalyst were take like NiMo, yield increased from 90 to 100% from 260°C to 270°C after one hour of reaction time [120]. Nimkarde et al. [55] hydroprocessed Karanja oil on a

sulfide CoMo/Al₂O₃ and NiMo/Al₂O₃ on a fixed bed reactor. It was observed from the studies that higher temperature and H₂/oil ratio made the conversion fast. At NiMo/Al₂O₃ 90.5% yield was obtained. Monnier et al. [148] prepared nitrides of Mo/Al₂O₃, W/Al₂O₃ and Va/ Al₂O₃ with ammonia for hydrotreatment by removing oxygen of Canola oil and oleic acid at a temperature range of 380°C to 410°C and 7.15 MPa pressure. Molybdenum nitride performed superior to W and vanadium in removing oxygen and converting oleic acid to straight chain alkanes. Decarbonylation and decarboxylation helped in deoxygenating oleic acid supported on Vanadium catalyst. Molybdenum-nitride produced 8times more octadecane to that of vanadium and tungsten nitride. Pomace oil was hydrotreated by using HZSM-5, FCC and CoMo catalysts. CoMo catalyst gave highest percentage of alkanes while FCC and HZSM-5 gave aromatic components [149].

Apart from nitrides, phosphide catalysts as well play vital part in improving the catalyst's action. Soyabean oil was hydro-deoxygenated (HDO) by using 25% of each Ni₂P/SiO₂, Ni₂P/H-Y zeolite catalyst by Zarchin et al. [150]. Ni₂P/H-Y zeolite showed an active inclination towards hydrocracking and isomerization. During HDO, water vapours were produced which hindered the activity of catalysts by reducing its acidity. 99.5% of oxygen was removed during HDO and Ni₂P/H-Y zeolite was found to be stable even after running for more than 250hours and producing 50% of light H-C compounds. Ayodele et al. [151] added fluoride to NiMoFO_x/zeolite catalyst to increase the surface area by increasing pore area and volume. Temperature 633K, pressure 20bars and 100ml of hydrogen/min was found to be optimized condition for producing n-octadecane (75%) and i-octadecane (23%).

Zeolites is used in converting triglycerides to saturated compounds. Li et al. [152] examined Meso-Y, SAPO-34 and HY zeolites. Meso-Y gave 53% of alkanes and 13.4% of aromatic hydrocarbon compounds. 40.5% was the maximum yield with Meso-Y at 673K from WCO. Jatropha oil was hydroprocessed using bimetallic NiMo and NiW supported on

mesoporous SAPO-11. Under 648 to 723K, 60 to 80 bars, 84% by weight liquid hydrocarbon compound was produced with 40% of kerosene and 20% of light-weight gasoline. It was also concluded that little variations in silica percentage in SAPO-11, catalyst remain unaffected during HDO of Jatropha oil [153].

Researchers have also studied model compounds and their effect on hydro-deoxygenation. Deliy et al. [154] used hydro-deoxygenation process using model compounds like methyl Palmitate and methyl heptanoate were used. CoMo/ γ - Al₂O₃ and NiMo/ γ - Al₂O₃ catalysts were used at temperature 573 K and pressure 35 bars. NiMo/ γ - Al₂O₃ gives higher conversion for C16 hydrocarbon chain. Decanoic acid, oleic acid, stearic acid, Palmitic acid and linoleic acid are some of the model compounds used by researchers. Snare et al. [108] Pd/C5 catalyst of weight 5% for temperature range of 573 to 633K and 15 to 27 bars was used for unsaturated fatty acid, and methyl oleate model compounds. Siew et al. [155] studied the morphology of two different SBA-15 having sphere-like and necklace-like structures which were created as supports for Pd. Pd diffusion on necklace-like SBA-15 was higher than sphere-like SBA-15 which further helped in substantial removal of oxygen.

Cotton seed oil underwent co-hydroprocessing in a trickle bed reactor at 30 bar and 578 to 618 K on sulphided CoMo/Al₂O₃ [21]. Catalyst was stable beyond 300 hrs. The authors discovered that the selectivity of diesel-like fuel was 91% and conversion efficiency was 90%. Activated carbon is inexpensive, has a large BET surface area, many pores, a low acidity, and allows for easy metal recovery from used catalyst [156]. Jatropha oil (5, 15, 25%) with gas oil was also co-hydroprocessed by Rajesh et al. [157] on CoMo/C catalyst and an increase in n- and i-paraffins was found and pure Jatropha oil was hydrotreated on mesoporous titanasilicate support. Blends of Sunflower oil and a gas oil was co-hydroprocessed and catalyzed on sulphided NiO (3%), MoO₃ (12%) - γ - Al₂O₃ with 0, 15 and 30 % of zeolite by weight and 100% conversion to H-C compound was obtained [63].

This literature review on catalyst has served an in-depth understanding of active metals, catalyst supports, promoters, catalytic activity, yield, selectivity in hydroprocessing of triglycerides and fatty acids. Acidic support and zeolites are favorable for hydrocracking and removal of oxygen. To achieve high selectivity using deoxygenation process on triglycerides and fatty acids, catalyst are incorporated high metal dispersion and moderate acidic support.

2.5.2 Temperature and its Effect on Production of Renewable Diesel

Like catalyst, temperature also has vital role in forming of products under hydroprocessing. Sunflower oil was hydroprocessed in the 360 to 420 °C range, producing hydrocarbon mixtures with a high concentration of saturated hydrocarbons and little aromatic content. The reaction temperature has a substantial impact on products' configuration. Authors concluded that when the reaction temperature was raised from 360°C to 420°C, composition of main hydrocarbon products of hydroprocessed Sunflower oil like n-alkanes (C₁₇ and C₁₈) dipped from 53 to 5% by wt. However, the product of hydro-processing at 420 °C included more than 5% by weight of aromatic hydrocarbons, but the percentage of aromatics in the products formed at 360 °C was negligible [35]. Catalyst sulfideTMN/ α - Al₂O₃ was used on Jatropha oil. With raise in temperature (300°C to 340°C), C₁₅ to C₁₈ hydrocarbon compounds increased [126]. Nimkarde et al. [55] in their work have shown that Karanja oil when hydro-processed on Ni/ γ - Al₂O₃ at a higher temperature of 653 K, 90.5% of oil conversion was reported. Bezergianni et al. [102] however concluded from their studies that with increase in reaction temperature the conversion efficiency decreases. At 330°C, 90% of conversion was obtained from WCO to n-paraffins. At the same time, it was observed by the authors that increased temperature favored removal of 99% of nitrogen and Sulphur. Bromine index decreased with increased temperature which further increases saturation of double bonds, however hydrogen consumption increased. Anand et al. and Jha et al. [125,126] both worked on Jatropha oil using sulfideTMN/ α - Al₂O₃ and CoMo respectively found that with

increase in temperature C15 to C18 hydrocarbon compounds were formed and at lower temperatures oligomerised compounds are formed. Kikhtyanin et al. [41] observed that decarboxylation or decarbonylation increases the C17-C18 ratio by increasing the reaction temperature and decreasing supply of feedstock oil on catalyst Pd/SAPO-31. Additionally, it was noted that i-paraffins reduced as temperature rose. For operating temperatures of 330°C to 350°C, it was revealed that the proportion of C17 to C18 H-C chain spanned from 75 to 80%.. Hancsok et al. [114] used Pt/HZSM-22/Al₂O₃ and at 350°C, isomerization of pre-hydrogenated sunflower oil was 100% converted. It was found in Kubicka et al. [120] experiments that Rapeseed oil was converted 100% into n-alkanes at 270°C and below 270°C, only 80 to 90% conversion was seen. Whereas, Simacek et al. [35] found similar results at 360°C with n-C17 and n-C18. Kiatkittipong et al. [69] also worked on pre-hydrogenated Palm oil and took three different categories like crude Palm oil (CPO), degummed Palm oil (DPO) and Palm fatty acid distillate (PFAD). They were studied under different operating conditions of temperature, pressure and WHSV. It was found out that CPO at 400°C and 40 bar gave a yield of 51%. For DPO, yield calculated was 70% and for PFAD diesel yield of 81% was calculated at 375°C. Pinto et al. [149] hydro-processed olive pomace oil at adequate temperature range of 300 to 430°C to produce H-C compounds. From their experiments it was concluded that olive pomace oil (OPO) without using any catalyst can have the conversion efficiency of above 90% by volume. With increase in reaction temperature to 430°C and reaction time, H-C conversion further increased to 99% by volume. However, authors also reacted OPO with different catalyst like CoMo/Al₂O₃, fluid catalytic cracking and HZSM-5. CoMo/ Al₂O₃ produced n-alkanes whereas, rest of the two catalysts produced aromatic compounds. Under the cracking reactions, they also observed the increase in Co and CO₂ gases by 30 to 40%. Srifa et al. [70] presented in their work that with rise in temperature, yield of Palm oil to hydrocarbons also increased from 270°C to 300°C. It was observed that

when Palm oil was hydroprocessed at 270°C, it started to solidify at ambient temperature due to the existence of some Palmitic and stearic acid. However beyond 420°C, it was also observed that the conversion percentage dipped to 37.9% from 89.8%.

Rajesh et al. [157] co-processed Jatropha oil with gas oil at various temperatures and studied their effect on the hydrocarbon compounds produced. 5, 10 and 20% of JO was taken in gas oil. Hydro-desulphurization was evaluated at three varying operating temperatures of 330°C, 350°C and 380°C. Amongst all these temperatures maximum removal of Sulphur was found at 350°C and beyond which the removal rate decreased. 40ppm, 124 ppm, 154ppm and 220ppm of sulphur proportion was in neat gas oil (GO), 5%, 10% and 15% of JO in GO respectively. Alike effects were obtained by Bezergianni et al. [109] co-processed WCO with heavy atm gas oil (HAGO) and operated it at varying temperatures as mentioned above. They also observed that at 370°C Sulphur elimination rate increased from 89% to 99.24%. However while using catalyst CoMo and 10 and 30% of WCO in HAGO, desulphurization rate reduced to 87.12% and 80.93% respectively.

Only saturation and heteroatom elimination occur when the temperature is low, but cracking also takes place when the temperature is high. On the same terms hydrogen consumed is less at lower temperatures. Bezergianni et al. [158] deliberated the temperature effect on the mixture of WCO and heavy gas oil (HGO). More hydrogen is consumed with increase in proportion of WCO in HGO as it helps in removal of oxygen molecule from the triglycerides and improves cracking activity. Boyas et al. [143] deliberated the outcome of temperature on hydro-cracking of Rapeseed oil from 300 to 400°C. At 350°C, product obtained was semi-solid. At temperatures 350°C, 375°C and 380°C, yield procured was 78%, 76% and 52% respectively. This drop was attributed to cracking of C₁₇ to C₂₂ hydrocarbons and developing of lighter chain hydrocarbons like C₁₃ to C₁₆. Rising temperature from 375°C to 400°C, further increased the formation of light hydrocarbon compounds.

2.5.3 Outcome of Hydrogen Pressure on Production of Renewable Diesel

Presence of hydrogen at high pressure in hydroprocessing is vital. Hydrogen helps in removing of oxygen and other heteroatoms from the feedstock which is to be converted into the fuel. At the same time, it is also very critical to check on hydrogen consumption. Pinto et al. [149] have hydro-treated olive pomace oil (OPO) at temperature range of 300°C to 430°C with the supply of H₂ pressure of 11bar initially. This hydrogen pressure led to the conversion of organic compounds in which hydrocarbons was in dominance. Without utilizing any catalysts, 90% by volume of hydrocarbons were produced. Nimkarde et al. [55] researched that hydrogen pressure whose involvement is pivotal on the hydrogenation process, isomerization mechanism and cracking of triglycerides. Feedstock selected was Karanja oil and hydrogen pressure was varied from 1.5MPa to 3MPa with catalyst like CoMo and NiMo. At 1.5 MPa using CoMo and NiMo catalysts separately conversion efficiency was found to be 60.1% and 62.1% respectively which further increased with 3MPa with CoMo and NiMo to 85.6% and 88.4% respectively. However authors brought this also to notice that with increase in hydrogen pressure, operating cost also increases. Yuhan et al. [159] hydrotreated C₁₈ fatty acid, octadecanoic acid (C₁₈:0 -Stearic acid, C₁₈:1 -oleic acid, C₁₈:2 -linoleic acid) along with impurities C₁₆ to C₂₀ at pressures 2 to 8MPa. At 3MPa C₁₇ yield dipped from 10.19% to 7.39% from 3MPa to 8MPa and for C₁₈ yield at 3MPa was 7.18% which increased to 10.68% at 8MPa. This decrease and increase in yield with rise in pressure is because, C₁₇ is obtained via HDCX or HDCN reaction mechanism and C₁₈ follows de-oxygenation reaction mechanism. This concluded that higher hydrogen pressure favour the HDO reaction mechanism. Alike outcomes were achieved by Sotelo et al. [143] which emphasized that n-C₁₇:n-C₁₈ yield ratios at various temperatures of 350°C, 375°C, and 400°C were 2.2, 1.6, and 1.5, respectively in a batch-reactor. This implies that with decrease in pressure decarboxylation and decarbonylation decreases. However Huber et al. and Simacek et al.

[129,160] have shown that yield of n-C₁₇ > n-C₁₈ at constant hydrogen pressure (7MPa) in a continuous reactor. Sotelo et al. [143] also concluded that in batch reactor hydrogen pressure decreases which leads to decrease in decarbonylation. Chen [161] in his work has shown that both temperature and pressure play vital role in formation of gaseous products but in an opposite way. With increase in pressure, gaseous products decrease, whereas with increase in temperature, gaseous products increase. It was also reviewed that increasing pressure reduces making of aromatic hydrocarbons, maximum diesel conversion was found at 40 bar by Kiatkittipong et al. [69]. Palm oil conversion increased with surge in H₂ pressure, whereas, pressure did not affect the diesel conversion in case of degummed pal oil and crude pal, oil. Reverse gas-shift reaction occurred at higher hydrogen pressure and led to good amount of CO which declines the active sites of catalyst. Fatty acids consume less hydrogen in contrast to degummed and crude Palm oil.

Guzman et al. [113] established that aromatic compounds were seen in maracuja and soybean oil at a higher pressure of 90 bars and none was located at lower pressure of 25 bars.. The reason for this is attributed to Palm oil's components like linoleic (C_{18:2}) and linolenic in the molar ration of C_{18:2} and C_{18:3} respectively. Whereas, maracuja and soybean oil contains 71% and 64% by wt. respectively. Bezergianni et al. [162] studied the efficiency of using three parameters: hydrogen:oil, pressure, and LHSV. Three tests covered a range between 82.7 and 96.5 bar were used to study hydrotreatment pressure, a crucial factor in hydrotreatment reactions. The highest production of 71.36 % for alternative fuel that resembles diesel is achieved at the maximum pressure. Additionally, when pressure rises, the output of fuel that is similar to diesel declines. Yield of 5.16% at 82.7 bar decreased to 4.03% at 96.5 bar. Additionally, as pressure rises, oxygen removal efficiency rises as well.

2.6 Characteristics of Renewable Diesel used in CI Engines

Fuel properties, performance, emission and combustion characteristics will be studied in this topic.

2.6.1 Physio-chemical Properties of a Renewable Diesel

Physio-chemical properties are important to know before any fuel can be run on an existing CI engine.

Renewable diesel is deliberated as drop-in-fuel as already mentioned in previous chapter due to its similar molecular structure alike diesel. The viscosity of Renewable diesel is more than diesel but much lesser than biodiesel [163]. From the various researches conducted the viscosity for Renewable diesel lies in between 3 to 4mm/s² which is at par with diesel as its value also lies in the same range [66,74]. It is imperative to have viscosity as per ASTM D445 standards, otherwise very less viscosity can lead to leakages from fuel pumps and can hence lead to malfunction of an engine in the longer run [163]. Higher viscosity means, higher surface tension which leads to lesser Webber number. Therefore, Renewable diesel has higher Webber number than diesel. Density is dependent of temperature. Bezergianni et al. [74] and Das et al. [164] and many other researchers have shown in their work that the density is measured at 15°C and some of them like Simacek et al. [128] and Koul et al. [49] have shown density to be measured at 40°C. depending upon the different feedstocks taken for conversion, the density of Renewable diesel was found in between 775 to 816kg/m³ [60,62,65,165].

Density of Renewable diesel is lesser than diesel which leads to more consumption of fuel for producing same output as while using diesel fuel [20,65,73,74]. Fuel quantity is raised by 3 to 6% for Renewable diesel [166,167]. Kuronen et al. [166] suggested that blending Renewable diesel with diesel can improve its density. Since Renewable diesel has more

hydrocarbons in its H-C chain, therefore its density is lesser than diesel. This Renewable diesel under hydroprocessing can form n-alkanes as well as iso-alkanes.

Straight-chain hydrocarbons have a high cetane number, whereas iso-alkanes or branched hydrocarbons have better cold flow properties [73,168]. A higher cetane number leads to lesser ignition delays and improves the speed of auto-ignition [76]. Since Renewable diesel is free from heteroatoms, so its cetane number ranges from 80 to 99 [49,66,74,76,81,163,169]. Sugiyama et al. [170] experimented on NExBTL to understand the effect on emission and performance characteristics. They also observed that spray characteristics for Renewable diesel and diesel were very similar.

Renewable diesel has enhanced cold-flow characteristics than both diesel and much-explored biodiesel spanned from -31°C to -6°C [49]. Hartikka et al. [171] and Knothe [76] have shown in their studies that cloud point (CP) can further be improved by isomerization which drops the temperature further to -55°C , but the cetane number decreases. Branched-chain hydrocarbons can flow better than n-alkanes. Simacek et al. [128] showed in their paper that Rapeseed when converted to Renewable diesel at 420°C , the cold flow characteristics were similar to the diesel. Alike outcomes were achieved by Pitz et. al [172]. Hydroprocessing done on sunflower oil using Pt/HZSM-22/ alumina by Hancsok et al. [114] showed a decline in cloud point from 23°C to -23°C . Bezergianni et al. [109] also showed that during the hydro-cracking process, by increasing temperature, isomerization is preferred.

Calorific value is another significant physico-chemical property of the fuel. CV of Renewable diesel is smaller than diesel but greater than biodiesel. Aatola et al. [173] conveyed CV to be between 42 to 47MJ/kg. Renewable diesel's CV is marginally lower than diesel but significantly superior to biodiesel [163]. This is because Renewable diesel has a better CV than biodiesel as during hydroprocessing oxygen is removed from the feedstock, improving its calorific value as well as oxidation stability. Al-Muhtaseb et al. [174] evaluated

CV of Renewable diesel using the feedstock as waste dates in presence of Pd/C and Pt/C catalysts which were 44.1MJ/kg and 43.8 MJ/kg respectively. Whereas Pinto et al. [149] showed in their paper that Renewable diesel produced from Crambe oil has CV of 40.6MJ/kg. Singh et al. [175] stated that due to the very good cetane index of Renewable diesel, it can also be considered a very good option for a cetane index improver for organic fluids.

These physico-chemical properties also help in determining the emission and performance parameters. Makinen et al. [71] stored hydro-processed fuel for 8 months and found it to be unaltered which confirmed oxidation stability. Few researchers have worked on the bulk modulus of fuel as well. Lapuerta et al. [176] showed that hydro-processed vegetable oil is less compressible and hence has a higher bulk modulus between 5MPa to 15MPa which is more than diesel.

2.6.2 Performance Characteristics of a Renewable Diesel

Renewable diesel has lesser density and lesser calorific value than diesel. During combustion, the heat released by Renewable diesel is 4 to 5% lower than diesel fuel. Also, due to less density the fuel intake is more for an engine with same specifications running on both diesel as well as Renewable diesel. The consumption of Renewable diesel is increased by 4% to 6% [166,167]. Some researchers have shown that the efficiency of a diesel engine operated on Renewable diesel was observed to be increased by 1% [72,173,177]. Due to higher cetane index of Renewable diesel, Sugiyama et al. [170] verified that the time taken for injection was 3 to 5% higher than that of diesel with working pressures of 40MPa to 200MPa. Additionally, they came to the conclusion that both diesel and renewable diesel had identical droplet sizes and spray angles. Crepeau et al. [96] results were also in synchronization with Sugiyama et al. [170] but for Gas-to-liquid fuel. Based on these studies conducted it was inferred by authors that despite 5% lesser energy content in the fuel there was no power loss, reason being higher ignition duration of Renewable diesel than diesel and

according to Bernoulli's equation, fuel flow rate is inverse proportion to square root of density [72,96,167,170].

Ogunkoya et al. [178] have verified from their experiments that isomerized Renewable diesel when produced from Canola oil undergoing deoxygenation had potential to replace diesel fuel. At BMEP of 1.26 bar had a mechanical efficiency of 59.8% which is just 3.2% lesser than diesel. Also, the pressure inside the cylinder was high with rising load on an engine. Kim et al. [179] tested sixteen different kinds of fuels. The samples consisted of iso-alkanes, biodiesel and diesel. 1.5 lt of engine and passenger car was used for conducting experiments. Minimum power loss was seen with iso-alkanes and diesel blends and maximum loss was evaluated in case of bio-diesel and diesel compositions. With increase in proportion of alkanes or iso-alkanes with diesel, BSFC decreases and for the same conditions BSFC increased for diesel and biodiesel (BD) blend. The reason for this is accredited to the H-C chain of n- and iso-alkanes which is from C-15 to C-18. Fuel efficiency of n-alkanes and iso-alkanes blended with diesel was far superior than BD+diesel compositions due to nonexistence of oxygen atoms in their molecular arrangement [74,170,179–181]. It was shown by Sugiyama et al. [170] that by advancing injection rate of fuel at a low load of 32Nm and 110Nm, BSEC decreased and optimized value was obtained at -4° after TDC and $+6^\circ$ after TDC respectively. Also, fuel consumption of Renewable diesel at low and medium load decreased by 4.3% and 5.3% respectively. Due to HRD's higher CV by 14% in comparison to BD, it showed lesser BSFC [182].

Kumar et al. [61,65] worked on spray mean diameter (SMD) of diesel, hydro-processed vegetable oil (HVO), and their blends. SMD of HVO is 20.4mm and Diesel is 16.1mm. The experiments resulted that with rise in proportion of HVO in a blend, SMD also increased. Due to lower CV of HVO, heat release rate was lesser by 4 to 15% than diesel which also resulted in lesser cylinder crowning pressure. This further led to lower BTE and

more BSEC. For hydrotreating fatty acids produced from Canola oil, both a batch technique and a continuous process were used by Ogunkoya et al. [178]. At 12.6 MPa, the most effective brake thermal efficiency is found in biodiesel, and there was a drop of 8% in Renewable diesel prepared from batch procedure. At higher pressure of 3.77 bar, Jet fuel efficiency exceeded Renewable diesel's efficiency by 5%. Caprotti et al. [183] performed test on Toyota truck using 5% BD and different proportions of iso-HVO in diesel. Fuel consumption drops as the percentage of iso-HVO rises. Due to isomerized HVO, the startability in cold regions was found to be at par with diesel. It was recommended by authors to use 20% of HVO in diesel to improve the cold flow properties. Miller 50 and Miller 70, advanced valve timings were tested upon HVO by Imperato et al. [184]. NO_x reduced by 3% and fuel was conserved by 5% by mass. When Miller timing was kept at 50° CA and scavenging angle was -30° CA, the fuel consumed was similar to the base timing of 15°CA and at scavenging of 60°CA. Reducing scavenging angle by -45°CA leads to increase in consumption of fuel by 230g/kWhr. Fuel consumption increased by 13% when Miller timing was 50°CA and negative scavenging, however emissions remained same. Hartikka et al. [171] also concluded that spray angle for HVO and diesel is similar by running heavy duty engine and passenger car on neat HVO. For BD and diesel blends many researchers have suggested to use higher carbon chain alcohols which help in lowering down the flash point and hence helps in reducing long ignition delays [169,185,186]. Mattson et al. [36] stated during pre-mixed combustion phase, Renewable diesel released lesser heat rate than diesel, however with increase in load that is during diffusion combustion phase more heat was released which helped in kindling the fuel-air mixture sufficiently. Caton et al. [187] have shown in their experiments on turbocharged CI engine which was fuelled with HRD produced from algae that at varying rpm and load conditions, the combustion duration (CD) showed an increase of 1.5 deg CA from 0.5 deg CA with respect to fossil fuel. Comparable results were acquired from algae HRD by Petersen et

al. [188] on DI-2-S marine diesel engine. The cause for this was credited to lesser and longer pre-mixing and combustion duration respectively due to shorter ignition delay. Aatola et al. [173] and Gomez et al. also obtained extended combustion duration and credited this to lack of aromatic compounds, lesser oxygen and shorter ID.

2.6.3 Emission Characteristics of a Renewable Diesel

Controlling emissions have become a major challenge for all researchers. Finding a suitable and sustainable fuel which is environment friendly is something researchers are researching for tirelessly. Kim et al. [179] in their study have shown that paraffins and iso-paraffins emit lesser THC and CO harmful emissions than that of biodiesel. With 50% of iso-paraffin, paraffin and BD with diesel showed reduction in particulate matter than neat diesel. However NO_x was higher at full load conditions for all blends than diesel. Ogunkoya et al. [178] represented that due to Renewable diesel's better ignition qualities like shorter ignition delay, lack of aromatic and better calorific value leads to complete combustion which in turn leads to lower carbon-dioxide, carbon-monoxide, NO and smoke opacity. However HC emissions are slightly on the higher side. Hartikka et al. [171] have shown decrease in HC emissions as well along with NO_x, CO and PM. They have attributed the reason to H:C ratio, higher cetane number along with absence of aromatics in H-C chain. Due to lesser carbon atoms in relation to hydrogen leads to lesser flame temperature and hence quenching in combustion chamber leads to lesser NO_x formation than diesel fuel. They also attributed lesser NO_x to exhaust gas reheat system, diesel particulate filter, and oxidation catalyst installed in a CI engine on which experiment was conducted. NO_x and PM emission was reduced by 2% and 39% respectively. Sugiyama et al. [170] shown in their study that by advancing rate of injection at lower load of 1400rpm, 32N-m and injection pressure of 50MPa) HC and CO emissions did not surpass the setting point for diesel and smoke opacity did not worsen. With medium load of 2000rpm, 110N-m and 100MPa injection pressure, optimum value was

obtained at $+6^\circ$ after TDC and HC, CO did not worsen. Singh et al. [182] observed that Renewable diesel produced from Jatropha methyl ester and Rapeseed methyl ester had lesser NO_x in comparison to the base biodiesel. Singh et al. [182] Emission results obtained authors showed decrease in PM, HC and CO emissions when CI engine was run on hydro-processed Renewable diesel (HRD) and BD. However there was a rise in NO_x emissions. NO_x was 29% more in BD than HRD and PM more by 27% for HRD than BD. With rise in the engine load, CO and HC decreased but NO_x increased. Kumar et al. [61] have concluded from their work that hydroprocessed fuel obtained from WCO and a blend of D70H30 (70% of Diesel and 30% of HVO) is an enhanced combination to substitute diesel in CI engine. HC and CO emissions reduced till H30, after which it started to increase. At all loads, NO and smoke was lesser than diesel because of the existence of small quantity of oxygen which helped in complete combustion and lowered combustion temperature. Imperato et al. [184] performed test on HVO by using Miller timing technique which helped in reducing NO_x by 3% and smoke was reduced to 0.06 from 0.18. Along with advancement of crank angle, scavenging angle was also mottled. If Miller timing (MT) is increased from 30°CA to 70°CA then ignition delay becomes longer by 3°CA which gives more time for mixing/combustion and thus increasing peak pressure of cylinder which is as high as four times to that of the base line. Due to creation of high pressure, high temperature spots are created which can lead to increase in NO_x emissions. For lesser NO_x emissions, Miller timing was decided as 50°CA with negative scavenging angles, however fuel consumption increased.

Hartikka et al. [171] studied the technical specifications of HVO on heavy duty vehicles. From their study, it was concluded that running CI engine on neat HVO reduces NO_x by 95, particulate emissions by 32%, and carbon-monoxide emissions by 255 and hydrocarbon emissions by 31%. Whereas, using same fuel in passenger cars helps in reducing NO_x by 2% PM by 39% and other unfettered emissions were also reduced. There was no

clogging or any chemical instability seen while using HVO in an engine. Due to lower viscosity of Renewable diesel and its run carried over NEDC, it showed reduced emissions in comparison to BD working on same conditions [189–191]. As per study done by Singh et al. [62], they concluded that HRD when run on a CI engine showed reduction in fuel consumption by 17% and increase in BTE by 10%. Many researchers have shown that NO_x emissions either rises or dips. It was concluded that only cetane number is not the factor that can show reduction in NO_x however, oxygen present in the molecular arrangement is also one of the reason. Karavalakis et al. [192] and Devendra et al. [62] conducted experiment trial on a Cummins ISX15 vehicle with 400 hp engine (2014 model) and on a Cummins ISB6.7 vehicle with 220 HP engine (2010 model) [62]. However a 43% of reduction was seen in particulate matter. The particle size of Renewable diesel was evaluated as 23% lesser than diesel. Due to good reactivity of Renewable diesel at lower temperatures, which improves the diesel particulate filter's (DPF) ability to regenerate.

2.7 Summary

From the exhaustive literature review, the subsequent major findings can be drawn:

- Renewable diesel actually works as a drop-in fuel, meaning that it can work on an existing CI engine without any modifications and existing pipeline infrastructure can be used without causing any operational problems.
- Reaction temperature, hydrogen pressure, and catalyst play a vital role in the diesel selectivity. A higher reaction temperature causes the products to crack, which further lowers the diesel selectivity. Higher hydrogen pressure reduces the gaseous products formation but it inhibits the isomerization. Catalytic hydro-treatment of liquid biomass leads to higher calorific value, paraffinic nature, better oxidation stability and non-corrosive in nature.

-
-
- Mild-hydrocracking leads to higher cetane index of the products formed but at the same time it deteriorates cold flow properties as products formed are n-alkanes instead of i-alkanes. Because of high cetane number of renewable diesel, combustion starts more quickly under low and medium loads than under high loads. A high cetane number enhances cold starts and lowers smoke, noise, and emissions percentage.
 - Adding smaller quantity of vegetable oil to petroleum feedstock for co-hydroprocessing can increase the production of fuel products and some of their attributes.
 - Higher LHSV helps in improving the isomerization. Iso-Renewable diesel blended with diesel has higher cetane value, calorific value, and oxidation stability than BD or Renewable diesel.
 - Due to the lower density of renewable diesel compared to diesel, fuel consumption rises by 3-6%.
 - The intake of hydrogen increases along with the ratio of hydrogen to oil. Efficiency of conversion diminishes as the hydrogen to oil ratio rises.
 - Spray characteristics which are fuel permeation, for both Renewable diesel and diesel, the droplet size and spray angle are nearly identical.
 - Due to desired physio-chemical characteristics but low acidity, acidic support materials such as ZrO₂, TiO₂, and zeolites are favoured over basic and neutral support materials. The most popular active metals, however, are noble metals like palladium and platinum and transition metals like nickel, molybdenum, and cobalt. Bimetallic complexes also often exhibit increased activity for hydro-deoxygenation at lower reaction temperatures.
 - A reduction in particulate matter, NO_x, HC, CO, smoke opacity and unregulated emissions was observed for heavy duty and light-duty vehicles. Also, oxidation stability of Renewable diesel was far better than FAME.

2.8 Research Gaps

Based on the exhaustive literature review, subsequent research gaps were enumerated.

- Only Soybean, Karanja, Rapeseed, Palm oil and waste cooking oil have been extensively used for producing Renewable diesel using hydro-processing technology. There are many other vegetable oils that are yet to be explored.
- Existing catalyst are used for commercial heteroatom removal which are less effective for hydroprocessing of biomass-based oils.
- Water vapours generated during a hydro-deoxygenation reaction at a high temperature decrease the catalyst's activity, longevity, and selection.
- Work on testing of fuel for vehicle application is limited, most of the work done is based on New European Driving Cycle (NEDC) with limited vehicles in comparison to the engines used for agriculture.

2.9 Objectives

The following research objectives are envisaged for the current research work.

1. Selection of a suitable Indian based feedstock vegetable oil for the production of Renewable diesel.
2. Selection of appropriate catalyst for the hydroprocessing.
3. Study of effect of various parameters that is reaction temperature, hydrogen pressure on diesel selectivity.
4. Production of Renewable diesel using the parameters such as temperature, pressure and appropriate catalyst.

-
-
5. To check the storage stability.
 6. Determination and analysis of the physicochemical properties of the Renewable diesel produced and blends of Renewable diesel, diesel and ternary blends of Renewable diesel, diesel and ethanol and compare the results with the diesel.
 7. Determining and exploring a diesel engine's performance, combustion, and emission characteristics while using the produced renewable diesel as well as binary and ternary blends.
 8. Response Surface Methodology is used to optimize fuel blends and engine operating conditions for optimal performance and emission characteristics.

SYSTEM DEVELOPMENT AND METHODOLOGY**3.1 Introduction**

The chapter elucidates all the steps executed to carry out the research in a proper methodical way as highlighted in preceding chapter of the problem statement section. Figure 3.1 below gives the summary of research work carried out in a flowchart.

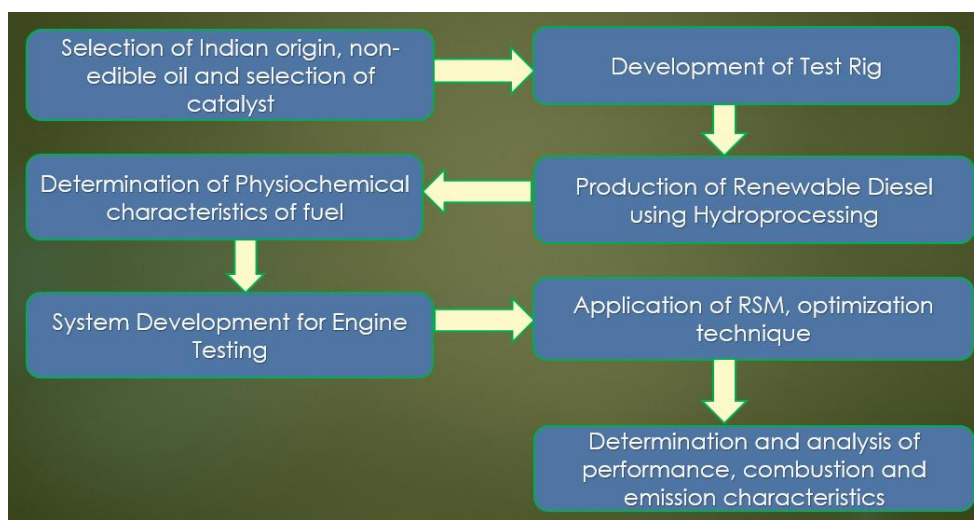


Figure 3.1. Research Methodology Flowchart

The flowchart shows that based on literature survey, Indian origin, non-edible feedstock was chosen to undergo hydroprocessing. A noble metal catalyst was selected to carry out the hydroprocessing at an elevated temperature and pressure in high pressure stirred reactor (HPSR) to obtain Renewable diesel and its characterization was elucidated. The production and characterization of biodiesel is also explained. Moreover, the characterization of catalyst was also studied. Various physiochemical characteristics were found out and compared to conventional fuel, Diesel. The storage stability of Renewable diesel was tested for twelve months and is discussed in detail. Several fuel samples were made by mixing Renewable diesel and Diesel and ternary blends were also formed by mixing ethanol with Diesel and Renewable diesel and were tested on developed CI engine test rig for their

performance and emissions. The blend was optimised using the Response Surface Methodology (RSM) optimization method, which can produce results that are optimal in terms of emissions and performance. In the end, accuracy and uncertainty of all equipment used for experimentation purpose is also discussed.

3.2 Selection of Vegetable Oil and Catalyst

Jatropha curcas belongs to a family of Euphorbiaceae. Jatropha curcas was chosen for the present work due to its various advantages of being cultivated on barren lands with minimum water requirements. Its by-products like straw, husk, twigs, leaves etc can be used as a manure. It can be easily grown in Indian environment. It contains 72% of unsaturated fatty acids (UFA) and 28.23% saturated fatty acids (SFA) [49]. For the present work ruthenium was selected as a catalyst. Ruthenium is a noble metal [119,144,193]. Ruthenium is effective than nickle-copper supported alumina, copper-molybdenum supported alumina, nickle - molybdenum supported alumina etc. Little work has been performed on Jatropha oil and ruthenium (Ru) combination. Since ruthenium is a noble metal so, it is pricier but it has an advantage of carrying out reactions at a lower temperature which usually does not happen in case of other base catalyst, nitrides or sulphides [23,68,134]. It also saves on time of chemical reaction process. On commercializing ruthenium on a larger front will help in reducing the cost of fuel production with substantial profits.

3.3 Preparation of a Catalyst

As already discussed in section 3.3 about ruthenium catalyst and its advantages. So, in hydroprocessing of JO, catalyst preparation was done using wet-impregnation technique. This technique is used for heterogeneous catalyst as it is simple and cost effective. Three different aqueous solution of cerium nitrate hexahydrate (5gm) mixed with 15 ml of distilled H₂O, manganese acetate (0.274gm) mixed with 50ml of distilled H₂O and ruthenium chloride (0.248gm) mixed with 50 ml of distilled H₂O were prepared. These solutions were poured

drop-wise over support of calcined alumina (5gm) to make it totally wet. This support obtained was then dried at 100°C into a solid substance, which was further calcined for 180 minutes at 500°C. The support included 5% each of cerium and magnesium and 2% of ruthenium of the catalyst weight. For hydroprocessing process, the catalyst prepared was first activated under hydrogen pressure of 2 bar at 200°C for 180 minutes each time.

3.4 Production of Renewable Diesel using Hydroprocessing

Renewable diesel was produced with the help of High Pressure Stirred Reactor (HPSR) of Amar equipment. It consisted of a batch reactor in which reactants like Jatropha oil and catalyst was kept. It had a capacity of 100 ml. Reactor had a capacity to withhold the temperature till 500°C and pressure up to 100 bars. It has a heater temperature controller that goes up to 500 °C and an electrical ceramic band heater with insulation and coating. The reactants will be stirred inside the reactor with the help of a four bladed turbine stirrer. It has a programmable Proportional Integral Derivative (PID) SS controller, alarm for an elevated temperature and motor speed controller. Water was allowed to flow through a spiral cooling pipe so that temperature could be regulated. The picture and the line diagram of the HPSR is shown below in Plate.3.1 and Figure 3.2 respectively.

In the present work, cerium (Ce) and manganese (Mn) promoted catalyst containing ruthenium (Ru) was selected. Ru was supported on aluminium oxide (Al₂O₃) as a catalyst. In a reactor vessel, 20 gm (w/w) of Jatropha oil (JO) was mixed with 0.40 gm of catalyst which was 0.02 times the weight of JO. Reactor was tightly sealed and nitrogen (N₂) gas was purged into the vessel so as to prevent any chemical alteration due to oxygen present inside the reactor. Then hydrogen (H₂) gas was supplied and kept constant at 4.5 MPa with the supply of heat until the temperature reached 320°C. The reaction time was 3.5 hours. As soon as the chemical reaction was over, vessel was permitted to cool down to the surrounding conditions. Gases were released by slowly opening the valve. Reactor was opened and the liquid called

as Renewable diesel was collected in a beaker and was filtered and weighed. Reactor was cleaned with an acetone. Renewable diesel then underwent fractional distillation following the ASTM D2892 and 5236 standards. Renewable diesel's boiling range was found out to be in between 190 - 360°C.

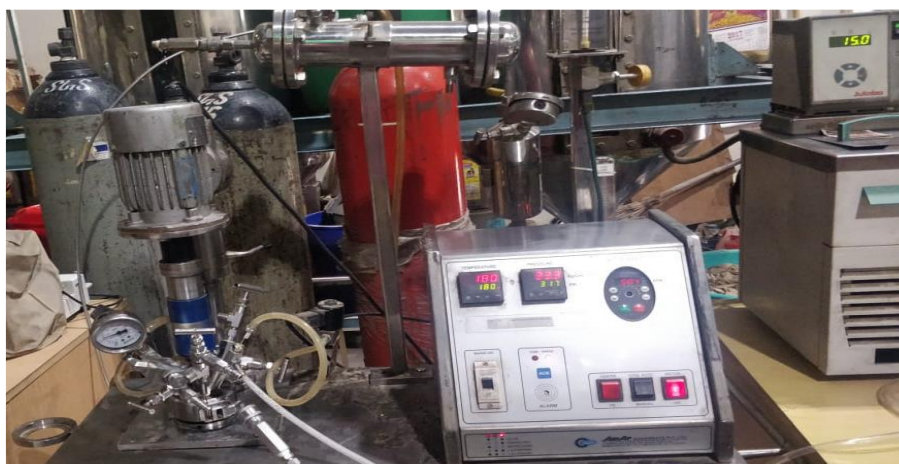


Plate. 3.1. Experimental set-up for Renewable diesel production high pressure stirred reactor (HPSR)

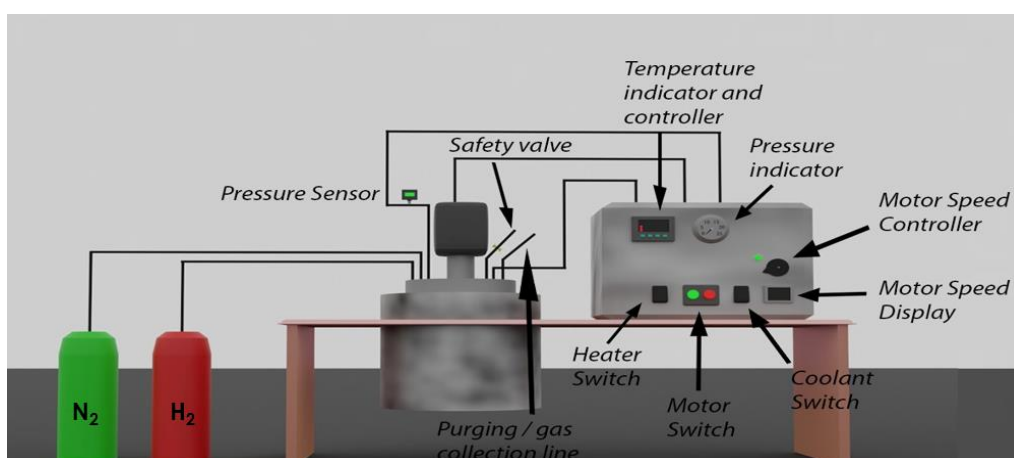


Figure 3.2. Schematic diagram of HPSR

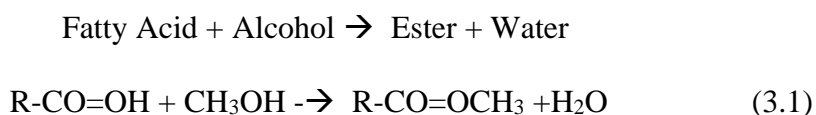
3.5 Production of Biodiesel

For the present work, JO was accessed from 'Gobind Machinery Works', New Delhi. It has fatty acid upto 13.2%. Due to JO's higher fatty acid content, first esterification process and then transesterification process was conducted for biodiesel production. During

esterification process, JO was mixed with KOH and H₂SO₄ to reduce free fatty acid below 2% [194].

3.5.1 Esterification of Jatropha Oil

In the first stage JO was heated at 120°C for an hour to remove any water content in oil. After this JO was cooled down to 60°C. To reduce free fatty acid content to 2% and to avoid saponification, p-toulene sulphonic acid (PTSA) is mixed with 20% (w/w) methanol (CH₃OH) in a different beaker to obtain the catalyst concentration of 0.5% (w/w). The catalyst prepared was added to the solution of Jatropha oil and CH₃OH which was heated at 60°C for about two hours on a hotplate magnetic stirrer. The chemical equation of esterification process is shown in equation 3.1



3.5.2 Transesterification of Esterified Jatropha Oil

Esterified Jatropha oil and CH₃OH was taken in 6:1 ratio. This molar ratio of esterified oil and methanol was mixed with 0.5% concentration of sodium hydroxide (NaOH). The solution was covered and heated on magnetic stirrer at 60°C for 45 minutes till a clear layer of glycerol is visible at the flask's bottom. The resultant solution was placed in a separating funnel and allowed to sit for 24 hours. By-product glycerol was settled at the bottom and was then removed. The remaining solution was the Jatropha oil biodiesel, which was further washed with warm water so that any surplus catalyst or an alcohol will be removed. Washing continued till a transparent layer of water was settled at the bottom and hence removed. Final product of biodiesel formed was again heated at 100°C to remove any moisture content if present. Transesterification process is chemically represented in Figure 3.3 below. Various steps in making of biodiesel from Jatropha oil are presented in Plate 3.2.

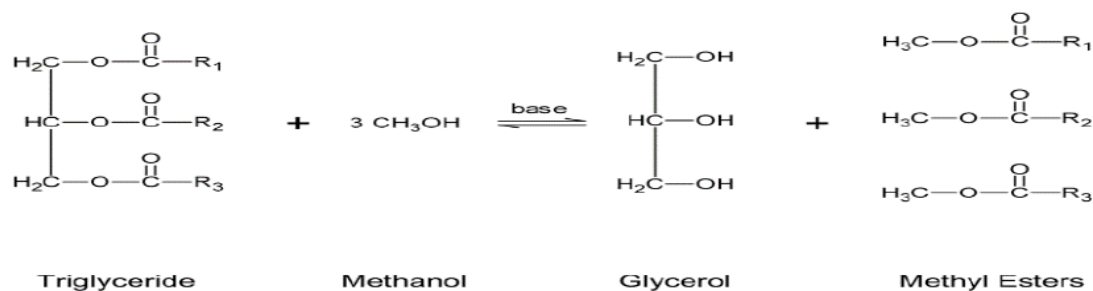


Figure 3.3. Chemical reaction during transesterification process

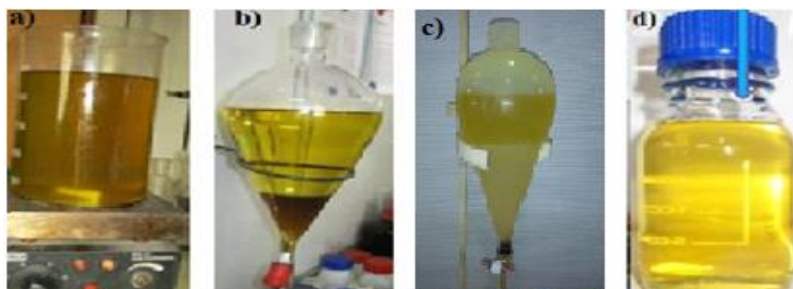


Plate 3.2. Steps in biodiesel production from Jatropha oil

a) Transesterification b) Glycerol separation c) Washing d) Biodiesel (B100)

3.6 Ethanol

Ethanol is an alcohol. Ethanol was obtained from Agarwal Chemicals, Delhi. It was 99% anhydrous. Ethanol being renewable source can be produced from agricultural wastes. Various processes involved in the production of ethanol are thermochemical process, biochemical process or carbon-monoxide hydrogenation. Both thermochemical and biochemical fall under cellulosic production processes. Ethanol is usually supplied through specially designed pipelines due to its high volatility and affinity for water

3.7 Preparation Fuel Sample Test Blends

Diesel was mixed with renewable diesel obtained by hydroprocessing in a variety of volumetric ratios. To create a one-litre sample of fuel for the various tests to be carried out, 10%, 20%, 30%, 40%, and 50% of renewable diesel were mixed with 90%, 80%, 70%, 60%, and 50% of diesel, respectively. These fuels were blended on a volume basis. Apart from these blends, ternary blends were also formed by mixing Diesel, Renewable diesel and ethanol on volume basis. Ethanol was taken as 5%, 10% and 15%, Renewable diesel was taken as 20%

and 30% and rest was diesel fuel. Percentage of ethanol was limited to 15% as beyond 15%, phase separation was observed in fuel samples. Table 3.1 and Table 3.2 below demonstrates the various proportions in which these fuels were blended with each other with their nomenclature. The prepared fuel samples are shown in Plate 3.3 and Plate 3.4. Also, phase separation of ternary fuel samples having 20% of ethanol is represented in plate 3.5.

Table 3.1 Composition of various fuel samples blends of Diesel and Renewable diesel

Nomenclature of a blend formed	% of Diesel in a blend	% of Renewable diesel in a blend
D100	100	0
R100	0	100
D90R10	90	10
D80R20	80	20
D70R30	70	30
D60R40	60	40
D50R50	50	50

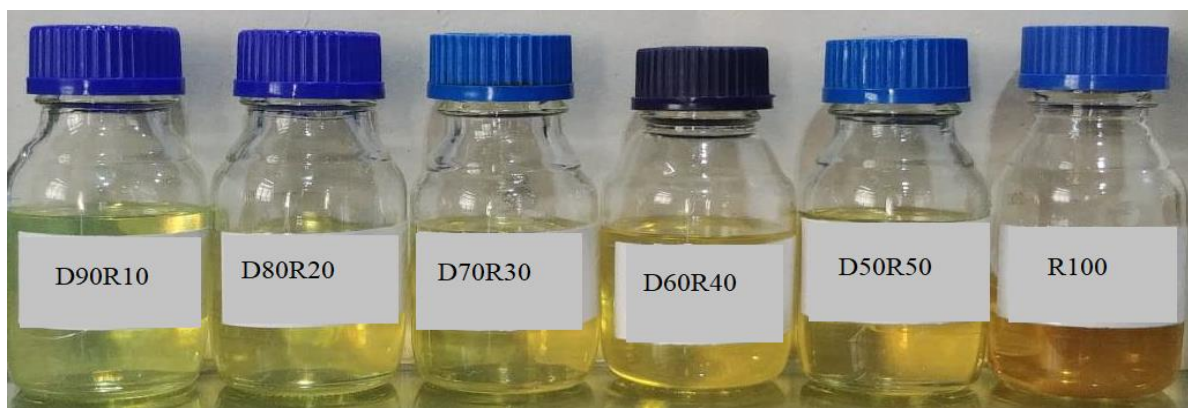


Plate 3.3 Fuel sample blends of Diesel and Renewable diesel

Table 3.2 Composition of ternary fuel sample blends of diesel Renewable diesel and Ethanol

Nomenclature of a blend formed	% of Diesel in a blend	% of Renewable diesel in a blend	% of Ethanol in a blend
R20 E5	75	20	5
R20 E10	70	20	10
R20 E15	65	20	15
R30 E5	65	30	5
R30 E10	60	30	10
R30 E15	55	30	15



Plate 3.4. Ternary fuel samples blends of Diesel, Renewable diesel and ethanol

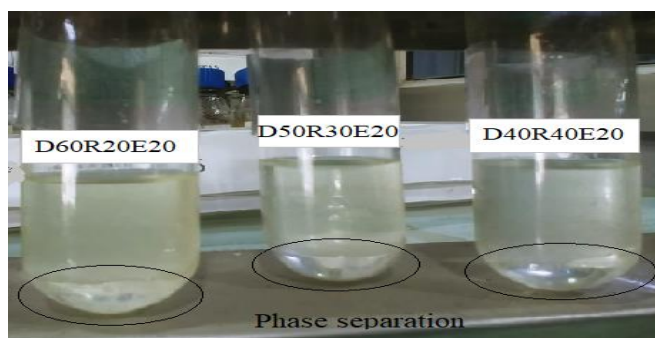


Plate 3.5 Phase separation in fuel sample blends with 20% as ethanol

3.8. Test Methods for Determination of Physicochemical Properties

Different test samples of 500 ml each was taken to determine the fuel sample's physicochemical characteristics. These characteristics like viscosity, density, calorific value, cloud point etc., must always be assessed for better understanding of the trends observed during engine trials. Equipment used for assessing the various characteristics of fuels are explained in following sub-topics. The characteristics of the test samples

3.8.1 Kinematic Viscosity

Kinematic viscosity was measured with the Viscometer, by Petrotest as shown in Plate 3.6. Fuel samples were tested for viscosity at a temperature of 40°C using plate 3.6 following ASTM D445 principles. The capillary tube was opened and a specific amount of measured sample was allowed to freely pass through it. Fuel sample was passed through a capillary tube with an upper level till it passed through the lower level. Time was recorded in seconds

and was multiplied by capillary constant as shown in eq 3.2, to get the value of kinematic viscosity in mm²/s, or cSt.

$$v = k * t \quad (3.2)$$

Where;

v : Kinematic viscosity in mm²/sec;

k : is the Constant; in mm²/sec² (k= 0.005675 mm² / sec²) and

t : is Time, in sec

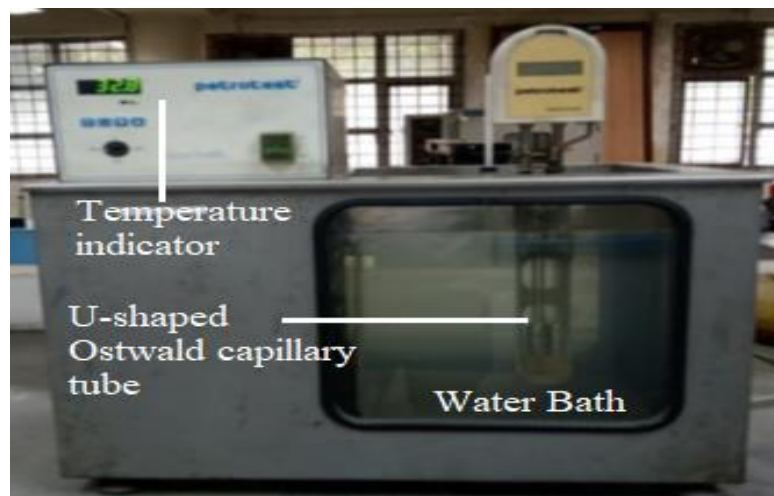


Plate 3.6 Viscometer

3.8.2 Density Meter

Plate 3.7 shows the "Anton Par Density Meter, Model DMA 4500" was used to measure density of fuel samples. Equipment measured the specific gravity of test fuel samples using ASTM D-4052 at a temperature of 15°C. Firstly, 10ml of toluene was injected through the sample injection port to rinse the test fuel pipeline thoroughly. Then 10 ml of fuel sample was injected into the injection port. The repeatability was tested three times and found to be adequate each time. Furthermore, the average of the three measurements was used as the final value for each sample.



Plate 3.7 Density meter

3.8.3 Calorific Value

The term “calorific value” refers to how much heat a substance emits when it completely burns [163]. Heating value of a substance is also known as a CV[163]. A Parr 6100 O₂ bomb calorimeter presented in Plate 3.8, is utilized to find CV of fuel samples by placing them in a crucible. Crucible filled with measured fuel sample was then placed in a hermetically sealed bomb. It has nichrome wire which was connected to electrodes touching the fuel sample. Thereafter, O₂ is supplied to a bomb. Bomb is then filled with oxygen. Bomb is then kept in water filled jacket in a calorimeter. The fuel sample is lit, causing it to burn. The heat released is displayed on the bomb calorimeter system's panel.

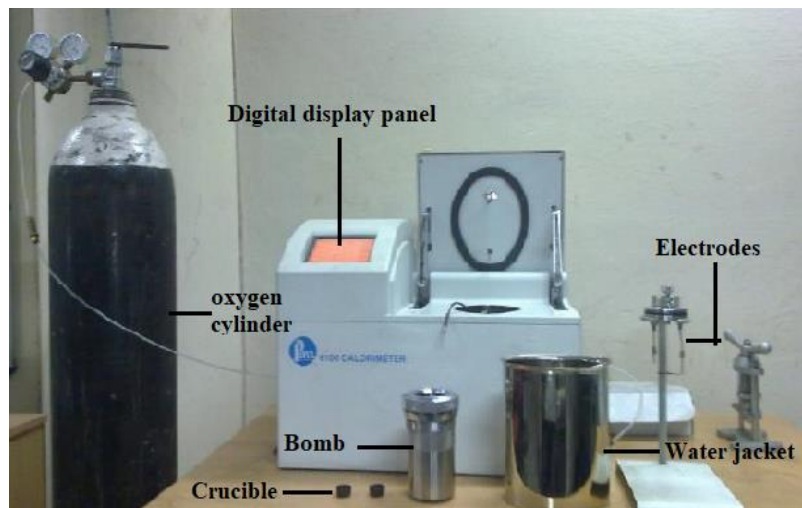


Plate 3.8 Bomb Calorimeter

3.8.4 Flash Point

The lowest temperature at which a combustible substance will burn when subjected to an incendiary device is known as the flash point (FP) [163]. The concentration of generated vapours, on the other hand, is inadequate to support combustion. Fuel with a low FP has a high level of volatility. In terms of fuel storage and transportation, the flashpoint is an essential characteristic. As indicated in Plate 3.9, the flash point was established in this experiment using Pensky-Martens Automatic Flash Point equipment per ASTM D93 guidelines. A measured amount of fuel sample is put in a cup and then carefully sealed with a cap. Sample is then heated. Apertures are periodically unlocked to allow O₂ to enter. The ignition source is then mechanically immersed into the cup over apertures to check fuel sample's flash [163]



Plate 3.9 Flash point apparatus

3.8.5 Cetane Index

The cetane index is essential for determining how well a fuel ignites [163]. A high cetane index considerably improves performance and combustion with a reduced ignition delay. [163]. Cetane index also describes the fuel's ability to self-ignite in CI engines. Cetane index of fuel must be accurately moderate. Too low cetane index will result in knocking of an engine resulting in its rupturing and too high cetane index will lead to inadequate blending of fuel/ air resulting in poor performance and more smoke. In present work, ASTM D4737 standards were followed to calculate cetane index which is shown in equation 3.3 below.

$$\text{Cetane index} = 45.2 + (0.0892) * T_{10A} + [0.131 + (0.901 * X) * T_{50A}] + [0.0523 - (0.420 * X) * T_{90A}] + [0.00049 * (T_{10A})^2 - (T_{90A})^2] * (107X + 60X^2) \quad (3.3)$$

$$X = [e^{-3.5Z}] - 1,$$

$$Z = D - 0.85,$$

D : Density of the fuel sample measured at 15 °C,

T_{10A}, T_{50A}, T_{90A} : Recovery/Boiling temperature for obtaining 10%, 50% and 90% vol. /vol. distilled fuel.

3.8.6 Distillation

The basic process of separation known as distillation identifies the characteristics of a liquid [49]. The equipment used for conducting distillation of the fuel samples is shown in Plate 3.10 below. It works as per ASTM D86 norms. Distillation equipment has a distillation flask for keeping the fuel. The temperature is recorded at the moment when the first condensed drop leaves the condenser [195]. At regular intervals, condensate temperature and the corresponding volume is measured and recorded.



Plate 3.10 Distillation equipment

3.8.7 Cold Flow Properties

For transportation fuel to be practically applicable during winters, three indispensable parameters are measured: a) Cloud point (CP), b) Pour point (PP), and c) Cold Flow Plugging

Point (CFPP). In regions with lower temperatures, fuel crystal clouds are formed and makes fuel viscous [20,49,74–76].

3.8.7.1 Cloud Point and Pour Point

The moment at which fuel cools to its low temperature and crystals begin to form visibly forming hazy or cloudy is referred to as the fuel's cloud point. [163]. Pour point of the fuel is termed as the lowermost temperature wherein fuel is unable to pour [196]. Both cloud point and pour point play a crucial role in operation ability of an engine during low temperatures. An equipment of the Koehler brand, as shown in Plate 3.11, is used to measure the fuel's cloud point and pour point. Cloud point and pour point was measured following ASTM D2500 and ASTM D97 standards respectively. Fuel sample is put into the test tube and placed inside the cold chamber through an aperture on the top. The test tube is fitted with a cork with small opening in the middle for inserting RTD (Resistance Temperature Detector) temperature sensor. The temperature at which fuel stops flowing is noted as pour point and the temperature at which test tube starts becoming cloudy is recorded as the cloud point.

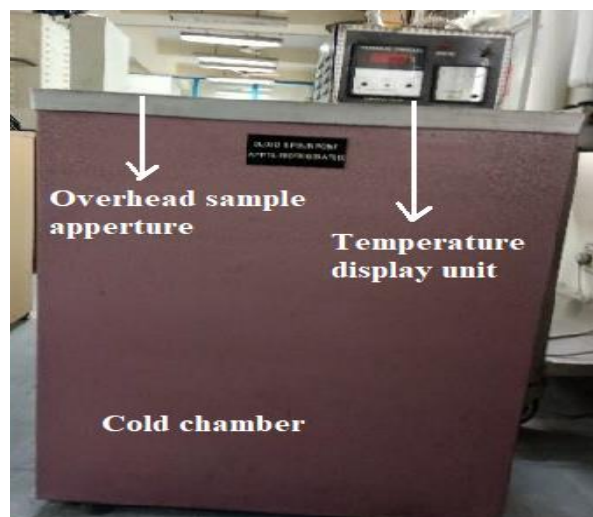


Plate 3.11 Cloud Point and Pour Point equipment

3.8.7.2 Cold Filter Plugging Point

The lowest temperature of fuel at a specific time, beyond which fuel cannot pass through the filter is CFPP [163]. Equipment used for determining cold filter plugging point

(CFPP) is set up by Linetronic Technologies as shown in Plate 3.12 It was following ASTM D6371 standards. In this set-up, specified amount of fuel sample is sucked into capillary through vacuum mechanism and cooled in a pre-cooled bath at $-34\text{ }^{\circ}\text{C}$ temperature. As soon as fuel stops to flow through the 10-micron filter within one minute, is noted as the CFPP of the fuel sample.

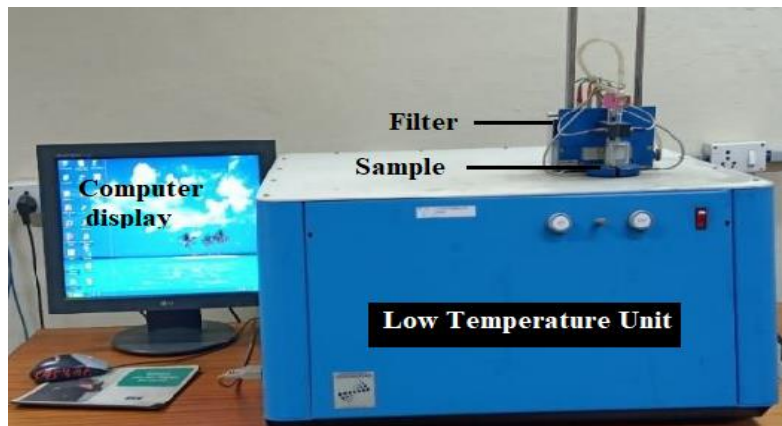


Plate 3.12 Cold Filter Plugging Point Apparatus

3.8.8 Lubricity

A lubricant plays a vital part in maintaining lubricity. Fuel works like a lubricant in an engine. The lubricity of fuel was determined with the High Frequency Reciprocating Rig (HFRR), make Ducom TR-282 as shown in Plate 3.13 below following ASTM D 6079 standards. A 2 ml of fuel sample is placed into a reservoir at a standard temperature. A vibrator arm is weighed with 200 gm of weight and lowered till it touches the test disk, sunken in fuel sample. Reciprocating arm starts reciprocating at 50Hz with 1mm of stroke for approximately 1hr and 15 minutes allowing the ball to rub on the test disk. Due to rubbing, a wear scar is formed on the test ball, which is measured under CCD camera with a 5-layer optical lens having a focusing range from 3cm to infinity. The size of wear scar is viewed on a PC using SCARVIEW software. The dimension of the wear scar is noted as the lubricity of the fuel sample.

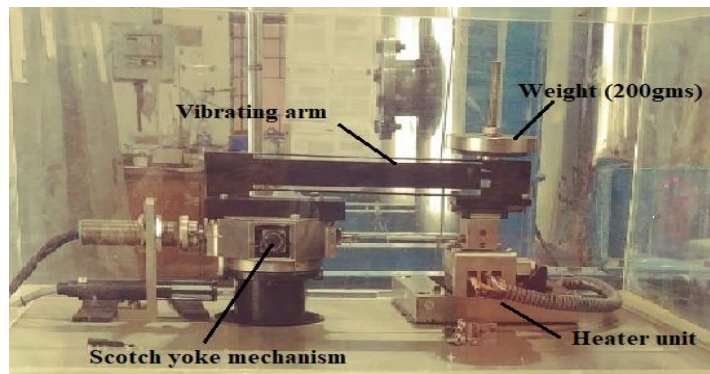


Plate 3.13 High Frequency Reciprocating Rig

3.8.9 Gas Chromatograph and Mass Spectrometer (GC-MS)

The gas-chromatograph mass-spectrometer (GC - MS) accurately separates and analyses the fuel samples into various constituents that it comprises. A Shimadzu QP-2010 equipped with Agilent DB-2887 column with specifications as 10m*0.53mm*3.0 μ m, and flame ionization detector was used for biodiesel and Renewable diesel derived from Jatropha oil. GC-MS is shown in Plate 3.14. The main components of a GC setup are a) gas cylinder with a regulator, b) a gas flow regulator, c) an injection port, d) a column, e) an indicator, and f) recorder. A predetermined temperature is set for the injection port, column, and detector. In GC the components are separated in gaseous state (mobile phase) and liquid (stationary state). Compounds are boosted by an inert gas. Depending upon the boiling point of each component present in a compound decides its elution from column. This separates the components from the mixture. Retention time is how long it takes for elusion to happen. Once the components are separated from the compound and leave from GC-column, mass spectrometer ionises and fragments these components and expedites these ionised molecules using electron or chemical ionisation sources. These disintegrated ions are a function of their mass / Charge ratios. Peak zones represent an amount of a compound. Each peak shown in a GC - MS graph, generates a unique mass spectrum which shows a specific compound.

Fuel sample of 0.1 μ l, was added into a column at 350 $^{\circ}$ C, keeping detector and injector temperatures constant. A programmable temperature checker was used to adjust the

GC oven's temperature, which was raised gradually at an interval of 15°C/min. Nitrogen, an inert gas transported liquid samples through the column. Thus, GC-MS helps in analysing the constituents present in the fuel sample and furthermore aids in determining their physicochemical properties.

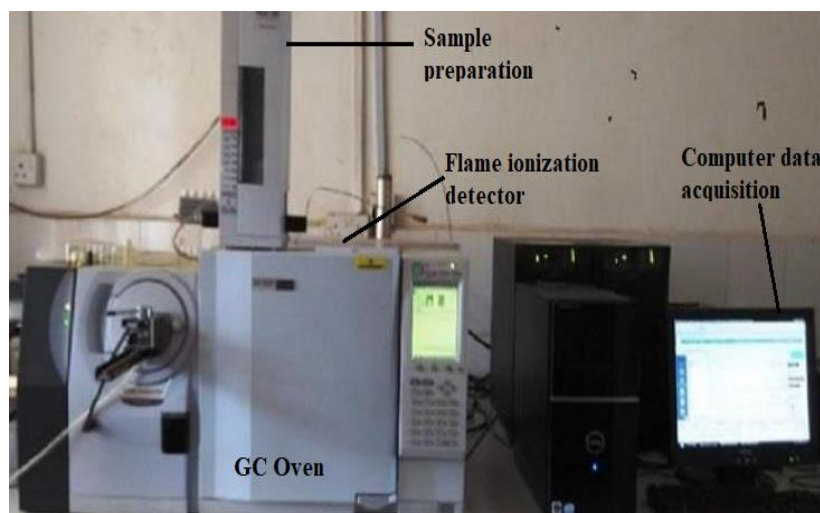


Plate 3.14 Gas Chromatograph and Mass Spectrometer

3.8.10 Fourier Transform Infra-Red Spectroscopy (FTIR)

The Nicolet 380 model from Thermo Fisher Scientific is used for the FTIR analysis of the fuel sample. Plate 3.15 depicts the equipment. The instrument is a Fourier transform infrared spectrometer, which splits an infrared beam into two components that, after passing through an optical system, produce an interference pattern when they recombine.

The molecular arrangement of chemical groups, particularly functional groups which is present in a molecule is determined by Fourier Transform Infrared Radiation (FTIR) based upon the explicit vibrational energy of a specific molecular bond [49]. The reference spectrum is formed by applying the FT to a standard infrared (I.R.) plot, and then inserting sample into the I.R.'s trail to obtain inserted sample's spectrum. To create an FTIR spectrum, the reference and sample spectrums were combined and entered into the software.



Plate 3.15 FTIR set-up

3.9 Selection of Compression Ignition Engine

In a country like India, where economy largely depends on agriculture, almost 5 million light and medium duty diesel engines are still in use. Knowing the fact that diesel engines is the core reason to the prevailing environmental conditions, diesel engines are still in use. Modifying an engine is an option but it will take its own time to reach and gear up to rural places in India. Therefore, considering this fact that modifying an engine is not a good option in present scenario, the renewable fuel and its blend with Diesel should be tested on the existing engine design. It will be a significant step towards moving ahead with the alternative fuel in the existing design engine and at the same time mitigating environmental pollution.

In the present experiment, a Kirloskar single-cylinder, 4-stroke, light duty, upright, stationary, H₂O cooled, DI, 3.5kW power and rated speed of 1500rpm was used. **Appendix 1** gives diesel engine's specifications. These engines are robust. Cylinder make was of cast iron, had a liner of toughened high phosphorous cast iron. Engine has a wet-sump lubrication system. Oil is sent to crankshaft. This helps in resistance to wear. An overhead camshaft operates the inlet and exhaust valves. This crankshaft drives the overhead camshaft with the help of two-pairs of bevel gears. Camshaft end drove the fuel pump. Engine is attached with

tank of water and blower, which helps in cooling the engine while in operation. Engine set-up is presented in Plate 3.16. Engine is fitted with eddy current dynamometer shown in the labelled Plate 3.17, which measures torque and power supply.

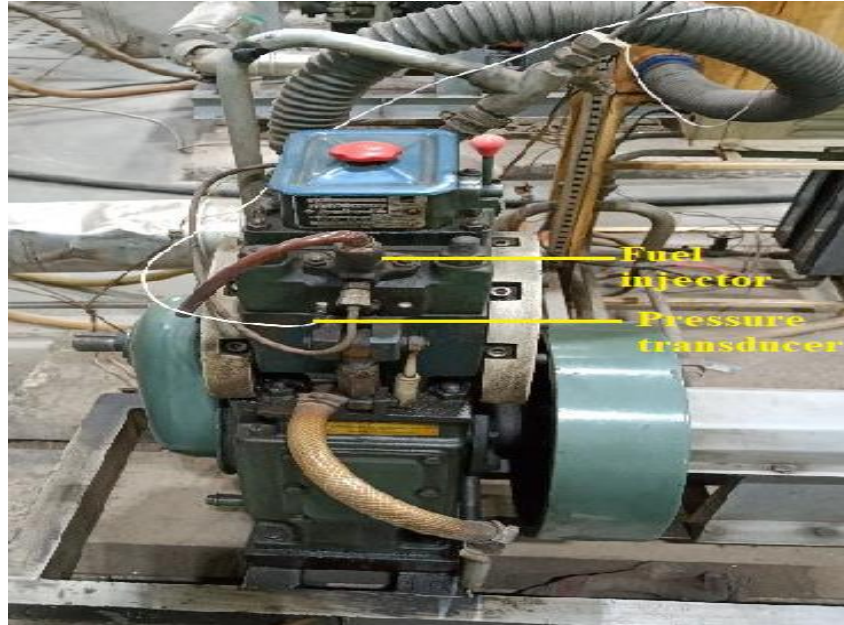


Plate 3.16. Test Engine

For proper load transmission, a high precision strain gauge is fixed to the dynamometer. At the arm of the dynamometer, is attached a magnetic pick-up type of sensor which determines the rpm. Strain gauge, magnetic pick-up type sensor are fixed to a dynamometer is shown in Plate 3.18. The engine and dynamometer were supplied with 350 litre and 120 litre of cooling water per hour respectively. Water flow was controlled by two rotameters installed on the panel as shown in Plate 3.19. ‘Kubeler’ make piezoelectric transducer measured in-cylinder pressure. Crank angle encoder was placed towards end of the eddy current dynamometer to load an engine. These sensors sent signals to the computer with an aid of NI USB 6210, a data acquisition system shown in Plate 3.20. The data sent, was read and analysed by ‘ENGINESOFT’ software, installed on a computer. The complete assembly of an engine system is presented in Figure 3.4.



Plate 3.17 Eddy current dynamometer

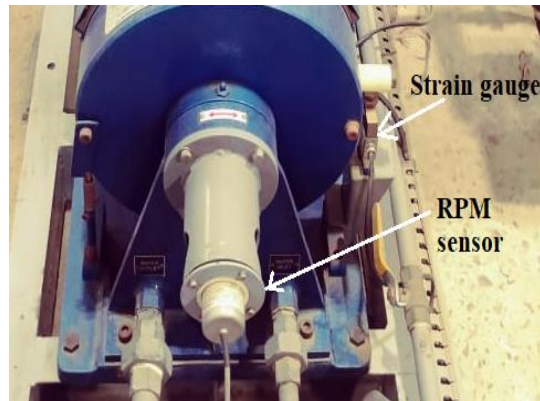


Plate 3.18 Strain gauge and RPM sensor



Plate 3.19 Rotameters



Plate. 3.20 NI USB 6210 Data acquisition system

Two separate fuel chambers were connected to the engine test rig. One tank contained diesel and another tank contained alternate fuel or diesel blends. Fuel flow was measured by calibrated standard burette (20cc by volume) and a stop watch. The control panel shown in Plate 3.17 shows sensor indicator, fuel burette, fuel valve, manometer for air, load indicator, rpm indicator and rotameters. Control panel was also responsible for loading and unloading of an engine.

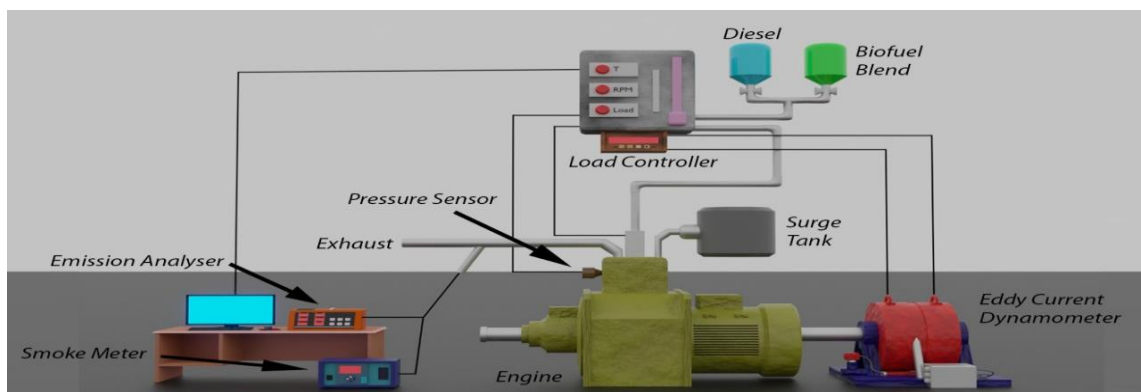


Figure 3.4. Engine experimental set-up

During combustion of the fuel, harmful exhaust emissions are emitted. Pollutants like CO, CO₂, NO_x and UBHC were measured by AVL 1000 gas-analyser. Smoke was measured with AVL DISMOKE 480 BT smokemeter. Gas analyser and smokemeter used in the present experimental work are showed in Plate 3.21 and specifications are listed in **Appendix-2** and **Appendix-3** respectively.



Plate 3.21. AVL DISMOKE smoke meter and AVL DITEST gas analyser

3.10 Selection of Engine Test Parameters

Engine research necessitates identification of relevant test parameters. The engine was tested per IS:10000. The engine's most important parameters and calculated engine parameters are given below:

A) Observed parameters

1. Engine load
2. Engine speed
3. Air flow rate
4. Fuel consumption rate
5. Temperature
6. In-cylinder pressure
7. Engine-exhaust emissions CO, CO₂, HC and NO_x
8. Smoke opacity

B) Calculated parameters

-
1. Brake Thermal Efficiency (BTE)
 2. Brake Specific Energy Consumption (BSEC)
 3. Pressure rise rate
 4. Heat release rate (HRR)
 5. Ignition delay
 6. Duration for combustion

3.11. Observation and Calculation Methods

Two fuel tanks, a fuel intake reading device, unit for determining the rate of airflow, an eddy current dynamometer, an RPM meter, a temperature display unit, an in-cylinder pressure instrument, and emissions measuring devices are the main components of the experimental setup. It was customary to run an engine on diesel initially for half an hour to heat it before the experiment was carried out. The observations for reference of diesel data were obtained only after running an engine for 30 mins. Following the warm-up stage, fuel line was substituted for alternate fuel and its blends, by linking to an engine for readings. The load on the drive shaft was adjusted using the eddy current dynamometer.

3.11.1 Brake Power (BP) and Brake Mean Effective Pressure (BMEP)

Brake power is the power generated at the driving shaft of an engine. BP is calculated by using the formula given below in equation 3.4 to 3.6.

$$BP = \frac{2\pi NT}{60 \times 1000} \quad (\text{kW}) \quad (3.4)$$

Where N : speed of an engine, rpm and T : Torque in Nm

$$T = \text{Force applied on dynamometer (F)} * \text{Length of the dynamometer arm (L)} \quad (3.5)$$

From equation 3.3 and 3.4

$$BP = \frac{2\pi NFL}{60 \times 1000} \quad (\text{kW}) \quad (3.6)$$

$$L = 0.185 \text{ m}$$

Rated power of the selected engine for the present experimental work was 3.5 kW. The minimum and maximum load calculated for the engine attached to dynamometer is 0.3 Kg and 17.3 Kg. All engine trials were carried out at different loads for emission and performance characteristics.

BMEP is the average pressure applied during the combustion process on the piston. It is calculated by using the equation 3.7 given below.

$$BMEP = \frac{120 * BP}{L * A * N * 101.325} \quad (3.7)$$

All the performance, emission and combustion readings were documented on every load for different test fuel samples.

Brake specific energy consumption (BSEC): Amount of energy of fuel utilised by engine to give one unit of power. From equation 3.8 it is clear that BSEC is closely attributed to the CV of the fuel. It is also dependent upon the viscosity of fuel. It is represented in MJ/kWh.

$$BSEC = \frac{m_f * CV * 3600}{BP (kW)} \quad ; m_f : \text{mass of fuel in kgs, CV: calorific value in MJ} \quad (3.8)$$

Brake Thermal Efficiency (BTE) specifies the efficiency with which the chemical energy of fuel is transformed into useful work. It is represented in % and its symbol is η_{BTE} . From the equation 3.9, it clearly shows that BTE \propto BP and indirectly proportional to mass of the fuel (m_f) and calorific value (CV).

$$\eta_{BTE} = \frac{BP * 100}{CV * m_f} \quad (3.9)$$

3.11.2 Measurement of Engine Speed

The toothed end of the dynamometer shaft was fitted with a magnetic pick up type rpm sensor. Magnetic pick-up type of sensor contained permanent magnet, yoke, and coil. This sensor was in close proximity to a toothed gear. An AC voltage pulse was created in the coil as each tooth moved by the sensor. Each tooth produced a pulse. More pulses were created when the gear turned faster. The data acquisition system received these impulse signals

digitally. The data acquisition system's calculated engine rpm, which was then displayed on the control panel and in the computer's ENGINESOFT database. Plate 3.18 already shows the rpm sensor.

3.11.3 Measurement of Air Flow Rate

An air sensor (turbine type flow metre) was mounted within the control panel to measure air flow. The air flow sensor is shown in plate 3.22 below. Utilizing the fluid's mechanical energy to turn a "pinwheel" (rotor) in the flow stream, turbine flow metres measure the flow rate. The rotor's blades are arranged to allow energy from the air stream to be converted into rotational energy. Bearings serve to support the rotor shaft. The rotor rotates faster in response to the fluid's velocity. Each blade or implanted piece of metal produces a pulse, making magnetic blade movement detection common. The pulse signal is processed by the transmitter and sent to the data acquisition system, which determines the fluid flow. The air flow data was stored in the enginesoft database and the sensor indication on the control panel. Furthermore, another approach for validating sensor data was available. It was based on the air box and orifice approach.



Plate 3.22 Air flow sensor

Equation 3.10 below shows the differential pressure across the orifice that is inserted in the air flow channel provides the air flow rate.

$$\text{Mass of air (m)} = C_d * A * \sqrt{2gh_w\rho_w\rho_a} \quad (3.10)$$

Where C_d = Co-efficient of discharge of orifice (0.6 in the present case); A = Orifice area;

g : acceleration due to gravity;

h_w : height of water column;

ρ_w : density of water, and

ρ_a : density of air

3.11.4 Measurement of Fuel Consumption Rate

The amount of fuel consumed is determined by how long it takes an engine to use a certain amount of fuel. Product of volumetric fuel consumption and fuel's density gives the mass of fuel consumed. A fuel flow sensor (Plate 3.23) installed inside the control panel measured fuel consumption volumetrically in current setup. The data acquisition system received the sensor signal. Fuel consumption could be obtained automatically as well as manually. At several instances, the sensor data was verified by manually timing 20cc fuel consumptions in the burette while blocking the fuel cock. The fuel sensor data, on the other hand, was found to be more accurate.



Plate 3.23 Fuel flow sensor

3.11.5 Measurement of Temperature

To measure exhaust gas temperatures, Chromel-Aluminum K-type thermocouples shown in Plate 3.24 were attached to a six-channel digital panel metre. A millivolt source was used to calibrate the metre up to 800 °C. The sensor was installed near the engine's exhaust manifold. The temperature data was recorded in the ENGINESOFT database as well as the

sensor indicator on the control panel. The emission data was manually obtained from the analysers' printed results as well as the computer's engine-soft database.



Plate 3.24 K-type thermocouple

3.11.6 Measurement of In-cylinder Pressure

The pressure generated inside the cylinder due to combustion was calculated using a 'Kubeler' piezoelectric transducer. A transducer's signals were sent to a charge amplifier, which boosted the signals while reducing signal noise. The signals were then transferred to a data acquisition system, which combined them with the outputs from the crank angle encoder to create a pressure versus crank angle graph in software placed on a computer. For each degree of crank angle rotation, pressure data was generated. For the in-cylinder pressure vs crank angle data in this investigation, fifty continuous cycles were averaged. Pressure sensor is attached on an engine's head in Plate 3.25 shown below.



Plate 3.25 Kubeler piezoelectric transducer

3.11.7 Measurement of Exhaust Emissions

On combustion of fuel, exhaust gases are emitted out from the diesel engine. Exhaust emission majorly constitute UBHC, CO, CO₂, NO_x and smoke. The probe of AVL di-gas

analyser and smoke meter is introduced into the exhaust outlet of an engine to measure the concentration levels of major pollutants. These concentration levels are displayed on the personal computer which is connected to gas analyser and smoke meter. Gas analyser and smoke meter is shown in plate 3.21 and their specifications in Appendix-2 and Appendix-3 respectively.

3.11.8 Calculation of Heat Release Rate (HRR)

The quantity of chemical energy produced by fuel upon combustion is referred to as "heat release" [197]. For studying combustion properly, assessing HRR is of great prominence as it affects engine efficiency and power output. To evaluate HRR, Heywood's [8] method was adopted for the current study and it is represented in equation 3.10. According to this method HRR is in accordance with 1st law of thermodynamics, which states that combustion chamber is treated as a single zone wherein, change in pressure is directly correlated to quantity of energy liberated by fuel undergoing burning [8,198]. Apart from single zone model, there is multi-zone model wherein burned and unburned areas are considered separately and an operator has to keep a continuous track of it [195]. It also comes with certain disadvantages due to uncertainties during separating burned and unburned zone [199] which is why single zone was preferred in the present work. Equation to calculate HRR is given below in equation 3.11

$$\frac{dQ}{d\theta} = \frac{\gamma}{\gamma-1} * P * \frac{dV}{d\theta} + \frac{1}{\gamma-1} * V * \frac{dP}{d\theta} - \frac{dQ_w}{d\theta} \quad (3.11)$$

$dQ/d\theta$: Time taken wrt net heat release in engine's cylinder (J/°CA);

$dQ_w/d\theta$: Heat transfer rate wrt wall (J/°CA),

γ : ratio of specific heats;

P : Cylinder pressure (bar);

V : Gas volume (m³)

θ : Crank angle (°)

The time fuel takes for combustion to start after fuel injection is called the ignition delay. The ignition delay was computed in this study as the time interval in terms of crank angle degree. The amount of time it takes for heat to be emitted from fuel from beginning to end is known as the combustion duration.

3.12 Engine Trial Methodology

In engine set-up as shown in Figure 3.4, there are two tanks, one for diesel fuel and another one for fuel samples. The pipeline from tank to the common valve is checked for any air bubble. Before cranking an engine, the fuel level in the tanks is kept at sufficient level for operating an engine smoothly. Engine was initially fed with neat Diesel and run at no load condition until the time engine warmed up and was stabilized. During this time, data acquisition system was connected to LabVIEW-based ENGINESOFT software which was installed on the personal computer. Sensors placed at various location on an engine started to receive signals and sensors were set to minimum resolution.

After attaining steady state conditions, the valve for the diesel supply was closed and valve of fuel test sample chamber was switched open. Engine was run for at least thirty minutes on test sample until engine got stabilized following steps by Bekal et al. [200]. All the readings were taken on each fuel sample with the periodically calibrated instruments. Load varied from 0% to 100% in an interval of 20%. At each load, airflow rate, fuel-flow rate, rpm, exhaust temperature and pollutants were recorded. Average of 50 cycles were taken for recording combustion data. All trials were carried out, following IS:10000 standards. Engine was run on neat Diesel, neat Renewable diesel, binary blends and ternary blends as explained earlier. All test were carried out at normal temperature and atmospheric pressure conditions.

3.13 Experimental Accuracies and Uncertainties

Any instrument used for measurement in the present experimental work were all calibrated periodically and it was made sure that they display higher accuracy. Table 3.3 below

shows accuracy, range and uncertainty percentage associated with various measurements and calculated parameters. All the measurements taken were repeated during the experimental trials and the average of was found in the permissible range, hence exhibiting higher accuracy.

Table 3.3 Accuracy of measuring instruments

Measuring Parameters	Measurement Principle	Limits	Precision	Uncertainty %
Engine Load	Strain gauge load cell	0 to 25 kg	±0.1kg	± 0.2
Engine Speed	Magnetic pick-up	0 to 200 rpm	±20 rpm	± 0.12
Time	Stop-watch	-	± 0.5 %	± 0.2
Exhaust Temperature	K-type thermocouple	0 to 1000 °C	± 1 °C	± 0.2
Crank angle encoder	Optical	0 to 720° CA	± 0. 2° CA	± 0.25
Cylinder Pressure	Piezoelectric	0 to 200 bar	± 1 bar	± 0.2
Fuel consumption	Turbine flow type	-	-	± 0.25
Air consumption	Level sensor	-	-	± 0.5
BP	-	-	-	± 0.5
BTE	-	-	-	± 0.5
BSEC	-	-	-	± 0.4
HC	Non-dispersive infrared (NDIR)	0 to 30000ppm	± 10ppm	± 0.12
NO	Electrochemical	0 to 5000ppm	± 50ppm	± 1.1
CO	Non-dispersive infrared (NDIR)	0 to 15%	± 0.01%	± 0.5
Smoke opacity	Light extinction measurement	0 to 99%	0.1%	± 1.5

Uncertainty provides the broadest possible absolute alteration between reported value and true value [201,202]. Uncertainty can be found out by the equation 3.12 given below.

$$U_o^2 = U_1^2 + U_2^2 + U_3^2 + U_4^2 + \dots \quad (3.12)$$

Where, U_o : overall uncertainty (%)

U_1, U_2, U_3 , etc are the uncertainty percentages of different physiochemical properties like, kinematic viscosity, density and other parameters. For physiochemical properties, reading was

taken five times and the uncertainty percentage was found out to be less than 0.1%, hence it was neglected. Observed values were similar in each test as the equipment underwent timely calibration and had high precision.

3.14 Optimization of Output Factors Using Response Surface Methodology

Series of experiments were conducted on an engine to calculate performance and emission characteristics using many blends. However, it was viable to use an optimization technique to cut down on the time and expense of experimentation. The optimization method known as Response Surface Methodology (RSM) was used to find the optimal ratio of Renewable Diesel and Diesel to achieve the optimum BTE and reduced emissions. RSM is the huge range of statistical and numerical methodologies that are valuable for exhibiting and analysing issues, comprising of various response variables. Every factor has an impact on each response variable. This technique intends to optimize the response variable by studying an impact of various input factors so that cost is reduced and time is saved on the number of experiments to be executed. Designing of experiment was performed with the help of MINITAB 17 software. Figure 3.5 shows the step wise flowchart for applying RSM technique carried out in the present study.

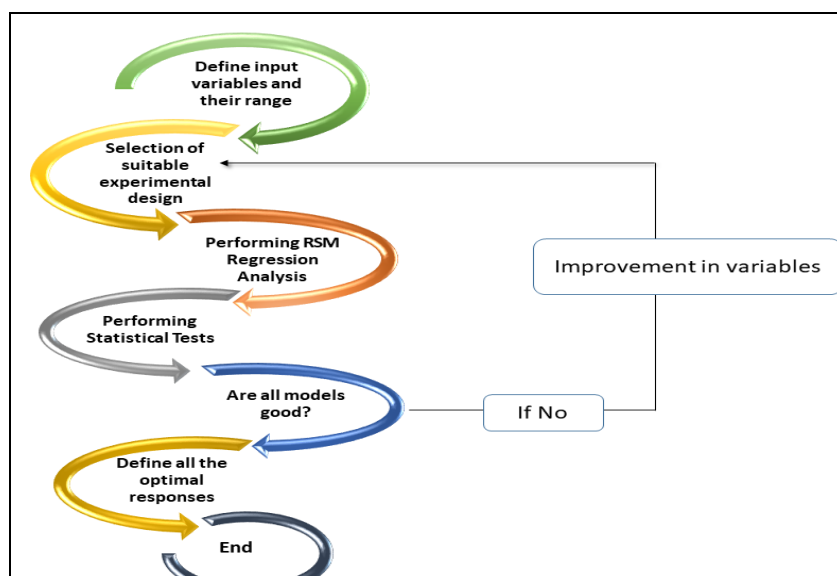


Figure 3.5 Step-by-step mechanism for applying RSM model

The first step in the RSM technique is to define the input variable and response variables and selection of suitable experimental design. Response variables are the ones who are effected by input variables. Various response variables considered are as BTE, CO, HC, NO and smoke opacity. Input factors taken are BMEP in bar and percentage of Renewable diesel, and ethanol in a diesel by volume. Lower, and higher range was defined for input factors as presented in Table 3.4 below.

Table 3.4. Various input factors and their levels

Input Variables / Factors	Levels	
	Low	High
BMEP (bar)	0.7812	4.1670
Renewable diesel (%)	20	30
Ethanol (%)	5	15

Once the input variables are selected, an appropriate design, Central Composite Face Centred Design (CCFCD) was selected. CCFCD helps in predicting the results precisely and practically only fewer number of experiments can be conducted, saving both on time and cost [122,203,204]. CCFCD optimization allows for the assessment of a large number of variables and also the significance of each factor [205]. As shown in Figure 3.6, CCFCD has six axial points, eight cube points and six centre-points in a cube. Various experimental trials conducted on CCFCD design are tabulated in Table 3.4 below. Factor values which are in the mid-range level are located at the centre points whereas other factor values (extreme range) are located at the corner points.

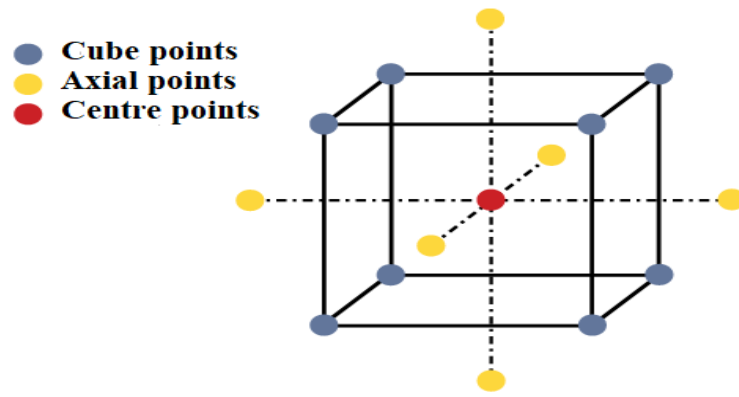


Figure 3.6 Geometric structure of CCFCF

As is known that various variables in CI engine during combustion hold a non-linear relation, so it is a complex phenomenon. To portray these complex non-linear relationships of various variables, a second-order regression equation is generated between various responses and input variables, selected in the beginning of the model, shown in eq 3.13

$$Z = \beta_0 + \sum_{k=1}^l \beta_k x_k + \sum_{k=1}^l \sum_{m>1}^l \beta_{km} x_k x_m + e \quad (3.13)$$

Where,

Z = Forecasted value of a response, k= linear coefficient, m= quadratic coefficient, β = regression coefficient, l= number of input factors, e= random error in the response value.

Number of trials conducted on CCFCF model are tabulated in Table 3.5 below. Twenty trials of experiments were conducted in accordance with the input factors.

$$\text{Total no. of runs} = 2^m + 2m + q \quad (3.14)$$

where,

m : number of independent variables,

2^m : number of factorial points or corner points,

2m : number of axial points and

q : number of replicated centre points.

Hence, total number of experimental runs = 20

Table 3.5 Design array of experimental trials

S.No.	BMEP (bar)	RENEWABLE DIESEL (%)	ETHANOL (%)	BTE (%)	CO (g/kWhr)	HC (g/kWhr)	NO (g/kWhr)	SMOKE (%)
1	0.7812	20	5	17.847	4.750345	9.823	13.78044	3.5
2	2.4741	25	10	28.48	4.426419	4.5801	4.864206	17.1615
3	2.4741	25	5	28.884	4.213069	4.3298	5.141933	18.15
4	2.4741	25	15	26.15	4.604569	4.7301	4.807369	16.4115
5	0.7812	30	15	14.85	4.678345	11.1337	12.34744	1.4
6	2.4741	30	10	28.32	4.354269	4.7126	4.757206	16.823
7	4.167	20	15	28.35	31.289	3.167	3.482412	49.9
8	2.4741	25	10	28.48	4.524	4.867	5.0235	17.265
9	4.167	25	10	30.502	30.4999	3.176	3.161195	50.9
10	4.167	30	5	30.47	30.161	3.186	3.298195	52.1
11	2.4741	25	10	28.543	4.6264	4.766	4.9652	17.065
12	2.4741	25	10	28.333	4.3264	4.5129	4.73239	16.948
13	2.4741	20	10	28.64	4.498569	4.4476	4.971206	17.5
14	4.167	20	5	30.97	30.412	2.87	3.458791	55
15	0.7812	30	5	17.48	4.579345	10.265	13.1339	2.3
16	4.167	30	15	27.9	30.889	3.385	3.317412	48.5534
17	2.4741	25	10	28.4973	4.2265	4.62986	4.86433	17.365
18	0.7812	20	15	15.524	4.8703	10.447	12.55744	2.2
19	0.7812	25	10	17.425	4.68819	10.54035	12.7993	2.4
20	2.4741	25	10	28.232	4.4876	4.786	4.5488	17.056

Results and Discussions**4.1 Introduction**

The findings from a number of experiments are thoroughly explained in this chapter. The characterization of the catalyst prepared from wet impregnation technique is explained with the help of the figures obtained. The physio-chemical physiognomies of diesel and biodiesel are compared to Renewable diesel. Also the effect on the physiochemical properties was observed when Renewable diesel and diesel were blended as a binary fuel. Ethanol being environment friendly was also added in certain percentages in the blend of diesel and Renewable diesel making it a ternary blend and change in the physiochemical properties was studied and is explained in detail. In the later stage, CI engine was run on various binary and ternary blends. Performance characteristics (BTE, BSEC, exhaust gas temperature), exhaust emissions (NO, CO, CO₂, HC, smoke opacity) and combustion characteristics (HRR, P- θ curve, combustion duration and ignition delay) was studied and elucidated in detail with figures, curves etc. in the end, RSM multi-objective optimization model is discussed and an optimum binary and ternary blend is obtained which can make CI engine run efficiently.

4.2 Catalyst Characterization

Preparation of a catalyst is discussed in section 3.4. Figure 4.1 shows the XRD profile of a catalyst prepared from a wet impregnation method. The highest peak is observed at 66.89° and second and third highest at 46.54° and 37.59° respectively. Metals used in the preparation of a catalyst are low in percentage and high dispersion on the support, individual peaks of metals cannot be seen. The nature of aluminium oxide is not affected by the impregnation technique used for metals. Outcomes obtained by Sankaranarayanan et.al and Mishra et.al were comparable [63,206]. Figure 4.2 presents Scanning Electron Microscope (SEM) pictures

of a catalyst at 20, 10 and 5 μm . SEM is carried out to study morphology and surface topography of the catalyst prepared.

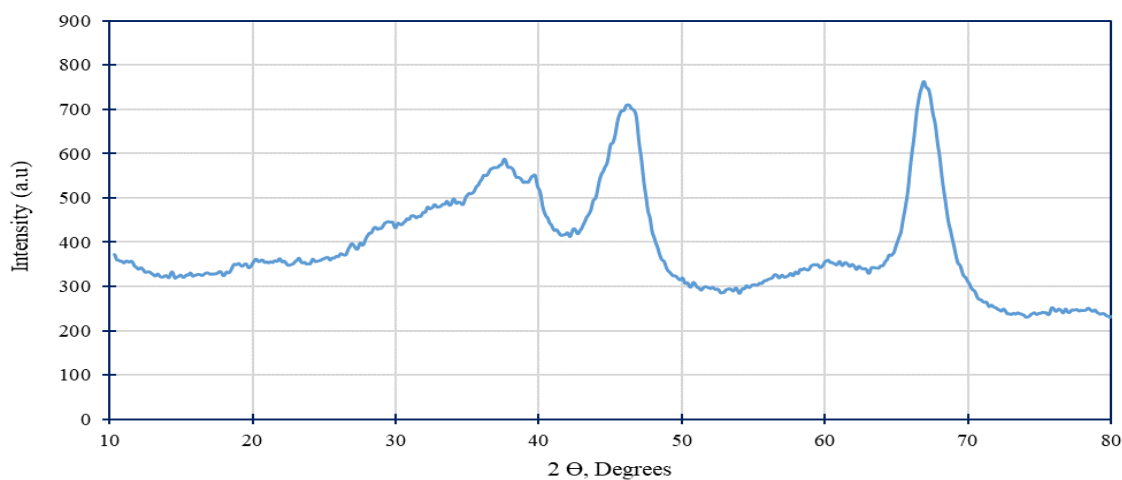


Figure 4.1. XRD profile of a catalyst

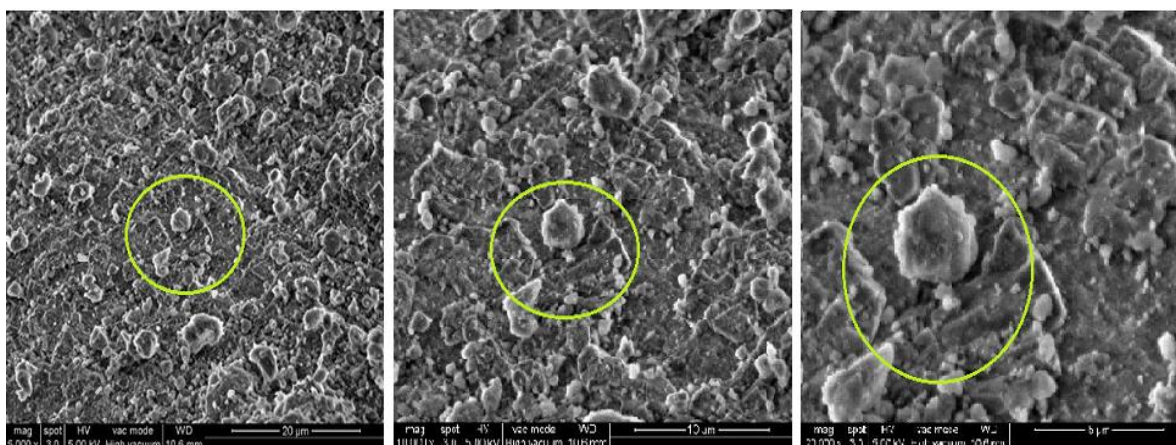


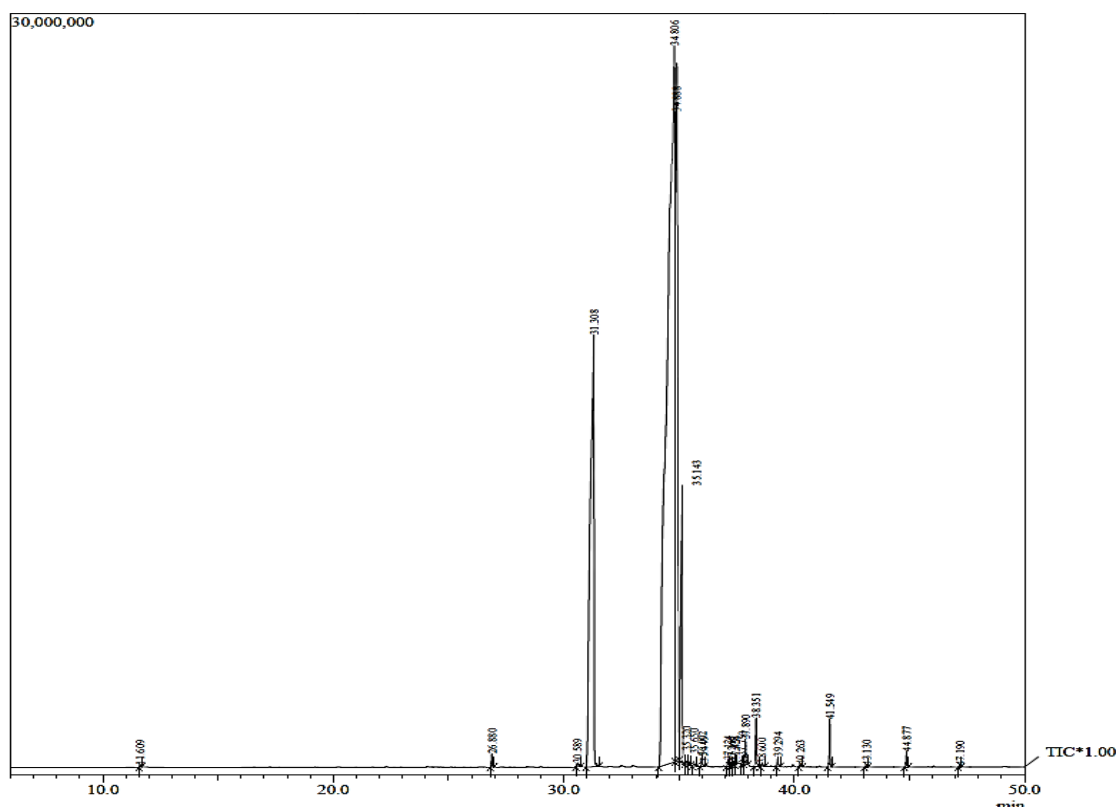
Figure 4.2. SEM images of a catalyst at 20 μm , 10 μm and 5 μm

4.3 Product Analysis

Product analysis is one of the important parameters in identifying the various components, chemical mixtures, chemical groups like functional groups present in any organic material at a molecular level [49]. GC-MS and FTIR are the two different techniques considered for product analysis. It is very essential as it identifies esters, alcohols, aldehydes etc. as they have substantial influence on the physiochemical properties of a compound.

4.3.1 GC-MS of Biodiesel Derived from Jatropha Oil

Figure 4.3 shows the GC outline of a biodiesel having a hydrocarbon chain length from C-15 to C-25. The total percentage of SFA and USFA found in the derived biodiesel was found to be 27.59% and 71.93% respectively. SFA like methyl Palmitate (16.8%) and methyl stearate (10.79%) and USFA like methyl linoleate (39.58%) and methyl oleate (32.41%) were the major constituents of the biodiesel. Methyl linoleate being the dominant constituent.



increase in H-C sequence length, increases the energy density and decreases volatility. This enhances the fuel's ability to ignite [178]. Additionally, it was noted that JO initially had 28.23% SFA, which after undergoing hydrogenation process was increased to approximately 62%. There are few isomers also that are formed which help in improving the cold flow properties of a fuel.

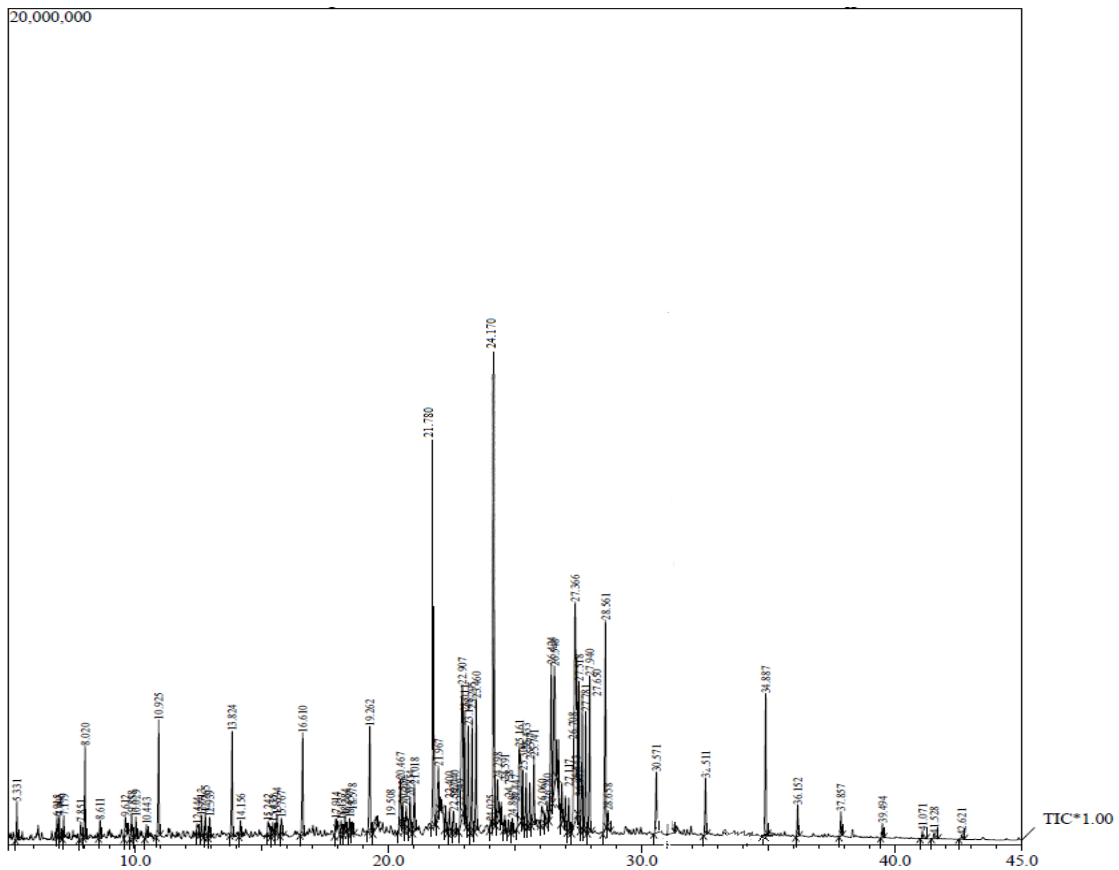


Figure. 4.4 Gas- chromatograph of a Renewable diesel derived from Jatropha oil

4.3.3. FTIR Analysis of Biodiesel Derived from Jatropha Oil

In FTIR, under the exposed I.R radiations, various molecules with single and double bonds existing in any fuel sample like CH, NH, OH C=O bonds are delicate and are measured in a wavelength spectral of 400 to 4000 per cm [208,209]. Figure 4.5 shows that transmittance of C-O bond is on the higher side with peak intensity at 1171 per cm which falls in the range of 1100 to 1300 per cm. Transmittance percentage is very low at 1740 per cm which corresponds to COOH group (1740 to 1755 per cm). This also infers that there is a small

presence of esters which is also confirmed in GC-MS analysis. C-H bond stretching is observed in biodiesel at wavenumber 2855 per cm and 2925 per cm and it is on the lower side. Outcomes are in synchronization with Rajeshwari et.al [209]. Methyl group in biodiesel infrared adsorption range is shown in between wavelength spectral of 1362 to 1385 per cm.

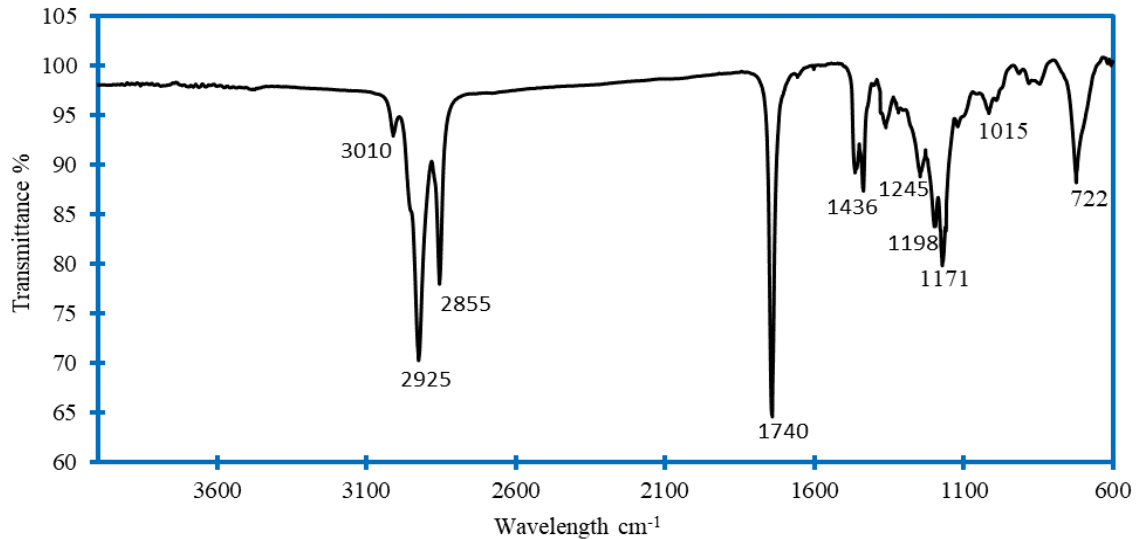


Figure 4.5. FTIR analysis of Biodiesel derived from Jatropha oil

4.3.4. FTIR Analysis of Renewable Diesel Derived from Jatropha Oil

Each molecule in its molecular structure has its vibration and energy associated with it. Figure 4.6 shows transmittance percentage for R100 at 1740 per cm is high which concludes removal of carboxylic group (COOH) due to hydroprocessing. C-H absorption falls in between the range of 2700 to 3100 per cm and same is seen for Renewable diesel at 2855 per cm, 2923 per cm and 2956 per cm. The peaks at 1377 and 1463 wavenumber show the presence of methyl group inferring presence of large number of n-paraffins and smaller number of isomers. The conclusion is in-line with the work done by Chatterjee et al. [209] and Janampelli et al. [210].

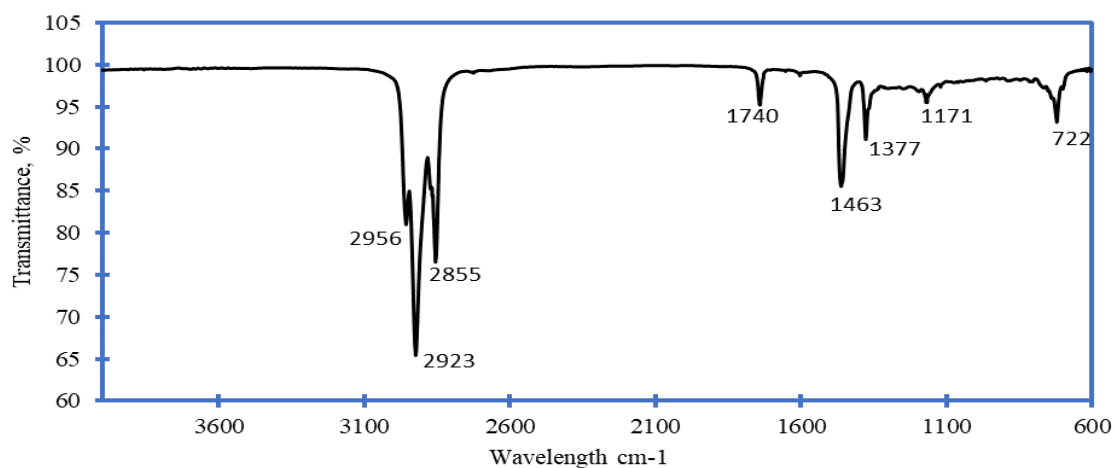


Figure 4.6. FTIR analysis of Renewable diesel derived from Jatropha oil

4.4. Physio-chemical Properties of Fuel and its Blends

Physicochemical properties are one of the important characteristics for any fuel. Section 3 already provides an explanation of the various instruments used to measure the physical-chemical characteristics of fuel and blends. According to ASTM standards, an assessment of the chemical characteristics was done. Various physio-chemical properties are explained in the section below in detail. Table 4.1 and Table 4.2 shows the various physio-chemical properties of blends of diesel and Renewable diesel and blends of diesel, Renewable diesel and ethanol.

Table 4.1 Comparison in Properties of Diesel, Biodiesel, Renewable Diesel, and blends

Property	D100	B100	R100	R10D90	R20D80	R30D70	R40D60	R50D50
Kinematic Viscosity at 40°C, cSt	2.42	5.09	2.75	2.55	2.60	2.64	2.68	2.71
Density at 15°C, kg/m ³	837	859.6	819.2	834.4	831.87	830.6	829.5	828.22
Flash Point, °C	59	162	67.2	60.0	60.6	61.9	63.2	63.7
Calorific Value, MJ/kg	42.57	40.9	41.80	42.42	42.30	42.09	41.93	41.87
Cloud Point, °C	-0.82	4	-5.9	-1.2	-1.7	-2.6	-2.7	-3.3
CFPP, °C	-12	-6	-14	-12.3	-12.8	-13.1	-13.3	-13.5

Cetane index	46.77	47.97	66.3	48.52	50.01	51.54	51.7	54.4
Lubricity, microns	177	371	196	175.7	152.3	146	100.1	94.6

Table 4.2 Comparison in Properties of Diesel, Renewable Diesel, Ethanol and their blends

Property	Diesel	R100	E100	R20E5	R20E10	R20E15	R30E5	R30E10	R30E15
Viscosity, cSt	2.42	2.75	1.076	2.55	2.52	2.47	2.61	2.57	2.5
Density, gm/cm³	837	819.2	764.1	830.65	828.44	824.14	829.09	826.11	823.46
Calorific Value, MJ/kg	42.57	41.8	26.8	40.19	39.51	39.01	39.88	39.17	38.92
CFPP, °C	-12	-14	-51	-16.08	-16.92	-17.81	-17.22	-18.11	-19.99
Cloud Point	-1.09	-5.9	-117.3	-2.76	-3.01	-3.37	-3.66	-3.95	-4.31
Cetane index	46.77	66.3	7.2	51.16	49.08	47.29	53.29	51.21	50.06
Flash point	59	67.2	13.5	61.51	60.76	59.81	62.11	61.32	60.34
Lubricity	177	196		178.9	178.6	178.2	181.1	180.8	180.4

4.4.1 Density

Density is one of the significant properties for any fuel. Density of Jatropha oil is highest which is 920 kg/m³. Density of a biodiesel and Renewable diesel derived from Jatropha oil is 859.6 kg/m³ and 819.2 kg/m³ respectively and density of diesel is 837 kg/m³. The density of Renewable diesel is lesser than diesel. As per the ASTM D1298 and EN590 standards the density of the fuel should be in between 820 to 860 kg/m³ and 820 to 845 kg/m³ respectively. The figure 4.7 below shows the density of diesel, Renewable diesel and various blends of Diesel and Renewable diesel of different percentage by volume. From figure 4.7 it is evidently noted, with addition of Renewable diesel in diesel the density of blends further decreases. D100 is the densest fuel among the fuel samples and R100 is the lowest. Since the density of Renewable diesel is less, which aids in proper atomization which further leads to less exhaust emissions than diesel [112,211]. However, due to surge in temperature of fuel while undergoing burning process, density is further decreased, which leads to lesser energy content,

and lesser power. Consequently, fuel usage is increased to make up for the loss of power [49,53,166,171].

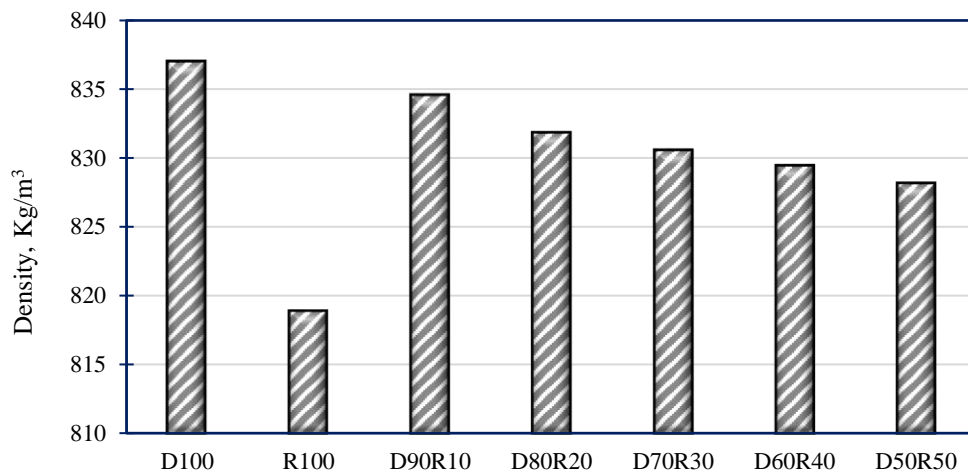


Figure 4.7. Density variation for test fuel samples

Figure 4.8 shows the variation in density of ternary blends of various proportions by volume. It is observed that ethanol's (764.11 kg/m^3) density is lowest amongst all the test fuel samples. Due to less density of an ethanol and Renewable diesel, pour speed is high and energy content is low. Pouring speed of any fuel is inversely proportional to $\sqrt{\text{density}}$ [20,24,65,212]. From the bar graph it is clear that with an increase in ethanol percentage (5%-15%) and Renewable diesel (20%-30%), density of fuel samples decreases due to their lesser density than diesel and they replace diesel's share in blends. From the Table 4.2 and Figure 4.8 it is observed that blends like D75R20E5, D70R20E10 and D60R30E5 have density values as 830.65 kg/m^3 , 828.44 kg/m^3 and 829.09 kg/m^3 which is at par with diesel and could be deliberated as an another option to replace diesel fuel. All the values of density measured for blends is within the range as per ASTM D1298 and EN590 standards.

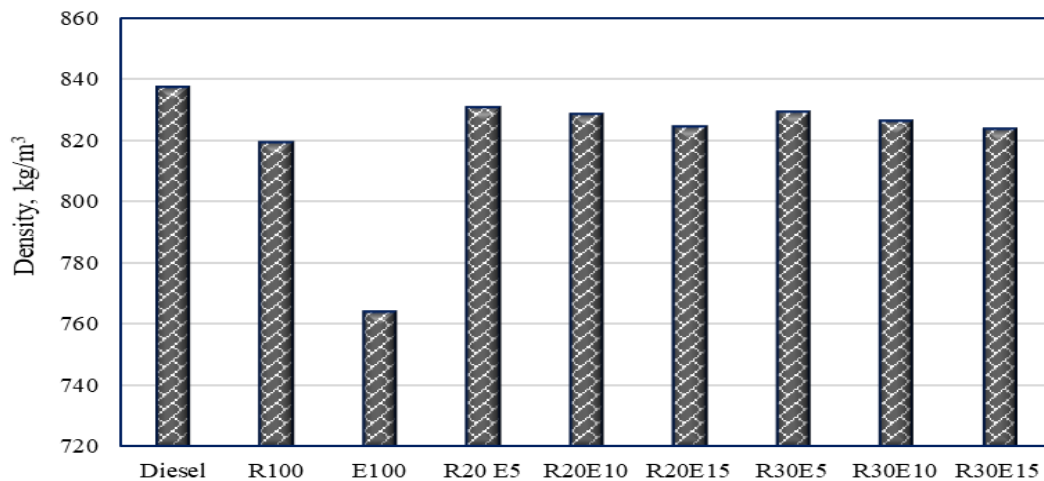


Figure. 4.8. Density variation for ternary test fuel samples

4.4.2 Kinematic Viscosity

Viscosity is a property which makes combustion process easier and affects emission quality. Less viscosity, high atomization, better mixing will lead to lesser emissions and vice-versa. As per ASTM D445 and EN590 standards kinematic viscosity of the fuel to be operational in a diesel engine should be in between 1.9 to 4.1cSt. Temperature also has an impact over the viscosity. If the temperature decreases, viscosity increases which can lead to plugging of filters, inadequate lubrication, leakage which can further result into less power output and higher fuel consumption [20,163,176,213]. From the Figure 4.9 and Table 4.2 viscosity of D100, R100, D90R10, D80R20, D70R30, D60R40, D50R50 is 2.42, 2.75, 2.55, 2.60, 2.64, 2.68, 2.71cSt respectively. From the Figure 4.9 and the values of viscosity for each test sample, it is seen with a rise in Renewable diesel proportion, the viscosity of the blend is increasing, but it is within the range as per ASTM D445 standards. Also, viscosity of R100 is lesser than biodiesel (5.09cSt) [73,75]. Renewable diesel has very little or no oxygen than biodiesel leading to lesser surface tension, which is one more reason for Renewable diesel's lesser viscosity [100,146,214].

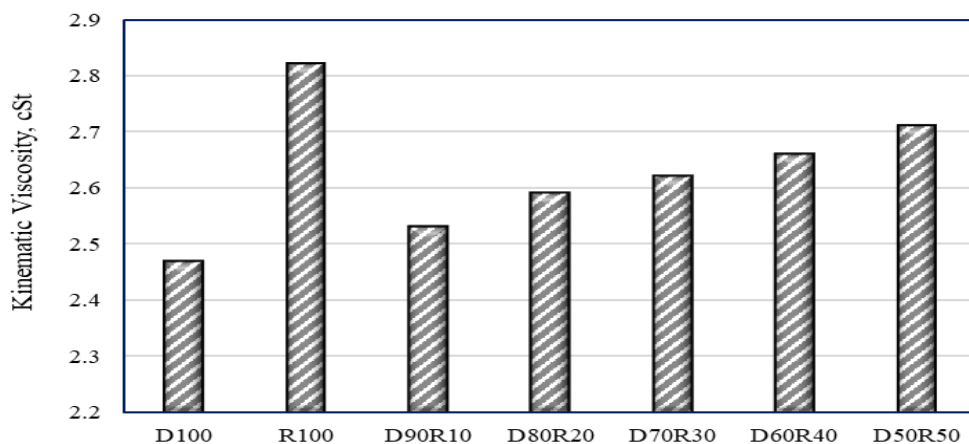


Figure 4.9. Kinematic viscosity variation for test fuel samples

Table 4.2 apart from showing the viscosity of D100 and R100, the viscosity of E100, D75R20E5, D70R20E10, D65R20E15, D65R30E5, D60R30E10, D55R30E15 is 1.076, 2.55, 2.52, 2.47, 2.61, 2.57, 2.50 cSt respectively. According to Figure 4.10, viscosity decreases as ethanol's percentage in a blend increases because it has a lower cetane index and more oxygen. Nonetheless, lesser cetane index and more oxygen can lead to better mixing and better combustion rate [215]. It is also observed by keeping the percentage of ethanol constant and increasing the percentage of Renewable diesel the viscosity increases from 2.55cSt (R20E5) to 2.61cSt (R30E5) which compensates for the decreased viscosity otherwise. Due to the volume proportion of Renewable Diesel being higher than that of ethanol in all blends, it is dominant. The viscosity of binary and ternary blends spans between R100 and D100.

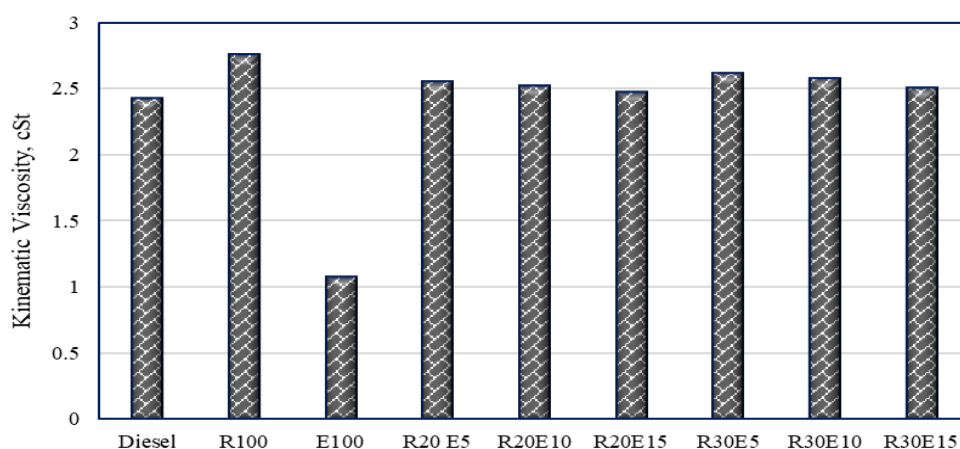


Figure. 4.10. Kinematic viscosity variation of ternary test fuel samples

4.4.3 Calorific Value

Calorific value is also called the heating value of any organic compound. Calorific value is the energy that is liberated by an organic substance when it undergoes the combustion in presence of oxygen and gives by-products like carbon di-oxide and water [20,60,73,74,206,216]. From the Figure 4.11, it is seen that the calorific value of the diesel is highest due to no oxygen present in its molecular structure. CV for Renewable diesel is lesser than diesel and higher than biodiesel, as it undergoes hydroprocessing and most of the oxygen molecules are removed [20,49]. CV of D100, R100, D90R10, D80R20, D70R30, D60R40, D50R50 is 42.57, 41.80, 42.42, 42.30, 42.09, 41.93 and 41.87MJ/kg respectively. From the values it is elucidated that with an addition of Renewable diesel in diesel by volume the calorific value decreases, but is in between the diesel and Renewable diesel. Other way round, it can also be said that more percentage of diesel in Renewable diesel, CV for Renewable diesel was enhanced at the same time.

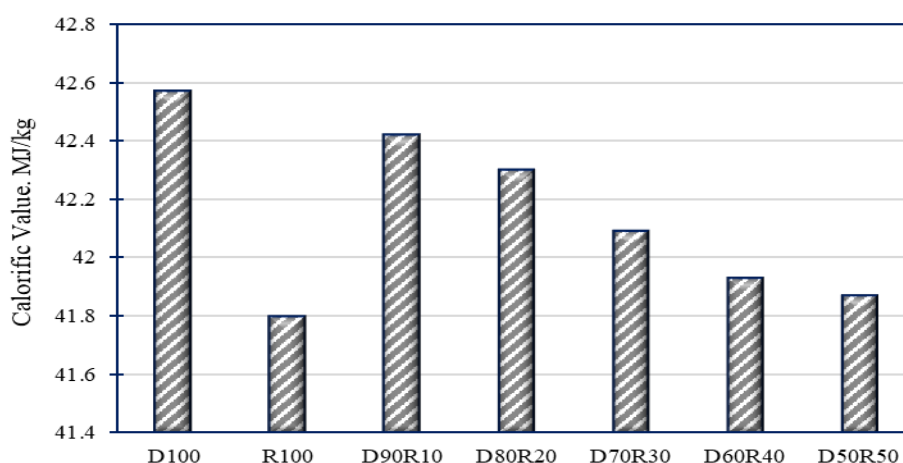


Figure. 4.11. Calorific value variation for test fuel samples

Figure 4.12 shows the CV for the ternary blends in which ethanol (26.8MJ/kg) has the lowest CV. Calorific value of D75R20E5, D70R20E10, D65R20E15, D65R30E5, D60R30E10, D55R30E15 is 40.19, 39.51, 39.01, 39.88, 39.17, 38.92 MJ/kg. It is also

observed, when keeping ethanol percentage constant and increasing R100 percentage by volume, CV of ternary blends is higher than when increasing percentage of E100 by volume.

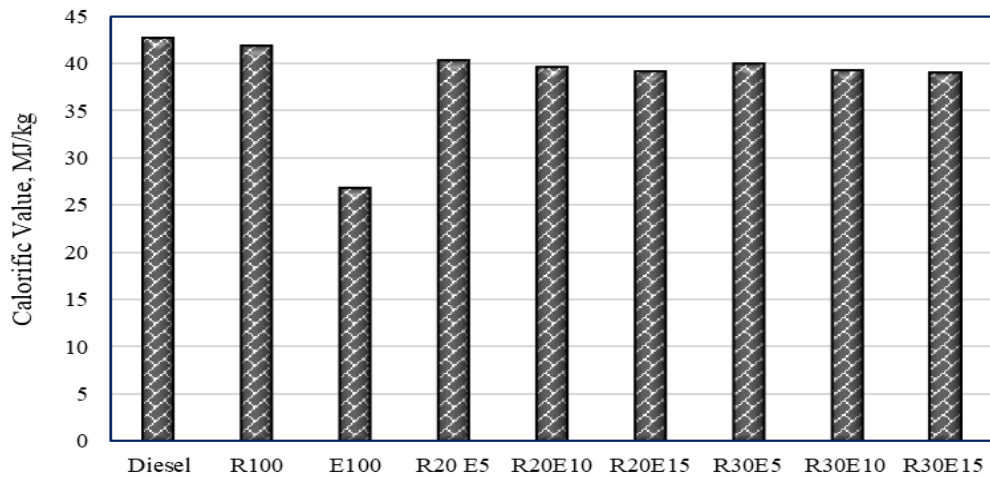


Figure. 4.12. Calorific value variation for ternary test fuel samples

4.4.4 Distillation

Distillation is a process where a compound having different mixtures in it are separated from each other depending upon their boiling temperature. Vaporization and condensation is the basic fundamental for any distillation. Diesel has a hydrocarbon chain length from C-10 to C-16, and its boiling point ranges from 155°C to 345°C [92]. If any fuel comes in a similar range to that of diesel, it has a high probability to replace diesel fuel as per the Brazilian National Agency of Petroleum, Natural Gas and Biofuels (NAP)[217]. In present study, diesel had a boiling temperature of 342°C and Renewable diesel 326°C. From the Figure 4.13 it is observed that the concluding temperature of R100 is 326°C and binary blends lies between 331°C to 336°C, which shows that these fuel samples are volatile in nature which leads to better atomization, better mixing and lesser smoke. On the similar terms when biodiesel's concluding temperature is studied, it is 356°C which shows less volatility, improper mixing, incomplete combustion, more unburnt particles and higher smoke opacity [49,217]. It is also detected at 98% of distillation, renewable diesel's end temperature is lower than diesel, so lesser emission is seen in Renewable diesel due to presence of lesser number of compounds

with higher molecular weight. It is in line with Stella, Koul et al., Panel et al. and Sonthalia et al. [49,68,81,82,218].

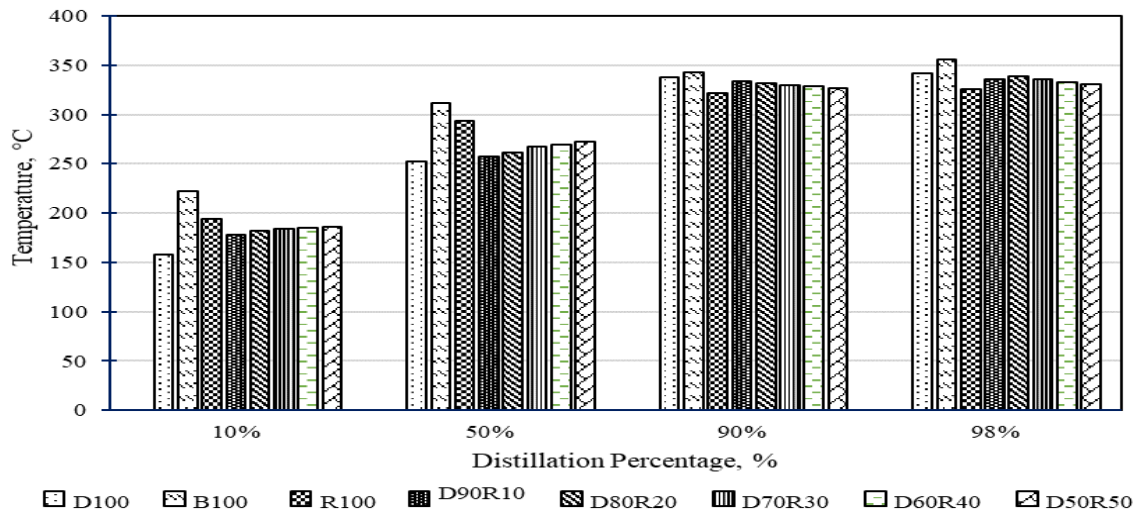


Figure. 4.13. Distillation at 10%, 50%, 90% and 98% recovery for diesel, Renewable diesel, biodiesel and blends.

4.4.5 Cetane Index

One of the crucial factors that determines how well a fuel will ignite and contributes to maintaining the burning process is the cetane index. More the value of cetane index, less is the ID and more is the CD [112]. Reduced ID also corresponds to longer combustion durations, which will result in complete combustion and less smoke and emissions. [73,208]. From the Figure 4.14, it is witnessed that cetane index of the Renewable diesel is highest amongst all the fuel samples which is 66.3 and lowest is of diesel, 46.77. With an addition of Renewable diesel in diesel it is indicated in Figure 4.14 that cetane index of the binary blends increases and is greater than that of diesel. R100 and various binary blends have better ignition probability than diesel. Cetane index for various binary blends like D90R10, D80R20, D70R30, D60R40, D50R50 is 48.52, 50.01, 51.54, 51.7 and 54.4 respectively.

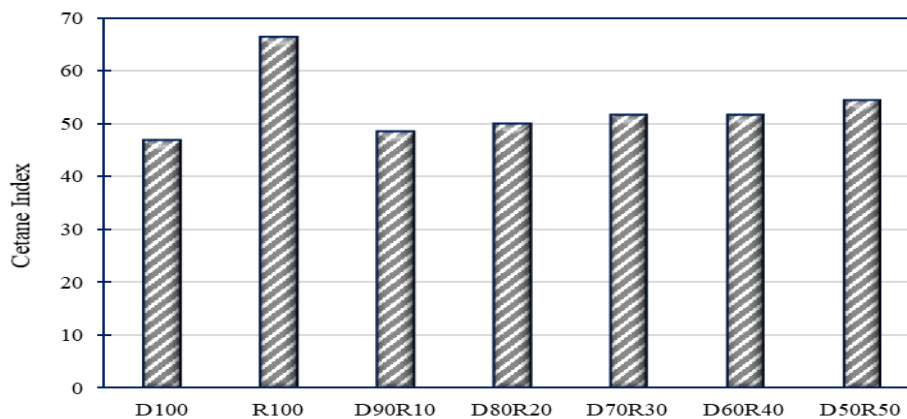


Figure 4.14. Cetane index variation for various diesel, Renewable diesel and binary test fuel samples

In Figure 4.15, ethanol has cetane index of 7.2 which is the least in the test samples. It is also observed that since cetane index of E100 is lowest, so when it is added with Renewable diesel and diesel, cetane index decreases but throughout in all ternary blends, cetane index is more than diesel. Keeping volume percentage of Renewable diesel constant and increasing E100 percentage, cetane index of the blend slightly decreases. However when ethanol percentage by volume is kept constant and proportion by volume of Renewable diesel is augmented, a slight increase in cetane index of ternary blend can be witnessed which is due to the presence of renewable diesel’s higher cetane index and its percentage of share increasing in a blend formed. The results are in synchronization with De-gang Li [208]. Cetane index of R20E5, R20E10, R20E15, R30E5, R30E10, R30E15 is 51.16, 49.08, 47.29, 53.29, 51.21, and 50.06 respectively.

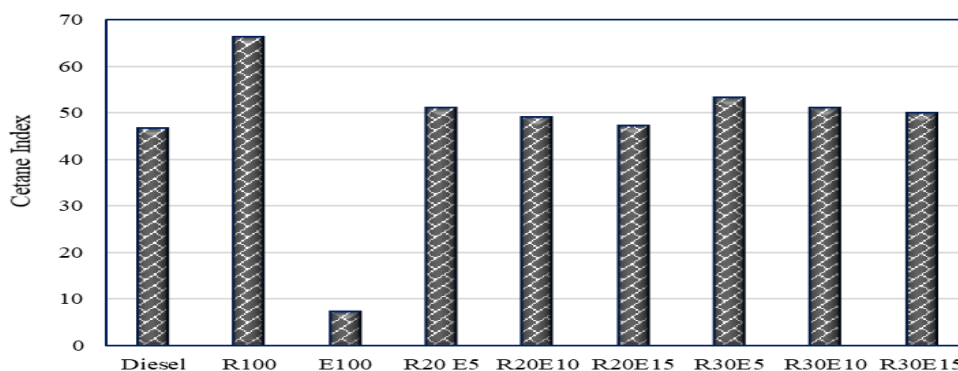


Figure. 4.15. Cetane index variation for diesel, ethanol, Renewable diesel and ternary blends

4.4.6 Cold Flow Properties

For any diesel engine to work in lower temperature regions is also important and for that it is imperative to check the cold flow properties (CFP) of fuel. CFP of the n-paraffin is comparatively lesser than iso-paraffin. However n-paraffin have better cetane index than iso-paraffin. In the present research cloud point (CP) and cold filter plugging point (CFPP) were studied. Both CFPP and CP are the indicators which show the ability of the fuel to be operational in low temperature zones. Figure 4.16 and 4.17 shows the CP of binary blends and ternary blends respectively. From Figure 4.16 it is clearly observed that R100 (-5.883°C) has highest and diesel (-0.81°C) has lowest cloud point. This can also be validated from GC graph (Figure 4.4) as well which shows R100 has isomers which are responsible for its better cold flow properties. Additionally, the CP of blends has increased due to the inclusion of renewable diesel, allowing these blends to run in CI engines with ease in extremely low temperatures. The CP for various binary blends like D90R10, D80R20, D70R30, D60R40, and D50R50 is -1.2 , -1.7 , -2.6 , -2.7 and -3.3°C respectively. The CP of ethanol is -117.3°C for ethanol which is more than Renewable diesel also. So with addition of ethanol in ternary blends, it is seen that CP of all the blends have further improved in comparison to binary blends. CP for D75R20E5, D70R20E10, D65R20E15, D65R30E5, D60R30E10, D55R30E15 is -2.76 , -3.01 , -3.37 , -3.66 , -3.95 , and -4.31°C . As far as CFPP is concerned, both R100 (-14°C) and E100 (-51°C) have lesser CFPP than diesel (-12°C) which is an added advantage for them to work in low temperature areas. With an addition of R100 and E100, CFPP improved. Figure 4.18 and 4.19 shows the CFPP values for binary and ternary blends along with diesel, Renewable diesel and ethanol. CFPP for various binary blends are D90R10 (-12.3°C), D80R20 (-12.8°C), D70R30 (-13.1°C), D60R40 (-13.3°C), D50R50 (-13.5°C). Similarly CFPP for ternary blends are R20E5 (-16.08°C), R20E10 (-16.92°C), R20E15 (-17.81°C), R30E5 (-17.22°C), R30E10

(-18.11°C), R30E15 (-19.99°C). Additionally, it has been noticed that the CFPP has improved more since the inclusion of ethanol.

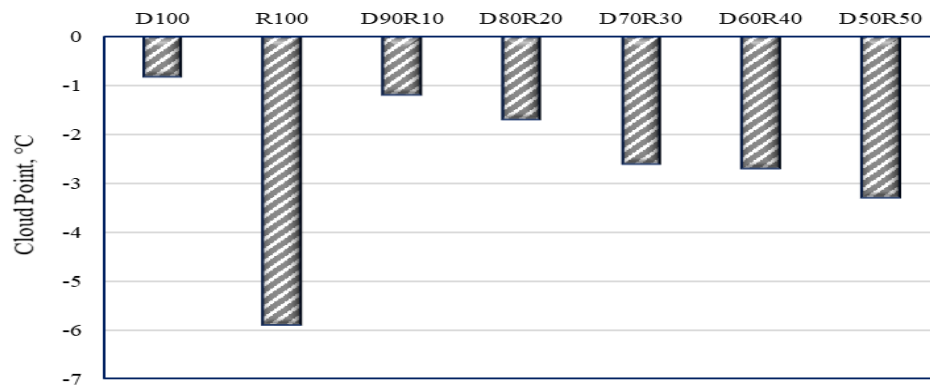


Figure 4.16. Cloud Point variation for various diesel, Renewable diesel and binary test fuel samples

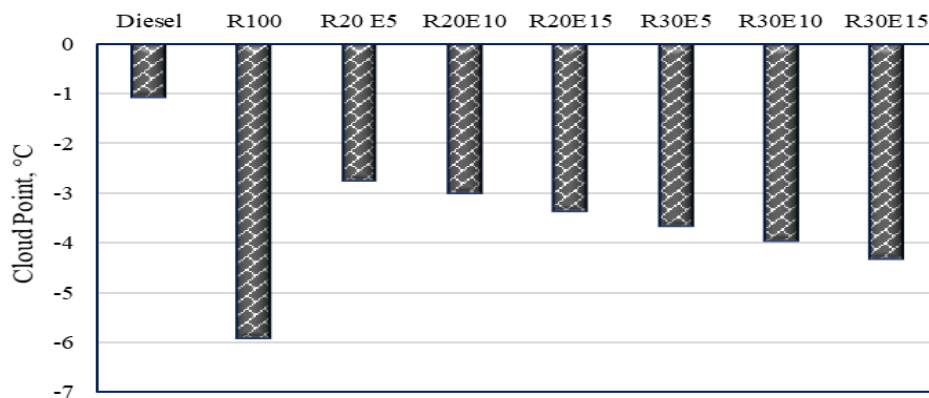


Figure 4.17. Cloud point variation for diesel, Renewable diesel and ternary blends

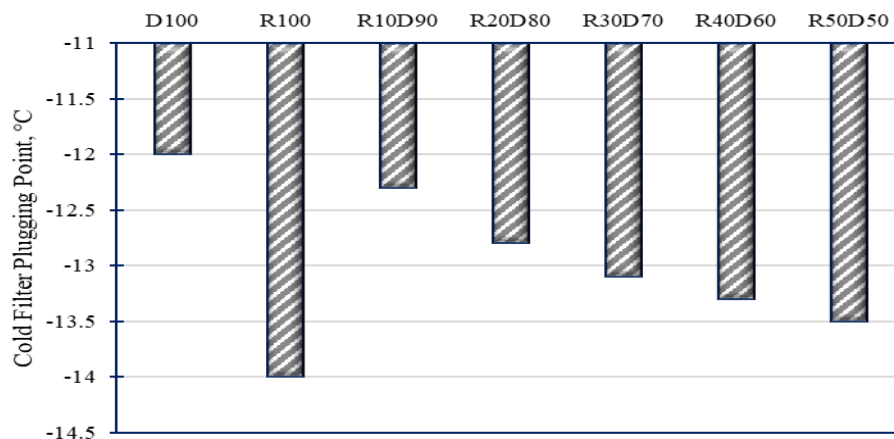


Figure 4.18. Cold filter plugging point variation for diesel, Renewable diesel and binary test fuel samples

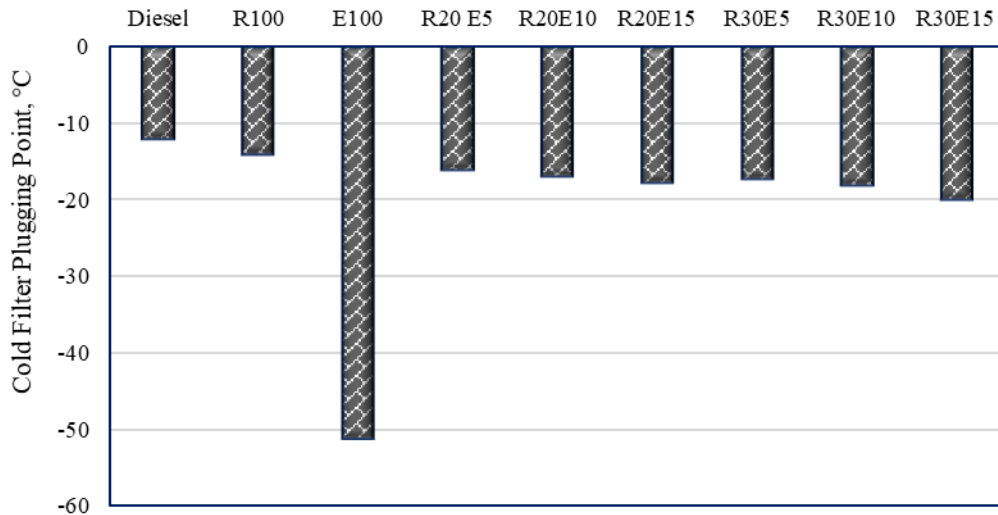


Figure 4.19. Cold filter plugging point variation for diesel, Renewable diesel, ethanol and their ternary blends.

4.4.7 Flash Point

Flash point is an indicator for security. High the flash point, safer is the fuel. When flash point is high, volatility is low and less vapours are formed and chances of catching fire is minimum. As per ASTM D975 guidelines, FP is supposed to be more than 52°C. Diesel has FP of 59°C, R100 has 67.2°C and ethanol has 13.5°C which is lowest. Ethanol has a tendency to evaporate very easily and thus effecting its lubrication property as well. Ethanol is one of the additive that is added in biodiesel (162°C) to improve its FP. From Figure 4.20, with increase in R100 in diesel, FP of blends improved and was in between diesel and Renewable diesel. Similarly with addition of ethanol in ternary blends FP decreased. It is observed from Figure 4.21, when ethanol percentage by volume is kept constant and R100 percentage is increased, FP increased but vice-versa when R100 is kept constant and E100 percentage is increased.

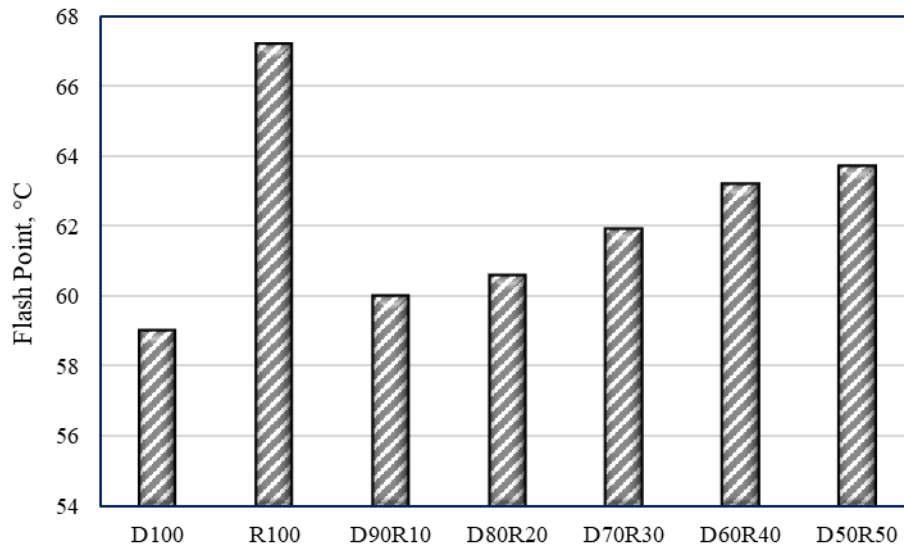


Figure 4.20. Flash point variation for diesel, Renewable diesel and binary test fuel samples

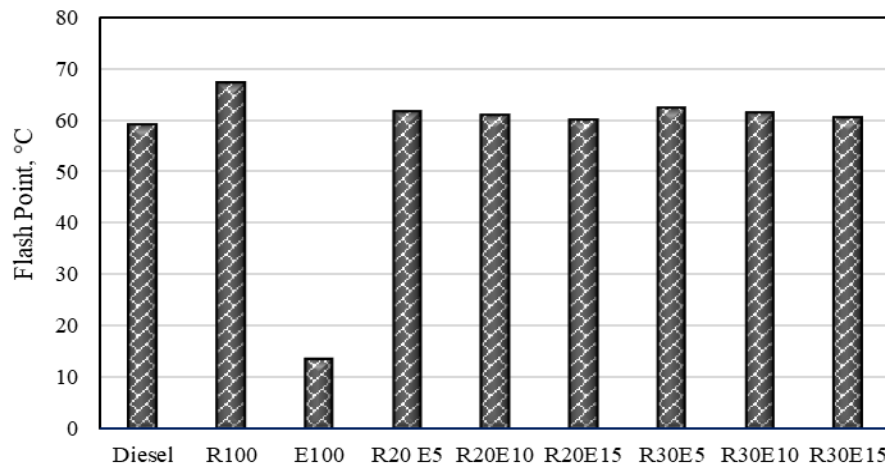


Figure 4.21 Flash point variation for diesel, Renewable diesel, ethanol and their ternary blends.

4.4.8 Lubricity

One of the crucial elements for any engine's effective operation is lubrication.. During hydroprocessing of feedstock, various heteroatoms like sulphur, nitrogen etc., are removed which results in low lubricity. Biodiesel (371 microns) has higher lubricity than diesel (177 microns) and R100 (196 microns). Due to small scar diameter and more unsaturation than R100 and diesel, biodiesel has more lubricity. With the addition of approximately 2% of biodiesel in R100 or D100, their lubricity can be improved [219]. However no such addition was done in present research. From Figure 4.22 with an increase in the amount of R100 in

blends, it has been noted, their lubricity improved. Lubricity of various binary blends like D90R10, D80R20, D70R30, D60R40, and D50R50 is 178.7, 179.3, 181.6, 182.7 and 183.6 microns respectively.

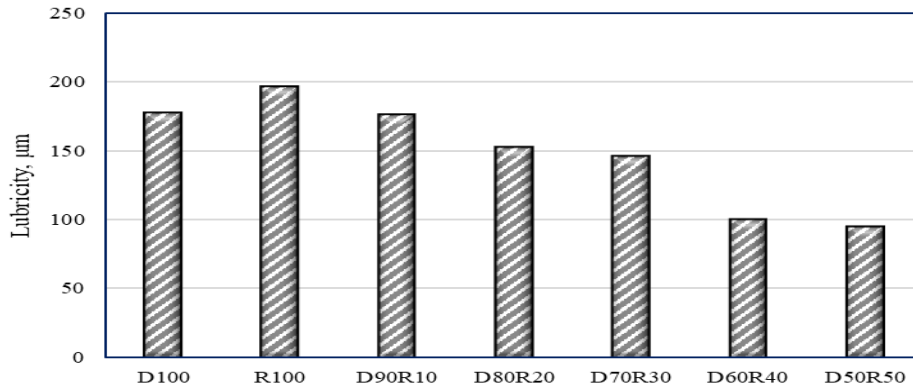


Figure 4.22. Lubricity variation for diesel, Renewable diesel and binary test fuel samples

Lubricity of ethanol is lowest as its vaporization speed is very high. With addition of ethanol, the lubricity slightly decreased. There was hardly any major change found in lubricity of ternary blends to that of binary blends as seen from Figure 4.23. It is in synchronization with Kuszewski et. al [220].

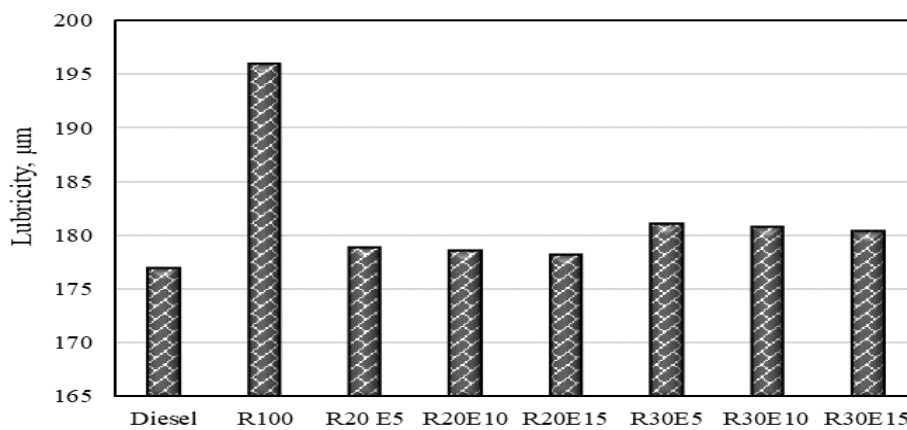


Figure 4.23. Lubricity variation for diesel, Renewable diesel and ternary blends of ethanol, diesel and Renewable diesel.

4.5. Storage Stability and its Effect on Fuel Properties

Fuel has to be stored for the period of six months to one year so that it can be used as and when required. Due to the presence of double or triple bonds, oxygen, and sulphur in its

fuel's molecular structure, as well as physical circumstances like light, air, and temperature, several chemical reactions within the fuel occur during the storage time. In the present work, over the course of a year, changes in kinematic viscosity, density, and calorific value were noted monthly. All these blends made out of diesel and Renewable diesel were kept covered in glass beakers under normal room temperature, away from direct sunlight. Figure 4.24 shows the change in viscosity for twelve months. It is understood that there is a surge in viscosity of neat Renewable diesel and slight increase in blends. It is due to the fact that Renewable Diesel's molecules contain very little oxygen. Out of all fuel samples, R100 had the maximum increase in viscosity, however it was in a specified range as per ASTM D4625 and ASTM D5304 [221]. It is imperative to have viscosity as per ASTM standards, otherwise with high viscosity, fuel filters can get clogged and improper atomization will take place. Kinematic viscosity of R100 has increased from 2.82 to 3.19cSt, D100 (2.47 to 2.76cSt), D90R10 (2.53 to 2.83cSt), D80R20 (2.59 to 2.87cSt), D70R30 (2.62 to 2.91cSt), D60R40 (2.66 to 3.0cSt) and D50R50 (2.71 to 3.06cSt).

The density of the fuel samples also showed a small increase. From the Figure 4.25, maximum increase of 0.42% was seen in R100 which might be because of the existence of small amount of O₂ in its molecular arrangement and lesser number of hydrocarbons and lowest 0.346% in case of D100. Density of other binary blends like D90R10, D80R20, D70R30, D60R40, and D50R50 also increased by 0.42, 0.36, 0.33, 0.35 and 0.37% respectively but it was lesser than that of R100. So, it better to use blends wherein density change is minimum over a year [73,74,180].

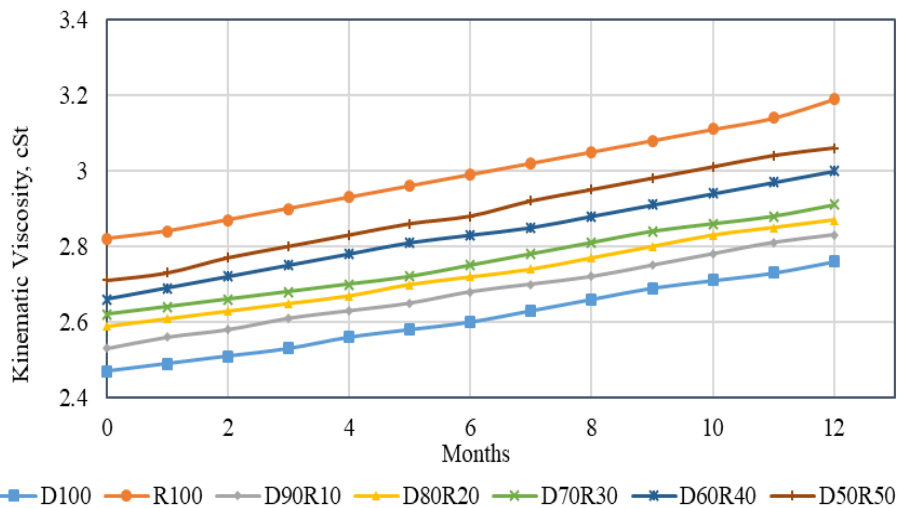


Figure 4.24. Variation in Kinematic Viscosity of diesel, Renewable diesel and their blends for twelve months

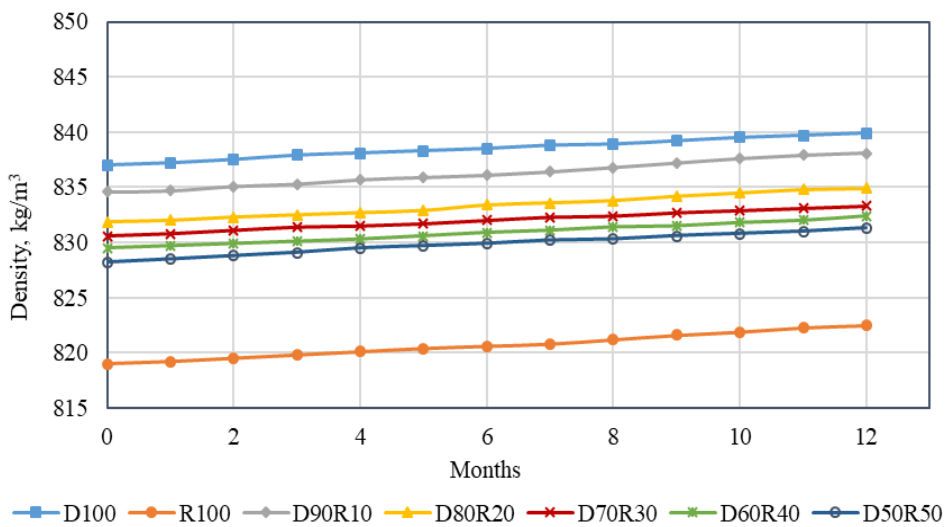


Figure 4.25. Variation in Density of diesel, Renewable diesel and their blends for twelve months

Contrary to viscosity and density, fuel samples calorific value dropped during the course of a year. It is a known fact that CV of biodiesel is very low due to presence of oxygen in it. However R100 (41.8MJ/kg) has better CV than biodiesel (40.9MJ/kg) and at par with diesel (42.57 MJ/kg). CV for diesel is the best amongst all the fuel samples prepared. Calorific value for diesel decreased from 42.57 to 41.77MJ/kg and for Renewable diesel (41.8 to 40.31MJ/kg). This is due to the reason that diesel has no oxygen content in its H-C chain and

R100 has slight presence of oxygen in its H-C chain. For other blends like D90R10, D80R20, D70R30, D60R40, and D50R50, their CV also decreased slightly.

From the studies conducted for viscosity, density and calorific value it can be observed that these blends can be used in operating CI engine even after storing for one year without having any marginal change in their above-mentioned properties.

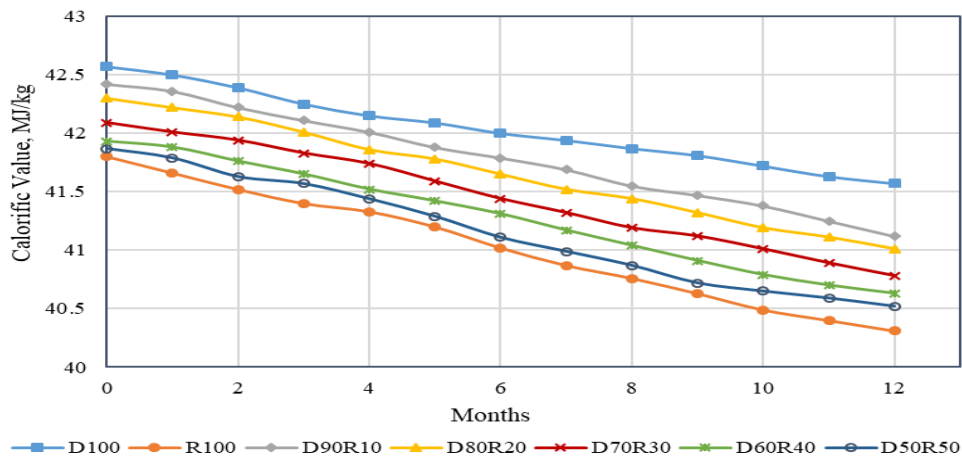


Figure 4.26. Variation in calorific value of diesel, Renewable diesel and their blends for twelve months

4.6. Engine Combustion Characteristics for Diesel, Renewable Diesel and their Blends

Burning fuel with oxygen present causes it to generate heat during the combustion process. If there is complete combustion, it will give less emissions.. Calorific value and cetane index have pivotal role to play in carrying out proper combustion in a CI engine. Various parameters checked during combustion are heat release rate (HRR), Pressure-angle curve (P- θ), peak pressure etc.

4.6.1 Heat Release Rate (HRR)

HRR for various fuel samples is compared to that of diesel in Figure 4.27. It is seen that maximum HRR is for diesel which is 56.14J/°CA and lowest for Renewable diesel which is 45.69 J/°CA at full load. Highest HRR of diesel can be credited due to its higher calorific value and better atomization. It is witnessed that with increase in Renewable diesel percentage,

HRR for the blends decreases. However the values of HRR lies in between the diesel and Renewable diesel. The reason for lesser HRR for binary blends and R100 is its early start, less ignition delay due to high cetane index. In addition to this, more heat is released in diffusion phase than in a premixed phase. Due to shorter ignition delay, fuel quantity burnt is less, hence lesser HRR. Same outcomes were attained by Sugiyama et. al [170], Singh et. al [222] and Sonthalia et. al [144].

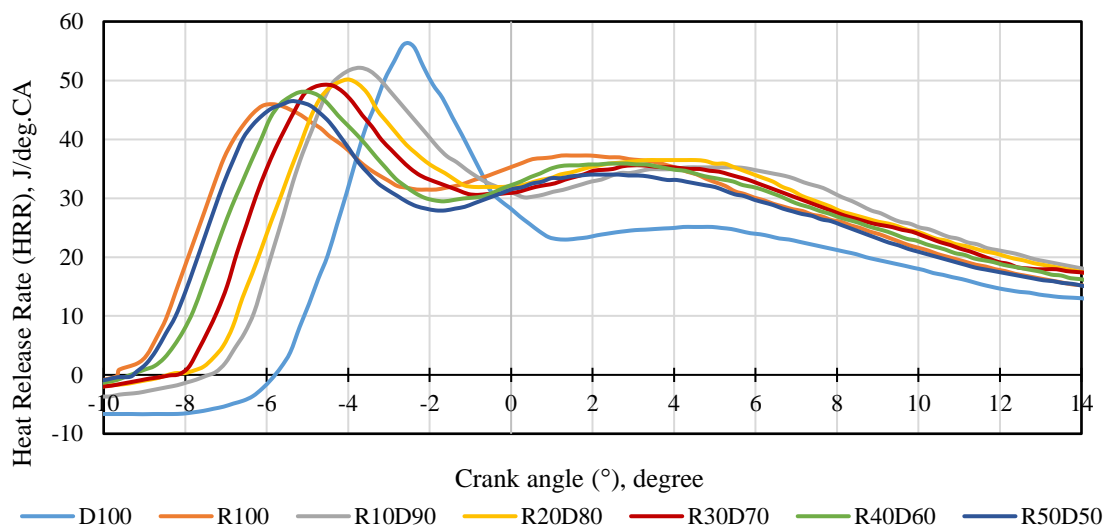


Figure. 4.27. Heat release rate variation of diesel, Renewable diesel and their blends at full load

4.6.2 In-cylinder Pressure (P- θ curve)

The most crucial factor in determining the pressure rise and fall with respect to the combustion phases occurring within the combustor of a CI engine is the inside-cylinder pressure curve. During the first stage which is premixed phase, piston is close to top dead centre (TDC), hence pressure is maximum during that stage. Consequently, during expansion stroke which is the diffusion phase, pressure starts receding and is lowest at the end when piston reaches bottom dead centre (BDC). Pressure transducer is installed on an engine which is described in detail in chapter 3, is used to sense pressure at different crank angles of an engine. In Figure 4.28, it is seen, diesel has highest peak pressure (72.65bar) and lowest is for R100 (66.54bar). Various binary blends like D90R10, D80R20, D70R30, D60R40 and

D50R50 have highest peak pressure as 71.07, 70.28, 69.01, 67.71 and 67.512 bar respectively. From these values and Figure 4.28, it is witnessed that with adding of Renewable diesel, the peak pressure falls because of lesser HRR in pre-mixed phase. Furthermore, a possible additional factor is an improvement in cetane index, which further results in a shortened ignition timing. It is also seen from the smooth curve obtained for Renewable diesel, the pressure is rising gradually.

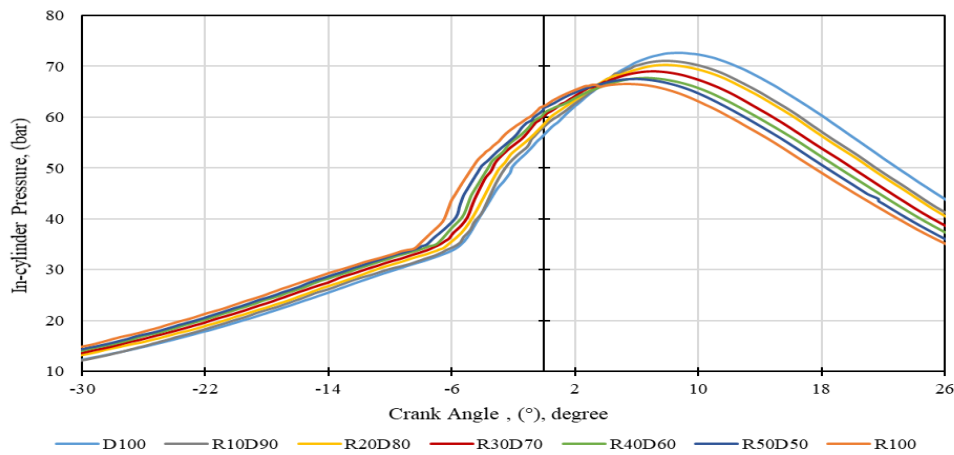


Figure. 4.28. Variation in in-cylinder pressure of diesel, Renewable diesel and their blends at different crank angles at full load

4.6.3. Variation in In-cylinder Pressure at Various Loads

From the Figure 4.29 it is witnessed, with rise in load, pressure is increasing. It is observed that as load rises, additional fuel is pumped into system leads to more HRR and hence pressure will increase gradually. So, with increase in load, peak pressure will increase. From the bar graphs it is clearly depicted that diesel's peak pressure has been high throughout on all loads and Renewable diesel's has been lowest. As explained earlier in section 4.6.1 that due to higher cetane index leading to shorter ID and amount of fuel burnt is less which leads to less HRR and less peak pressure. Also, for renewable diesel, lesser fuel is burnt in comparison to diesel is due to R100's lesser density than D100. On the same reasons, same trend can be seen in blends with higher percentage of Renewable diesel.

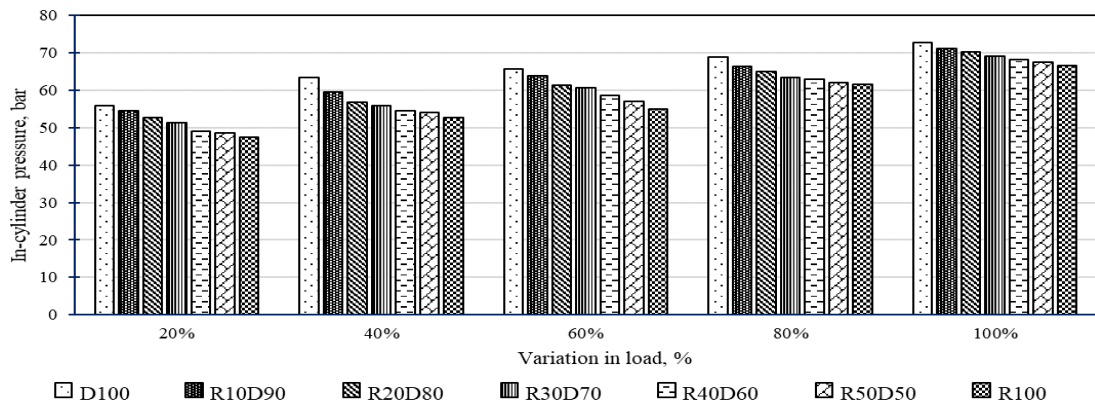


Figure. 4.29. Variation in peak pressure of diesel, Renewable diesel and their blends at varying loads.

4.6.4 Ignition Delay (ID)

The period of time between the moment fuel is injected and the beginning of combustion is known as the ignition delay. Combustion was considered to commence when the heat release turned into positive. Ignition delay is measured in degree crank angles ($^{\circ}$ CA). From the Figure 4.30, it is detected with rise in load, ID is reduced. When load on an engine is increased, more fuel is burnt which releases more temperature and more pressure which increases heat release rate and thus results in a reduced igniting lag. Renewable diesel due to its higher cetane index property has the shortest ID amongst all fuel samples. At full load, ID of Renewable diesel is the lowest due to its high cetane index. Highest being of diesel as its cetane index is lesser than that of Renewable diesel.

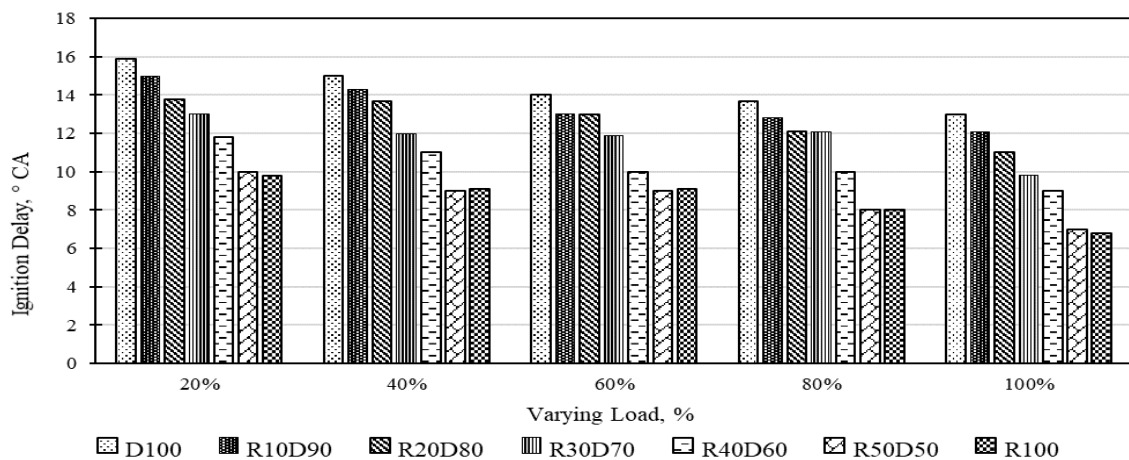


Figure. 4.30. Variation in ignition delay of diesel, Renewable diesel and their blends at varying loads.

4.6.5 Combustion Duration (CD)

Combustion duration is the time period when mass fraction is burnt from 10% to 90% of the mixture [144]. It has been shown that as the load increases, the combustion duration increases leading to increased power output. Fuel quantity likewise rises as the load does and to burn it, the duration for combustion also increases [61]. It is seen in Figure 4.27 that due to shorter ignition delay in Renewable diesel heat released during pre-mixed phase is less and due to accumulation of fuel in diffusion phase heat released is quicker and more than diesel. Due to this quick heat release, time duration for combustion is less. Figure 4.31 shows distinctly that with rising proportion of Renewable diesel, the combustion duration decreases and as we move towards diesel, the combustion duration increases due to diesel's lesser CI and renewable diesel's higher CI. The results are similar to Thiyagarajan et al. [211]. There was an increasing trend seen in CD for all fuel samples while increasing load from 20% to 100%. For diesel it was 42.5 to 62.5°C_A, D90R10 41.5 to 60.5 °C_A, D20R80 40.5 to 58.5°C_A, D70R30 39.5 to 57.5°C_A, D60R40 38.5 to 56.5°C_A, D50R50 37.5 to 54.5°C_A and R100 35.5 to 52.5°C_A.

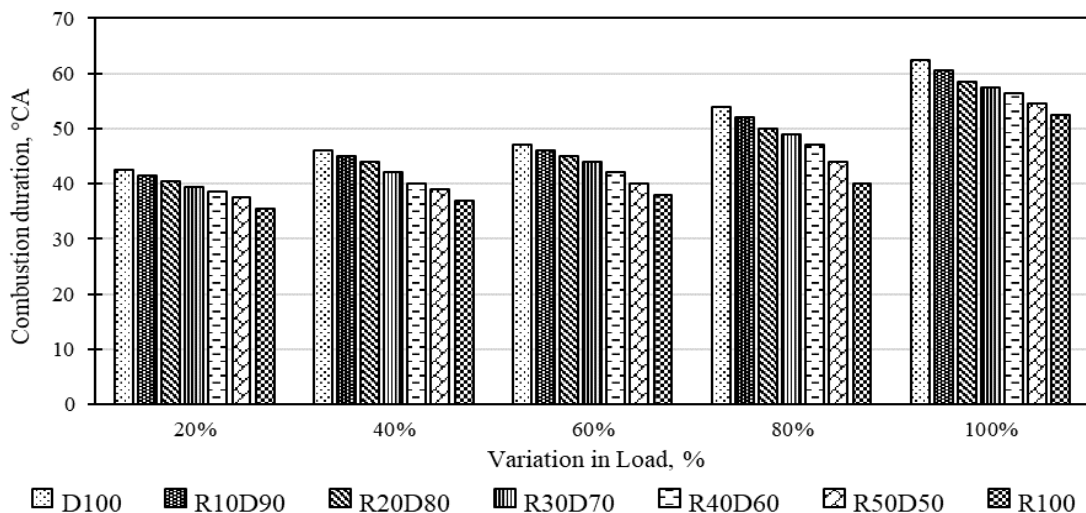


Figure. 4.31. Variation in combustion duration of diesel, Renewable diesel and their blends at varying loads.

4.6.6 Burning Rate at Different Crank Angles

Figure 4.32 shows the various crank angles at which 10, 50 and 90% of heat is released by burning 10, 50 and 90% of the fuel sample. The bar graphs also signifies the crank angle at full load. 10% of CA (10CA) was considered as the commencement of combustion, CA50 showed close of pre-mixed combustion stage and CA90 showed the end of combustion or diffusion phase. It is observed from Figure 4.32 that CA10 is lowest for R100 which implies that due to higher cetane index of R100, ignition starts earlier than D100. Similarly, CA90 occurs earlier for R100 than D100 due to rapid combustion taking place in diffusion stage which is also seen in section 4.6.5. It is observed here that though the cetane index for Renewable diesel is highest amongst all test fuels, however, its rate of burning is lesser than diesel. Furthermore, it is seen that for diesel CA50 is highest and lowest for Renewable diesel which is the reason for lesser HRR and is also verified in section 4.6.1. With addition of Renewable diesel in a blend, CA50 decreases. CA50 for diesel happens at 19.2°C, D90R10 at 18.3°C, D80R20 17.4°C, D70R30 17°C, D60R40 16.6°C, D50R50 15.8°C and R100 14.8°C. The decrease is due to the fact of shorter ignition delay as is also verified in section 4.6.5 above.

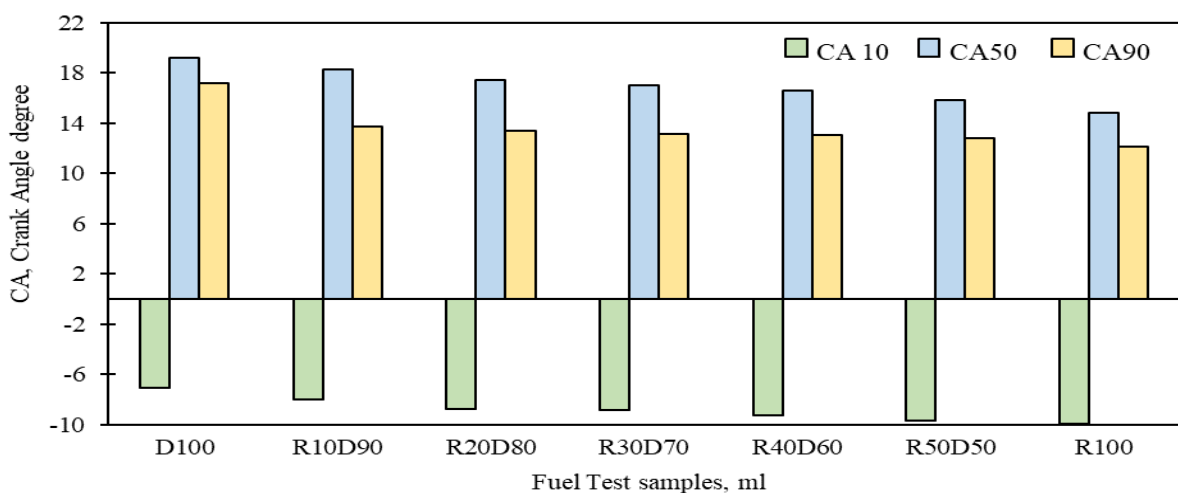


Figure. 4.32. Crank angle versus MFB at full load for various fuel samples

4.7 Engine Performance Characteristics of Diesel, Renewable diesel and their Blends

Engine performance is one of the basic and vital feature for knowing about the engine's efficiency and its operation ability successfully. It helps in optimizing the fuel consumption and helps beforehand in predicting any faults or repairs. In this research work, BTE, BSEC and EGT were studied and are explained in detail with the help of graphs in below mentioned sub-sections.

4.7.1 Brake Thermal Efficiency (BTE)

Using Figure 4.33, it is shown that when engine load increases, BTE also rises. The reason for the increase in BTE at greater loads is because more fluid is pumped at higher loads, making A/F mixture rich, which releases greater energy and results in a higher BTE. Additionally, it has been noted that a blend's BTE falls as the proportion of Renewable diesel increases. This is because of the lesser CV and high viscosity of Renewable diesel. Due to high viscosity of R100, there might not be the proper mixing of R100 with air which releases less heat and leading to lesser BTE [112]. BTE of diesel, D90R10, D80R20, D70R30, D60R40, D50R50 and Renewable diesel is 31.19%, 29.68%, 28.94%, 28.24%, 27.68% and 27.21% respectively. Diesel has the highest BTE and lowest for Renewable diesel. Comparable outcomes are found by Singh et al. [62], Sonthalia et al. [144] and Dolanimiti et al. [178].

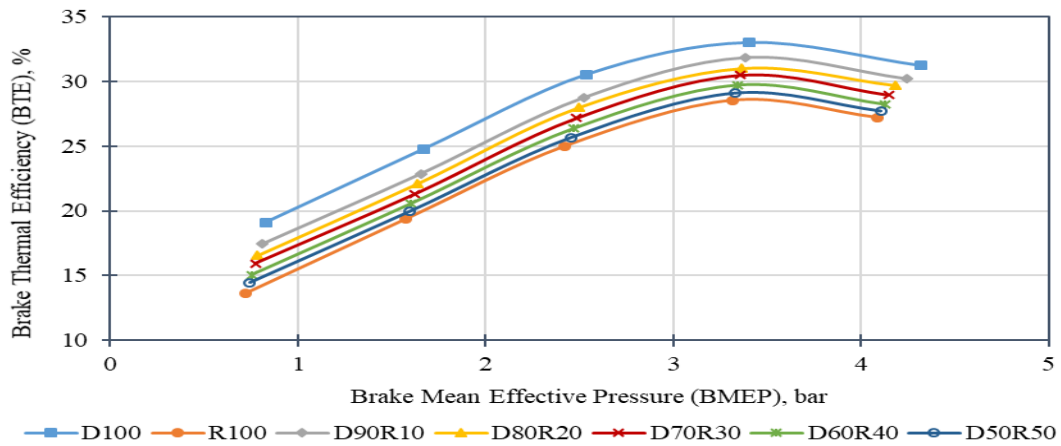


Figure 4.33. Brake thermal efficiency of various fuel samples at varying load

4.7.2. Brake Specific Energy Consumption (BSEC)

Brake specific energy consumption of fuel samples at various loads are shown in Figure 4.34 below. It is seen with increasing load, BSEC of fuel is decreasing which results in higher BTE as discussed in section 4.7.1. With addition of Renewable diesel in the blends, the BSEC is increasing due to lesser CV of R100 in contrast to diesel. Higher calorific value implies lesser brake specific energy consumption. Due to lesser CV, the air-fuel mixture heating value reduces and energy consumption increases [200,222]. It is seen that diesel has lowest BSEC and highest is for Renewable diesel. BSEC at full load for diesel, D90R10, D80R20, D70R30, D60R40, D50R50 and Renewable diesel is 11.54, 11.93, 12.13, 12.44, 12.75, 13, and 13.27MJ/kWhr respectively.

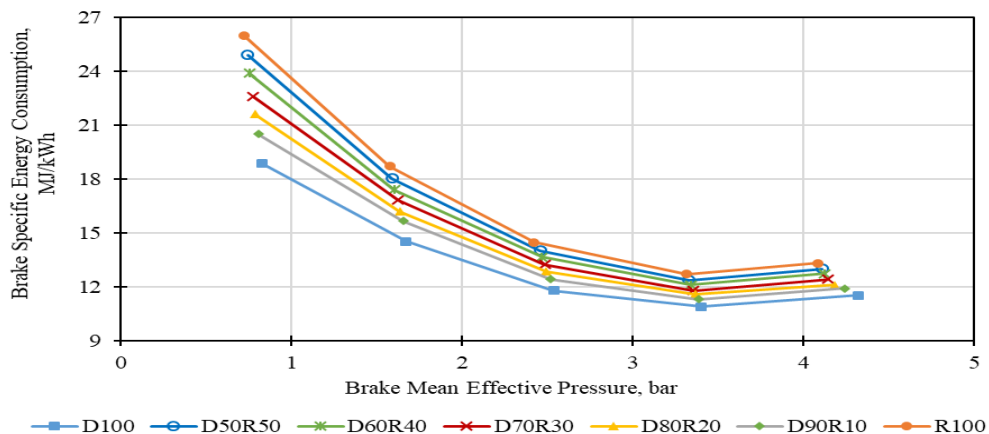


Figure 4.34. Brake specific energy consumption of various fuel samples at varying load

4.7.3. Exhaust Gas Temperature (EGT)

Exhaust gas temperature of diesel, Renewable diesel and their blends is shown in Figure 4.35 at varying load conditions. EGT rises as the load increases. R100 possesses the greatest EGT in compared to diesel. Additionally, it has been found that when the percentage of R100 in blends rises, so does the EGT. The reason can be attributed to the heat release rate which is more in diffusion combustion stage. Moreover the density of Renewable diesel is less which leads to more fuel intake, hence high BSEC and high EGT. In addition to that another reason for higher EGT than diesel can be given to a small amount of oxygen included in renewable diesel, which aids in complete combustion and releases more carbon-dioxide, hence more heat and higher exhaust temperature during end stages of combustion. EGT at full load for diesel, D90R10, D80R20, D70R30, D60R40, D50R50 and Renewable diesel is 416°C, 420.6°C, 426.3°C, 431.4°C, 436.5°C, 440.8°C and 449.5°C respectively.

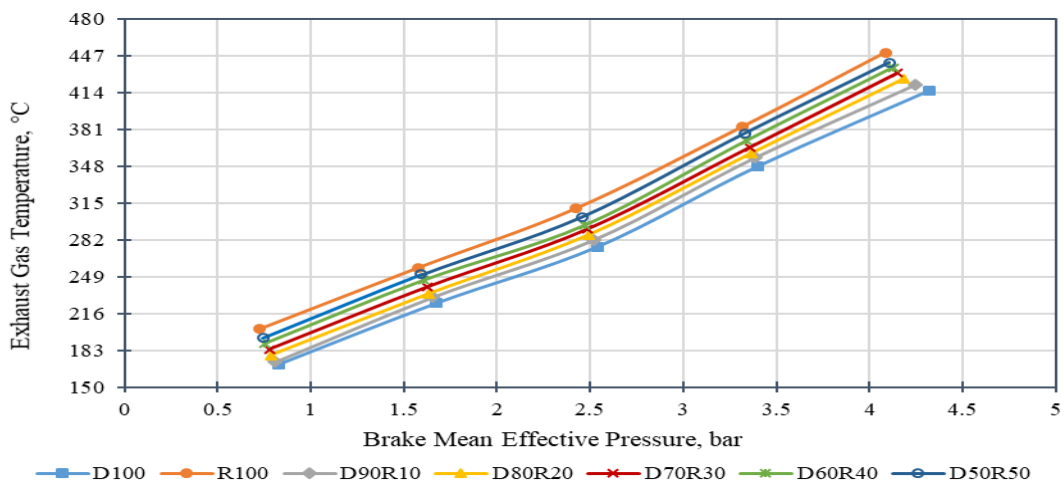


Figure 4.35. Exhaust Gas Temperature of various fuel samples at varying load

4.8 Engine Exhaust Emission Characteristics of Diesel, Renewable diesel and their Blends

This section discusses numerous exhaust pollutants that are produced as a by-product of fuel combustion inside CI engines. Hydrocarbon (HC), Carbon-monoxide (CO), Nitrogen

oxide (NO) and smoke opacity are studied in detail. All these listed emissions are calculated with AVL gas analyzer and smokemeter as discussed in Chapter 3 in detail.

4.8.1 Hydrocarbon Emissions (HC)

Hydrocarbon emissions are shown for various blends at varying load in Figure 4.36 below. Due to the quenching effect, leaner air-fuel mixture, and low flame turbulence, it is observed that HC emissions are maximum for all fuel samples at the beginning of the combustion at the lowest load. However, when load increases, HC emissions fall as a result of increased heat release and improved fuel mixing once combustion starts to sustain [20]. It is observed that highest HC emissions are emitted by R100 (2.75g/kWh) and lowest by D100 (2.501g/kWh). In Figure 4.36 at full load, maximum HC emissions is reduced in case of D70R30 by 14.48%, in comparison to other blends (D90R10: 5.8%, D80R20: 10.32%, D60R40: 7.48% and D50R50: 2.52%). Even though the heat released by these blends is lower than diesel still HC emission was lesser than diesel. The reason for lesser HC emission can be attributed to better combustion because of more paraffinic structure and lesser aromatic structure. As is known that longer hydrocarbon chains require more energy to break the bonds but in case of Renewable diesel, hydrocarbon chain length is smaller, so it requires lesser amount of energy for breaking bonds [178]. With addition of Renewable diesel up to 30% by volume in the blend, the HC emissions have reduced due to reduced heat release capacity. However with increase in Renewable diesel percentage, HRR further decreases and it is unable to withstand combustion leading to increased HC emissions. Also, from Figure 4.36 it is seen that at full load, till D70R30, hydrocarbon emissions have reduced but on further increasing Renewable diesel proportion by volume, HC emission increases. There was an increase of 9.76% seen in case of R100 when compared to D100.

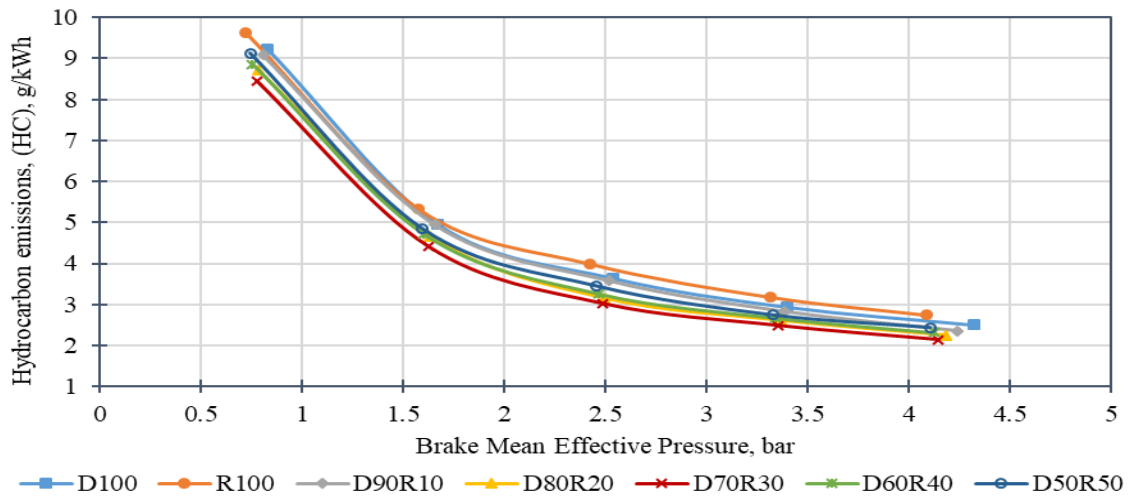


Figure 4.36. Hydrocarbon emissions by different fuel samples at varying load conditions

4.8.2. Carbon-monoxide Emissions (CO)

Carbon-monoxide emissions for different fuel samples at varied load conditions is depicted in Figure 4.37 below. It is seen that till 50% of the applied load, CO is less and after that it starts to increase. At full load, CO emissions are highest. More fuel is fed into the combustion chamber when the engine is completely loaded, keeping the air-fuel mixture rich and lowering the amount of oxygen [182,223]. Due to less oxygen present in rich mixture, incomplete combustion takes place leading to high CO. Amongst all the fuel samples present, Renewable diesel has highest percentage of CO (32.49%). This is due to the reason that lesser amount of heat is released leading to lesser combustion temperature, further leads to incomplete combustion. Hence highest CO emission. For other blends like D90R10, D80R20, D70R30, D60R40, D50R50, CO emission decreased by 5.09%, 9.56%, 13.84%, 12.46% and 6.86% respectively. This is due to the reason that due to presence of more paraffinic structure and higher cetane index, better combustion occurred, which contributed to a fall in CO emissions. Also, it is inferred from experimental results that D70R30 has the maximum percentage decrease of CO whereas, 3.403% CO increase was observed in R100. The trend seen for CO emission is similar to that of HC emission with respect to decrease in emissions till D70R30.

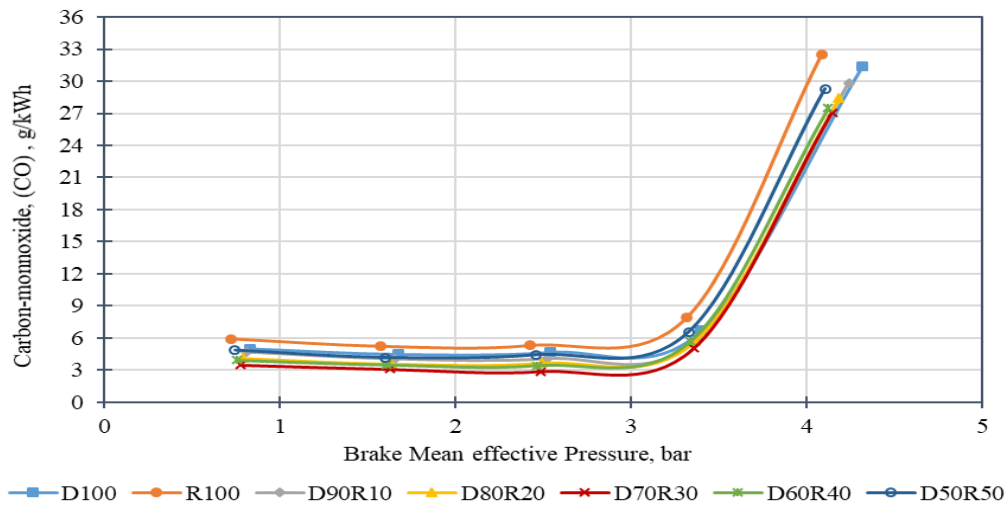


Figure 4.37. Carbon-monoxide emissions by different fuel samples at varying load conditions

4.8.3 Nitrogen-oxide Emission (NO)

With an increase in combustion chamber's temperature at the exhaust, NO also increases. As per Zeldovich mechanism, NO is formed at higher temperature [61,182]. Higher temperatures result in reactant molecules having greater thermal energy and a higher frequency of collisions, which speeds up the reaction. Apart from combustion temperature, NO formation also depends upon time taken for chemical reaction to take place and availability of oxygen. During stoichiometric A/F mixture, NO formation is very high. From Figure 4.38, it is observed that at full load Renewable diesel (3.101g/kWhr) has lowest NO emissions and diesel (4.039g/kWh) has the highest. Renewable diesel has higher cetane index which leads to shorter ignition delay. Due to reduced ignition lag in Renewable diesel and the blends, the time taken to release heat during pre-mixed combustion phase is lesser which leads to low combustion temperature and hence lesser NO emissions. Similar results were obtained by Singh et al. [224]. It is seen that with increased load and increased proportion of Renewable diesel, NO emissions decreases. NO emission for D90R10, D80R20, D70R30, D60R40, D50R50 and Renewable diesel has decreased by 2.86%, 9.98%, 12.66%, 15.6%, and 16.76% and by 23.23% at full load respectively.

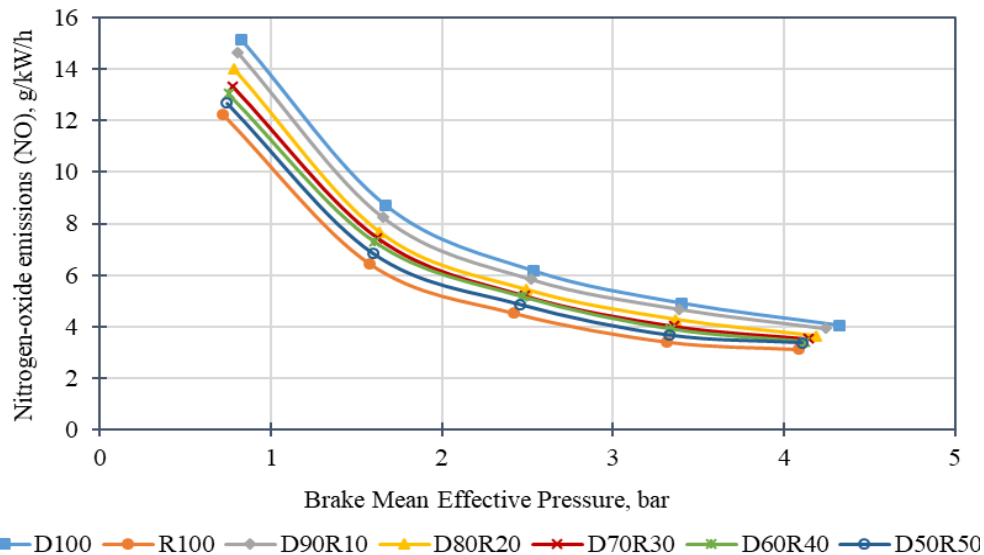


Figure 4.38. Nitrogen-oxide emissions by different fuel samples at varying load conditions

4.8.4 Smoke Opacity

The reason for smoke opacity to arise happened due to incomplete combustion taking place. Figure 4.39 depicts the deviation in smoke opacity for different fuel samples at varying loads when compared with each other. It is learnt that smoke opacity is seen to be decreasing for fuels which have lesser aromatic content and whose diffusion combustion stage is away from TDC [222]. In the experimental results presented in terms of the curves, shows that with increase in load, smoke increases. Smoke opacity of R100 and its blends is lesser than D100. Smoke opacity of D90R10, D80R20, D70R30, D60R40, D50R50, R100 and D100 is 59.1%, 55.9%, 54.1%, 55.8%, 56.3%, 57.8% and 62.4% respectively at full load. Since Renewable diesel has less aromatic structure so smoke formed is less. In addition to it, higher cetane index of renewable diesel and lower premixed combustion stage, air and fuel got sufficient time to mix which resulted in complete combustion and hence less smoke opacity. Comparable outcomes were achieved by Singh et al. [224], Ogunkoya et al. [178] and Prokopowicz et al. [165]. It was also observed that D70R30 blend has the lowest (54.1%) and diesel has highest (62.4%) smoke opacity amongst all fuel samples. Smoke is observed to increase with an increase in renewable diesel beyond D70R30. It is because combustion temperature starts

decreasing due to lesser HRR and is unable to sustain combustion and leads to increase in smoke opacity.

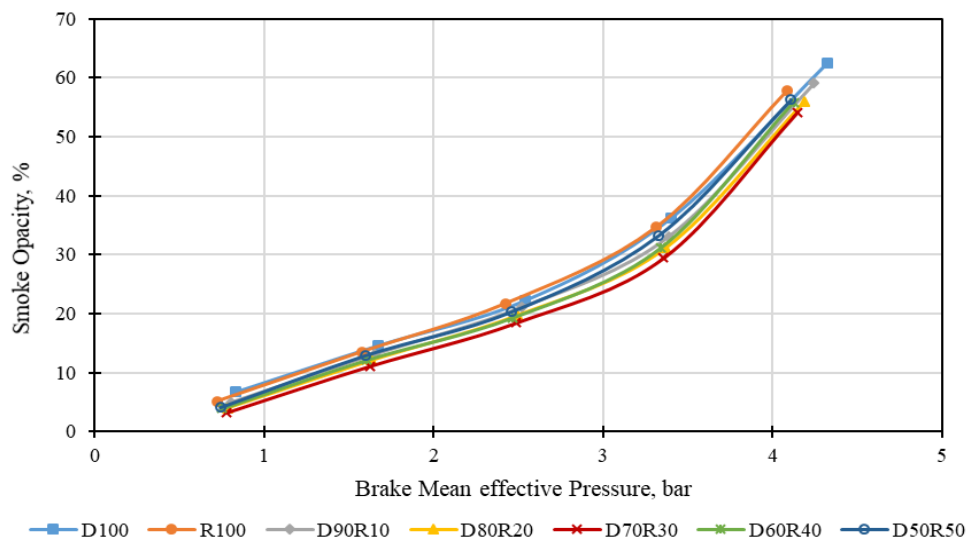


Figure 4.39. Smoke Opacity of different fuel samples at varying load conditions

4.9. Combustion Characteristics of Diesel, Renewable Diesel and Ethanol Blends (Ternary blends)

In earlier section binary blends' combustion, performance and emission characteristics were deliberated on the basis of various tests conducted on CI engines. It was observed that D70R30 has least emissions than diesel but BTE was lower. At the same time D80R20 has lesser emissions but higher BTE than D70R30. To compensate for the loss in BTE, ethanol was explored by making a ternary blend of diesel, Renewable diesel and ethanol. The combustion, performance, and emission characteristics of D80R20, D70R30, R100, and D100 were evaluated and compared to those of 20% and 30% of Renewable Diesel blended with 5%, 10%, and 15% of ethanol by volume.

4.9.1. Heat Release Rate for Ternary Blends

Heat release rate for various ternary blends was studied at peak load. D80R20, D70R30 results were compared to that of R20E5, R20E10, R20E15, R30E5, R30E10 and R30E15.

From the Figure 4.40, 4.41 and 4.42, it is observed that HRR for ternary blends is more than binary blends (D80R20 and D70R30). As the concentration of ethanol has increased, HRR has also increased. It is realized that maximum heat release has been with 15% of ethanol and this was higher than that of diesel. HRR for D100, R30E15 and R20E15 is 56.13J/°CA, 59.83J/°CA and 61.74 J/°CA and. Comparable outcomes were derived by Rakopoulos et al. [140] and Wu-goia et al. [225]. The primary physio-chemical properties of ethanol include a low cetane index, which increases ignition lag and shortens combustion period. During premixed combustion stage, due to ethanol's low density and low viscosity, better atomization leads to better mingling which further leads to quick burning and hence higher HRR than diesel. Also, during ignition delay, at some points fuel gets accumulated and many hot spots are created. These hot spots in presence of oxygen present in ethanol helps in combustion process during the flame propagation. Although the calorific value of ethanol is low but ignition delay gives fuel sufficient time to release maximum heat [112].

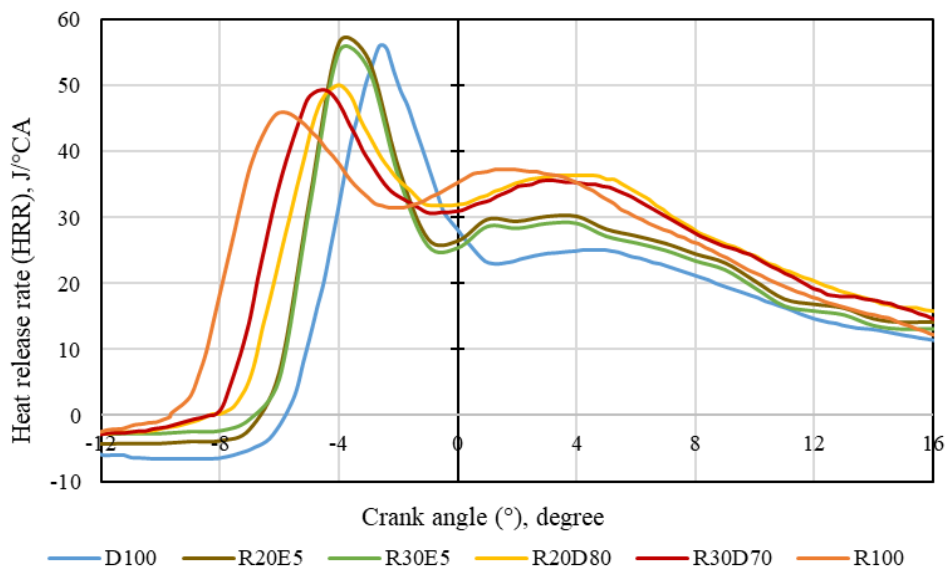


Figure 4.40 Heat Release Rate at peak load with 5% blending of an ethanol

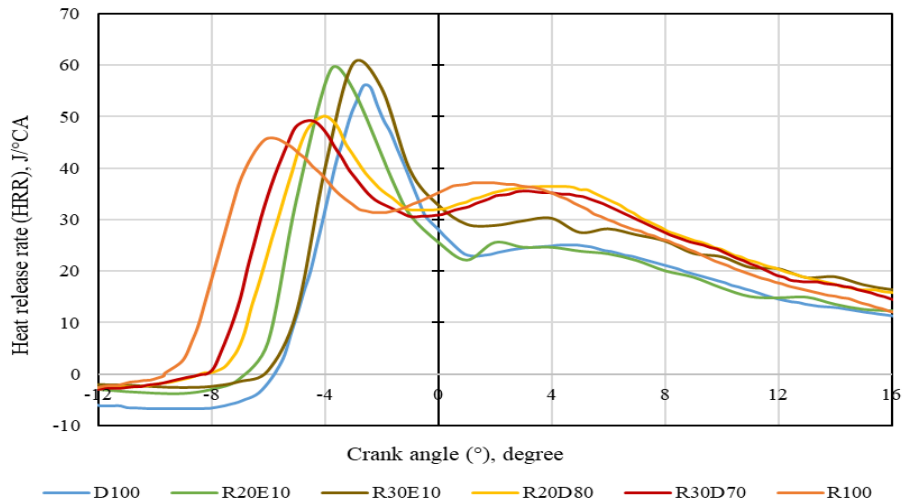


Figure 4.41 Heat Release Rate at peak load with 10% blending of an ethanol

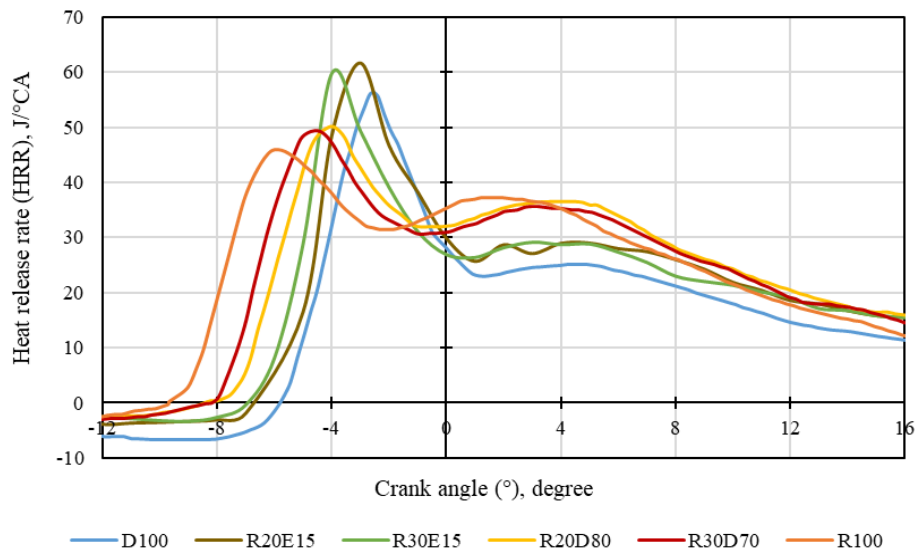


Figure 4.42 Heat Release Rate at peak load with 15% blending of an ethanol

4.9.2. In-cylinder Pressure (P- θ Curve) for Ternary Blends

Figure 4.43, 4.44 and 4.45 below shows the deviation in peak pressure for several ternary blends at the highest load. Peak pressure indicates maximum burning pressure. Peak pressure of ternary blends is seen to be more than binary blends. Since ethanol has a low cetane index and a low ignition delay, combustion time has risen, leading to a rise in pressure rise. Moreover, due to increase in ignition delay, oxygen gets accumulated at various locations inside the combustion chamber which creates hot spots for Renewable diesel and diesel.

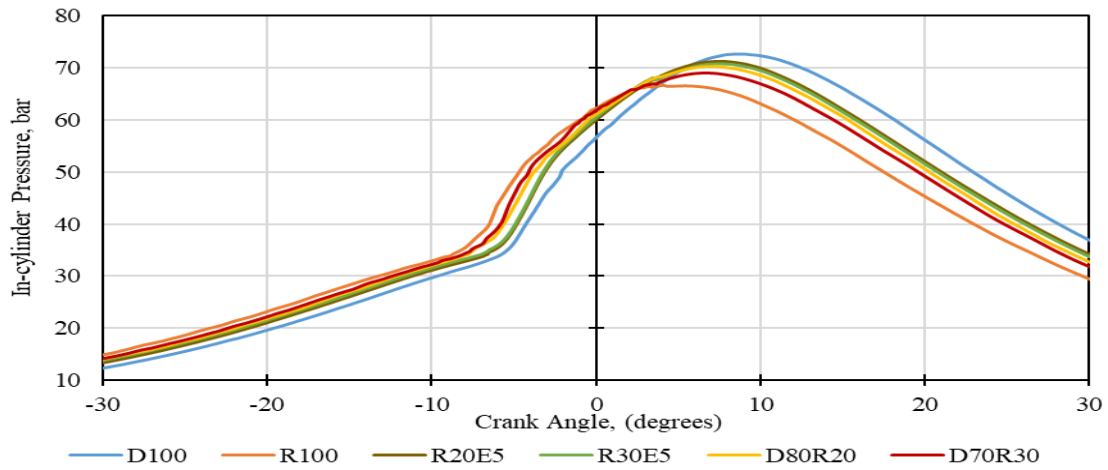


Figure 4.43 Variation in in-cylinder peak pressure at peak load with 5% blending of an ethanol

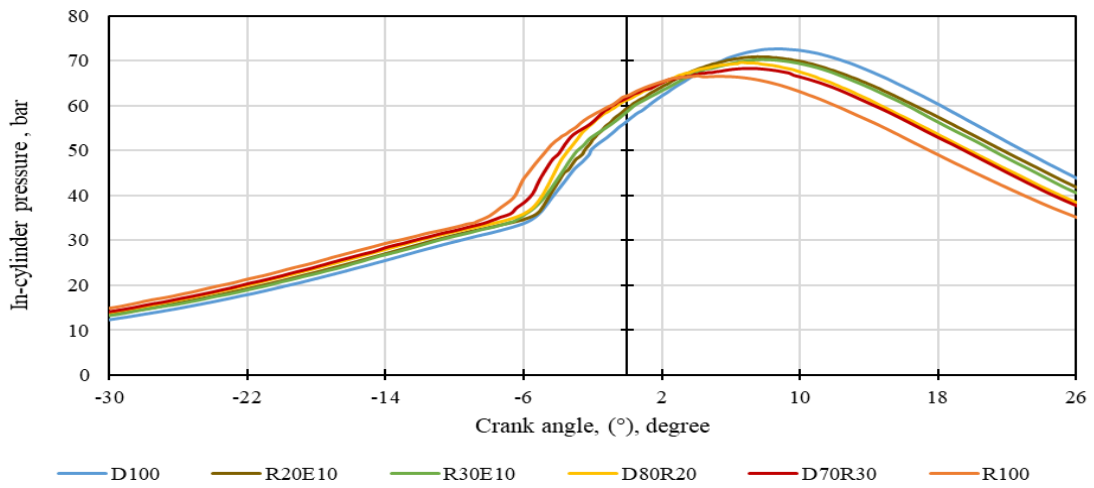


Figure 4.44 Variation in in-cylinder peak pressure at peak load with 10% blending of an ethanol

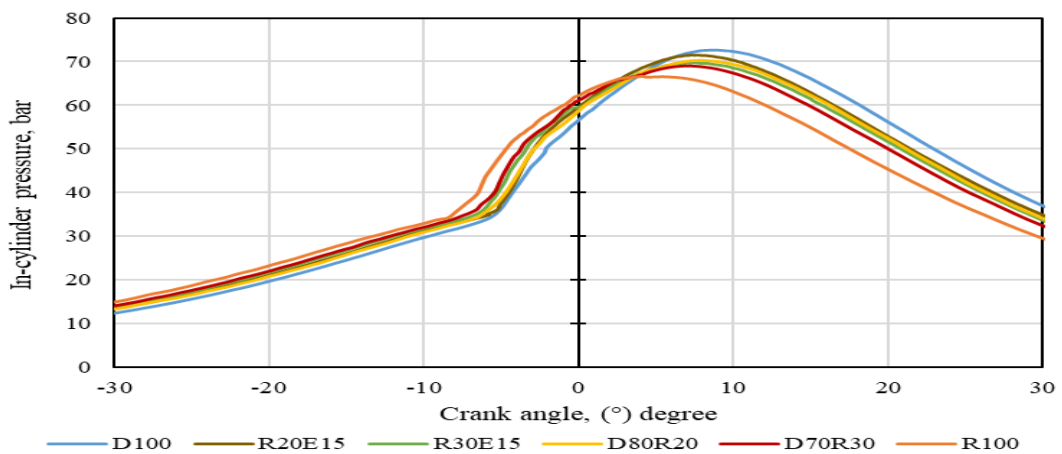


Figure 4.45. Variation in in-cylinder peak pressure at peak load with 15% blending of an ethanol

At these hot spots Renewable diesel and diesel in ternary blends gets more oxygen and enough time to burn which releases quick heat release rate and high peak pressures. However, throughout the combustion process, peak pressure of ternary blends has been lesser than the diesel's peak pressure. The cause is accredited to E100's high latent heat of vaporization which cools down air temperature and in turn reduces pressure. Also, CV of ethanol is lesser than D100 and with increasing ethanol share, peak pressure reduces. Comparable outcomes are in-line with Li et al. [140], Ning et al. [116] and Kim et al. [141]. Highest peak pressure amongst all ternary blends is for R20E5 which is 71.25 bar and for diesel is 72.65 bar.

4.9.3. Variation in In-cylinder Pressure of Ternary Blends at Various Loads

Peak pressure of various binary as well as ternary blends with 5%, 10% and 15% of ethanol is studied at different loads and is represented as a bar graph in Figure 4.46, 4.47 and 4.48 respectively. It is observed in all the figures shown below that with increase in load, peak pressure also increases. Amongst all these fuels, R100 has the lowest peak pressure (66.6 bar) due to its high cetane index which results in less ignition delay, lesser HRR in pre-mixed combustion stage and hence lesser peak pressure. Also, with increase in renewable diesel proportion by volume, keeping ethanol constant the oxygen content present in both renewable diesel and ethanol creates a quenching effect and since CV of both the mentioned fuels is lesser than D100, so the peak pressure reduces. Moreover, high hidden heat of evaporation of E100 leads to reduced temperature, hence reduced combustion pressure. R20E5 has higher peak pressure of 71.25bar than R30E5 has a peak pressure of 70.78bar at full load. Similarly R20E10, R20E15, R30E10 and R30E15 have 70.89 bar, 70.56 bar, 70.23 bar, and 69.62bar respectively. With increase in share of ethanol, ID is increased due to low cetane index, which further increases CD and peak cylinder pressure shift towards TDC which results in decrease of peak pressure. This is in synchronization with Hulwan et al. [215], Geo et al. [112] and Ning et al. [116].

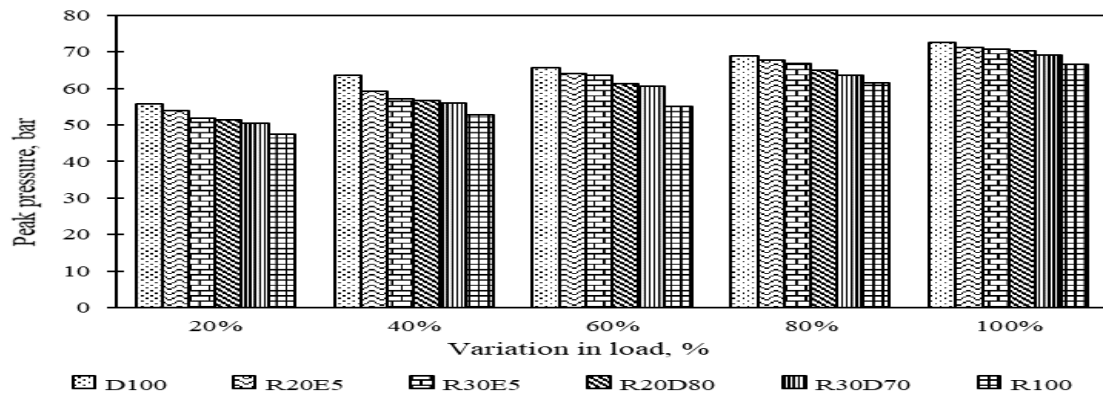


Figure 4.46. Variation in in-cylinder peak pressure at various load with 5% blending of an ethanol

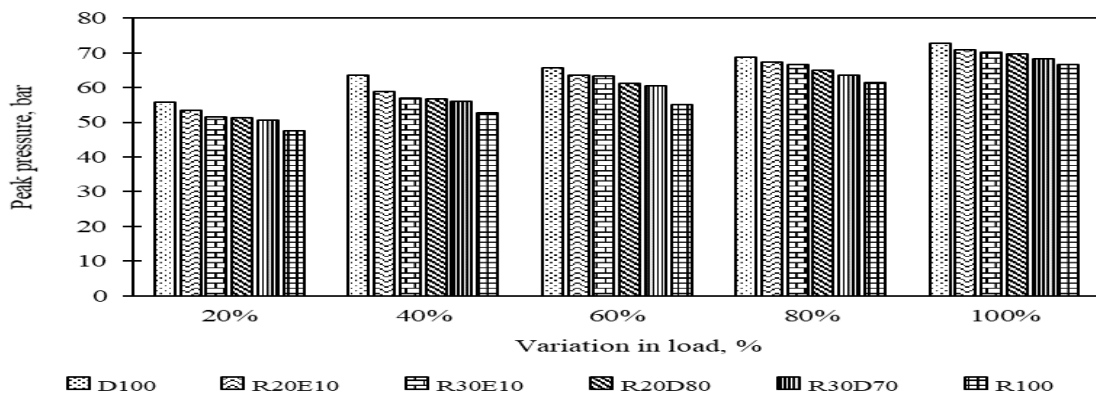


Figure 4.47. Variation in in-cylinder peak pressure at various load with 10% blending of an ethanol

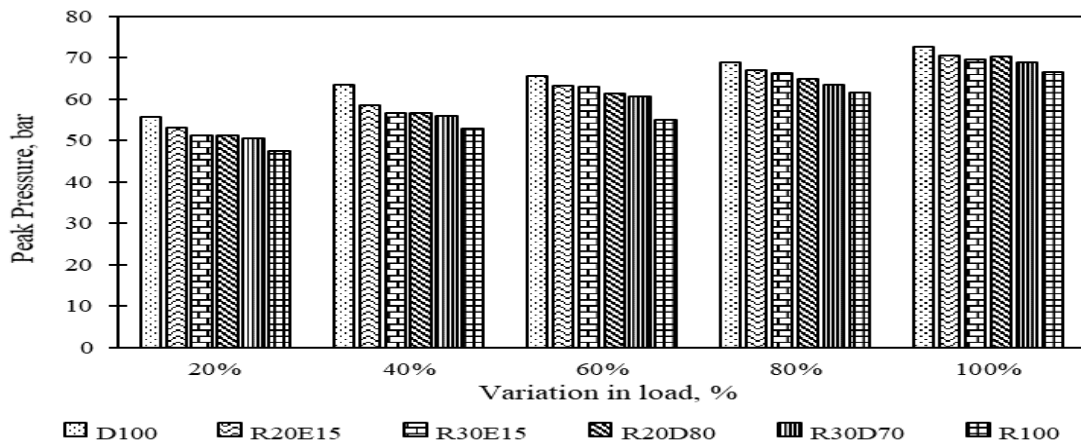


Figure 4.48. Variation in in-cylinder peak pressure at various load with 15% blending of an ethanol

4.9.4. Variation in Ignition Delay for Ternary Blends

Variation in ignition delay for diesel, Renewable diesel, binary and ternary blends is shown at varying loads in Figure 4.49, 4.50 and 4.51. It is observed that with increasing load,

ID for each sample fuel is decreasing. It is also observed that least ignition delay is for Renewable diesel amongst all fuel samples tested at all loads. The reason for this is Renewable diesel's highest cetane index amongst all fuel samples and reduced combustion duration. Highest ignition delay is for R30E15. It is seen that when percentage of ethanol is increased keeping the percentage of Renewable diesel constant, ID increases. This is because of less value of cetane index of ethanol which replaces diesel's share. On same lines, when ethanol percentage is kept constant and Renewable diesel percentage is increased, ignition delay decreases, like ID of R20E5 is more than R30E5. The reason for this decreased ignition delay is because of higher cetane index of Renewable diesel and it is being dominant with increase in its percentage in a blend. This is in-line with Geo et al. [112].

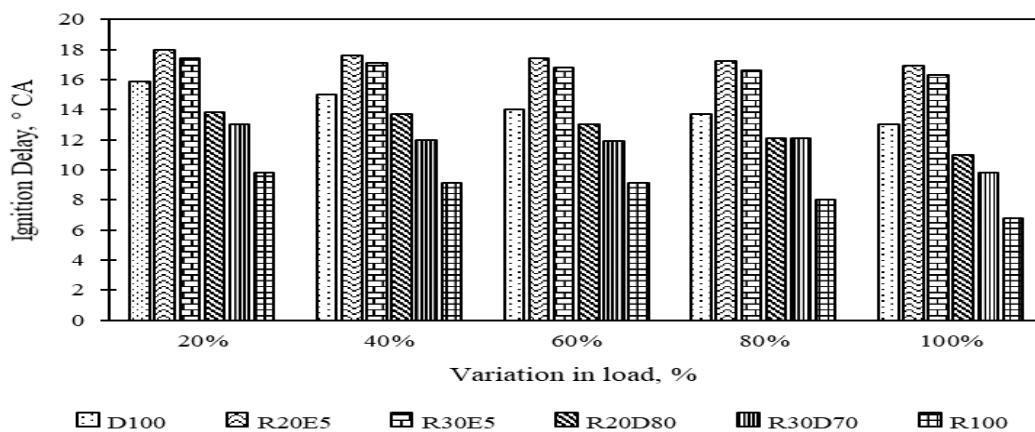


Figure 4.49. Variation in ignition delay at various load with 5% blending of an ethanol

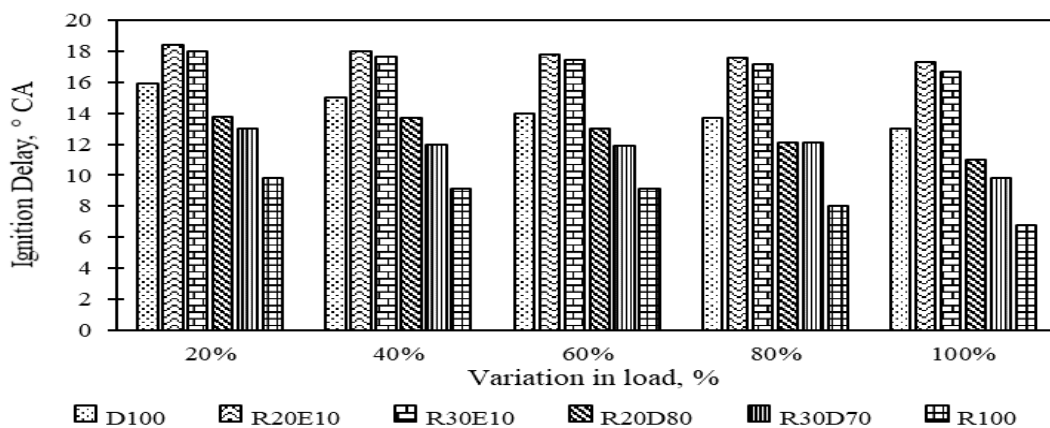


Figure 4.50. Variation in ignition delay at various load with 10% blending of an ethanol

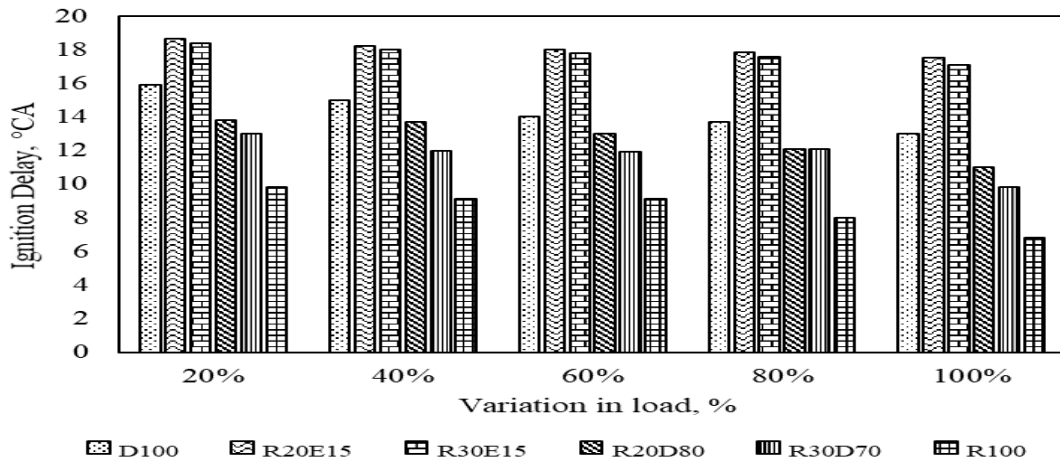


Figure 4.51. Variation in ignition delay at various load with 15% blending of an ethanol

4.9.5. Variation in Combustion Duration for Ternary Blends

From the Figure 4.52, 4.53 and 4.54 it is shown combustion duration for different fuel samples at varying load. From the figures given below, it is clearly depicted that with increase in load, combustion duration increases as this is the time period in which 10 to 90% of the fuel is burnt. Combustion duration at full load is highest for diesel (62.5°CA) and R20E5 (61.4°CA), R20E10 (61.1°CA), R30E5 (61°CA) and R30E10 (60.8°CA) are at par with diesel fuel due to faster diffusion combustion stage. Whereas Renewable diesel has lowest CD (52.5°CA) due to shorter pre-mixed stage and longer diffusion combustion stage. This is also the reason why binary fuels like D80R20 and D70R30 have lesser combustion duration than ternary blends. It is seen, with increasing ethanol and R100 percentage, combustion duration decreases. With increase in percentage of ethanol which replaces diesel percentage by volume, more oxygen is available and hence forms number of hot spots leading to quick combustion and improving diffusion combustion stage, thereby making combustion duration faster [112].

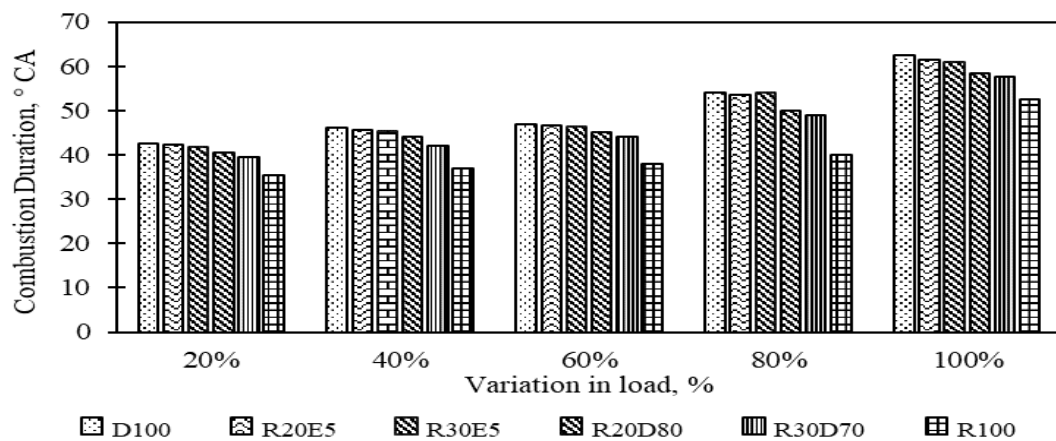


Figure 4.52. Variation in combustion duration at various load with 5% blending of an ethanol

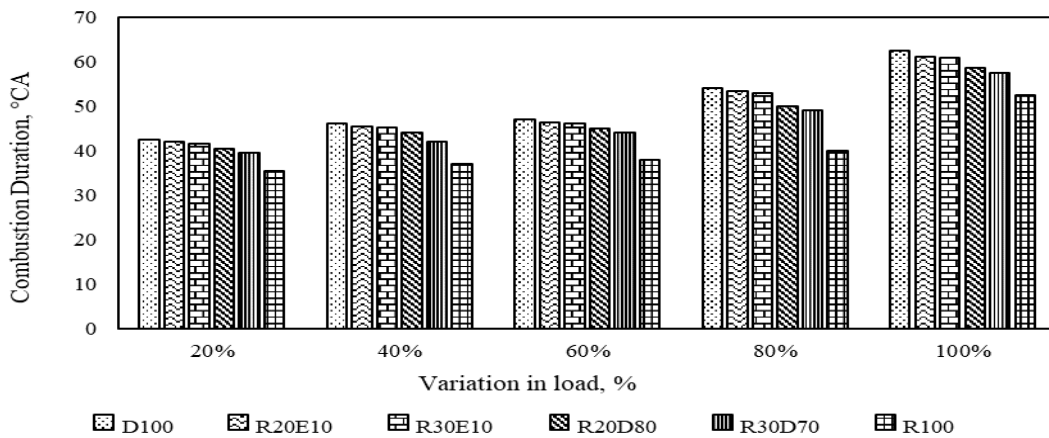


Figure 4.53. Variation in combustion duration at various load with 10% blending of an ethanol

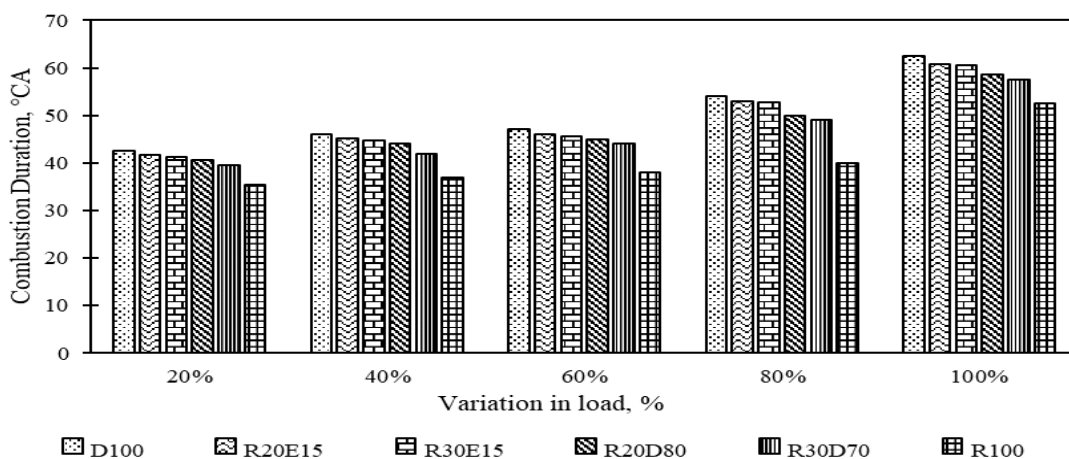


Figure 4.54. Variation in combustion duration at various load with 15% blending of an ethanol

4.10 Engine Performance for Ternary Blends

4.10.1 Brake Thermal Efficiency

Figure 4.55, 4.56 and 4.57 shows variation in BTE for 5, 10 and 15% blending of an ethanol respectively and its comparison to binary fuel samples (D80R20 and D70R30) and with D100 and R100. It is clearly observed from all three figures given below that BTE of the diesel fuel (31.69%) is maximum and Renewable diesel has least (27.21%) amongst all fuel samples. In binary fuels it was seen that with an increase of Renewable diesel percentage BTE decreased however it was more than R100. In addition to this, when binary was made ternary by adding ethanol in it, it was detected that BTE was more in comparison to binary fuels till 10% of ethanol in a blend. Since ethanol has high volatility, less density, temperature of charge slightly goes down because of high hidden heat of vaporization which further increases the premixed air-fuel mixture density. Due to this drop in temperature and low cetane index of ethanol, ignition delay further increases giving more time in the pre-mixed combustion stage and hence BTE progresses [112,215]. Apart from this, it was also observed that when ethanol percentage was increased beyond 10%, its BTE decreased. Delay in combustion increased the charge's heat capacity, raising temperature and lowering density, which was the cause of BTE decline. Due to low density, more fuel is consumed for the same output, hence BTE decreases as shown in Figure 4.47. This is alike to Edwin et al. and Sayin et al. [112,226]. For R20E5, R20E10, R20E15, R30E5, R30E10 and R30E15 brake thermal efficiency is 30.97, 30.8, 28.35, 30.47, 30.12 and 27.9 respectively.

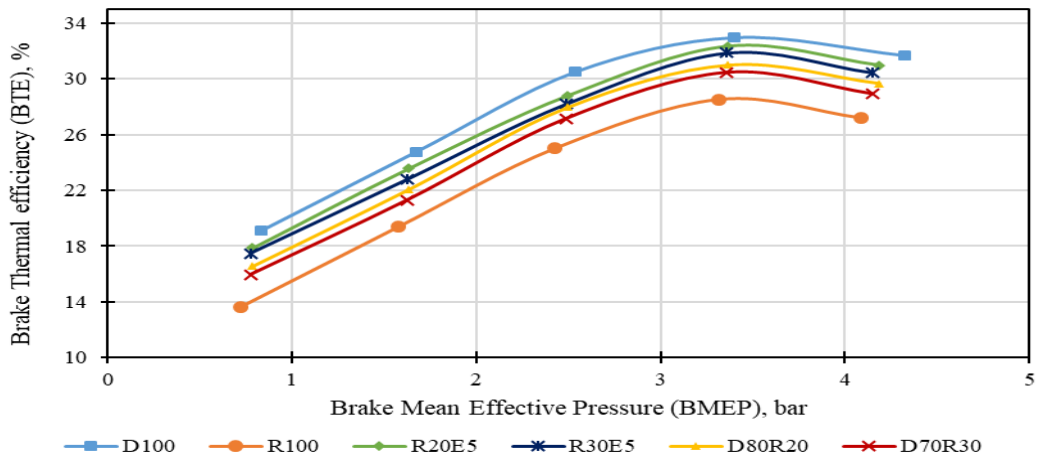


Figure 4.55 Variation in Brake Thermal efficiency at different loads with 5% blending of an ethanol

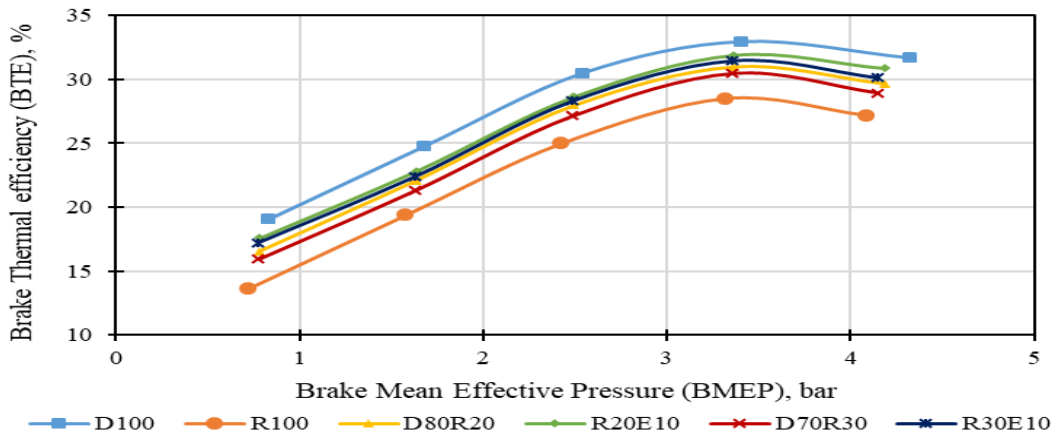


Figure 4.56 Variation in Brake Thermal efficiency at different loads with 5% blending of an ethanol

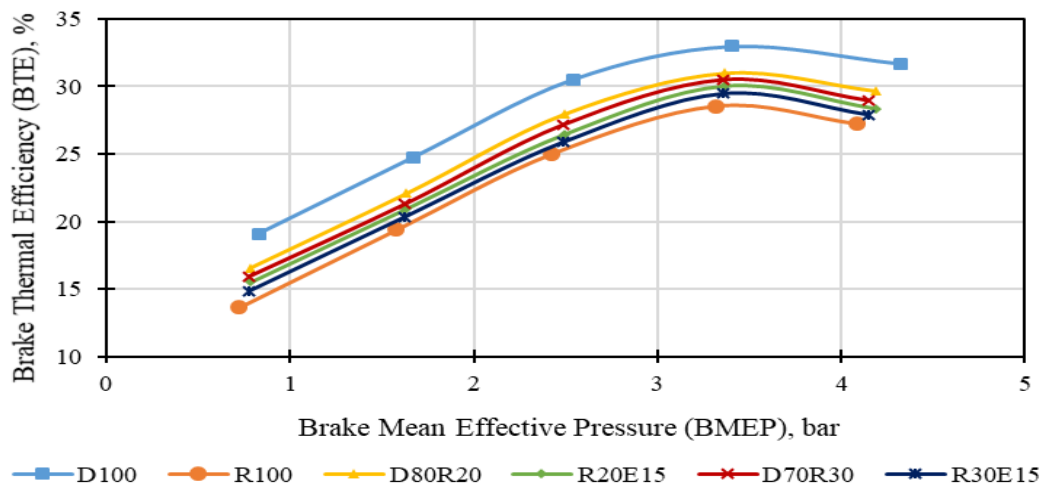


Figure 4.57 Variation in Brake Thermal efficiency at different loads with 15% blending of an ethanol

4.10.2 Brake Specific Energy Consumption of Ternary Blends

Figure 4.58, 4.59 and 4.60 represent the variation in brake specific energy consumption of ternary blends along with D80R20, D70R30, R100 and D100. BSEC of R100 is highest as its BTE is lowest amongst all fuel samples tested. Exactly opposite trend can be seen to what was seen in BTE curve. This is because when less energy is consumed, BTE is higher and vice-versa. R100, D80R20, D70R30 has higher BSEC than R20E5, R30E5, R20E10 and R30E10. Because R100 and E100 have lower calorific value than D100, higher energy or fuel must be used to create the same amount of output on a CI engine as is given by D100. As the percentage of ethanol is beyond 10%, more percentage of fuel is taken up by ethanol replacing diesel so BSEC further increases as fuel becomes leaner. The increase in BSEC is also due to less volatility of ethanol [215].

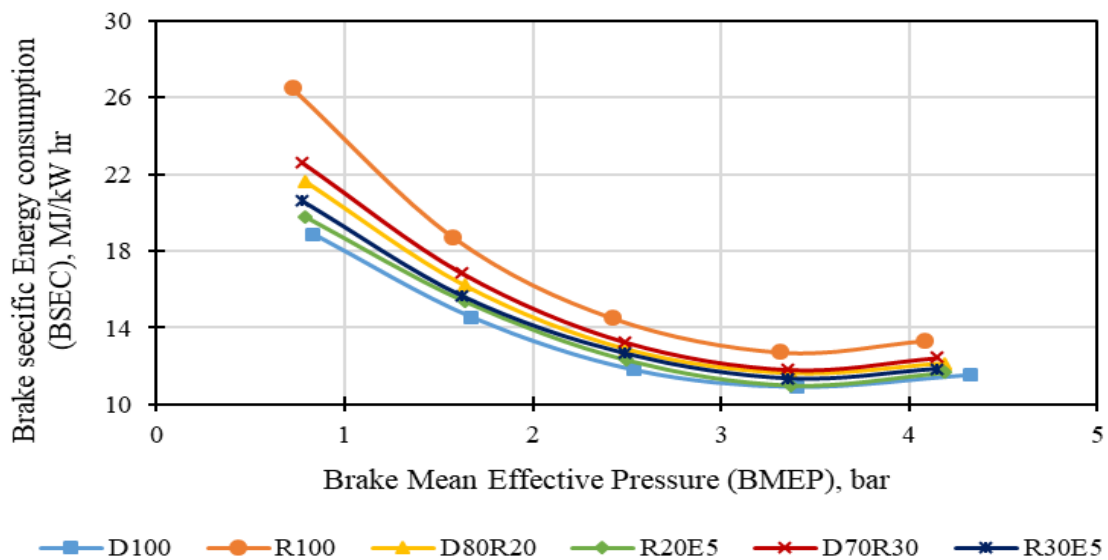


Figure 4.58 Variation in Brake specific energy consumption at different loads with 5% blending of an ethanol

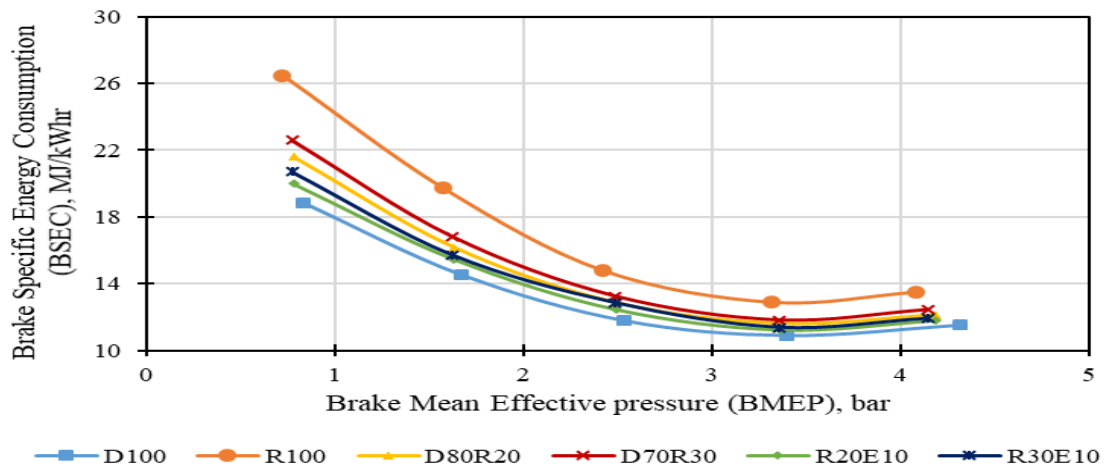


Figure 4.59 Variation in Brake specific energy consumption at different loads with 10% blending of an ethanol

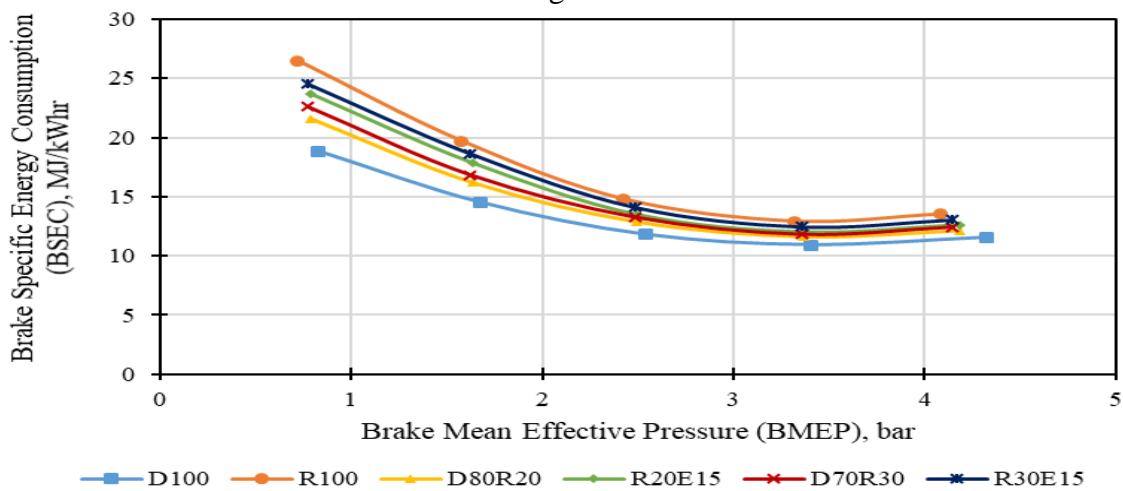


Figure 4.60 Variation in Brake specific energy consumption at different loads with 15% blending of an ethanol

4.10.3 Exhaust Gas Temperature for Ternary Blends

Renewable diesel has highest exhaust gas temperature (449.5°C) and diesel has the lowest, 416°C at full load. From the Figure 4.61 to 4.63 it is observed that with increasing ethanol%, EGT decreases. Decrease in EGT is because of more amount of O₂ present in ethanol and lesser heat release rate in diffusion combustion stage which leads to quenching effect and hence lesser EGT. It was also observed, when percentage of ethanol was kept constant and percentage of Renewable diesel percentage was increased, EGT increased comparatively. The cause is due to a larger heat release rate during the diffusion combustion stage and a lower density, which causes a higher fuel intake and higher BSEC and EGT. EGT

for R20E5, R20E10, R20E15, R30E5, R30E10 and R30E15 is 417, 415, 413, 420, 419, 417.4°C respectively at full load.

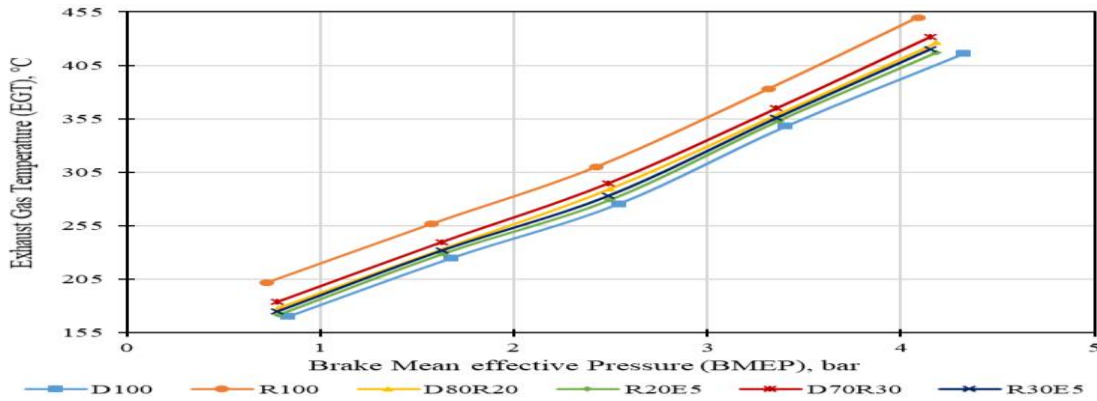


Figure 4.61 Variation in exhaust gas temperature at different loads with 5% blending of an ethanol

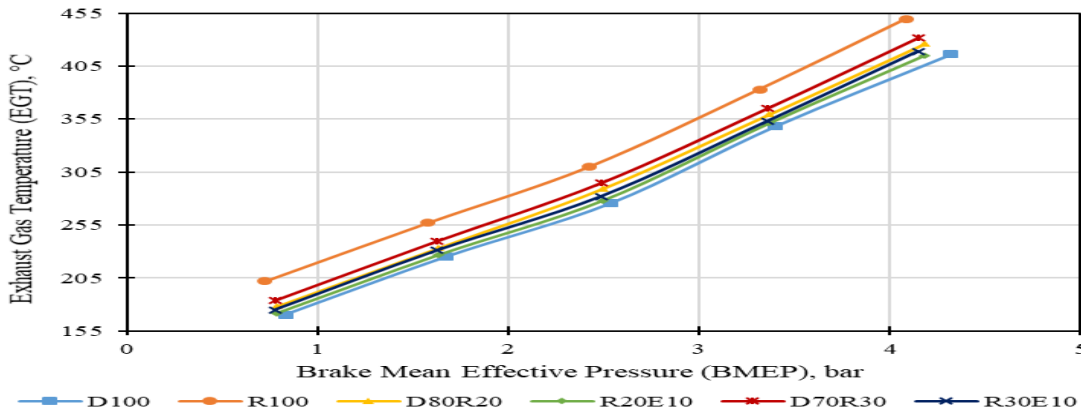


Figure 4.62 Variation in exhaust gas temperature at different loads with 10% blending of an ethanol

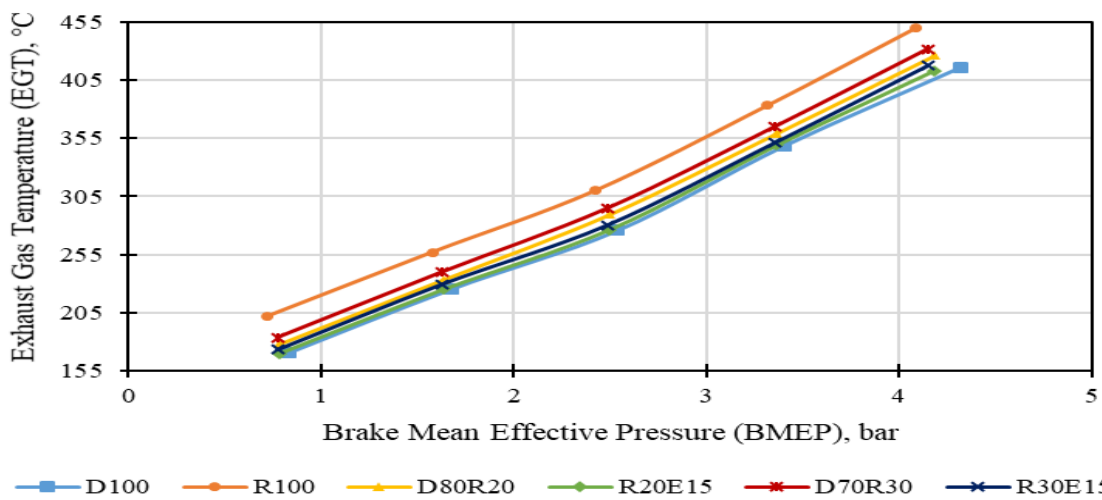


Figure 4.63 Variation in exhaust gas temperature at different loads with 15% blending of an ethanol

4.11. Engine Exhaust Emissions for Ternary Blends

4.11.1 Hydro-carbon Emissions for Ternary Blends

Hydrocarbon emissions produced by various fuel samples at various loads have been represented graphically in Figure 4.64, 4.65 and 4.66 with ethanol as 5%, 10% and 15% respectively. The comparison of ternary blends is done with R100, D100, D80R20 and D70R30. From the graphs it is seen that for all fuel samples, with increasing load, HC emission decreases. This is because, initially the charge is rich and doesn't get enough of oxygen to burn completely because of which flame also can't speed up till end of the cylinder walls and hence HC in the beginning is higher. With increase in load, charge is mixed in better way, gets enough time to mix and burns which leads to increase in temperature and pressure and hence HC emission reduces. It is seen with increasing ethanol% in ternary blends, HC emissions are increasing. This increase can be accredited to low temperature inside combustion compartment due to a presence of ethanol having high volatility which forms quenching layer of unburnt HC. So, due to this low temperature, ethanol is not burnt completely resulting in formation of unburnt HC emission during an expansion stage [112]. So, as ethanol percentage increases, HC emissions also increases. Lowest HC emission is seen in D70R30 (2.139g/kWhr) and highest in R30E15 (3.39g/kWhr). Additionally, it has been found that binary blends emit fewer HC emissions than ternary blends. This is because of the less aromatic structure in renewable diesel, combustion is sustained and complete combustion takes place leading to lesser HC emissions.

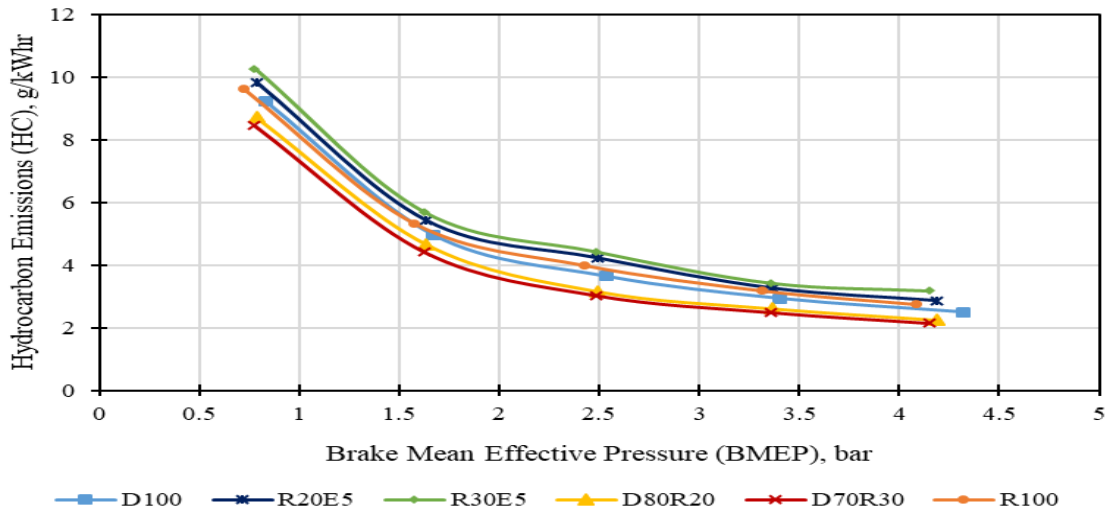


Figure 4.64 Variation in hydro-carbon emission at different loads with 5% blending of an ethanol

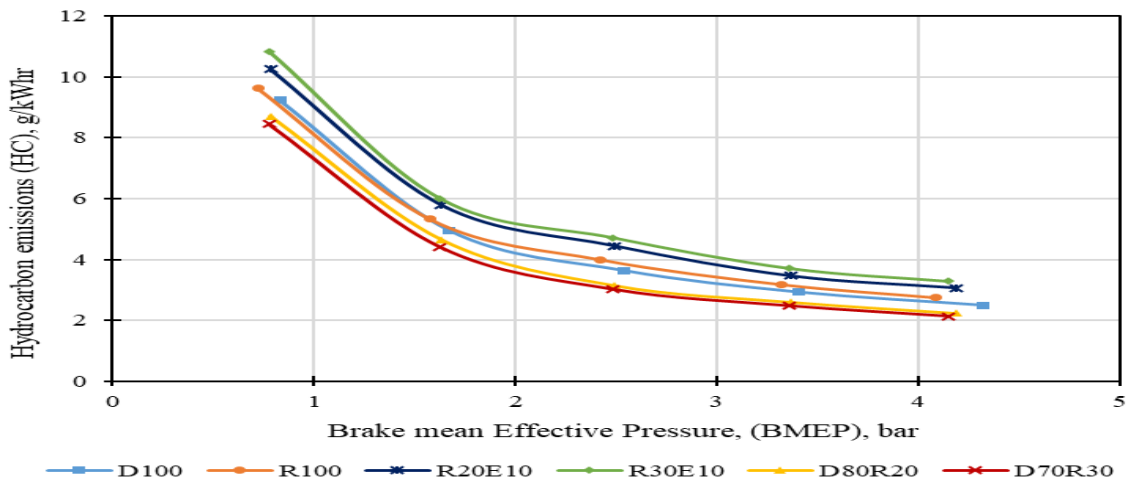


Figure 4.65 Variation in hydro-carbon emission at different loads with 10% blending of an ethanol

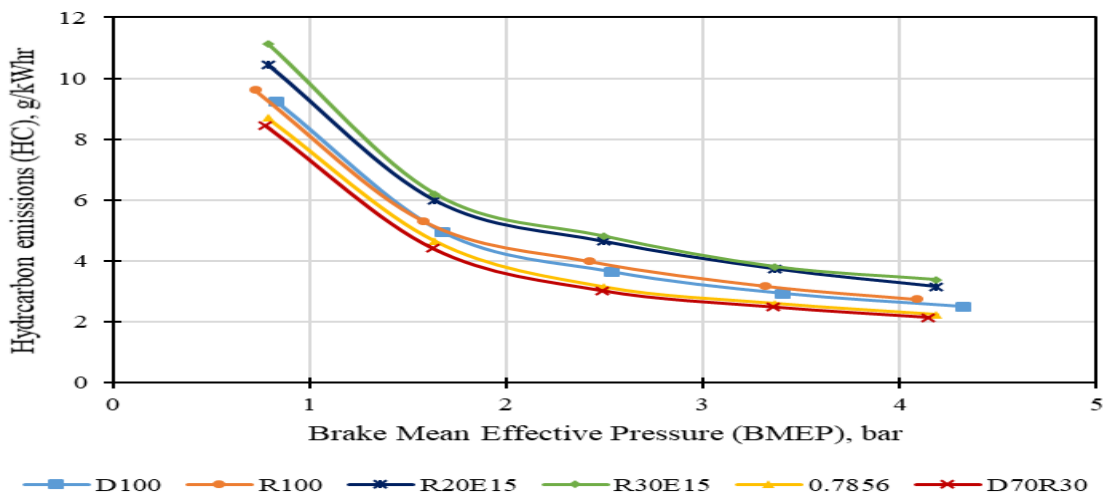


Figure 4.66 Variation in hydro-carbon emission at different loads with 15% blending of an ethanol

4.11.2 Carbon-monoxide Emissions of Ternary Blends

Carbon-monoxide emissions are shown for different sample fuels at varying loads from Figure 4.67 to 4.69 with 5, 10 and 15% ethanol blending respectively and all these are compared with D100, R100, D80R20 and D70R30. In all graphs it is represented that R100 has highest CO emissions due to less HRR leading to incomplete combustion. With the addition of an ethanol in fuel samples, it is observed that CO emission further increases. Since ethanol has very low viscosity, it vaporizes quickly and hence time available for it to mix properly with oxygen is very less during compression stroke and hence leads to incomplete combustion and increase in CO emission. When renewable diesel percentage is increased and ethanol is kept constant, CO emission still increases. This is because oxygen present in both renewable diesel and ethanol creates a quenching layer which leads to low temperature zone and less heat release because there is less time available for combustion to happen completely. Lower CO emission was seen in D70R30 (27.07g/kWhr) and in ternary fuel samples R20E5 (30.41g/kWhr) and R30E10 (30.26g/Kwhr).

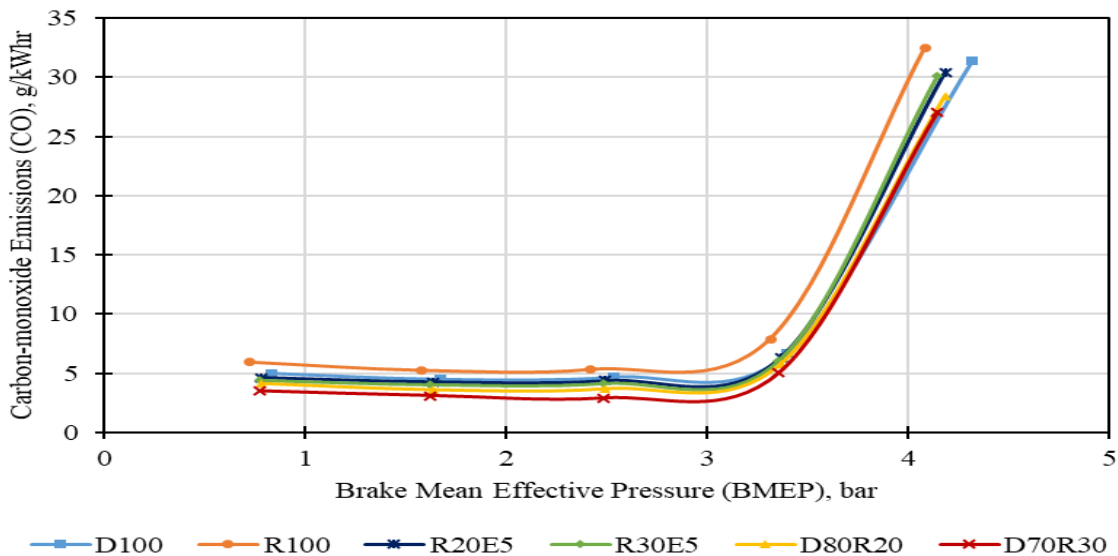


Figure 4.67 Variation in carbon-monoxide emission at different loads with 5% blending of an ethanol

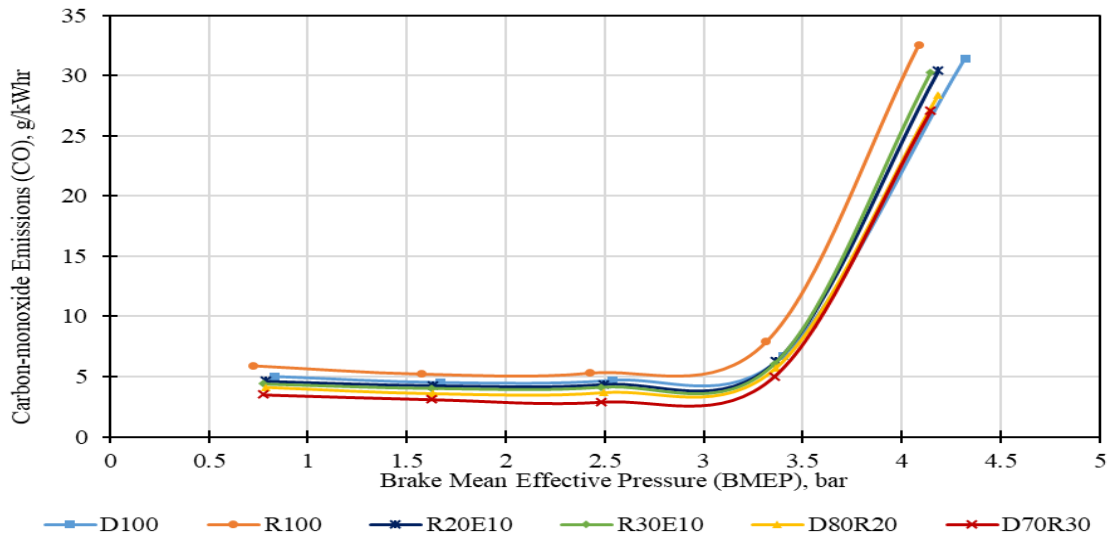


Figure 4.68 Variation in carbon-monoxide emission at different loads with 10% blending of an ethanol

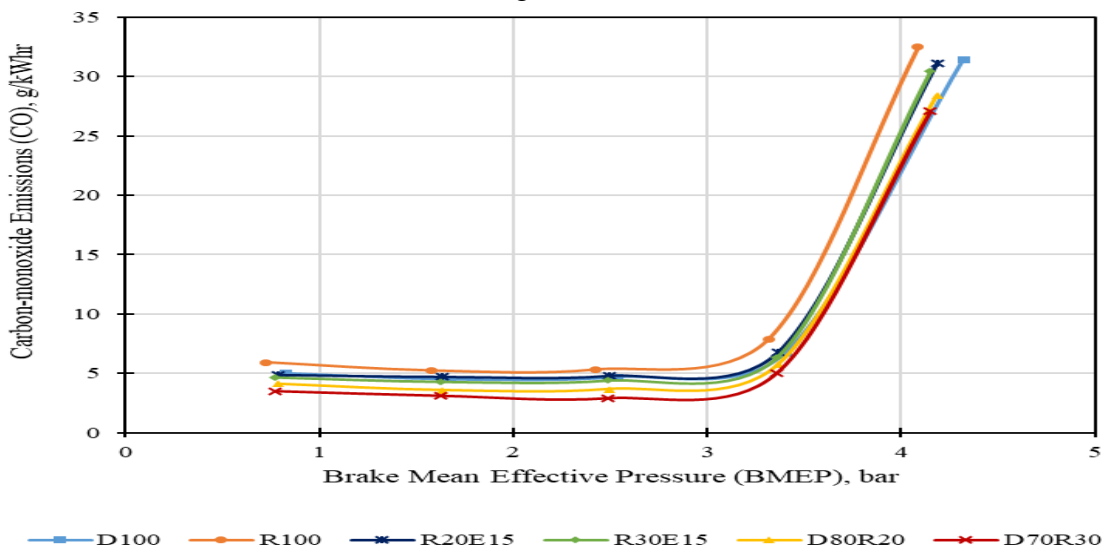


Figure 4.69 Variation in carbon-monoxide emission at different loads with 15% blending of an ethanol

4.11.3 Nitrogen-oxide Emission for Ternary Blends

More the temperature generated in combustion chamber, more will be the NO formed. In Figure 4.60, 4.61 and 4.62 variation in NO emission at various loads is represented graphically. It is observed that diesel has maximum NO emission (4.04g/kWhr) which is harmful for the environment. R100 has lowest NO emission (3.1g/kWhr) due to lower pre-mixed combustion stage which lowers the temperature of combustion chamber and time

available for nitrogen reactions to take place is also less. NO formation declines as ethanol addition increases. Owing to lower CV, more oxygen content and high volatility of ethanol, there is a cooling effect which lowers down the flame temperature. When flame temperature is lowered, it affects the flame propagation as well which lowers down the overall temperature and hence lesser NO emissions. Also more CO formation and lesser heat release rate during expansion stage also leads to decrease in NO formation. R20E5, R30E5, R20E10, R30E10, R20E15 and R30E15 produced 3.46, 3.29, 3.26, 3.06, 3.48 and 3.32g/kWhr of NO during combustion.

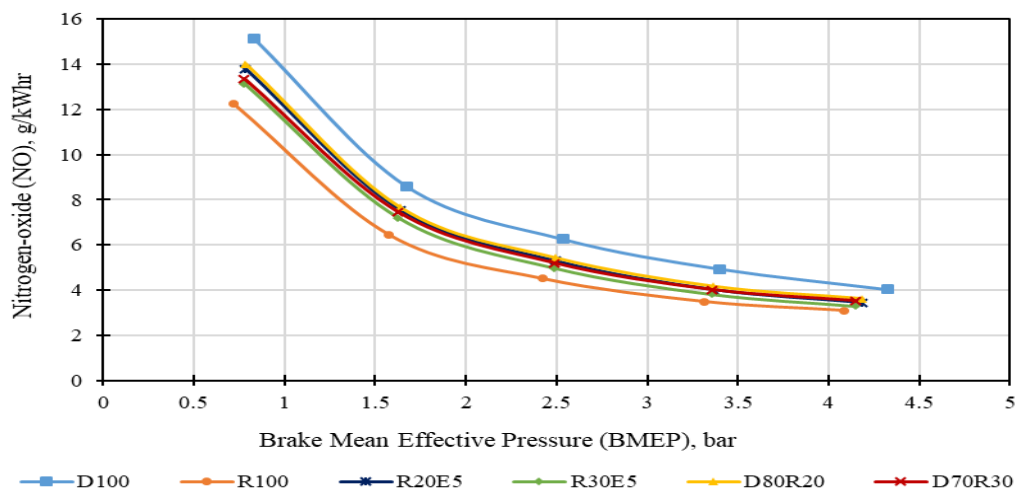


Figure 4.70 Variation in Nitrogen-oxide emission at different loads with 5% blending of an ethanol

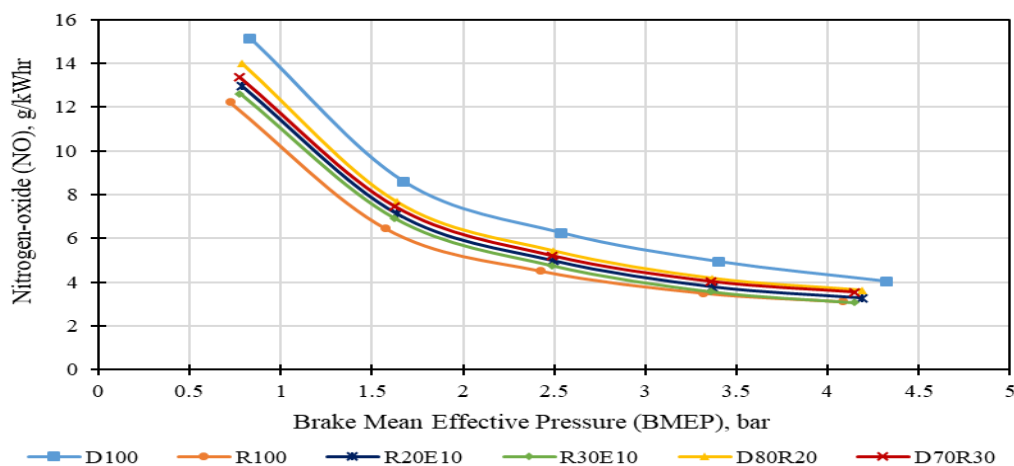


Figure 4.71 Variation in Nitrogen-oxide emission at different loads with 10% blending of an ethanol

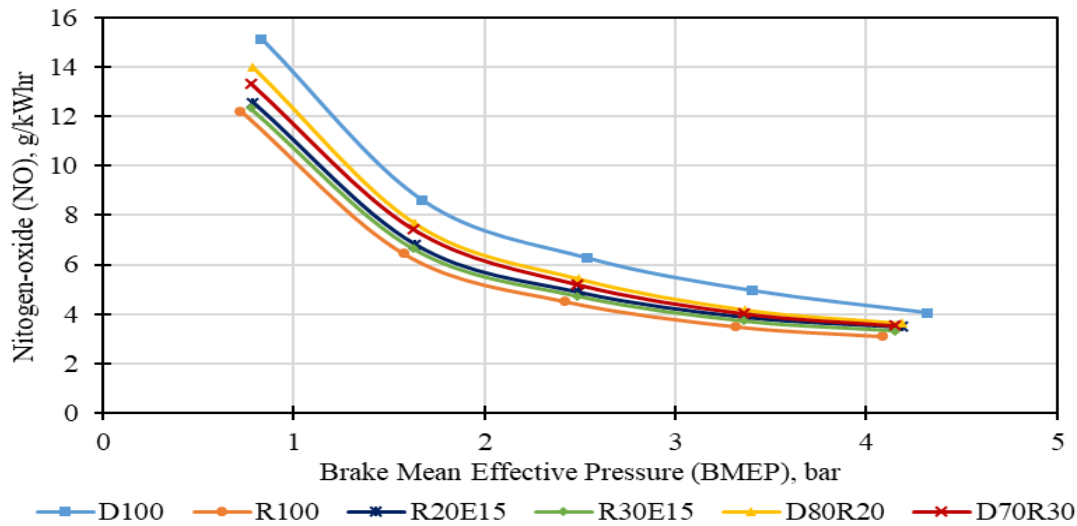


Figure 4.72 Variation in Nitrogen-oxide emission at different loads with 15% blending of an ethanol

4.11.4 Smoke Opacity of Ternary Blends

Graphic representations of the difference in smoke density for various fuels at various loads are shown in figures 4.73, 4.74, and 4.75. Amongst particulate matter (PM), soot is responsible for production of smoke. Soot is usually formed when long H-C chains are thermally cracked in absence of oxygen. At full load, highest smoke was obtained for D100 (62.4%) and lowest was for R30E15 (48%). As conferred previously, presence of renewable diesel decreases smoke opacity due to lesser aromatic content and smaller H-C chain, PM emissions are less. With addition of ethanol in a blend, further reduces smoke. Smoke is usually formed in absence of oxygen. Since ethanol has more oxygen content, very low cetane index which increases the delay period, so more time is provided for proper mixing of air and fuel which hence releases less smoke. Presence of oxygen both in renewable diesel and ethanol even in rich zones and proper mixing of air-fuel mixture seems to be dominant in reducing smoke. Since oxygen is vital part of ethanol's structure so it helps in oxidation of soot particles. This is in synchronization with Edwin et al. [112] and Sayin et al. [226]. At full load, smoke opacity for R100, R20E5, R20E10, R20E15, R30E5, R30E10 and R30E15 is 57.8, 55, 52.1, 49.9, 52.1, 49.7 and 48% respectively.

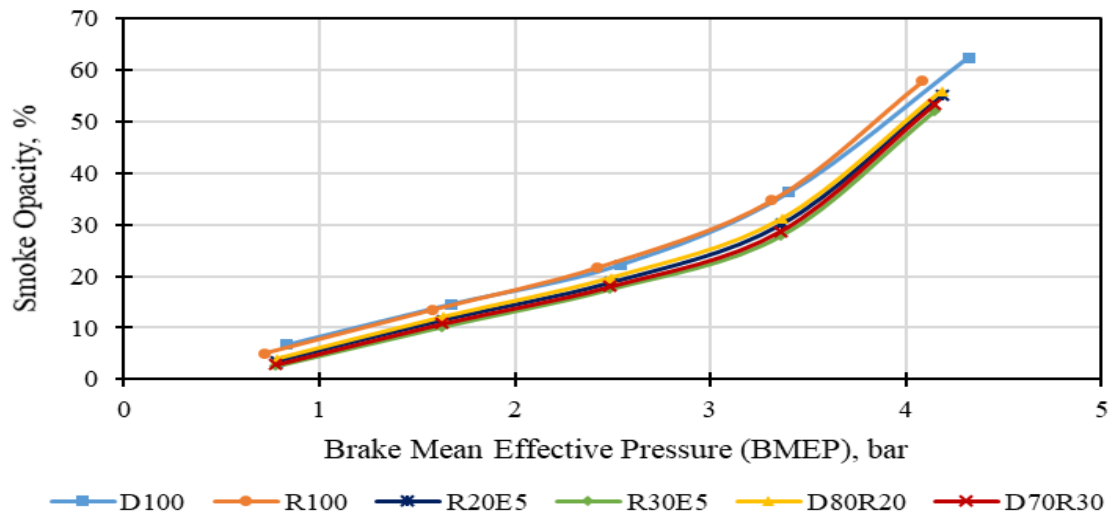


Figure 4.73 Variation in Smoke opacity at different loads with 5% blending of an ethanol

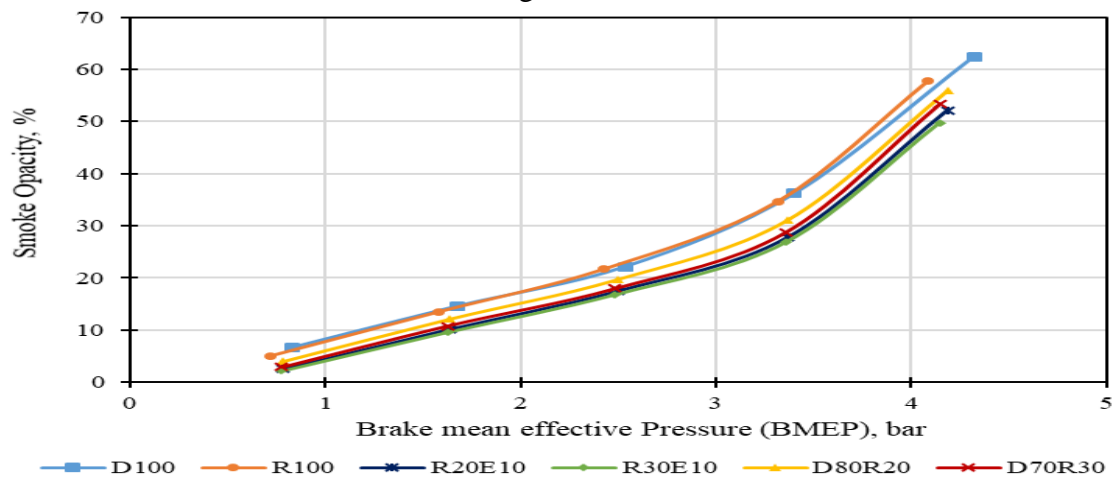


Figure 4.74 Variation in Smoke opacity at different loads with 10% blending of an ethanol

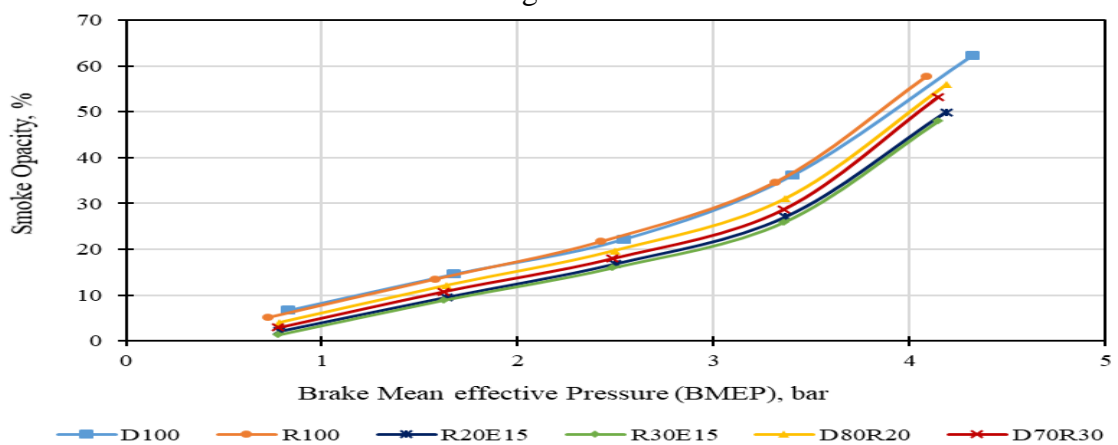


Figure 4.75 Variation in Smoke opacity at different loads with 15% blending of an ethanol

4.12. Response Surface Methodology Model Estimate

Input variables and response variables are of utmost importance in RSM technique. Their relationship is represented in terms of second order degree polynomial equations shown in **Appendix-4**. Response value depends upon input value which is further taken up by specifying lower and upper limit. In present case BMEP was between 0.7812 to 4.167 bar and Renewable diesel was between 20 to 30% and ethanol 5 to 15%. The response received from RSM technique was confirmed by implementing and choosing ANOVA (Analysis Of Variance) test. The statistical technique known as ANOVA divides observed variance data into many components to be utilized in further testing. In order to understand more about the connection between the dependent and independent variables, an ANOVA is employed for data sets with three or more groups. Simply it identifies whether the correlations obtained are substantial for full quadratic model or not. Table 4.3 shows the ANOVA for BTE, Table 4.4 and 4.5 shows ANOVA for emissions CO, HC and NO, smoke opacity respectively. On the extreme left side, it represents Model. Model represents the dependent variables, like in this case it is BMEP, Renewable diesel and ethanol. Along with models, tables include adjacent square (SS), probability value (P-value) and fit value (F-value). If the value of P for an input factor is less than 0.05 then it means all the dependent variables are significant with the confidence level of 95%. From the Tables 4.3, 4.4 and 4.5 it is clearly observed that all three input factors have significant effect on the responses. Table 4.6 shows the coefficient of Determination (R^2) and adjusted R^2 (adj R^2). The difference between R^2 and adj R^2 should be less than 2%. Value for R^2 represents how much fit or precise is the model. This displays the correlation between the model's accuracy with the experimental data. Whereas, adj R^2 is used to counterbalance the effect which is due to any variation done in the model. If the value of adj R^2 is closer to 100%, it shows that the model is more precise. Predicted R^2 helps in representing the prediction data for the model.

Table. 4.3 ANOVA for BTE

Source	Adj SS	F- Value	P- Value
Model	574.858	4835.63	0.000
Linear			
BMEP (bar)	423.358	32051.14	0.000
Renewable diesel (%)	0.534	40.43	0.000
Ethanol (%)	16.582	1255.35	0.000
Square			
BMEP (bar) * BMEP (bar)	56.434	4272.44	0.000
Renewable diesel (%) * Renewable diesel (%)	0.001	0.04	0.894
Ethanol (%) * Ethanol (%)	2.623	198.55	0.000
2-Way Interaction			
BMEP (bar) * Renewable diesel (%)	0.001	0.08	0.785
BMEP (bar) * Ethanol (%)	0.007	0.53	0.483
Renewable diesel (%) * Ethanol (%)	0.008	0.63	0.448
Error	0.132		
Total	574.990		

Table 4.4 ANOVA for CO and HC Emissions

Source	Adj SS	F- Value	P- Value	Adj SS	F- Value	P- Value
	CO Emissions			HC Emissions		
Model	2560.09	21832.16	0.000	157.225	1232.32	0.000
Linear						
BMEP (bar)	1681.80	129039.31	0.000	132.678	9359.29	0.000
Renewable diesel (%)	0.13	10.29	0.009	0.372	26.21	0.000
Ethanol (%)	0.49	37.66	0.000	0.571	40.26	0.000
Square						
BMEP (bar) * BMEP (bar)	479.97	36826.88	0.000	13.792	972.92	0.000
Renewable diesel (%) * Renewable diesel (%)	0.01	0.40	0.628	0.541	0.29	0.603
Ethanol (%) * Ethanol (%)	0.00	0.14	0.714	0.022	1.53	0.245
2-Way Interaction						
BMEP (bar) * Renewable diesel (%)	0.01	0.80	0.393	0.044	3.12	0.108
BMEP (bar) * Ethanol (%)	0.24	18.43	0.002	0.124	8.76	0.014
Renewable diesel (%) * Ethanol (%)	0.00	0.28	0.610	0.003	0.19	0.672

Error	0.10		0.142	
Total	2561.03		157.367	

Table 4.5 ANOVA for NO Emissions and Smoke Opacity

Source	Adj SS	F- Value	P- Value	Adj SS	F- Value	P- Value
	NO Emissions			Smoke Opacity		
Model	284.179	1700.25	0.000	6478.26	6591.45	0.000
Linear						
BMEP (bar)	229.446	12355.04	0.000	5985.53	54810.96	0.000
Renewable diesel (%)	0.195	10.50	0.009	4.79	43.90	0.000
Ethanol (%)	0.530	28.51	0.000	15.84	145.04	0.000
Square						
BMEP (bar) * BMEP (bar)	27.358	1473.15	0.000	249.75	2286.98	0.000
Renewable diesel (%) * Renewable diesel (%)	0.004	0.21	0.653	0.00	0.04	0.840
Ethanol (%) * Ethanol (%)	0.061	3.27	0.101	0.07	0.65	0.439
2-Way Interaction						
BMEP (bar) * Renewable diesel (%)	0.035	1.90	0.198	0.63	5.78	0.037
BMEP (bar) * Ethanol (%)	0.526	28.35	0.000	5.19	47.57	0.000
Renewable diesel (%) * Ethanol (%)	0.023	1.26	0.288	0.48	4.37	0.063
Error	0.186			1.09		
Total	284.365			6479.35		

Table 4.6 Model Evaluation

Model	BTE (%)	CO (g/kWh)	HC (g/kWh)	NO (g/kWh)	Smoke Opacity (%)
R²	99.98	99.99	99.91	99.93	99.98
Adjusted R²	99.96	99.98	99.83	99.88	99.97
Predicted R²	99.87	99.94	99.58	99.69	99.84

4.13 Surface and Contour Plots for Input Factors and Response Variables

The relationship represented between two independent variables with a dependent / response variable geometrically is called as contour plot. Contour plots are represented in 2-dimensional. Whereas Surface plot is a 3-dimensional figure. Both plots are shown on X, Y and Z axis.

From Figure 4.76 a, b and c to Figure 4.79 a, b and c shows BTE/CO/HC/NO/Smoke opacity vs Renewable diesel, Ethanol and BMEP. All these three input factors (BMEP, Renewable diesel and ethanol) are varied in such an arrangement that one out of these three factors is held constant at a time.

In Figure 4.76 a) ethanol is kept constant and BMEP and Renewable diesel are varied to study BTE. It is seen with increase in BMEP, BTE is increased. However as it tends to increase towards full load, BTE slightly drops. Increase in load leads to increase in fuel consumption, which decreases BTE. Similarly with increase in Renewable diesel keeping ethanol constant, it is seen that there is a minor decrease in BTE which is because of less viscosity and lesser CV of both renewable diesel and ethanol. Similar results are seen in Figure 4.76 b), where renewable diesel is kept constant and ethanol and BMEP are varied.

While holding Renewable diesel constant at a specific amount, BTE first marginally increases and then falls with a surge in BMEP and rise in ethanol %. Initially BTE increases because ethanol has high heat of vaporization which leads to increase in pre-mixed charge density releasing heat which can sustain combustion and hence high BTE. However when ethanol percentage is increased, oxygen amount present in renewable diesel and majorly in ethanol increases, leading to high temperature because of complete combustion which further reduces density of the charge. Due to less density, more fuel is consumed which lowers down BTE [112,215].

Similar trend is seen in Figure 4.76 c) for constant load, BTE declines with rise in proportion of renewable diesel from 20 to 30% due to lesser HRR during pre-mixed stage which happened due to renewable diesel's higher CI and lesser ID. Also, in case of increasing ethanol from 5 to 15%, BTE first increases due to high HRR. Since ethanol density is very less and with increase in heat, density of fuel further reduces and consumption of fuel

increases and a decrease in BTE can be observed beyond E10. The outcomes are comparable to Edwin et al. [112], Bekal et al. [200].

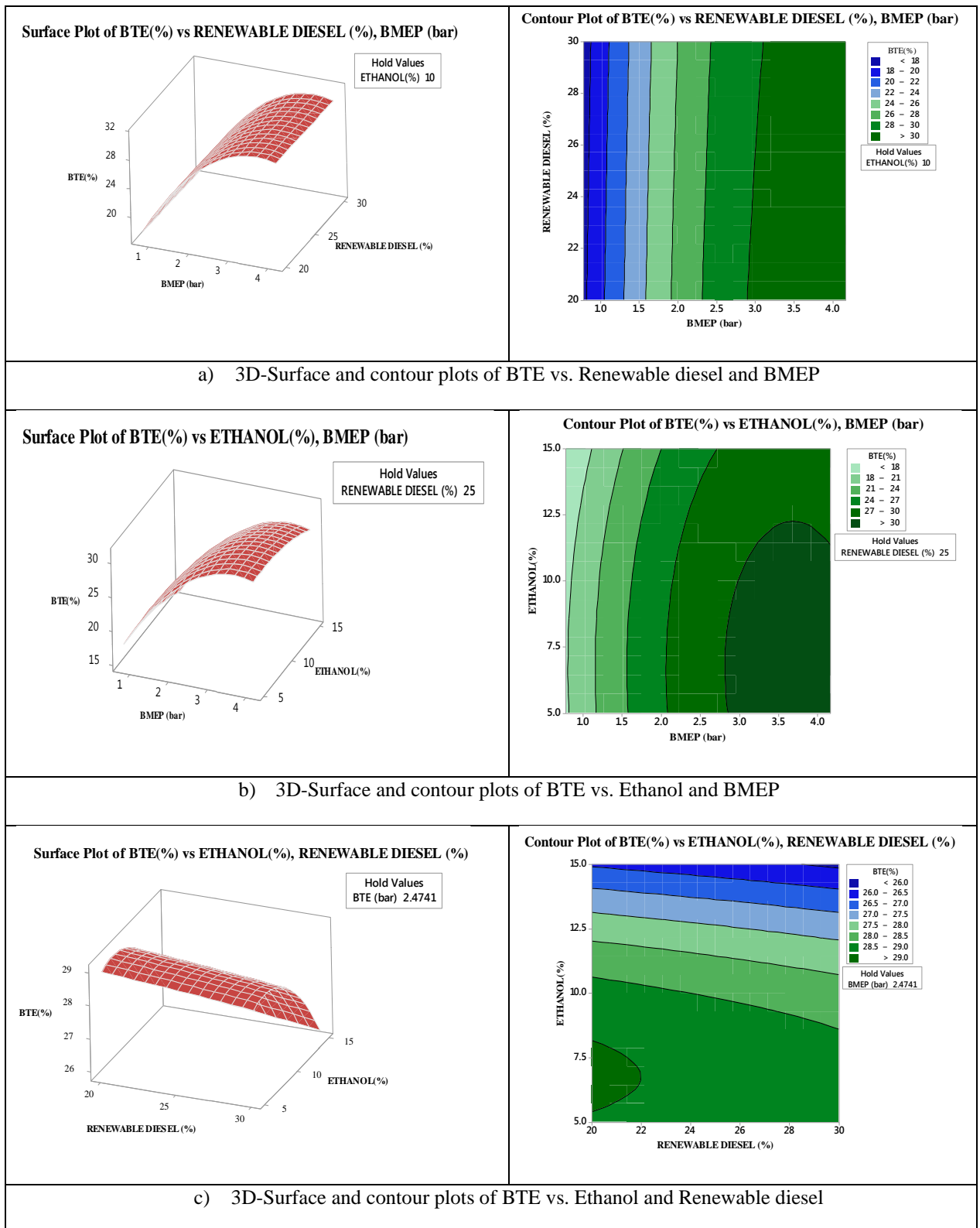


Figure 4.76. 3D-Surface and contour plots of BTE vs. various input variables

3D surface plots and contour plots for carbon-monoxide for various input variables are shown below in Figure 4.77 a, b and c. From the surface and contour plots in Figure 4.77 (a) and (b), it is seen that with increment in BMEP, keeping ethanol and renewable diesel constant respectively, CO emission is seen to be increasing. This is due to the fact that ethanol has very low viscosity, it vaporizes quickly and hence time available for it to mix properly with oxygen is very less during compression stroke which leads to incomplete combustion and increase in CO emission. Similarly renewable diesel has less HRR and shorter pre-mixed combustion stage which is not able to sustain complete combustion with increasing load, so CO increases.

In Figure 4.77 (b) CO emissions are observed for varying ethanol, keeping renewable diesel constant. With increase in ethanol, keeping Renewable diesel constant, increase in CO emission is observed. This is due to the reason, ethanol replaces the percentage volume of renewable diesel and diesel and blend's oxygen content increases leading to cooling effect and incomplete combustion.

In addition, with increase in Renewable diesel in Figure 4.77 (c) load constant leads to decrease in CO as Renewable diesel has lesser aromatic structure and more paraffinic content which leads to slightly better combustion and hence slight decrease in CO [112,215]. However this is true only when the load is fixed at a mid-value. It is also observed from surface and contour plots that by increasing ethanol at constant BMEP, CO emissions increases. Ethanol has more amount of oxygen and leads to quenching effect as it vaporises quickly. So there is not enough heat to sustain the combustion hence CO increases. From contour plots (Figure 4.77 c) it is seen that when Renewable diesel is between 29 to 30%, CO is less than 4.2g/kWhr and ethanol nearing to 15% has CO greater than 4.68g/kWhr. Same thing can be verified from surface plots.

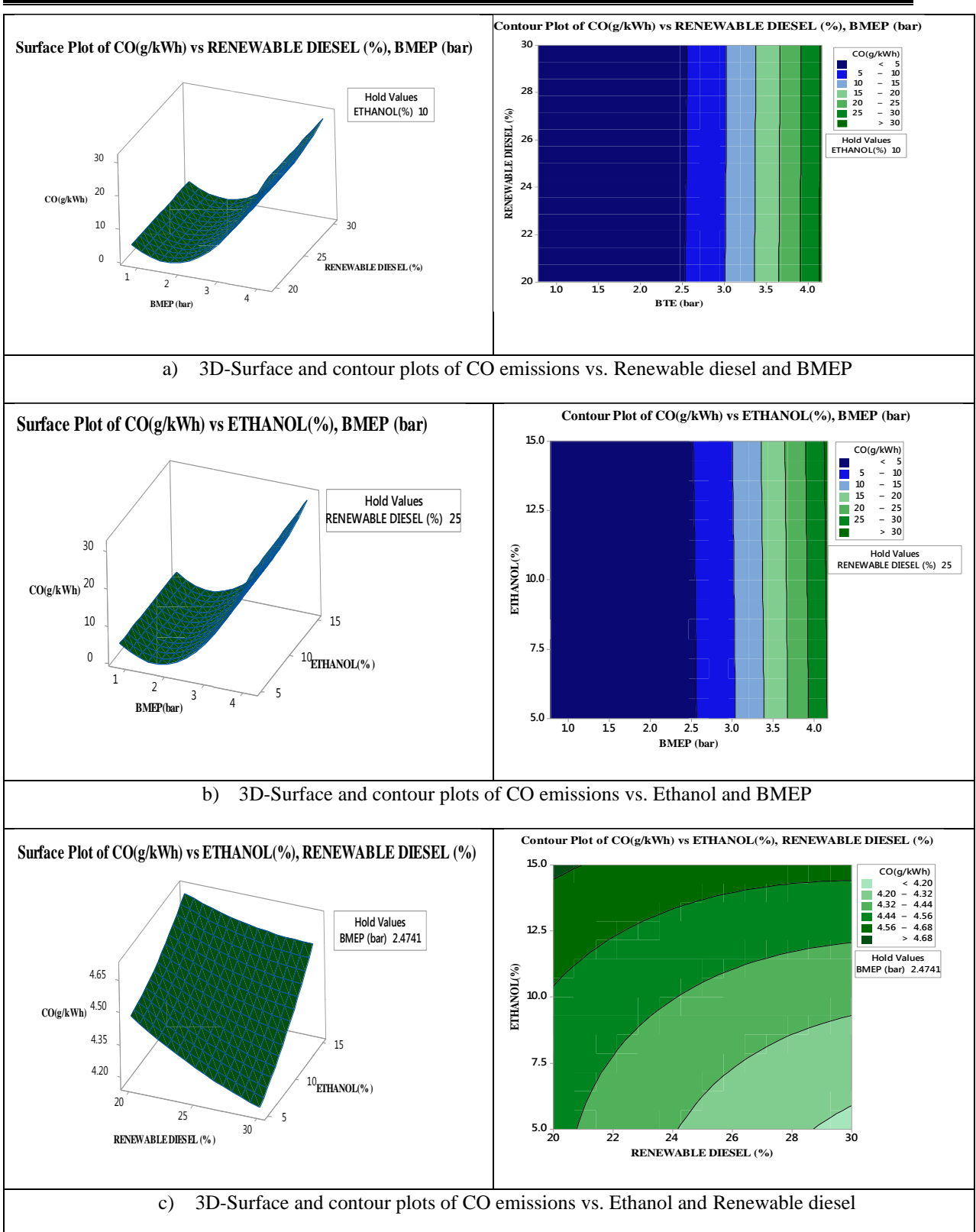


Figure 4.77. 3D-Surface and contour plots of CO emissions vs. various input variables

Figure 4.78 a, b and c displays the 3-D surface plot and contour plots for hydrocarbon emission with respect to various input factors. In Figure 4.78 a, it is seen that with increase in

BMEP, HC emissions is first highest in the beginning and then it decreases keeping ethanol constant. Initially HC is highest due to low volatility of ethanol and it doesn't get enough time to mix and results in unburnt HC. Gradually with increase in load, and percentage of ethanol being constant, more fuel is supplied and charge gets enough time to mix and burn and hence HC emission reduces. Similar results were obtained experimentally. From the contour plots also, it is depicted, value of HC emission is less than 4g/kWhr for BMEP spanning in between 3 to 4 bar. Similarly, keeping ethanol constant and increasing Renewable diesel, HC emissions marginally is increased. It is because Renewable diesel also has slight oxygen present and its H-C chain is smaller which requires lesser amount of energy to break the bonds and heat released is less which leads to more HC emission.

Similar trend is seen for Figure 4.78 (b), keeping Renewable diesel constant and increasing BMEP, HC decreases and similarly increasing ethanol HC slightly increases which is in synchronization with the reasons given earlier for Figure 4.78 (a).

In Figure 4.78 c), keeping BMEP constant and increasing Renewable diesel and ethanol separately, HC emissions increases which is in synchronization with both (a) and (b) figures. From the contour plots also, it is seen that when ethanol is above approx. 13.5% and Renewable diesel is above 29%, HC emissions are highest, more than 4.95g/kWhr. Considering the cumulative effect, similar results were obtained experimentally as well.

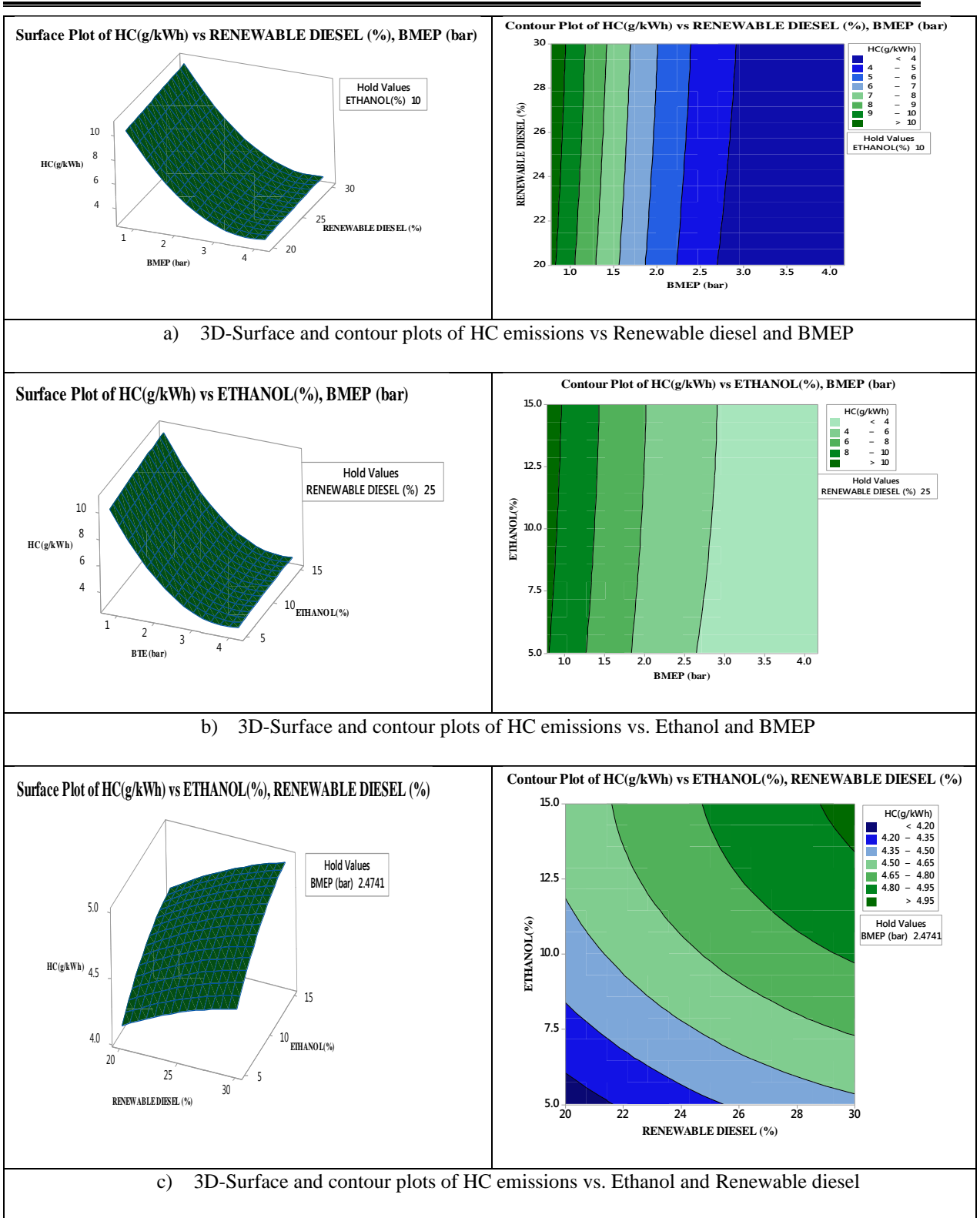
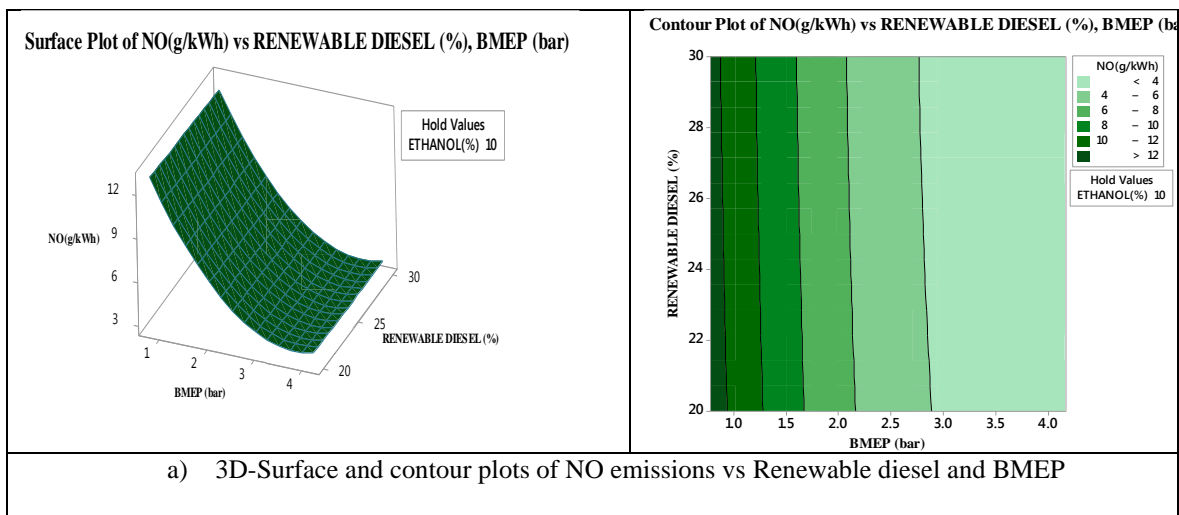


Figure 4.78. 3D-Surface and contour plots of HC emissions vs. various input variables

3-D surface plots and contours plots have been shown in Figure 4.79 a, b and C for NO emissions with respect to various input variables. Figure (a) shows NO emissions when

ethanol is kept constant. With increase in BMEP, NO emission decreases significantly and with increase in Renewable diesel, NO emission decreases slightly. The decrease is due to the fact that presence of ethanol's high vaporization ability and lower heating value resulted in decrease in combustion chamber temperature and hence NO emissions decreases.

Similar trend is seen for Figure 4.79 (b). Furthermore, because of the low cetane index of ethanol and the increase in ethanol proportion, the charge becomes leaner, which results in a decrease in flame temperature and a reduction in NO emissions. Also due increase in Renewable diesel and shorter ignition delay, the time taken to release heat during pre-mixed combustion phase is lesser which leads to low combustion temperature and hence lesser NO emissions as depicted in Figure 4.79 (c). With rise in load, keeping renewable diesel constant, renewable diesel (high cetane index) does not get enough time for nitrogen reactions to occur. Also HRR is low which leads to lower combustion temperature, hence decreased NO emission. This is in synchronization with Kim et al. [112,179,215].



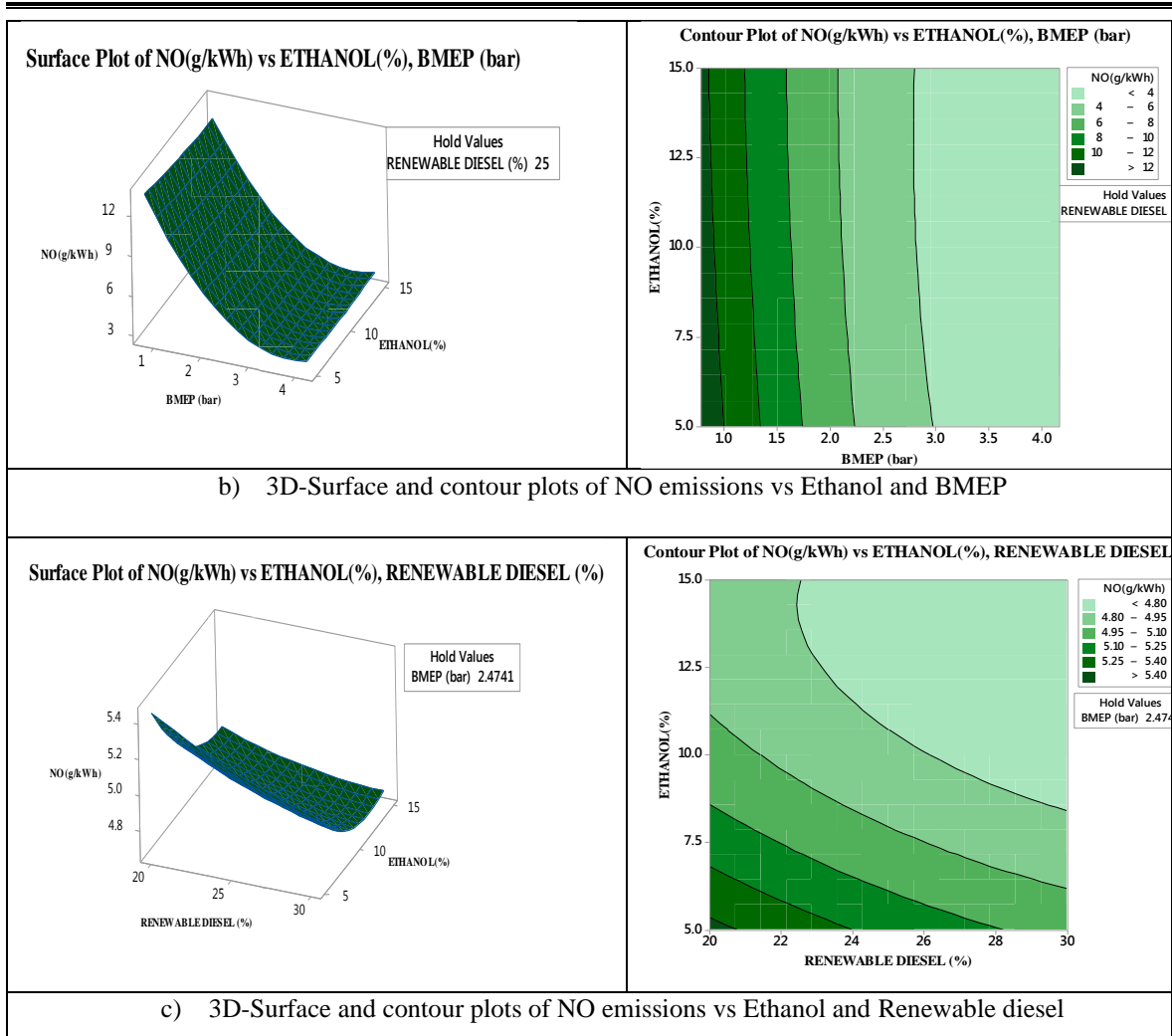


Figure 4.79. 3D-Surface and contour plots of NO emissions vs. various input variables

Figure 4.80 a, b and c depicts the 3-D surface and contour plots of smoke opacity with respect to various input variables. From Figure 4.80 (a) and (b) it is evident that while keeping ethanol constant or Renewable diesel constant, with increase in BMEP, smoke opacity increases. This is attributed by the incomplete combustion that occurs at peak load and causes an increase in smoke.

On the same lines, in Figure 4.80 (c), it is detected that with increasing ethanol content and Renewable diesel content, keeping BMEP constant, smoke opacity decreases. This is because Renewable diesel's lesser aromatic structure and less premixed combustion stage, air and fuel got sufficient time to mix which resulted in complete combustion and hence less smoke opacity. This also supports reason for lesser CO in Figure 4.77(c) at mid-value of

BMEP. In addition to this ethanol's presence of oxygen increases as it replaces diesel fuel in a blend, leads to complete combustion and hence lesser smoke. Moreover, on cumulative basis, both Renewable diesel and ethanol when added to diesel in certain proportions, help in smoke reduction. This is also verified from contour plots and experiments as well.

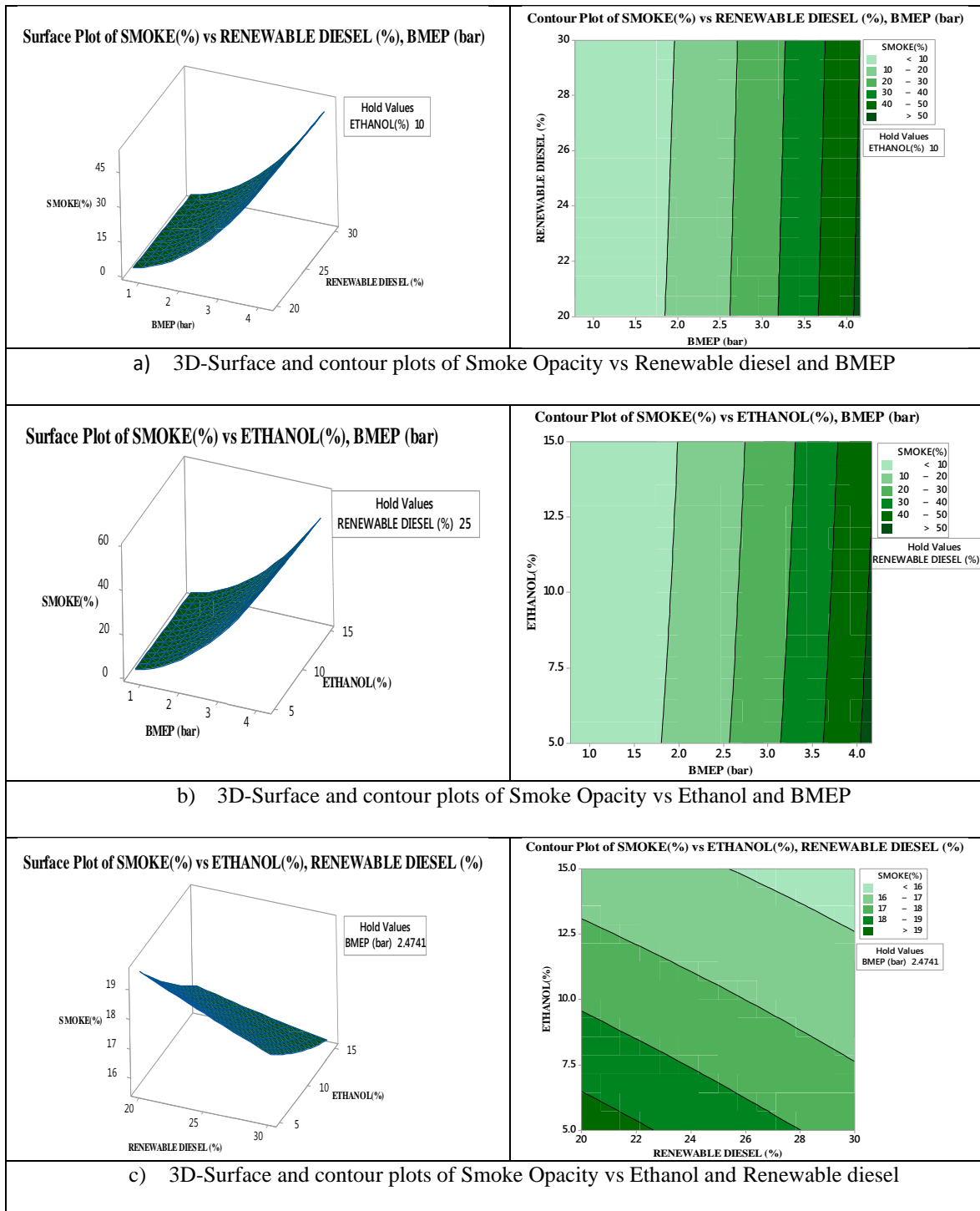


Figure 4.80. 3D-Surface and contour plots of Smoke Opacity vs. various input variables

4.13.1 Optimization Plot and Validation Test

RSM uses an optimization strategy at the end of methodology to get the optimal values and see how it affects the response variables and the desirable outcomes. Desirability ranges in between 0 to 1. Closer the desirability value is to '1' represents that value is closer to ideal value, whereas '0' represents vice-versa. In the present work, optimization technique was implied so as to find the optimized value for BMEP and the percentage of Renewable diesel and ethanol. This helps in reducing cost and saving experimentation time. Table 4.7 represents the given lower and upper limit values for input factors (BMEP, Renewable diesel and ethanol) along with weight and significance. Whereas, as far as response variables were concerned, BTE aim was fixed at maximum and all emissions were fixed at minimum values. Figure 4.7 is the optimization plot which shows the optimized condition as BMEP at 2.628 bar with optimized blend of Renewable diesel at 30% and ethanol at 7.05% and rest being diesel. At this optimized condition, the response variables like BTE, CO, HC, NO, Smoke opacity were optimized at 29.21%, 5.50 g/kWh, 4.32 g/kWh, 4.47 g/kWh, and 19.46 % respectively.

Table 4.7. Optimization values

Input Factors	Lower Limit	Upper Limit	Weight	Importance	Criterion
BMEP (bar)	0.7812	4.1670	1	1	Within range
Renewable diesel (%)	20	30	1	1	Within range
Ethanol (%)	5	15	1	1	Within range
Response Factors					
BTE (%)	14.85	30.97	1	1	Maximize
CO (g/kWh)	4.2135	31.289	1	1	Minimize
HC (g/kWh)	2.87	11.13	1	1	Minimize
NO (g/kWh)	3.161	13.78	1	1	Minimize
Smoke Opacity (%)	1.4	55	1	1	Minimize

Table 4.8 below is a validation table wherein, the values obtained from RSM model are validated with the values obtained by performing experiments. The desired output is the direct accuracy of the RSM model. With the engine's input values optimised, the test was run. Table 4.8 below gives the predicted values of BTE, CO, HC, NO and smoke emissions of the

optimized blend which were then compared to the experimental values obtained by performing experiment. The difference between experimental and anticipated results that is within the acceptable range is provided by residual percentage. Hence regression models created for optimization of BMEP and percentage of Renewable diesel and ethanol is beneficial in effectively envisaging experimental values with approximately 92% of accuracy.

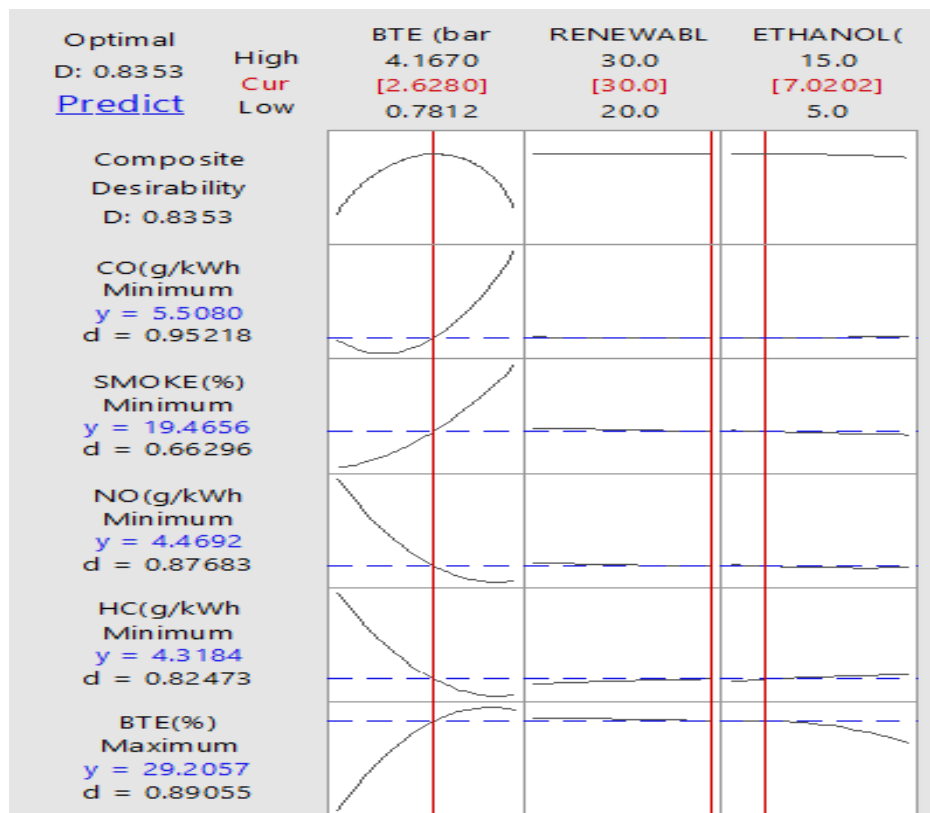


Figure 4.81 Optimization plot for smoke, CO, NO, HC and BTE

Table 4.8 Validation Test

Blend	BMEP (bar)		BTE (%)	CO (g/kWh)	HC (g/kWh)	NO (g/kWh)	Smoke Opacity (%)
D63R30E7	2.628	Predicted Value	29.21	5.5	4.32	4.47	19.46
		Experimental Value	29.19	5.05	4.16	4.66	20.31
		Residual %	0.07	8.18	3.7	4.25	4.36

CONCLUSIONS AND FUTURE SCOPE**5.1 Conclusions**

In the present study Renewable diesel was produced from Jatropha oil by undergoing the hydroprocessing. It has been shown that renewable diesel is a sustainable alternative fuel. Also, hydroprocessing is promising route to handle the increased environmental pollution from diesel and better than much researched transesterification process.

1. The physiochemical properties of the Renewable diesel and diesel blends, along with ternary blends had almost similar values to that of the diesel. All the values lied within the ASTM D standards.
2. Renewable diesel and its combinations were shown to have better cold flow characteristics and cetane index than conventional diesel.
3. Renewable diesel and its blends have lower HRR than diesel. Due to high cetane index, ignition started earlier in case of Renewable diesel and its blends. Peak pressure for Renewable diesel and its blends was lower than diesel. Same trend was seen for ternary blends.
4. Brake Thermal efficiency of Renewable diesel and its blends was lesser than diesel. Lowest BTE was for R100 and highest for D100 as 27.212% and 31.189% respectively. With increase in the percentage of R100, BTE decreases and BSEC increases. At full load BSEC for R100 is highest, 13.33 MJ/kW hr and D100 is lowest, 11.54 MJ/kW hr.
5. Values of CO, HC and smoke opacity dropped till R30D70 blend, thereafter, as the proportion of R100 in the blend rises, the value for smoke rises. At peak load for R30D70, HC, CO and Smoke was reduced by 14.47%, 13.84% and 13.3%

-
-
- respectively. There was a decrease in NO emissions with increase in percentage of Renewable diesel. At full load NO emissions were reduced by 12.66% for R30D70 and 23.23% for R100.
6. To further reduce emissions, ethanol was added into R20D80 and R30D70 blends. Ethanol percentage was chosen as 5, 10 and 15%. Beyond 15%, ethanol in a blend of diesel and renewable diesel proved highly insoluble.
 7. With increase in percentage of ethanol, HRR increased. At full load, maximum HRR for R20E15 was 61.74J/°CAD whereas, for D80R20 it was 50.16J/°CA. With increase in addition of ethanol pressure also increased.
 8. BTE increased with increase in percentage of ethanol till E10. Beyond E10, BTE decreased. BTE for R20E5 and R20E10 was increased by 4.35% and 4.05% than D80R20. Similarly, R30E5, R30E10 was increased by 5.28% and 4.16% than D70R30 respectively. For R20E15 and R30E15, BTE decreased by 4.69% and 3.74% than D80R20 and D70R30 respectively. BSEC was lower with ethanol in comparison to binary blends but was higher than diesel. Blends with 15% ethanol had highest BSEC.
 9. With increase in percentage of ethanol, CO and HC increases however, CO emissions are lesser than diesel. Moreover, with increase in ethanol percentage smoke opacity and NO decreases.
 10. At full load conditions, CO for R20E5, R20E10 and R20E15 was reduced by 3.21%, 2.86% and 1.056% and HC was increased by 12.85%, 22.63% and 26.63% than diesel.
 11. Ternary blend R30E10 has lowest NO and smoke emissions. NO and smoke opacity reduced by 24.25% and 20.35% respectively.
 12. RSM optimizer tool showed that 30% of Renewable diesel, 7% of ethanol at BMEP of 2.6 bar, optimized output can be attained.

5.2 Scope for Future Work

On the basis of the research work performed and knowledge gained, following suggestions are put forth for the future work.

1. More non-edible feedstock like nag-champa oil, rubber seed oil etc. can be explored using hydroprocessing for Renewable diesel production.
2. Different software like ASPEN or ANSYS can be applied to study combustion and other output parameters in detail which can also be experimentally validated.
3. Some additives can be considered while adding ethanol beyond 15% to avoid phase separation in blends.
4. Catalysts currently in use for industrial hydro-processing of oils derived from biomass perform less well. Commercial catalysts can be modified further with more work.

REFERENCES

- [1] Authority TG. India 3rd largest energy consumer : GAIL. Times of India 2018:8–10.
- [2] BP. Statistical Review of World Energy globally consistent data on world energy markets . and authoritative publications in the field of energy. BP Energy Outlook 2021 2021;70:8–20.
- [3] MoPNG Economics and Statistics Division. India PNG statistics 2019-20 2020:244.
- [4] Indian Bureau of Mines. Indian Minerals Yearbook 2019 (Part- III : Mineral Reviews) - Rare Earths 2020;2019:1–23.
- [5] Affairs E. Economic Survey 2018-19 2019;2:1–468.
- [6] Mayssara A. Abo Hassanin Supervised A. Petroleum Planning & Analysis Cell. Abr Ready Reckoner 2021.
- [7] Sahoo PK, Das LM. Combustion analysis of Jatropha, Karanja and Polanga based biodiesel as fuel in a diesel engine. Fuel 2009;88:994–9. doi:10.1016/j.fuel.2008.11.012.
- [8] Heywood JB. Internal Combustion Engine & Fundamentals. Mc-Graw Hills; 2018.
- [9] Stern AC. Air Pollution From Motor Vehicles and Its Control. 1974:449–72.
- [10] IQAir. World Air Quality Report. 2020 World Air Qual Rep 2020:1–41.
- [11] Reşitoğlu IA, Altinişik K, Keskin A. The pollutant emissions from diesel-engine vehicles and exhaust aftertreatment systems. Clean Technol Environ Policy 2015;17:15–27. doi:10.1007/s10098-014-0793-9.
- [12] Oda Y, Osafune S, Ueda H, Fujimura K. Clean Combustion Technology in Diesel Engines Operated with Dimethyl ether. Mitsubishi Heavy Ind Ltd Tech Rev 2004;40:2–6.
- [13] Dickens C, Carol AC. Clean and secure energy for the twenty- first century. Proc Inst Mech Eng Part A J Power Energy 2002;216:291–4. doi:10.1243/09576500260251138.
- [14] Pelemo J, Inambao FL, Onuh EI. Potential of used cooking oil as feedstock for hydroprocessing into hydrogenation derived renewable diesel: A review. Int J Eng Res Technol 2020;13:500–19. doi:10.37624/ijert/13.3.2020.500-519.
- [15] Vuyyuru KR. Conversion of Cellulosic Biomass into Chemicals using Heterogeneous and Electrochemical Catalysis. Inst Chem 2012;7–9. doi:10.14279/depositonce-3444.
- [16] Jeremiah Njeru Gatumu. Evaluation Of Combustion , Performance And Emission Of A Direct Injection Compression Ignition (Dici) Engine Running On A Diesel-Syngas Blend Master Of Science (Mechanical Engineering) Jomo Kenyatta University Of. Jomo Kenyatta University Of Agriculture And Technology, 2021.
- [17] Macedo T de O, Pereira RG, Pardal JM, Soares AS, Lameira V deJ. Viscosity of Vegetable Oils and Biodiesel and Energy Generation. World Acad Sci Eng Technol Int J Chem Mol Nucl Mater Metall Eng 2013;7:251–6.
- [18] Srivastava A, Prasad R. Triglycerides-based diesel fuels. Renew Sustain Energy Rev 2000;4:111–33. doi:10.1016/S1364-0321(99)00013-1.

-
-
- [19] Yang T, Jie Y, Li B, Kai X, Yan Z, Li R. Catalytic hydrodeoxygenation of crude bio-oil over an unsupported bimetallic dispersed catalyst in supercritical ethanol. *Fuel Process Technol* 2016. doi:10.1016/j.fuproc.2016.01.004.
- [20] Koul R, Kumar N, Singh RC. Environmental Effects A review on the production and physicochemical properties of renewable diesel and its comparison with biodiesel. *Energy Sources, Part A Recover Util Environ Eff* 2019;7036:1–21. doi:10.1080/15567036.2019.1646355.
- [21] Sebos I, Matsoukas A, Apostolopoulos V, Papayannakos N. Catalytic hydroprocessing of cottonseed oil in petroleum diesel mixtures for production of renewable diesel. *Fuel* 2009. doi:10.1016/j.fuel.2008.07.032.
- [22] Patel RL, Sankhavara CD. Biodiesel production from Karanja oil and its use in diesel engine: A review. *Renew Sustain Energy Rev* 2017;71:464–74. doi:10.1016/j.rser.2016.12.075.
- [23] Takase M, Zhao T, Zhang M, Chen Y, Liu H, Yang L, et al. An expatiated review of neem, jatropha, rubber and karanja as multipurpose non-edible biodiesel resources and comparison of their fuel, engine and emission properties. *Renew Sustain Energy Rev* 2015;43:495–520. doi:http://dx.doi.org/10.1016/j.rser.2014.11.049.
- [24] Mwangi JK, Lee WJ, Chang YC, Chen CY, Wang LC. An overview: Energy saving and pollution reduction by using green fuel blends in diesel engines. *Appl Energy* 2015;159:214–36. doi:10.1016/j.apenergy.2015.08.084.
- [25] Barnwal BK, Sharma MP. Prospects of biodiesel production from vegetable oils in India. *Renew Sustain Energy Rev* 2005;9:363–78. doi:10.1016/j.rser.2004.05.007.
- [26] Balat M. Modeling vegetable oil viscosity. *Energy Sources, Part A Recover Util Environ Eff* 2008;30:1856–69. doi:10.1080/15567030701457392.
- [27] Da Mota SDP, Mancio AA, Lhamas DEL, De Abreu DH, Da Silva MS, Dos Santos WG, et al. Production of green diesel by thermal catalytic cracking of crude palm oil (*Elaeis guineensis* Jacq) in a pilot plant. *J Anal Appl Pyrolysis* 2014. doi:10.1016/j.jaap.2014.06.011.
- [28] Uusitalo V, Väisänen S, Havukainen J, Havukainen M, Soukka R, Luoranen M. Carbon footprint of renewable diesel from palm oil, jatropha oil and rapeseed oil. *Renew Energy* 2014. doi:10.1016/j.renene.2014.03.020.
- [29] Sousa FP, Silva LN, de Rezende DB, de Oliveira LCA, Pasa VMD. Simultaneous deoxygenation, cracking and isomerization of palm kernel oil and palm olein over beta zeolite to produce biogasoline, green diesel and biojet-fuel. *Fuel* 2018. doi:10.1016/j.fuel.2018.03.020.
- [30] Srifa A, Faungnawakij K, Itthibenchapong V, Assabumrungrat S. Roles of monometallic catalysts in hydrodeoxygenation of palm oil to green diesel. *Chem Eng J* 2015. doi:10.1016/j.cej.2014.09.106.
- [31] Wakil MA, Kalam MA, Masjuki HH, Atabani AE, Rizwanul Fattah IM. Influence of biodiesel blending on physicochemical properties and importance of mathematical model for predicting the properties of biodiesel blend. *Energy Convers Manag* 2015;94:51–67. doi:10.1016/j.enconman.2015.01.043.
-
-

-
- [32] Balat M. Potential alternatives to edible oils for biodiesel production - A review of current work. *Energy Convers Manag* 2011;52:1479–92. doi:10.1016/j.enconman.2010.10.011.
- [33] Ramírez-Verduzco LF, García-Flores BE, Rodríguez-Rodríguez JE, Del Rayo Jaramillo-Jacob A. Prediction of the density and viscosity in biodiesel blends at various temperatures. *Fuel* 2011;90:1751–61. doi:10.1016/j.fuel.2010.12.032.
- [34] Oliveira L. E., Da Silva M. L. C. P. Comparative study of calorific value of rapeseed , soybean , jatropha curcas and crambe biodiesel. *Renew Energy Power Qual J* 2013;1:679–82.
- [35] Šimáček P, Kubička D, Kubičková I, Homola F, Pospíšil M, Chudoba J. Premium quality renewable diesel fuel by hydroprocessing of sunflower oil. *Fuel* 2011;90:2473–9. doi:10.1016/j.fuel.2011.03.013.
- [36] Sugami Y, Minami E, Saka S. Renewable diesel production from rapeseed oil with hydrothermal hydrogenation and subsequent decarboxylation. *Fuel* 2016;166:376–81. doi:10.1016/j.fuel.2015.10.117.
- [37] Agarwal AK, Dhar A, Gupta JG, Kim W II, Choi K, Lee CS, et al. Effect of fuel injection pressure and injection timing of Karanja biodiesel blends on fuel spray, engine performance, emissions and combustion characteristics. *Energy Convers Manag* 2015;91:302–14. doi:10.1016/j.enconman.2014.12.004.
- [38] Lianghui X, Hongbo G, Jialin L. Comprehensive suitability assessment of the coastline resources of Zhejiang Province, China. *Philipp Agric Sci* 2015;98:224–36. doi:10.1016/j.pecs.2006.08.003.
- [39] Fischer J, Connemann J. Biodiesel in Europe 1998: Biodiesel Processing Technologies. *Int Liq Biofuels Congr* 1998:1–16.
- [40] Smirnova MY, Kikhtyanin O V., Smirnov MY, Kalinkin A V., Titkov AI, Ayupov AB, et al. Effect of calcination temperature on the properties of Pt/SAPO-31 catalyst in one-stage transformation of sunflower oil to green diesel. *Appl Catal A Gen* 2015;505:524–31. doi:10.1016/j.apcata.2015.06.019.
- [41] Kikhtyanin O V., Rubanov AE, Ayupov AB, Echevsky G V. Hydroconversion of sunflower oil on Pd/SAPO-31 catalyst. *Fuel* 2010;89:3085–92. doi:10.1016/j.fuel.2010.05.033.
- [42] Krár M, Kovács S, Kalló D, Hancsók J. Fuel purpose hydrotreating of sunflower oil on CoMo/Al₂O₃catalyst. *Bioresour Technol* 2010;101:9287–93. doi:10.1016/j.biortech.2010.06.107.
- [43] Moniruzzaman M, Yaakob Z, Shahinuzzaman M, Khatun R, Aminul Islam AKM. Jatropha Biofuel Industry: The Challenges. *Front Bioenergy Biofuels* 2017. doi:10.5772/64979.
- [44] Khalil HPSA, Aprilia NAS, Bhat AH, Jawaid M, Paridah MT, Rudi D. A Jatropha biomass as renewable materials for biocomposites and its applications. *Renew Sustain Energy Rev* 2013;22:667–85. doi:10.1016/j.rser.2012.12.036.
- [45] Tikko A, Yadav SS, Kaushik N. Effect of irrigation, nitrogen and potassium on seed yield and oil content of Jatropha curcas in coarse textured soils of northwest India. *Soil*
-

Tillage Res 2013;134:142–6. doi:10.1016/j.still.2013.08.001.

- [46] Silitonga AS, Masjuki HH, Mahlia TMI, Ong HC, Atabani AE, Chong WT. A global comparative review of biodiesel production from *Jatropha curcas* using different homogeneous acid and alkaline catalysts: Study of physical and chemical properties. *Renew Sustain Energy Rev* 2013;24:514–33. doi:10.1016/j.rser.2013.03.044.
- [47] No SY. Inedible vegetable oils and their derivatives for alternative diesel fuels in CI engines: A review. *Renew Sustain Energy Rev* 2011;15:131–49. doi:10.1016/j.rser.2010.08.012.
- [48] Azam MM, Waris A, Nahar NM. Prospects and potential of fatty acid methyl esters of some non-traditional seed oils for use as biodiesel in India. *Biomass and Bioenergy* 2005;29:293–302. doi:10.1016/j.biombioe.2005.05.001.
- [49] Koul R, Kumar N, Singh RC. Comparative analysis of renewable diesel and biodiesel produced from *Jatropha* oil. *Environ Prog Sustain Energy* 2022:1–17. doi:10.1002/ep.13832.
- [50] Asikin-Mijan N, Lee H V., Abdulkareem-Alsultan G, Afandi A, Taufiq-Yap YH. Production of green diesel via cleaner catalytic deoxygenation of *Jatropha curcas* oil. *J Clean Prod* 2018;167:1048–59. doi:10.1016/j.jclepro.2016.10.023.
- [51] Jain A, Sirisha VL. Algal biodiesel: Third-generation biofuel. *Mar Bioenergy Trends Dev* 2015:423–57. doi:10.1201/b18494.
- [52] Rozmysłowicz B, Mäki-avela P, Murzin DY. Fatty Acids-Derived Fuels from Biomass via Catalytic Deoxygenation. *Biomass Convers.* 1st ed., 2020, p. 199–220. doi:10.1007/978-3-642-28418-2.
- [53] Bezergianni S, Dimitriadis A, Sfetsas T, Kalogianni A. Hydrotreating of waste cooking oil for biodiesel production. Part II: Effect of temperature on hydrocarbon composition. *Bioresour Technol* 2010;101:7658–60. doi:10.1016/j.biortech.2010.04.043.
- [54] Kovács S, Kasza Tt, Thernesz A, Horváth IW, Hancsók J. Fuel production by hydrotreating of triglycerides on NiMo/Al₂O₃/F catalyst. *Chem Eng J* 2011;176–177:237–43. doi:10.1016/j.cej.2011.05.110.
- [55] Nimkarde MR, Vaidya PD. Toward Diesel Production from Karanja Oil Hydrotreating over CoMo and NiMo Catalysts. *Energy and Fuels* 2016;30:3107–12. doi:10.1021/acs.energyfuels.6b00138.
- [56] Orozco LM, Echeverri DA, Sijánchez L, Rios LA. Second-generation green diesel from castor oil: Development of a new and efficient continuous-production process. *Chem Eng J* 2017. doi:10.1016/j.cej.2017.04.027.
- [57] Viêgas CV, Hachemi I, Freitas SP, Mäki-Arvela P, Aho A, Hemming J, et al. A route to produce renewable diesel from algae: Synthesis and characterization of biodiesel via in situ transesterification of *Chlorella* alga and its catalytic deoxygenation to renewable diesel. *Fuel* 2015;155:144–54. doi:10.1016/j.fuel.2015.03.064.
- [58] Casanave D, Duplan J, Freund E. Diesel fuels from biomass. *Pure Appl Chem* 2007;79:2071–81. doi:10.1351/pac200779112071.
- [59] Ramadhas AS, Jayaraj S, Muraleedharan C. Characterization and effect of using rubber seed oil as fuel in the compression ignition engines 2005;30:795–803.

doi:10.1016/j.renene.2004.07.002.

- [60] Pali HS, Sharma A, Singh Y, Kumar N. Sal biodiesel production using Indian abundant forest feedstock. *Fuel* 2020;273.
- [61] Kumar N, Sonthalia A, Tomar M, Koul R. An experimental investigation on spray, performance and emission of hydrotreated waste cooking oil blends in an agricultural engine. *Int J Engine Res* 2021;22:2305–17. doi:10.1177/1468087420928734.
- [62] Singh D, Subramanian KA, Garg M. Comprehensive review of combustion, performance and emissions characteristics of a compression ignition engine fueled with hydroprocessed renewable diesel. *Renew Sustain Energy Rev* 2017. doi:10.1016/j.rser.2017.06.104.
- [63] Sankaranarayanan TM, Banu M, Pandurangan A, Sivasanker S. Hydroprocessing of sunflower oil-gas oil blends over sulfided Ni-Mo-Al-zeolite beta composites. *Bioresour Technol* 2011. doi:10.1016/j.biortech.2011.08.127.
- [64] Veriansyah B, Han JY, Kim SK, Hong SA, Kim YJ, Lim JS, et al. Production of renewable diesel by hydroprocessing of soybean oil: Effect of catalysts. *Fuel* 2012;94:578–85. doi:10.1016/j.fuel.2011.10.057.
- [65] Sonthalia A, Kumar N. Hydroprocessed vegetable oil as a fuel for transportation sector: A review. *J Energy Inst* 2019;1–17. doi:10.1016/j.joei.2017.10.008.
- [66] Stegnar M, Uhrin P, Peternel P, Mavri A, Salobir-Pajnič B, Stare J, et al. The 4G/5G sequence polymorphism in the promoter of plasminogen activator inhibitor-1 (PAI-1) gene: Relationship to plasma PAI-1 level in venous thromboembolism. *Thromb Haemost* 1998;79:975–9. doi:10.1002/ep.
- [67] Plazas-González M, Guerrero-Fajardo CA, Sodr e JR. Modelling and simulation of hydrotreating of palm oil components to obtain green diesel. *J Clean Prod* 2018. doi:10.1016/j.jclepro.2018.02.275.
- [68] Bezergianni S. Catalytic Hydroprocessing of Liquid Biomass for Biofuels Production. *Liq Gaseous Solid Biofuels - Convers Tech* 2013:299–326. doi:10.5772/52649.
- [69] Kiatkittipong W, Phimsen S, Kiatkittipong K, Wongsakulphasatch S, Laosiripojana N, Assabumrungrat S. Diesel-like hydrocarbon production from hydroprocessing of relevant refining palm oil. *Fuel Process Technol* 2013;116:16–26. doi:10.1016/j.fuproc.2013.04.018.
- [70] Srifa A, Faungnawakij K, Itthibenchapong V, Viriya-empikul N, Charinpanitkul T, Assabumrungrat S. Production of bio-hydrogenated diesel by catalytic hydrotreating of palm oil over NiMoS₂/γ-Al₂O₃ catalyst. *Bioresour Technol* 2014;158:81–90. doi:10.1016/j.biortech.2014.01.100.
- [71] Mäkinen R, Nylund N, Erkkilä K, Saikkonen P. Bus Fleet Operation on Renewable Paraffinic Diesel Fuel. *Development* 2011;2012:10–1. doi:10.4271/2011-01-1965.
- [72] Murtonen T, Aakko-Saksa P, Koponen P, Lehto K, Sarjovaara T, Happonen M, et al. Emission Reduction Potential with Paraffinic Renewable Diesel by Optimizing Engine Settings or Using Oxygenate. *SAE Int* 2012. doi:10.4271/2012-01-1590.
- [73] Knothe G. Biodiesel and renewable diesel: A comparison. *Prog Energy Combust Sci* 2010. doi:10.1016/j.peccs.2009.11.004.

-
-
- [74] Bezergianni S, Dimitriadis A. Comparison between different types of renewable diesel. *Renew Sustain Energy Rev* 2013. doi:10.1016/j.rser.2012.12.042.
- [75] Erhan SZ, Dunn RO, Knothe G, Moser BR. Fuel Properties and Performance of Biodiesel. *Biocatal Bioenergy* 2008;1–57. doi:10.1002/9780470385869.ch1.
- [76] Knothe G. History of Vegetable Oil-Based Diesel Fuels. *Biodiesel Handb Second Ed* 2010;5–19. doi:10.1016/B978-1-893997-62-2.50007-3.
- [77] Arun N, Sharma R V., Dalai AK. Green diesel synthesis by hydrodeoxygenation of bio-based feedstocks: Strategies for catalyst design and development. *Renew Sustain Energy Rev* 2015. doi:10.1016/j.rser.2015.03.074.
- [78] Demirbas A. History of Biodiesel Fuel - Pacific Biodiesel. *Biodiesel* 2017.
- [79] De Sousa FP, Cardoso CC, Pasa VMD. Producing hydrocarbons for green diesel and jet fuel formulation from palm kernel fat over Pd/C. *Fuel Process Technol* 2016;143:35–42. doi:10.1016/j.fuproc.2015.10.024.
- [80] Diesel R, Christian R, Diesel K, September F. *Rudolf Diesel* 2018:162711.
- [81] Sonthalia A. Comparison of fuel characteristics of hydrotreated waste cooking oil with its biodiesel and fossil diesel. *Environ Energy Manag* 2019. doi:10.1007/s11356-019-07110-w.
- [82] Bezergianni S, Dimitriadis A, Chrysikou LP. Quality and sustainability comparison of one- vs. Two-step catalytic hydroprocessing of waste cooking oil. *Fuel* 2014;118:300–7. doi:10.1016/j.fuel.2013.10.078.
- [83] Mota SAP, Mancio AA, Lhamas DEL, Abreu DH De, Silva MS, Santos WG, et al. Production of green diesel by thermal catalytic cracking of crude palm oil (*Elaeis guineensis* Jacq) in a pilot plant. *J Anal Appl Pyrolysis* 2014;110:1–11.
- [84] He Z, Wang X. Hydrodeoxygenation of model compounds and catalytic systems for pyrolysis bio-oils upgrading. *Catal Sustain Energy* 2012. doi:10.2478/cse-2012-0004.
- [85] Ferreira CC, Costa EC, de Castro DAR, Pereira MS, Mâncio AA, Santos MC, et al. Deacidification of organic liquid products by fractional distillation in laboratory and pilot scales. *J Anal Appl Pyrolysis* 2017;127:468–89. doi:10.1016/j.jaap.2017.06.016.
- [86] Westphal GA, Krahl J, Munack A, Rosenkranz N, Schröder O, Schaak J, et al. Combustion of hydrotreated vegetable oil and jatropha methyl ester in a heavy duty engine: Emissions and bacterial mutagenicity. *Environ Sci Technol* 2013;47:6038–46. doi:10.1021/es400518d.
- [87] Kumara B, Prof B, Varma A. *Bioenergy for Sustainability and Security*. 1st ed. Springer Cham; 2019. doi:10.1007/978-3-319-96538-3.
- [88] Herskowitz M, Landau M V., Reizner Y, Berger D. A commercially-viable, one-step process for production of green diesel from soybean oil on Pt/SAPO-11. *Fuel* 2013. doi:10.1016/j.fuel.2013.04.044.
- [89] Bulushev DA, Ross JRH. Catalysis for conversion of biomass to fuels via pyrolysis and gasification : A review. *Catal Today* 2011;171:1–13. doi:10.1016/j.cattod.2011.02.005.
- [90] Kuchonthara P, Puttasawat B, Piumsomboon P, Mekasut L, Vitidsant T. Catalytic
-
-

-
- steam reforming of biomass-derived tar for hydrogen production with $K_2CO_3 / NiO / \gamma-Al_2O_3$ catalyst. *Energy* 2012;29:1525–30. doi:10.1007/s11814-012-0027-y.
- [91] Matsuoka K, Shimbori T, Kuramoto K, Hatano H. Steam Reforming of Woody Biomass in a Fluidized Bed of Iron Oxide-Impregnated Porous Alumina. *Energy & Fuels* 2006;20:2727–31. doi:10.1021/ef060301f.
- [92] Alberto D, Castro R De, Santos MC, Pereira AM. Fractional Distillation of Bio-Oil Produced by Pyrolysis of Açai (*Euterpe oleracea*) Seeds. *Conf COBEQ-2018 Intech Open* 2018.
- [93] Gayubo AG, Aguayo T, Atutxa A, Aguado R. Transformation of Oxygenate Components of Biomass Pyrolysis Oil on a HZSM-5 Zeolite . I . Alcohols and Phenols. *Ind Eng Chem Res* 2004;43:2610–8. doi:10.1021/ie030791o.
- [94] Samolada MC, Papafotica A, Vasalos IA. Catalyst Evaluation for Catalytic Biomass Pyrolysis. *Energy & Fuels* 2000;14:1161–7. doi:10.1021/ef000026b.
- [95] French R, Czernik S. Catalytic pyrolysis of biomass for biofuels production. *Fuel Process Technol* 2010;91:25–32. doi:10.1016/j.fuproc.2009.08.011.
- [96] Crepeau G, Gaillard P, Schaberg P. Engine Impacts and Opportunities of Various Fuels , Including GTL and FAME : Toward Specific Engine Calibration. *SAE Int* 2018;4970.
- [97] Yoon JY. What ' s the Difference between Biodiesel and Renewable (Green) Diesel. *Adv Biofuels* 2009:14.
- [98] Napolitano P, Guido C, Beatrice C, Pellegrini L. Impact of hydrocracked diesel fuel and Hydrotreated Vegetable Oil blends on the fuel consumption of automotive diesel engines. *Fuel* 2018. doi:10.1016/j.fuel.2018.02.097.
- [99] Li L, Quan K, Xu J, Liu F, Liu S, Yu S, et al. Liquidhydrocarbon fuels from catalytic cracking of waste cooking oils using basicmesoporous molecular sieves $K_2O/Ba-MCM-41$ as catalysts. *ACS Sustain Eng* 2013;11:1412–1416.
- [100] Wang F, Xu J, Jiang J, Liu P, Li F, Ye J, et al. Hydrotreatment of vegetable oil for green diesel over activated carbon supported molybdenum carbide catalyst. *Fuel* 2018. doi:10.1016/j.fuel.2017.12.059.
- [101] Putrasari Y, Lim O, Praptijanto A, Santoso WB. A review of Research and Development of Biodiesel as an Alternative Fuel in Indonesia. *Renew Sustain Energy Rev* 2017;72:497–509. doi:10.1016/j.rser.2017.01.001.
- [102] Bezergianni S, Dimitriadis A, Kalogianni A, Pilavachi PA. Hydrotreating of waste cooking oil for biodiesel production. Part I: Effect of temperature on product yields and heteroatom removal. *Bioresour Technol* 2010;101:6651–6. doi:10.1016/j.biortech.2010.03.081.
- [103] Ameen M, Azizan MT, Yusup S, Ramli A, Yasir M. Catalytic hydrodeoxygenation of triglycerides: An approach to clean diesel fuel production. *Renew Sustain Energy Rev* 2017. doi:10.1016/j.rser.2017.05.268.
- [104] Reaume SJ. Cold flow improvements to biodiesel through the use of heterogeneous catalytic skeletal isomerization. 2013. doi:10.1016/j.biombioe.2012.12.008.
- [105] Bezergianni S, Kalogianni A. Hydrocracking of used cooking oil for biofuels
-

-
- production. Bioresour Technol 2009;100:3927–32. doi:10.1016/j.biortech.2009.03.039.
- [106] Verduzco R, Adela M, Allieri A, Rosario M Del. HYDRODEOXYGENATION PROCESS OF VEGETABLE OILS FOR OBTAINING GREEN DIESEL. US 10,858,594 B2, 2020.
- [107] Blom P, Grøn ÆK. Hydroprocessing of Bio-Oils and Oxygenates to Hydrocarbons . Understanding the Reaction Routes. Top Catal Springer 2009;229–40. doi:10.1007/s11244-008-9159-z.
- [108] Snåre M, Kubic I, Murzin DY, A F-T. Heterogeneous Catalytic Deoxygenation of Stearic Acid for Production of Biodiesel. Ind Eng Chem Res 2006;45:5708–15. doi:10.1021/ie060334i.
- [109] Bezergianni S, Dimitriadis A, Sfetsas T, Kalogianni A. Bioresource Technology Hydrotreating of waste cooking oil for biodiesel production . Part II: Effect of temperature on hydrocarbon composition 2010;101:7658–60. doi:10.1016/j.biortech.2010.04.043.
- [110] Kim SK, Brand S, Lee HS, Kim Y, Kim J. Production of renewable diesel by hydrotreatment of soybean oil: Effect of reaction parameters. Chem Eng J 2013;228:114–23. doi:10.1016/j.cej.2013.04.095.
- [111] Bezergianni S, Dagonikou V, Sklari S. The suspending role of H₂O and CO on catalytic hydrotreatment of gas-oil; myth or reality? Fuel Process Technol 2016;144:20–6. doi:10.1016/j.fuproc.2015.12.007.
- [112] Geo VE, Sonthalia A, Nagarajan G, Nagalingam B. Studies on performance, combustion and emission of a single cylinder diesel engine fuelled with rubber seed oil and its biodiesel along with ethanol as injected fuel. Fuel 2017;209:733–41. doi:10.1016/j.fuel.2017.08.036.
- [113] Guzman A, Torres JE, Prada LP, Nun ML. Hydroprocessing of crude palm oil at pilot plant scale. Catal Today 2010;156:38–43. doi:10.1016/j.cattod.2009.11.015.
- [114] Hancsók J, Krár M, Magyar S, Boda L, Holló A, Kalló D. Investigation of the production of high cetane number bio gas oil from pre-hydrogenated vegetable oils over Pt/HZSM-22/Al₂O₃. Microporous Mesoporous Mater 2007;101:148–52. doi:10.1016/j.micromeso.2006.12.012.
- [115] Theilgaard A. Catalytic Production of Biodiesel. Technical University of Denmark, 2011.
- [116] Ning L, Duan Q, Chen Z, Kou H, Liu B, Yang B, et al. A comparative study on the combustion and emissions of a non-road common rail diesel engine fueled with primary alcohol fuels (methanol, ethanol, and n-butanol)/diesel dual fuel. Fuel 2020;266. doi:10.1016/j.fuel.2020.117034.
- [117] Šimáček P, Kubička D, Šebor G, Pospíšil M. Hydroprocessed rapeseed oil as a source of hydrocarbon-based biodiesel. Fuel 2009;88:456–60. doi:10.1016/j.fuel.2008.10.022.
- [118] Zandonai CH, Yassue-Cordeiro PH, Castellã-Pergher SB, Scaliante MHNO, Fernandes-Machado NRC. Production of petroleum-like synthetic fuel by hydrocracking of crude soybean oil over ZSM5 zeolite - Improvement of catalyst
-

-
- lifetime by ion exchange. *Fuel* 2016;172:228–37. doi:10.1016/j.fuel.2015.12.059.
- [119] Liu Y, Sotelo-Boyás R, Murata K, Minowa T, Sakanishi K. Production of Bio-Hydrogenated Diesel by Hydrotreatment of High-Acid-Value Waste Cooking Oil over Ruthenium Catalyst Supported on Al-Polyoxocation-Pillared Montmorillonite. *Catalysts* 2012;2:171–90. doi:10.3390/catal2010171.
- [120] Kubička D, Kaluža L. Deoxygenation of vegetable oils over sulfided Ni, Mo and NiMo catalysts. *Appl Catal A Gen* 2010;372:199–208. doi:10.1016/j.apcata.2009.10.034.
- [121] Prielcel P, Kubička D, Čapek L, Bastl Z, Ryšánek P. The role of Ni species in the deoxygenation of rapeseed oil over NiMo-alumina catalysts. *Appl Catal A Gen* 2011;397:127–37. doi:10.1016/j.apcata.2011.02.022.
- [122] Adam I, Aziz AAR, Suzana Y, Heikal MR, Adam IK, Rashid A, et al. Optimization of Performance and Emissions of a Diesel Engine Fuelled with Rubber Seed-Palm Biodiesel Blends using Response Surface Method. *Asian J Appl Sci* 2016;04:2321–0893.
- [123] Kordulis C, Bourikas K, Gousi M, Kordouli E, Lycourghiotis A. Development of nickel based catalysts for the transformation of natural triglycerides and related compounds into green diesel: A critical review. *Appl Catal B Environ* 2016. doi:10.1016/j.apcatb.2015.07.042.
- [124] Hsu KH, Wang WC, Liu YC. Experimental studies and techno-economic analysis of hydro-processed renewable diesel production in Taiwan. *Energy* 2018;164:99–111. doi:10.1016/j.energy.2018.08.208.
- [125] Kumar R, Farooqui SA, Anand M, Kumar R, Joshi R, Khan A, et al. Hydrotreatment of jatropha oil over NiMoS catalyst supported on thermostable mesoporous silica doped titania for the production of renewable drop-in diesel. *Catal Commun* 2017. doi:10.1016/j.catcom.2017.04.047.
- [126] Jha MK, Sinha AK, Agnihotri P. Hydroprocessing Of Jatropha Oil To Produce Green Fuels. *Int J ChemTech Res* 2013;5:765–70.
- [127] Kubička D, Horáček J. Deactivation of HDS catalysts in deoxygenation of vegetable oils. *Appl Catal A Gen* 2011;394:9–17. doi:10.1016/j.apcata.2010.10.034.
- [128] Šimáček P, Kubička D, Šebor G, Pospíšil M. Fuel properties of hydroprocessed rapeseed oil. *Fuel* 2010;89:611–5. doi:10.1016/j.fuel.2009.09.017.
- [129] Šimáček P, Kubička D, Šebor G, Pospíšil M. Hydroprocessed rapeseed oil as a source of hydrocarbon-based biodiesel. *Fuel* 2009. doi:10.1016/j.fuel.2008.10.022.
- [130] Kochetkova D, Blažek J, Šimáček P, Staš M, Beňo Z. Influence of rapeseed oil hydrotreating on hydrogenation activity of CoMo catalyst. *Fuel Process Technol* 2016;142:319–25. doi:10.1016/j.fuproc.2015.10.034.
- [131] Gusmão J, Brodzki D, Djéga-Mariadassou G, Frety R. Utilization of vegetable oils as an alternative source for diesel-type fuel: hydrocracking on reduced Ni/SiO₂ and sulphided Ni-Mo/ γ -Al₂O₃. *Catal Today* 1989;5:533–44. doi:10.1016/0920-5861(89)80017-3.
- [132] da Rocha Filho GN, Brodzki D, Djéga-Mariadassou G. Formation of alkanes, alkylcycloalkanes and alkylbenzenes during the catalytic hydrocracking of vegetable
-

-
- oils. *Fuel* 1993;72:543–9. doi:10.1016/0016-2361(93)90114-H.
- [133] Toba M, Abe Y, Kuramochi H, Osako M, Mochizuki T, Yoshimura Y. Hydrodeoxygenation of waste vegetable oil over sulfide catalysts. *Catal Today* 2011;164:533–7. doi:10.1016/j.cattod.2010.11.049.
- [134] Ameen M, Tazli M, Yusup S, Ramli A, Yasir M. Catalytic hydrodeoxygenation of triglycerides : An approach to clean diesel fuel production 2017;80:1072–88.
- [135] Chen R, Wang W. The production of renewable aviation fuel from waste cooking oil. Part I: Bio-alkane conversion through hydro-processing of oil. *Renew Energy* 2019. doi:10.1016/j.renene.2018.12.048.
- [136] Kordouli E, Pawelec B, Bourikas K, Kordulis C, Fierro JLG, Lycourghiotis A. Mo promoted Ni-Al₂O₃co-precipitated catalysts for green diesel production. *Appl Catal B Environ* 2018. doi:10.1016/j.apcatb.2018.02.015.
- [137] Mortensen PM, Grunwaldt JD, Jensen PA, Jensen AD. Influence on nickel particle size on the hydrodeoxygenation of phenol over Ni/SiO₂. *Catal Today* 2016. doi:10.1016/j.cattod.2015.08.022.
- [138] Furimsky E. Catalytic hydrodeoxygenation. *Appl Catal A Gen* 2000;199:147–90.
- [139] Şenol OI, Viljava TR, Krause AOI. Effect of sulphiding agents on the hydrodeoxygenation of aliphatic esters on sulphided catalysts. *Appl Catal A Gen* 2007;326:236–44. doi:10.1016/j.apcata.2007.04.022.
- [140] Rakopoulos DC, Rakopoulos CD, Kakaras EC, Giakoumis EG. Effects of ethanol–diesel fuel blends on the performance and exhaust emissions of heavy duty DI diesel engine. *Energy Convers Manag* 2008;49:3155–62. doi:10.1016/j.enconman.2008.05.023.
- [141] Kim HY, Ge JC, Choi NJ. Effects of ethanol-diesel on the combustion and emissions from a diesel engine at a low idle speed. *Appl Sci* 2020;10:1–15. doi:10.3390/APP10124153.
- [142] Liu Y, Murata K, Minowa T, Sakanishi K, Technology B. Production of Bio-Hydrogenated Diesel by Hydrotreatment of High-Acid-Value Waste Cooking Oil over Ruthenium Catalyst Supported on Al-Polyoxocation-Pillared Montmorillonite. *Catalysts* 2012;2:171–90. doi:10.3390/catal2010171.
- [143] Sotelo-Boyás R, Liu Y, Minowa T. Renewable diesel production from the hydrotreating of rapeseed oil with Pt/zeolite and NiMo/Al₂O₃ catalysts. *Ind Eng Chem Res* 2011;50:2791–9. doi:10.1021/ie100824d.
- [144] Kumar N, Sonthalia A, Koul R. Optimization of the Process Parameters for Hydrotreating Used Cooking Oil by the Taguchi Method and Fuzzy Logic. *J Energy Resour Technol ASME* 2020;142:1–9. doi:10.1115/1.4047405.
- [145] P Vincenzo. Green diesel. [Http://WwwOil-GasportalCom/Green-Diesel/](http://WwwOil-GasportalCom/Green-Diesel/) 2011;33:1.
- [146] Liu J, Lei J, He J, Deng L, Wang L, Fan K, et al. Hydroprocessing of Jatropha Oil for Production of Green Diesel over Non-sulfided Ni-PTA / Al₂O₃ Catalyst. *Sci Reports, Nat* 2015:1–13. doi:10.1038/srep11327.
- [147] Zhao X, Wei L, Cheng S, Kadis E, Cao Y, Boakye E, et al. Hydroprocessing of carinata
-

-
- oil for hydrocarbon biofuel over Mo-Zn/Al₂O₃. *Appl Catal B Environ* 2016;196:41–9. doi:10.1016/j.apcatb.2016.05.020.
- [148] Monnier J, Sulimma H, Dalai A, Caravaggio G. Hydrodeoxygenation of oleic acid and canola oil over alumina-supported metal nitrides. *Appl Catal A Gen* 2010;382:176–80. doi:10.1016/j.apcata.2010.04.035.
- [149] Pinto F, Varela FT, Gonçalves M, Neto André R, Costa P, Mendes B. Production of bio-hydrocarbons by hydrotreating of pomace oil. *Fuel* 2014;116:84–93. doi:10.1016/j.fuel.2013.07.116.
- [150] Zarchin R, Rabaev M, Vidruk-Nehemya R, Landau M V., Herskowitz M. Hydroprocessing of soybean oil on nickel-phosphide supported catalysts. *Fuel* 2015;139:684–91. doi:10.1016/j.fuel.2014.09.053.
- [151] Ayodele OB, Abbas HF, Daud WMAW. Catalytic upgrading of oleic acid into biofuel using Mo modified zeolite supported Ni oxalate catalyst functionalized with fluoride ion. *Energy Convers Manag* 2014;88:1111–9. doi:10.1016/j.enconman.2014.02.014.
- [152] Li T, Cheng J, Huang R, Zhou J, Cen K. Conversion of waste cooking oil to jet biofuel with nickel-based mesoporous zeolite Y catalyst. *Bioresour Technol* 2015;197:289–94. doi:10.1016/j.biortech.2015.08.115.
- [153] Verma D, Rana BS, Kumar R, Sibi MG, Sinha AK. Diesel and aviation kerosene with desired aromatics from hydroprocessing of jatropha oil over hydrogenation catalysts supported on hierarchical mesoporous SAPO-11. *Appl Catal A Gen* 2015;490:108–16. doi:10.1016/j.apcata.2014.11.007.
- [154] Deliy I V., Vlasova EN, Nuzhdin AL, Gerasimov EY, Bukhtiyarova GA. Hydrodeoxygenation of methyl palmitate over sulfided Mo/Al₂O₃, CoMo/Al₂O₃ and NiMo/Al₂O₃ catalysts. *R Soc Chem* 2014;4:2242–50. doi:10.1039/c3ra46164e.
- [155] Lee SP, Ramli A. Methyl oleate deoxygenation for production of diesel fuel aliphatic hydrocarbons over Pd/SBA-15 catalysts. *Chem Cent J* 2013;7:1–10. doi:10.1186/1752-153X-7-149.
- [156] Breyse M, Afanasiev P, Geantet C, Vrinat M. Overview of support effects in hydrotreating catalysts. *Catal Today* 2003;86:5–16. doi:10.1016/S0920-5861(03)00400-0.
- [157] Rajesh M, Sau M, Malhotra RK, Sharma DK. Hydrotreating of Gas Oil, Jatropha Oil, and Their Blends Using a Carbon Supported Cobalt-Molybdenum Catalyst. *Pet Sci Technol* 2015;33:1653–9. doi:10.1080/10916466.2015.1036291.
- [158] Bezergianni S, Dimitriadis A. Temperature effect on co-hydroprocessing of heavy gas oil-waste cooking oil mixtures for hybrid diesel production. *Fuel* 2013;103:579–84. doi:10.1016/j.fuel.2012.08.006.
- [159] Yang Y, Wang Q, Zhang X, Wang L, Li G. Hydrotreating of C18 fatty acids to hydrocarbons on sulphided NiW/SiO₂-Al₂O₃. *Fuel Process Technol* 2013;116:165–74. doi:10.1016/j.fuproc.2013.05.008.
- [160] Huber GW, Corma A. Synergies between Bio- and Oil Refineries for the Production of Fuels from Biomass. *Intersci Sustain Fuels* 2007;46:7184–201. doi:10.1002/anie.200604504.
-

-
- [161] Chen S. Green Oil Production by Hydroprocessing. *Int J Clean Coal Energy* 2012;1:43–55. doi:10.4236/ijcce.2012.14005.
- [162] Bezergianni S, Dimitriadis A, Kalogianni A, Knudsen KG. Toward hydrotreating of waste cooking oil for biodiesel production. Effect of pressure, H₂/oil ratio, and liquid hourly space velocity. *Ind Eng Chem Res* 2011;50:3874–9. doi:10.1021/ie200251a.
- [163] Kumar N, Koul R, Singh RC. Comparative analysis of ternary blends of renewable Diesel, diesel and ethanol with diesel. *Sustain Energy Technol Assessments* 2022;50:101828. doi:10.1016/j.seta.2021.101828.
- [164] Das LM, Kumar D, Pradhan S, Naik MK, Naik SN. Long-term storage stability of biodiesel produced from Karanja oil. *Fuel* 2009;88:2315–8. doi:10.1016/j.fuel.2009.05.005.
- [165] Prokopowicz A, Zaciera M, Sobczak A, Bielaczyc P, Woodburn J. The Effects of Neat Biodiesel and Biodiesel and HVO Blends in Diesel Fuel on Exhaust Emissions from a Light Duty Vehicle with a Diesel Engine. *Environ Sci Technol* 2015;49:7473–82. doi:10.1021/acs.est.5b00648.
- [166] Kuronen M, Mikkonen S. *Hydrotreated Vegetable Oil as Fuel for Heavy Duty Diesel Engines*. SAE Tech. Pap., Warrendale, USA: 2018.
- [167] Nylund N, Ahtiainen M, Saikkonen P, Amberla A, Aatola H. Optimized usage of NExBTL renewable diesel fuel. *JULKAISIJA – UTGIVARE*; 2011.
- [168] Gosling C, Marker T, Perego C. Vegetable oil- based diesel can offer better integration within crude-oil refineries for fuels blending. 2007.
- [169] Phoon LY, Hashim H, Mat R, Mustaffa AA. Flash point prediction of tailor-made green diesel blends containing B5 palm oil biodiesel and alcohol. *Fuel* 2016;175:287–93. doi:10.1016/j.fuel.2016.02.027.
- [170] Sugiyama K, Goto I, Kitano K, Mogi K, Honkanen M. Effects of Hydrotreated Vegetable Oil (HVO) as Renewable Diesel Fuel on Combustion and Exhaust Emissions in Diesel Engine. *SAE Int J Fuels Lubr* 2011;5:2011-01–1954. doi:10.4271/2011-01-1954.
- [171] Hartikka T, Kuronen M, Kiiski U. Technical Performance of HVO (Hydrotreated Vegetable Oil) in Diesel Engines. *SAE Int* 2018. doi:10.4271/2012-01-1585.
- [172] Pitz WJ, Mueller CJ. Recent progress in the development of diesel surrogate fuels. *Prog Energy Combust Sci* 2011;37:330–50. doi:10.1016/j.pecs.2010.06.004.
- [173] Aatola H, Larmi M, Sarjovaara T, Mikkonen S. Hydrotreated Vegetable Oil (HVO) as a Renewable Diesel Fuel: Trade-off between NO_x, Particulate Emission, and Fuel Consumption of a Heavy Duty Engine. *SAE Int J Engines* 2008;1:2008-01–2500. doi:10.4271/2008-01-2500.
- [174] Al-Muhtaseb AH, Jamil F, Al-Haj L, Al-Hinai MA, Baawain M, Myint MTZ, et al. Efficient utilization of waste date pits for the synthesis of green diesel and jet fuel fractions. *Energy Convers Manag* 2016. doi:10.1016/j.enconman.2016.09.004.
- [175] Singh D, Sandhu SS, Sarma AK. An investigation of green diesel produced through hydro-processing of waste cooking oil using an admixture of two heterogeneous catalysts. *Energy Sources, Part A Recover Util Environ Eff* 2018;40:968–76.
-

doi:10.1080/15567036.2018.1468508.

- [176] Lapuerta M, Rodríguez-fernández J, Fernández-rodríguez D. Cold flow and filterability properties of n -butanol and ethanol blends with diesel and biodiesel fuels. *Fuel* 2018;224:552–9. doi:10.1016/j.fuel.2018.03.083.
- [177] Nylund N, Hulkkonen T, Tilli A, Mikkonen S, Saikkonen P, Amberla A. Emission performance of paraffinic HVO diesel fuel in heavy duty vehicles. *Soc Automot Eng Japan, Inc SAE Int* 2018. doi:10.4271/2011-01-1966.
- [178] Ogunkoya D, Roberts WL, Fang T, Thapaliya N. Investigation of the effects of renewable diesel fuels on engine performance , combustion , and emissions. *Fuel* 2015;140:541–54. doi:10.1016/j.fuel.2014.09.061.
- [179] Kim D, Kim S, Oh S, No S-Y. Engine performance and emission characteristics of hydrotreated vegetable oil in light duty diesel engines. *Fuel* 2014;125:36–43. doi:10.1016/j.fuel.2014.01.089.
- [180] Panneerselvam N, Murugesan A, Vijayakumar C, Kumaravel A, Subramaniam D, Avinash A. Effects of injection timing on bio-diesel fuelled engine characteristics - An overview. *Renew Sustain Energy Rev* 2015;50:17–31. doi:10.1016/j.rser.2015.04.157.
- [181] Kim SK, Brand S, Lee HS, Kim Y, Kim J. Production of renewable diesel by hydrotreatment of soybean oil: Effect of reaction parameters. *Chem Eng J* 2013;228:114–23. doi:10.1016/j.cej.2013.04.095.
- [182] Singh D, Subramaniam KA, Singal SK. Emissions and fuel consumption characteristics of a heavy duty diesel engine fueled with Hydroprocessed Renewable Diesel and Biodiesel. *Appl Energy* 2015;155:440–6. doi:10.1016/j.apenergy.2015.06.020.
- [183] Caprotti R, Tang T, Ishibe N, R.In-ochanon, C.Tipdecho, S.Silapakampeerapap. Performance of Diesel containing Bio-Hydrogenated Component. *SAE Pap* 2011:2126–37. doi:10.4271/2011-01-1953.
- [184] Imperato M, Tilli A, Sarjovaara T, Larmi M. Large-bore compression-ignition engines: High NO_x reduction achieved at low load with hydro-treated vegetable oil. *SAE Tech Pap* 2011;5.
- [185] Cheah KW, Yusup S, Chuah LF, Bokhari A. Physio-chemical Studies of Locally Sourced Non-Edible Oil: Prospective Feedstock for Renewable Diesel Production in Malaysia. *Procedia Eng.*, 2016. doi:10.1016/j.proeng.2016.06.460.
- [186] Pidol L, Lecointe B, Starck L, Jeuland N. Ethanol-biodiesel-Diesel fuel blends: Performances and emissions in conventional Diesel and advanced Low Temperature Combustions. *Fuel* 2012;93:329–38. doi:10.1016/j.fuel.2011.09.008.
- [187] Caton PA, Williams SA, Hamilton LJ. HYDROTREATED ALGAE RENEWABLE FUEL PERFORMANCE IN A MILITARY DIESEL ENGINE. *Proc ASME Intern Combust Engine Div Spring Tech Conf* 2012:1–12.
- [188] Petersen J, Seivwright D, Caton P, Millsaps K. Combustion characterization and ignition delay modeling of low-and high-cetane alternative diesel fuels in a marine diesel engine. *Energy and Fuels* 2014;28:5463–71. doi:10.1021/ef500565t.
- [189] Anderson LG. Effects of Biodiesel Fuel Use on Vehicle Emissions. *Proc World Renew Energy Congr – Sweden*, 8–13 May, 2011, Linköping, Sweden 2011;57:3645–52.

doi:10.3384/ecp110573645.

- [190] Bielaczyc P, Szczotka A. A Study of RME-Based Biodiesel Blend Influence on Performance, Reliability and Emissions from Modern Light-Duty Diesel Engines. SAE Tech Pap 2008:1–14.
- [191] Zervas E. Regulated and non-regulated pollutants emitted from two aliphatic and a commercial diesel fuel. *Fuel* 2008;87:1141–7. doi:10.1016/j.fuel.2007.06.010.
- [192] Karavalakis G, Jiang Y, Yang J, Durbin T, Nuottimäki J, Lehto K. Emissions and Fuel Economy Evaluation from Two Current Technology Heavy-Duty Trucks Operated on HVO and FAME Blends. *SAE Int J Fuels Lubr* 2016;9:177–90. doi:10.4271/2016-01-0876.
- [193] Mendes MJ, Santos OAA, Jordão E, Silva AM. Hydrogenation of oleic acid over ruthenium catalysts. *Appl Catal A Gen* 2001;217:253–62.
- [194] Pali HS, Kumar N, Alhassan Y. Performance and emission characteristics of an agricultural diesel engine fueled with blends of Sal methyl esters and diesel. *Energy Convers Manag* 2015;90:146–53. doi:10.1016/j.enconman.2014.10.064.
- [195] Rahman SMA, Masjuki HH, Kalam MA, Sanjid A, Abedin MJ. Assessment of emission and performance of compression ignition engine with varying injection timing. *Renew Sustain Energy Rev* 2014;35:221–30. doi:10.1016/j.rser.2014.03.049.
- [196] Frantzi D, Zabaniotou A. Waste-based intermediate bioenergy carriers: Syngas production via coupling slow pyrolysis with gasification under a circular economy model. *Energies* 2021;14. doi:10.3390/en14217366.
- [197] Pali HS, Kumar N. Combustion, performance and emissions of Shorea robusta methyl ester blends in a diesel engine. *Biofuels* 2016;7:447–56. doi:10.1080/17597269.2016.1153363.
- [198] Grobbelaar E. The development of a small diesel engine test bench employing an electric dynamometer. Stellenbosch University, 2017.
- [199] Assanis DN, Filipi ZS, Fiveland SB, Syrimis M. A methodology for cycle-by-cycle transient heat release analysis in a turbocharged direct injection diesel engine. SAE Tech Pap 2000. doi:10.4271/2000-01-1185.
- [200] Bekal S, Babu TPA. Bio-fuel variants for use in CI engine at design and off-design regimes: An experimental analysis. *Fuel* 2008;87:3550–61. doi:10.1016/j.fuel.2008.07.001.
- [201] Hinrichs W. Uncertainty of measurement. *Mater Test* 1994;36:476–80. doi:10.4324/9780080499833-15.
- [202] Ghadikolaei MA, Cheung CS, Yung KF. Study of combustion, performance and emissions of a diesel engine fueled with ternary fuel in blended and fumigation modes. *Fuel* 2019;235:288–300. doi:10.1016/j.fuel.2018.07.089.
- [203] Krishnamoorthy V, Dhanasekaran R, Rana D, Saravanan S, Rajesh Kumar B. A comparative assessment of ternary blends of three bio-alcohols with waste cooking oil and diesel for optimum emissions and performance in a CI engine using response surface methodology. *Energy Convers Manag* 2018;156:337–57. doi:10.1016/j.enconman.2017.10.087.

-
-
- [204] Gopal K, Sathiyagnanam AP, Rajesh Kumar B, Saravanan S, Rana D, Sethuramasamyraja B. Prediction of emissions and performance of a diesel engine fueled with n-octanol/diesel blends using response surface methodology. *J Clean Prod* 2018;184:423–39. doi:10.1016/j.jclepro.2018.02.204.
- [205] Mohamad Said KA, Mohamed Amin MA. Overview on the Response Surface Methodology (RSM) in Extraction Processes. *J Appl Sci Process Eng* 2016;2. doi:10.33736/jaspe.161.2015.
- [206] Vibhanshu V, Kumar N, Mishra C, Sinha S, Pali HS, Bansal S. Experimental Investigation of Diesel Engine Fueled with Jatropha Oil Blend with Ethanol. *SAE Int* 2013;951–8. doi:10.4271/2013-24-0105.
- [207] Aromatics L, Zheng Y, Huang Y, Xu G, Kang J, Liu C, et al. Optimizing Catalytic Pyrolysis of Rubber Seed Oil for Light Aromatics and Anti-deactivation of ZSM-5. *J Anal Appl Pyrolysis* 2017. doi:10.1016/j.jaap.2017.06.010.
- [208] Li DG, Zhen H, Xingcai L, Wu-Gao Z, Jian-Guang Y. Physico-chemical properties of ethanol-diesel blend fuel and its effect on performance and emissions of diesel engines. *Renew Energy* 2005;30:967–76. doi:10.1016/j.renene.2004.07.010.
- [209] Chatterjee R, Kumar S. Spectroscopic Analysis and Performance Studies of Jatropha Extracted Bio-diesel. *Waste Biomass Valor Catal* 2017. doi:10.1007/s12649-017-9897-x.
- [210] Janampelli S, Darbha S. Metal Oxide Promoted Hydrodeoxygenation Activity of Platinum in Pt-MO_x / Al₂O₃ Catalysts for Green Diesel Production Catalysts for Green Diesel Production. *Energy & Fuels* 2018;1–48. doi:10.1021/acs.energyfuels.8b03588.
- [211] Boopathi D, Thiyagarajan S, Geo VE, Madhankumar S. Effect of the second generation and third generation biofuel blend on performance , emission and combustion characteristics of CI engine. *Int J Ambient Energy ISSN* 2018;1–28. doi:10.1080/01430750.2018.1492439.
- [212] Lapuerta M, Armas O, Garcı R. Effect of Ethanol on Blending Stability and Diesel Engine Emissions. *Energy & Fuels* 2009;4343–54. doi:10.1021/ef900448m.
- [213] Lapuerta M, Rodríguez-fernández J, Fernández-rodríguez D, Patiño-camino R. Modeling viscosity of butanol and ethanol blends with diesel and biodiesel fuels. *Fuel* 2017;199:332–8. doi:10.1016/j.fuel.2017.02.101.
- [214] Pattanaik BP, Jena J, Misra RD. The effect of oxygen content in soapnut biodiesel-diesel blends on performance of a diesel engine. *Int J Automot Mech Eng* 2017;14:4574–88. doi:10.15282/ijame.14.3.2017.14.0361.
- [215] Hulwan DB, Joshi S V. Performance, emission and combustion characteristic of a multicylinder DI diesel engine running on diesel-ethanol-biodiesel blends of high ethanol content. *Appl Energy* 2011;88:5042–55. doi:10.1016/j.apenergy.2011.07.008.
- [216] Tomar M, Dewal H, Sonthalia A, Kumar N. Optimization of spark-ignition engine characteristics fuelled with oxygenated bio-additive (triacetin) using response surface methodology. *Proc Inst Mech Eng Part E J Process Mech Eng* 2020. doi:10.1177/0954408920971110.
- [217] Mancio AA, Mota SAP, Ferreira CC, Carvalho TUS, Neto OS, Zamian JR, et al.
-
-

-
- Separation and characterization of biofuels in the jet fuel and diesel fuel ranges by fractional distillation of organic liquid products. *Fuel* 2018;215:212–25. doi:10.1016/j.fuel.2017.11.029.
- [218] Fabrizi A, Guarini G, Meliciani V. Green patents, regulatory policies and research network policies. *Res Policy* 2018. doi:10.1016/j.respol.2018.03.005.
- [219] Barbour RH, Rickeard DJ, Elliott NG. SAE TECHNICAL Understanding Diesel Lubricity. SAE Tech. Pap., 2018.
- [220] Kuszewski H, Jaworski A, Ustrzycki A. Lubricity of ethanol–diesel blends – Study with the HFRR method. *Fuel* 2017;208:491–8. doi:10.1016/j.fuel.2017.07.046.
- [221] Fu J, Turn SQ. Characteristics and stability of biofuels used as drop-in replacement for NATO marine diesel. *Fuel* 2019;236:516–24. doi:10.1016/j.fuel.2018.09.042.
- [222] Singh D, Sarma AK, Sandhu SS. A comprehensive experimental investigation of green diesel as a fuel for CI engines. *Int J Green Energy* 2019;16:1152–64. doi:10.1080/15435075.2019.1653882.
- [223] Singh D, Subramanian KA, Juneja M, Singh K, Singh S. Investigating the Effect of Fuel Cetane Number , Oxygen Content , Fuel Density , and Engine Operating Variables on NOx Emissions of a Heavy Duty Diesel Engine 2016;00:1–8. doi:10.1002/ep.
- [224] Singh D, Subramanian KA, Bal R, Singh SP, Badola R. Combustion and emission characteristics of a light duty diesel engine fueled with hydro-processed renewable diesel. *Energy* 2018;154:498–507. doi:10.1016/j.energy.2018.04.139.
- [225] Wu-gao Z, Li D, Zhen H, Jian-guang Y. Physico-chemical properties of ethanol – diesel blend fuel and its effect on performance and emissions of diesel engines. *Renew Energy* 2005;30:967–76. doi:10.1016/j.renene.2004.07.010.
- [226] Sayin C, Canakci M. Effects of injection timing on the engine performance and exhaust emissions of a dual-fuel diesel engine. *Energy Convers Manag* 2009;50:203–13. doi:10.1016/j.enconman.2008.06.007.

APPENDIX 1

Specifications of Engine Test-Rig

Parameters	Specifications
Engine make	Kirloskar
Number of cylinders	1
Strokes	4
Rated power	3.5 kW
Speed at rated power	1500 rpm
Bore x Stroke	87.5 x 110 mm
Length of connecting rod	234 mm
Orifice diameter	20 mm
Cooling type	Water cooled
Compression ratio	17.5:1
Dynamometer	Eddy current
Dynamometer arm length	185 mm
Inlet valve opening	4.5° before TDC
Exhaust valve opening	35.5° before BDC
Inlet valve closing	35.5° after BDC
Exhaust valve closing	4.5° after TDC
Fuel injection timing	23° before TDC
Fuel injection pump	MICO inline (mechanical governor, flange mount)
Injection duration	18° CA
Number of injector holes	3
Nozzle diameter	0.148 mm

APPENDIX 2

Specifications AVL DITEST 1000 Gas Analyzer

Parameters		Specifications	
Make		AVL	
Gases measured		O ₂ (Electro-chemical) CO, CO ₂ , HC (Infrared) NO (Electro-chemical)	
Dimensions (D*W*H), mm		85*270*320	
Weight		2.5 kg	
Humidity (non-condensing)		In between 10 to 90%	
Temperature		Operating	5°C to 40°C
		Storage	0°C to 50°C
Voltage, Volts		11 to 25, DC	
Power consumed , VA		20	
Measurement Range			
Parameter		by Volume	
CO	Measurement Range	0 to 15%	
	Resolution	0.01%	
	Precision	± 0.01%	
CO ₂	Measurement Range	0 to 20%	
	Resolution	0.1%	
	Precision	± 0.2%	
HC	Measurement Range	0 to 30000 ppm	
	Resolution	1ppm	
	Precision	± 10ppm	
NO	Measurement Range	0 to 5000 ppm	
	Resolution	1ppm	
	Precision	± 50ppm	
O ₂	Measurement Range	0 to 55%	
	Resolution	0.01%	
	Precision	± 1%	

APPENDIX-3

Specifications of AVL MDS 480 Smoke-meter

Parameter	Specifications
Make	AVL
Dimensions (D*W*H), mm	136*395*285
Weight	3.5 kg
Humidity, non-condensing	Lesser than 90%
Power consumed, VA	~ 78
Heating Chamber temp	100°C
Maximum emission temperature	200°C
Source of Light	Halogen bulb, 12V, 5W
Detector	Selenium Photocell
Measurement	
Principle	Light Extinction Measurement
Range	0 to 99%
Precision	0.1%
Uncertainty	2.1%
Length	215mm + 2mm

APPENDIX-4

Optimization Data of Non-Dimensional 2nd Order Differential Equations

Response	Equation
BTE, %	8.43+ 11.666 [BMEP (bar)]- 0.010 [RENEWABLE DIESEL (%)]+ 0.5645 [ETHANOL (%)]- 1.5807 [BMEP (bar)]*[BMEP (bar)]- 0.00054 [RENEWABLE DIESEL (%)]* [RENEWABLE DIESEL (%)]- 0.03906 [ETHANOL(%)]*[ETHANOL(%)]+ 0.00134 [BMEP (bar)]*[RENEWABLE DIESEL (%)]- 0.00350 [BMEP (bar)]*[ETHANOL(%)]- 0.00128 [RENEWABLE DIESEL (%)] * [ETHANOL(%)]
CO, g/kWh	14.87- 15.232 [BMEP (bar)]- 0.073 RENEWABLE DIESEL (%)- 0.0196[ETHANOL (%)]+ 4.6066 [BMEP (bar)]*[BMEP (bar)]+ 0.00138 [RENEWABLE DIESEL (%)]*[RENEWABLEDIESEL (%)]+ 0.00168 [ETHANOL(%)]*[ETHANOL(%)]- 0.00425 [BTE (bar)]*[RENEWABLE DIESEL (%)]+ 0.02047 [BMEP (bar)]*[ETHANOL(%)]- 0.00085 [RENEWABLE DIESEL (%)]*[ETHANOL(%)]
HC, g/kWh	11.28- 5.652 [BMEP (bar)]+ 0.130 [RENEWABLE DIESEL (%)]+0.1368[ETHANOL (%)]+ 0.7814 [BMEP (bar)]*[BMEP (bar)]- 0.00154[RENEWABLE DIESEL (%)]* [RENEWABLE DIESEL (%)]- 0.00355[ETHANOL(%)]*[ETHANOL(%)]- 0.00878 [BMEP (bar)]*[RENEWABLE DIESEL (%)]- 0.01472 [BMEP (bar)]*[ETHANOL (%)]+ 0.00073 [RENEWABLE DIESEL (%)]*[ETHANOL(%)]
NO, g/kWh	23.05- 8.774 [BMEP (bar)]- 0.145[RENEWABLE DIESEL (%)]- 0.2938[ETHANOL (%)]+ 1.1006 BTE (bar)*[BMEP (bar)]+ 0.00152[RENEWABLE DIESEL (%)]* [RENEWABLE DIESEL (%)]+ 0.00594 [ETHANOL(%)]*[ETHANOL(%)]+ 0.00784 [BMEP (bar)]*[RENEWABLE DIESEL (%)]+ 0.03031 [BMEP (bar)]*[ETHANOL (%)]+ 0.00216 [RENEWABLE DIESEL (%)]*[ETHANOL(%)]
Smoke Opacity, %	7.42- 0.221 [BMEP (bar)]- 0.237 [RENEWABLE DIESEL (%)]0.389 [ETHANOL(%)]+ 3.3252 [BMEP (bar)]*[BMEP (bar)]+ 0.00165[RENEWABLE DIESEL (%)]* [RENEWABLE DIESEL (%)]+ 0.00642 [ETHANOL(%)]*[ETHANOL(%)]- 0.0332 [BMEP (bar)]*[RENEWABLE DIESEL (%)]- 0.0952 [BMEP (bar)]*[ETHANOL(%)] + 0.00977 [RENEWABLE DIESEL (%)]*[ETHANOL(%)]

LIST OF PUBLICATIONS

International Journals

1. **Rashi Koul**, Naveen Kumar (2019): A review on the production and physicochemical properties of renewable diesel and its comparison with biodiesel, **Energy Sources, Part A: Recovery, Utilization, and Environmental Effects**, DOI: 10.1080/15567036.2019.1646355 (Publisher: Taylor & Francis SCIE Indexed)
2. Naveen Kumar, Ankit Sonthalia, Mukul Tomar, **Rashi Koul (2020)**, An experimental Investigation on Spray, Performance and Emission of Hydrotreated Waste Cooking Oil Blends in an Agricultural Engine. **International Journal of Engine Research. In Press**. DOI: 10.1177/1468087420928734. (Publisher: Institution of Mechanical Engineers, SAGE)
3. Naveen Kumar, Ankit Sonthalia, **Rashi Koul (2020)**, Optimization of the process parameters for hydrotreating used cooking oil by the Taguchi method and Fuzzy logic. **Journal of Energy Resources Technology**; 142(12): 123006 DOI: 10.1115/1.4047405 (Publisher: American Society of Mechanical Engineers)
4. **Rashi Koul**, Naveen Kumar and R C Singh (2021): Comparative analysis of ternary blends of renewable Diesel, diesel and ethanol with diesel, **Sustainable Energy Technologies and Assessment**, DOI: 10.1016/j.seta.2021.101828 (Publisher: Elsevier SCIE indexed)
5. Naveen Kumar, **Rashi Koul**, R C Singh (2022): Comparative analysis of renewable diesel and biodiesel produced from Jatropha oil. **Environmental Progress & Sustainable Energy** 2022:1–17. DOI:10.1002/ep.13832 (Publisher: Wiley SCIE indexed)

International Conferences

1. **Rashi Koul**, Naveen Kumar and R C Singh (2020): Emission Characteristics of Renewable Diesel and its Comparison with the Diesel Fuel on Single Cylinder Diesel engine. The 2nd International Conference on ‘Future Learning Aspects of Mechanical Engineering’, AUUP, Uttar Pradesh, India).
2. **Rashi Koul**, Naveen Kumar and R C Singh (2020): Emission and Performance Parameters of the Renewable Diesel Produced from Jatropha Oil on the Single Cylinder Diesel Engine. (International Virtual Conference on ‘Future Trends in Automotive Technologies’, VIT, Tamil Nadu, India).

A Brief Biographical Sketch



Rashi Koul was born on 18th September 1980 in Srinagar, J&K, India. She did her B.E. in Mechanical Engineering from Amravati University, Maharashtra, India in the year 2002; PGDM with specialisation in Human Resource from IGNOU in 2007, Delhi, India; M.Tech. with major in Thermal Engineering from Delhi Technological University, Delhi, India in the year 2013. She then enrolled herself in Delhi Technological University as a Ph.D. scholar in the Centre for Advanced Studies and Research in Automotive Engineering (CASRAE) at Mechanical Engineering Department.

Ms. Rashi Koul has over 13 years of experience in industry and teaching which includes 8 years in Amity University Haryana (AUH), Haryana. She has made significant and crucial contribution in setting up the biodiesel lab in AUH and has also guided many PG and UG students.

Ms. Rashi Koul is conducting research in alternative fuels with special emphasis on sustainable fuels and cleaner combustion techniques. She has worked on biodiesel, alcohol and now renewable diesel which is different and better than much-researched biodiesel. She has published 11 research papers in Scopus/SCI-indexed journals and conferences of repute. She is a member of ASME and IET. In recognition of her excellent research contribution, she has been nominated for Research Excellence award for executing commendable research work in the year 2022.

Curriculum Vitae

Personal Details:

Name: Rashi Koul
Date of Birth: 18 September 1980
Father's Name: Prof. Prediman Krishen Koul
Mother's Name: Mrs. Indra Mattoo
Marital Status: Married
Husband's Name: Mr. Amit Kaul
Permanent Address: Flat No. 28, Block G, Datta Ram CGHS, Sector 18, Rohini, New Delhi 110089
Nationality: Indian
Mobile No: + 91- 9718150288
Email Id: rashikoul@gmail.com
Languages known: English, Hindi, Kashmiri

Education Qualifications:

YEAR	COURSE	NAME OF INSTITUTE	Marks / Grade/ CGPA
2017	Ph.D. (Mechanical Engineering)	Delhi Technological University (formerly known as DCE)	
2013	M.Tech. (Thermal Engineering)	Delhi Technological University	7.84
2007	PGDM (Specialisation HR)	IGNOU	B
2002	B.E. Mechanical	Anuradha Engineering College, University of Amravati	70%

Papers Published:

- Koul, Rashi, Naveen Kumar, and R. C. Singh. "A review on the production and physicochemical properties of renewable diesel and its comparison with biodiesel." *Energy Sources, Part A: Recovery, Utilization, and Environmental Effects* 43.18 (2021): 2235-2255.
- Kumar, Naveen, Rashi Koul, and R. C. Singh. "Comparative analysis of ternary blends of renewable Diesel, diesel and ethanol with diesel." *Sustainable Energy Technologies and Assessments* 50 (2022): 101828.
- Kumar, Naveen, Ankit Sonthalia, Mukul Tomar, and Rashi Koul. "An experimental investigation on spray, performance and emission of hydrotreated waste cooking oil blends in an agricultural engine." *International Journal of Engine Research* 22, no. 7 (2021): 2305-2317.

-
-
- Kumar, Naveen, Ankit Sonthalia, and Rashi Koul. "Optimization of the process parameters for hydrotreating used cooking oil by the Taguchi method and Fuzzy logic." *Journal of Energy Resources Technology* 142, no. 12 (2020).
 - Koul, Rashi, Naveen Kumar, and R. C. Singh. "A review on the production and physicochemical properties of renewable diesel and its comparison with biodiesel." *Energy Sources, Part A: Recovery, Utilization, and Environmental Effects* 43, no. 18 (2021): 2235-2255.

Conferences Attended:

- Rashi Koul, Naveen Kumar and R C Singh (2020): Emission Characteristics of Renewable Diesel and its Comparison with the Diesel Fuel on Single Cylinder Diesel engine. The 2nd International Conference on 'Future Learning Aspects of Mechanical Engineering', AUUP, Uttar Pradesh, India).
- Rashi Koul, Naveen Kumar and R C Singh (2020): Emission and Performance Parameters of the Renewable Diesel Produced from Jatropha Oil on the Single Cylinder Diesel Engine. (International Virtual Conference on 'Future Trends in Automotive Technologies', VIT, Tamil Nadu, India).
- Advancements and Modern Innovations in Engineering and Technology, 2020
- 8th International Symposium on the fusion Science & Technologies (ISFT2020) held in JCBUST, YMCA, Faridabad, India from January 6-10, 2020. 20
- International Conference on New Frontiers in Engineering, Science and Technology (NFEST-2018) held in New Delhi, India from January 8-12, 2018.
- The Methanol Pathway to Hydrogen, Mission Hydrogen GmbH. April 2022

Academic Projects:

- Conversion of Waste Plastics to Liquid Fuel Using Thermo-Catalytic Pyrolysis Process For Effective Plastic Waste Management
- Properties of a Pre-Heated Jatropha Oil to be used in CI Engine as a Transportation Fuel
- Comparison of Chemical Properties of Diesel and Bio-Diesel from Jatropha Oil Produced from Bio Reactor Plant
- Design and Fabrication of Active Steering and Lane Control Mechanism for Automobiles
- Performance Characteristics of Biodiesel from Jatropha Oil
- Design and Construction of Foldable Electric Scooters
- Multi-Angular Gearless Drive
- Amphibian Robot

Work Experience:

Amity University, Gurgaon

Assistant Professor, Mechanical Engineering Department

Sept 2014 – May 2022

Responsibilities

University Grants Commission (UGC) -Departmental Coordinator

National Assessment Accreditation Council (NAAC) -Departmental Coordinator

Institution of Engineering and Technology (IET) -Departmental Coordinator

Set-up a Biodiesel Laboratory in AUH

Event Coordinator and Organiser of numerous guest lectures, expert talks, software programs trainings, alumni talks, farewells, fresher's orientation and induction, etc.

Technical Fest (Anveshan) -Coordinator

Overall 10 departmental labs in-charge (2019-2020)

Conference, Advancements and Modern Innovations in Engineering and Technology, 2020, Sessions Organiser, Rapporteur

Paper Reviewer in numerous National and International Journals and Conferences.

Editor of College Newsletter, Pragati

Faculty Coordinator for 'Shiksha Association' club in AUH.

Coordinator and Mentor for B.Tech, Mechanical Final Year and Third Year students

Member of American Society of Mechanical Engineers (ASME) and Institutions of Engineering and Technology (IET)

Subjects Taught: Engineering Thermodynamics, Heat Transfer, Fluid Mechanics and Fluid Machines, Refrigeration and Air Conditioning, Engineering mechanics, Basics of Mechanical Engineering, Gas Turbines, Internal Combustion Engines, Combustion and flames, Advanced Fluid Mechanics.

Dronacharya College of Engineering, Gurgaon

Assistant Professor, Mechanical Engineering Department

Jan 2014 – May 2014

Responsibilities

Responsible for Consultancy Development Cell for Mechanical Engineering Department

Responsible for Entrepreneurship Development Cell for Mechanical Engineering Department

Subjects Taught: Engineering Thermodynamics, Heat Transfer, Fluid Mechanics

Marathwada Institute of Technology, Aurangabad

Lecturer, Mechanical Engineering Department

Jan 2007 – Feb 2011

Responsibilities

Acted as an external examiner in PES Engineering College under University instructions

Head of the Ladies Redressal Cell for the college

Complete responsibility of Thermal Engineering Laboratory

Member in a disciplinary committee

Department conducted periodic students review with my feedback consistently being excellent, 98%

Organizing Member in Techno-Millennium (A Technical Event) in college

Organized an Industrial Visit for B.E. students

Subjects taught: Engineering Thermodynamics, Applied Thermodynamics, Fluid Mechanics & Hydraulic Machinery, Refrigeration and Air Conditioning, Engineering mechanics, Basics of Mechanical Engineering, , Refrigeration and Air Conditioning, Engineering mechanics, Basics of Mechanical Engineering

Model Institute Of Engineering & Technology, Jammu

Lecturer, Mechanical Engineering Department

May 2004 – Nov 2006

Responsibilities:

Member of Disciplinary Committee

Member of Guidance, Referral and Counselling Committee

Acted as Deputy Superintendent in the University Examination

Certified by NITTTR (National Institute of Technical Teachers' Training and Research), Chandigarh

Evaluated semester–end university examination answer sheets

Pass percentage of the students taught has always been between 80% - 90%

Received Letter of Appreciation from the Principal of the College for excellent results

Subjects taught: Mechanics, Thermal Engineering, and Machine Drawing

MGF TOYOTA, Gurgaon

Service Advisor

May 2003 – Feb 2004

Responsibilities:

Trouble shooting the technical faults in automobiles

Providing technical advice and directives for vehicle maintenance

Providing proper feedback to the technicians about the various repairs done on a vehicle and the rectification of the faults

Underwent intensive training for techniques to be followed in customer relationships conducted by the officials of Toyota Kirloskar Motor (TKM) Bangalore

Responsible for organizing and scheduling prioritized appointments and providing customers necessary details about servicing of vehicles including monitoring work progress, etc.

Technical, commercial and soft skills required

Awards and Recognition

- Awarded Best Paper in International Conference, The 2nd International Conference on 'Future Learning Aspects of Mechanical Engineering', AUUP, Uttar Pradesh, India).
- Recognized and selected two research papers for Research excellence Award at Delhi Technological University, Delhi
- Awarded 'Letter of Appreciation' by Principal MIET College of Engineering for Best Examination results.
- Chief Organizer, International Conference on New Frontiers in Engineering, Science and Technology (NFEST-2018) held in New Delhi, India from January 8-12, 2018.
- Organizer, 8th International Symposium on the fusion Science & Technologies (ISFT2020) held in JCBUST, YMCA, Faridabad, India from January 6-10, 2020. 20
- Awarded 'Appreciation Letter' by Chairman of Army Public School, Udhampur for qualifying for TEA (Test of Education Abilities)
- Stood 2nd in 'Skill Competition' Test held at MGF Toyota

Reviewer:

- Reviewed papers for Biofuels, Taylor & Francis.
- Reviewed paper for Asian Journal of Agricultural Extension, Economics & Sociology
- Reviewed paper for Asian Research Journal of Current Science

Memberships:

- Member of American Society of Mechanical Engineers (ASME) and ASME
- Member of Institutions of Engineering and Technology (IET)

Place: Delhi

Rashi Koul